Protein kinases that phosphorylate 14-3-3 isoforms

Samuel J. H. Clokie

A thesis submitted for the degree of Doctor of Philosophy
The University of Edinburgh
2005

DECLARATION

I declare that the thesis has been composed by me and the work presented is my own work, unless stated otherwise. This work has not been submitted for any other degree or professional qualification except as specified.

.....

Samuel JH Clokie

ACKNOWLEDGEMENTS

I thank my supervisor Professor Alastair Aitken for his help and providing me with the opportunity to undertake this project. I also thank members of the Aitken laboratory in particular Shaun Mackie, Alex Peden and Carolyn Brechin for advice and helpful discussions. I am grateful to the Medical research council for financial support.

Abstract

14-3-3 is an abundant, predominantly phospho-binding protein, intimately involved in the regulation of many diverse signal transduction events including cell cycle regulation, nucleo-cytoplasmic targeting of essential transcription factors and regulation of catecholamine synthesis. The 14-3-3 family consists of 7 isoforms (denoted α, β, γ, δ, ε, η and ζ) in mammals and shows a degree of isoform specificity in binding target proteins. 14-3-3 is phosphorylated in an isoform specific manner, for example SDK1/PKD phosphorylates 14-3-3 η, β and ζ, but not σ and τ. Our laboratory has previously identified *in vivo* 14-3-3 phosphorylation sites, S185 and S233. Phosphorylation of S233 by the serine/threonine protein kinase Casein kinase 1α (CK1α) was shown to negatively affect the interaction with Raf kinase. The group of Gotoh have recently shown that phosphorylation of S185 by the stress activated kinase c-Jun NH_2-terminal kinase (JNK) negatively effects the interaction with Bax. During studies in our laboratory that identified CK1α as a 14-3-3 kinase, several other proteins co-purified through four steps of chromatography, including centaurin-α_1 and CPI-17, suggesting a protein complex - these interactions have subsequently been characterised. CK1 has a potential phosphorylation dependent 14-3-3 binding site within the same region previously shown to be the interaction site for centaurin-α_1 and the aim of this investigation was to examine the possible interaction.

14-3-3 was found to associate with CK1 isoforms, with CK1α being studied further to reveal an interaction through serine residues 218 and 242 in a phosphorylation dependent manner, *in vivo*. Centaurin-α_1 was found to interact with a region corresponding to residues 214-226, only if S218 was in a dephosphorylated state, suggesting a possible regulatory mechanism. Mutagenesis of CK1α suggests that S242 is a high affinity binding site for 14-3-3, with S218 being of lower affinity. Investigations to identify possible kinase(s) responsible for phosphorylation of CK1 showed that stimulation of PKA can increase CK1α:14-3-3 association in cells, but PKA does not appear to phosphorylate CK1α *in vitro*.

As phosphorylation of 14-3-3 itself is an important regulatory mechanism, attempts were made to produce antibodies to phosphorylated S185 and S233 on 14-3-3. A phospho-specific antibody to S185 was successful, but antibodies to α-phospho-

S233 had no preference to the phosphorylation state of 14-3-3, although they were of high selectivity and affinity for 14-3-3 isoforms.

The kinase BCR (Breakpoint cluster region) is an important, but poorly understood protein that has been shown to associate with and phosphorylate 14-3-3. Investigations showed that BCR phosphorylates 14-3-3 on Ser233 *in vitro*. Additionally, BCR is shown to associate with another two isoforms of 14-3-3 (ε and η) both *in vitro* and *in vivo*. However 14-3-3 σ did not associate with BCR *in vitro*. BCR selectively phosphorylates 14-3-3 τ more than ζ, in contrast to CK1.

In summary, Interactions with CK1 and 14-3-3 are characterised in detail and a possible regulatory mechanism discussed for CK1:centaurin-α_1:14-3-3 interaction. Further insights into BCR signalling are revealed by identification of the phosphorylation site on 14-3-3 that has been shown to negatively affect binding to Raf kinase.

CONTENTS

DECLARATION....ii
ACKNOWLEDGEMENTS....iii
ABSTRACT....iv
CONTENTS....vi
LIST OF FIGURES....ix
LIST OF TABLES....xi
ABBREVIATIONS....xii

1. Introduction....2
1.1. Preamble....2
1.2. 14-3-3....3
1.2.1. Discovery of 14-3-3....3
1.2.2. 14-3-3 Sequence....5
1.2.3. Binding motifs....7
1.2.3.1. Phosphorylated ligands....7
1.2.3.2. Unphosphorylated ligands....8
1.2.4. Interacting partners....9
1.2.5. 14-3-3 structure....12
1.2.6. Regulation of interactions....21
1.2.6.1. Phosphorylation of 14-3-3....21
1.2.7. Isoforms and Dimers....23
1.2.7.1. Binding specificity and affinity....23
1.2.7.2. Heterodimerisation....24
1.2.7.3. 14-3-3 location and distribution....26
1.3. Breakpoint Cluster Region Kinase (BCR)....29
1.3.1. BCR Domain organisation....32
1.3.2. Regulation....36
1.3.3. Substrates....38
1.3.4. Localisation....38
1.4. Casein Kinase 1 (CK1)....39
1.4.1. Substrate specificity....40
1.4.2. Structure....46
1.4.3. Regulation of CK1....48
1.4.4. Sequence conservation between CK1 isoforms....50
1.4.5. Function....52
1.4.6. Localisation....53
1.4.7. Centaurin-α_1....55
1.5. AIMS....56
2. Materials and methods....58
2.1. Molecular biology....58
2.1.1. Agarose gel electrophoresis of DNA....58
2.1.2. Production of competent *Eschericia coli*....58
2.1.3. Preparation of plasmid DNA....59
2.1.3.1. Small scale, 'Mini-preps' of plasmid DNA....59
2.1.3.2. Large scale, 'Maxi-preps' of Plasmid DNA....59
2.2. DNA Manipulation....60

2.2.1. Prokaryotic vector manipulations – 14-3-3 60
2.2.1.1. 14-3-3 β isoform cloning 60
2.2.1.2. Polymerase chain reaction 60
2.2.1.3. Restriction enzyme digestion 60
2.2.1.4. 14-3-3 σ cloning 61
2.2.1.5. 14-3-3 η, γ ζ and τ cloning 61
2.2.2. Eukaryotic vector manipulations 61
2.2.2.1. *B*reakpoint *C*luster *R*egion (BCR) cloning 61
2.2.2.2. Casein Kinase 1 (CK1) cloning 62
2.2.3 62
2.2.4. Site-directed mutagenesis of CK1α 62
2.2.4.1. Polymerase chain reaction 62
2.2.4.2. Site Directed Mutagenesis of 14-3-3 63
2.3. Protein assay 64
2.4. Sodium-dodecyl sulphate polyacrylamide electrophoresis (SDS-PAGE) .. 64
2.4.1 65
2.4.2. Western blotting 65
2.5. Generation of antiserum to phospho-14-3-3 S185. 68
2.5.1. Peptide coupling and Immunisation of the sheep 68
2.5.2. Peptide affinity purification of anti-phospho-14-3-3 68
2.5.2.1. Immobilising the peptide 68
2.5.2.2. Binding and eluting the Antibody 69
2.5.2.3. Testing the Antibody 69
2.6. Purification of antibody to S233 site on 14-3-3 ζ 70
2.7. Cell culture 70
2.7.1. HEK293 cells, COS-1, COS-7 cells 70
2.7.2. Transfection of cells using electroporation 71
2.7.3. Transfection of cells using Lipids 71
2.7.4. Transfection of cells by calcium phosphate precipitation 71
2.7.5 72
2.7.6. Stimulation of 293 cells with dbcAMP 72
2.7.7. Lysis of mammalian cells 72
2.8. In vitro BCR kinase assay of 14-3-3 73
2.8.1. *In vitro* kinase assay using ^{32}P-ATP 73
2.9. Casein kinase 1 inhibitors 73
2.9.1. CKI-7 73
2.9.2. D4476 74
2.9.3. Phosphorylation of Centaurin-α_1 by all classes of Protein kinase C ... 74
2.10. Recombinant Protein Purification 75
2.11. In Vitro Transcription Translation 78
2.12. Protein digestion and mass spectrometry 79
2.12.1. Image analysis – Densitometry using AIDA/ImageJ software 79
3. Identification of phosphorylation site on 14-3-3 by BCR kinase. 82
3.1.1. DNA manipulation and purification of recombinant proteins used for kinase assays and binding experiments 85
3.1.2. GST-BCR and BCR-FLAG transfection in cells 86
3.1.3. Optimisation of BCR purification and phosphorylation of 14-3-3 by BCR. 89

3.1.4. BCR selectively phosphorylates 14-3-3 isoforms *in vitro* 91
3.1.5. BCR phosphorylates 14-3-3 tau and zeta on Ser/Thr 233..... 93
3.1.6. Endogenous CK1 does not co-precipitate and phosphorylate 14-3-3 in BCR-FLAG immunoprecipitations..... 95
3.1.7. Overexpression of BCR and CK1 97
3.1.8. D4476 does not affect BCR kinase auto- or trans-phosphorylation activity. 99
3.2. M2 FLAG antibody precipitates a cyclic A-like kinase: a cautionary tale101
3.2.1. PKA co-precipitates with the M2 anti-FLAG antibody from cell lysates 105
3.2.2. Investigation of BCR:14-3-3 interaction using an *in vitro* transcription translation system (IVTT) 107
3.2.3. GST-14-3-3 pull down of BCR..... 109
3.2.4. Co-expression of BCR and 14-3-3 isoforms in HEK293 cells. 111
3.2.5. Endogenous 14-3-3 association with BCR. 114
4. CK1α association with 14-3-3..... 119
4.1. Introduction..... 119
4.2. Results and Discussion..... 123
4.2.1. DNA manipulation and purification of recombinant proteins 123
4.2.2. Peptide synthesis and clean up of the synthetic peptide by HPLC and coupling of peptide to Sulfolink column..... 124
4.2.3. A phospho peptide corresponding to residues 214-226 of CK1α binds all 14-3-3 isoforms. 126
4.2.4. The CK1α phosphopeptide binds centaurin-α_1, only when dephosphorylated. 130
4.2.5. CK1 expressed by IVTT associates with 14-3-3, increasing with NaF treatment..... 132
4.2.6. All CK1α truncation mutants associate with 14-3-3. 134
4.2.7. CK1α associates predominantly with 14-3-3 η and γ in un-stimulated HEK 293 cells. 137
4.2.8. 14-3-3 isoforms associate with CK1α *in vitro* 139
4.2.9. Activation of PKA causes increased association of 14-3-3 with CK1α in HEK 293 cells. 141
4.2.10. Phosphorylation dependent binding of 14-3-3 η to CK1α..... 144
4.2.11. Inhibition of PKA reduces CK1α:14-3-3 association 147
4.2.12. 14-3-3 ζ binding mutant..... 149
4.2.13. Inhibition of CK1 binding to 14-3-3 using 14-3-3 antagonists..... 151
4.2.14. CK1α mutants retain autophosphorylation and catalytic activity 154
4.2.15. CK1 site directed mutants phosphorylate a CK1-specific peptide with similar kinetics 158
4.2.16. 14-3-3 binds to other CK1 isoforms. 160
4.2.17. PKC Phosphorylates Centaurin-α_1 on residue S87 and T276. 162
4.2.18. Phosphorylation of Centaurin-α_1 by PKC negatively affects interaction with CK1α..... 164
4.2.19. Computer modelling of 14-3-3 and CK1α 166
4.2.20. Discussion 169
5. Phospho-specific antibodies against 14-3-3..... 174
5.1. Introduction..... 174

5.2. Purification of Phospho S185 antibody using peptide affinity chromatography 175
5.2.1. Sensitivity of the pSPEKA antibody 178
5.2.2. Purification of Phospho S233 antibody 180
5.2.3. Cross reactivity of the 233L antibody 182
5.2.4. Immunoprecipitation of 14-3-3 using T233L antibody. 184
5.2.5. Discussion 186
6. General Discussion 188
6.1. BCR 189
6.2. CK1 192
6.3. CONCLUSION 200
7. Future work 202
8. Appendix 204
9. References 206
10. Publications 241

LIST OF FIGURES **Page number**

Figure 1.1 14-3-3 Domain organisation 4
Figure 1.2 Alignment of Human 14-3-3 isoforms 6
Figure 1.3 14-3-3 in Complex with a 'Mode 1' Peptide 13
Figure 1.4 14-3-3 monomer bound to a type 1 peptide 14
Figure 1.5 Crystal structure of 14-3-3 with AANAT 17
Figure 1.6 14-3-3 σ complexed with phosphopeptide 17
Figure 1.7 Sequence conservation on 14-3-3 19
Figure 1.8 Chromosomal translocation of BCR 30
Figure 1.9 Schematic showing BCR kinase 33
Figure 1.10 Crystal Structure of CK1 47
Figure 1.11 Schematic Representation of mammalian CKI Isoforms 49
Figure 1.12 Sequence alignment around proposed interaction region 51

Chapter 3

Figure 3.1 Summary of BCR:14-3-3 isoform interaction 84
Figure 3.2 Transfection efficiency in COS-1 and HEK293 cell types 88
Figure 3.3 Optimisation of lysis buffer for BCR immunoprecipitation and 14-3-3 τ phosphorylation 90
Figure 3.4 BCR kinase phosphorylates only 14-3-3 tau and zeta 92
Figure 3.5 Comparison of the 14-3-3 isoforms around residue 233 92
Figure 3.6 A Ser-Ala mutation at residue 233 abolishes phosphorylation of 14-3-3 τ *in vitro* 94
Figure 3.7 A Thr-Ala mutation at residue 233 abolishes phosphorylation of 14-3-3 ζ *in vitro* 94
Figure 3.8 CKI-7 has little effect on BCR phosphorylation of 14-3-3 96
Figure 3.9 Co-expression of BCR and CK1 98
Figure 3.10 CK1α does not co-immunoprecipitate with BCR kinase 100
Figure 3.11 Structures of CK1 inhibitors used in this study 100

Figure 3.12 M2 FLAG antibody co-purifies with a PKA-like kinase..... 102
Figure 3.13A Time Course of 14-3-3 γ phosphorylation..... 104
Figure 3.13B Densitometry of 14-3-3 γ phosphorylation..... 104
Figure 3.14 PKA co-precipitates with M2-FLAG antibody..... 106
Figure 3.15 co-precipitating PKA does not phosphorylate 14-3-3..... 106
Figure 3.16 *In Vitro* Transcription Translation (IVTT) of BCR-FLAG followed by pull down with GST-14-3-3zeta..... 108
Figure 3.17 BCR interacts with all 14-3-3 isoforms *in vitro*..... 110
Figure 3.18 Co-transfection of BCR-FLAG with 14-3-3 isoforms..... 113
Figure 3.19 BCR interacts with all 14-3-3 isoforms in 293 cells..... 115

Chapter 4

Figure 4.1 Centaurin-α1 co-purifies with CK1α from pig brain..... 122
Figure 4.2 CK1 binding partners investigated in this study..... 122
Figure 4.3 HPLC purification of the CK1 peptide corresponding to Residues *C*-^{214}FNRTpS^{218}LPWQGLKA^{226}..... 125
Figure 4.4 A phospho-peptide corresponding to residues 213-226 of CK1α associates with all 14-3-3 isoforms in a phospho-dependent manner..... 128
Figure 4.5 Densitometry analysis of CK1 phospho peptide binding to 14-3-3..... 129
Figure 4.6 Centaurin interacts with region corresponding to CK1 214-226 only if dephosphorylated..... 131
Figure 4.7 14-3-3 binds CK1a in a phospho-dependent manner..... 133
Figure 4.8 14-3-3 associates with all truncation mutants of CK1α..... 135
Figure 4.9 Coomassie stain of figure 4.10, showing equal loading of GST and GST-14-3-3 ζ..... 136
Figure 4.10 14-3-3 isoforms bind CK1α *in vivo*..... 138
Figure 4.11 14-3-3 isoforms associate with CK1 *in vitro*..... 140
Figure 4.12 Proposed interaction region within CK1α..... 142
Figure 4.13 Stimulation of PKA in 293 cells causes increased association of endogenous 14-3-3 with CK1α w/t..... 143
Figure 4.14 Residues S218 and S242 of CK1α are required for 14-3-3 association..... 146
Figure 4.15 Incubation of an inhibitor of PKA reduces association of CK1α with 14-3-3 ζ..... 148
Figure 4.16 Mutation of R5660A has no effect on CK1α association..... 150
Figure 4.17 Inhibition of CK1 binding to 14-3-3 using 14-3-3 agonists..... 153
Figure 4.18 Site-directed Mutagenesis of CK1 has little effect on autophosphorylation activity..... 156
Figure 4.19 Densitometry of PKA incubation with CK1α..... 157
Figure 4.20 Effect of CK1 mutants on the ability of CK1 to phosphorylate a CK1-specific peptide substrate..... 159
Figure 4.21 14-3-3 η binds to the CK1 ε isoform *in vitro*..... 161
Figure 4.22 PKC phosphorylates Centaurin-α_1 on residues S87 and T276..... 163
Figure 4.23 Phosphorylation of centaurin-α_1 by PKCε impairs association with CK1α..... 165

Figure 4.24 Computer modelling of CK1 and 14-3-3 interaction..... 168

Chapter 5

Figure 5.1A Scheme showing stages of antibody purification..... 178
Figure 5.1B. Dot blots of SPEKA/pSPEKA peptides..... 178
Figure 5.2A. Western blotting of recombinant 14-3-3 β, ζ and sheep brain extract..... 179
Figure 5.2B Ponceau load control..... 179
Figure 5.3 Serial dilutions of sheep brain, incubated with pSPEKA antibody.. 181
Figure 5.4 Testing of anti S233 antibody..... 183
Figure 5.5 Cross reactivity of T233L antibody with other 14-3-3 isoforms.... 185
Figure 5.6 Immunoprecipitation of 14-3-3 from cell and tissue lysates..... 187

Chapter 6

Figure 6.1 Proposed model for CK1 recruitment to the cell membrane..... 200
Figure 6.2 crystal structure of CK1, indicating interaction sites..... 203

LIST OF TABLES

Table 1.1 Sequences within mammalian proteins experimentally determined to bind 14-3-3..... 9
Table 1.2 Known kinases that phosphorylate 14-3-3 motifs..... 21
Table 1.3 14-3-3 binding proteins binding in an isoform-specific manner..... 24
Table 1.4 Summary of heterodimerisation of 14-3-3s..... 25
Table 1.5 Pathways activated/affected by BCR-ABL..... 29
Table 1.6 Phosphorylation sites *on* BCR..... 37
Table 1.7 CKI substrates and interacting proteins..... 41
Table 2.1 polymerase chain reaction..... 60
Table 2.2 Buffers and solutions for SDS-PAGE..... 64
Table 2.3 Transfer buffer..... 65
Table 2.4 Antibodies used for western blotting and immunoprecipitations..... 67
Table 2.5 binding buffer..... 68
Table 2.6 Clones used for protein over-expression in *E. coli*..... 75
Table 2.7 Clones Used for IVTT..... 78
Table 2.8 Media and buffers used..... 80
Table 4.1 summary of 14-3-3:CK1 interactions..... 173

ABBREVIATIONS

AKAP	A kinase anchoring protein
ATM	ataxia-telangiectasia mutated
ATP	adenosine-5'-triphosphate
ATR	ataxia-telangiectasia related
BSA	bovine serum albumin
CKI	casein kinase I
CKII	casein kinase II
CKI-7	N-(2-Aminoethyl)-5-chloroisoquinoline-8-sulfonamide
COS-1	SV40 transformed African green monkey kidney cells
Cpm	counts per minute
D4476	(4-[4-(2,3-dihydro-benzo[1,4]dioxin-6-yl)-5-pyridin-2-yl-1H-imidazol-2-yl]benzamide)
dbcAMP	dibutyryl cyclic adenosine monophosphate
DEAE-cellulose	Diethylaminoethyl - cellulose
DMEM	dulbecco modified Eagle medium
DMSO	dimethyl sulphoxide
dNTP	2'-deoxynucleoside 5'-triphosphate
DTT	Dithiothreitol
DYRK1A	Dual specificity tyrosine phosphorylated regulated kinase 1A
ECL	enhance chemiluminescence
EDTA	ethylenediaminetetra acetic acid
EGTA	ethyleneglycol-bis(β-aminoethylether)-N,N,N',N'-tetra acetic acid
FBS	foetal bovine serum

GST	glutathione-s-transferase
HA	influenza hemagglutinin-epitope (YPYDVPDYA)
HEK293	human Embryonic Kidney cells
HEPES	N-[2-hydroxyethyl]piperazine-N'-2ethanesulfonic acid
IC50	concentration required for 50% inhibition
IPTG	isopropyl-β-D-thiogalactopyranoside
IVTT	in vitro transcription/translation
MW	molecular weight
NP-40	Nonidet-P40 -octylphenolpoly(ethyleneglycolether)
PAGE	polyacrylamide gel electrophoresis
PBS	phosphate buffered saline
PCR	polymerase chain reaction
PKA	cAMP dependent protein kinase, protein kinase A
PKC	Protein kinase C
PMSF	Phenylmethylsulfonylfluoride
RPM	revolutions per minute
SDS	sodium dodecyl sulphate
SEM	standard error of mean
TAE	tris-acetate/EDTA
TBS	tris buffered saline
Tris-Hcl –	tris(hydroxymethyl)methylamine-hydrochloric acid)

CHAPTER 1
Introduction

1. Introduction

1.1. Preamble

The introduction provides a general overview of 14-3-3 biology, giving brief accounts of recent relevant developments and details on how 14-3-3 modulates the activity of bound proteins. The 14-3-3 interacting proteins examined in this study – BCR kinase (*B*reak point *C*luster *R*egion) and CK1 (formerly casein kinase I) are also discussed. The aim of this study was three fold. First was to identify the site of phosphorylation on 14-3-3 by the protein kinase BCR and examine in detail the interaction with 14-3-3 isoforms. The second aim was to further investigate a protein complex involving CK1, previously identified in our laboratory. In particular a possible CK1α: 14-3-3 interaction was examined and studies carried out to identify possible binding sites. Thirdly was to develop phospho-specific antibodies to 14-3-3 to probe how the phosphorylation status of 14-3-3 can affect binding to ligands.

Data shown here demonstrates that BCR can interact with the 14-3-3 γ and ε isoforms in addition to the previously reported 14-3-3 β, ζ and τ isoforms. The site of phosphorylation is mapped to S233 on zeta 14-3-3 and T233 on tau 14-3-3.

CK1α is shown to associate with all 14-3-3 isoforms in a phospho-dependent manner and the CK1α residues involved in this interaction are mapped to S218 and S242. This interaction occurs *in vitro* and *in vivo*. A model and possible function for this interaction is proposed.

1.2. 14-3-3

1.2.1. Discovery of 14-3-3

The name 14-3-3 was given to a group of small (28-33kDa), acidic proteins identified in a systematic screen of brain proteins by Moore and Perez in 1967 [1]. A combination of DEAE-cellulose chromatography and 2D starch electrophoresis resulted in the name 14-3-3, derived from the migration pattern [1]. A further systematic screen of cellular proteins from transformed human amnion cells by Celis et al [2] provides a good reference as to the location of 14-3-3 on a 2D gel. The first function ascribed to 14-3-3 was the activation of tryptophan hydroxylase by Yamauchi and co workers [3], however at this time, the 'activating protein' was not actually identified as 14-3-3 - it was not until several years later, when Ichimura et al, discovered the two are identical [4]. Shortly after, the same group identified and purified seven isoforms of 14-3-3 and denoted them α, β, γ, δ, ε, η and ζ after their respective elution position by HPLC [5]. They were also the first to clone 14-3-3 (the η isoform) [5]. At around the same time the laboratory of Aitken and co-workers identified a class of proteins that inhibited protein kinase C (PKC) as 14-3-3 [6]. Further studies into amino acid sequence of 14-3-3 by Aitken et al [7] revealed that the alpha and delta isoforms identified previously from brain, were the phosphorylated versions of beta and zeta respectively, bringing the actual number of isoforms to five. Subsequent studies have identified two further isoforms, named: 14-3-3 τ from T-cells [8] and 14-3-3 σ from epithelial cells (from *s*tratafin; the first name given to this isoform) [9], bringing the total number to seven. 14-3-3 τ has since been shown to be expressed in multiple cell types, whereas 14-3-3 σ has been found almost exclusively in epithelial cells.

Figure 1.1 shows a schematic of 14-3-3, outlining domain organisation and highlighting key regulatory phosphorylation sites. The existence of 14-3-3 as a dimer was one of the first insights into 14-3-3 structure and key residues required for dimerisation subsequently identified [10] and shown in figure 1.1. Also highlighted here are residues essential for phospho-peptide binding, as discussed in 1.2.3. Phosphorylation of 14-3-3 can have a significant affect on its ability to bind other proteins and is discussed in detail in section 1.2.6.

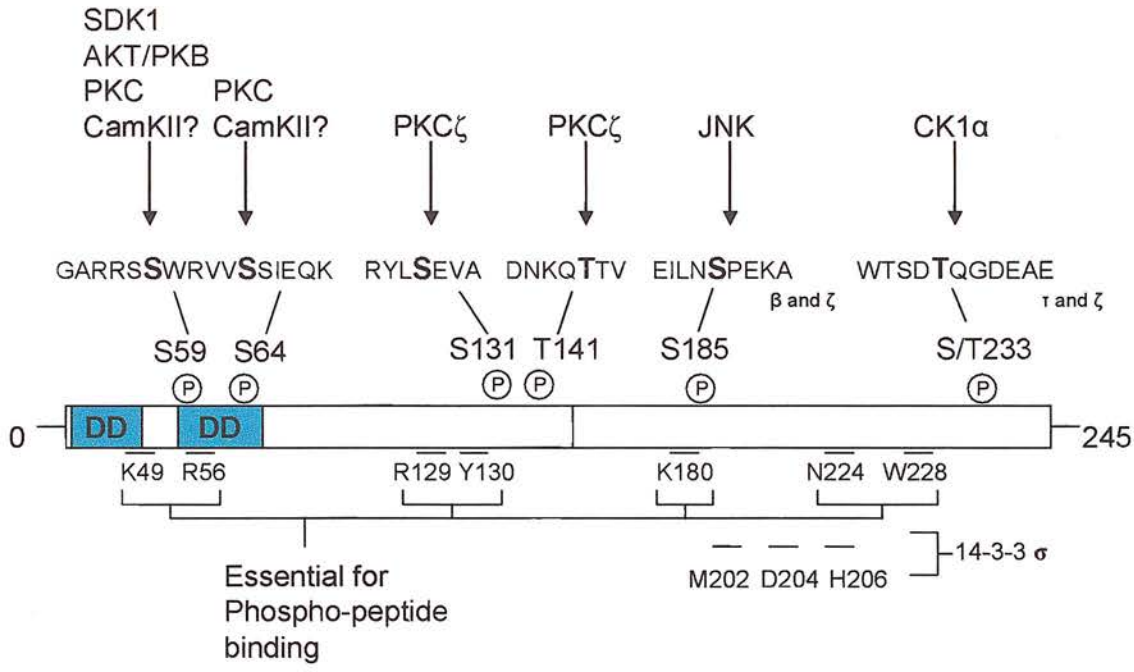

Figure 1.1 14-3-3 Domain organisation
14-3-3 is phosphorylated by a number of different kinases at different residues, with different consequences. DD represents the dimerisation domain. P in a circle represents phosphorylation sites with the respective kinase shown above. See text for specific details. Short bars indicate residues shown to be essential for phosphopeptide binding. Residues M^{202}, D^{204}, H^{206} are unique to σ and when mutated to I, G and D respectively, as in other 14-3-3 isoforms, gives σ the ability to bind the previously non-interacting ligand, Cdc25C [11].

1.2.2. 14-3-3 Sequence

14-3-3 isoforms shows a high degree of sequence conservation across a broad range of organisms [12, 13]. Sequence analysis reveals homologous sequences in most eukaryotes examined, indeed they are found in four of the major evolutionary lineages: fungi, Alveolata, plants and animals [13], whereas none so far have been found in prokaryotic organisms. The diversity of the organisms where 14-3-3 isoforms are found is sizable and indicates an ancient origin [12]. Evolution of such a large number of isoforms – at least 153 isoforms/alleles in 48 species of multicellular organisms (correct in 2000 [13]) is not obvious, but there are several possibilities why such a large number is expressed, as discussed by Rosenquist et al [13]. Among the possible reasons are: (i) to simply increase the amount of 14-3-3 available within a cell, (ii) to allow isoform-specific targeting (of 14-3-3) to a subcellular location, (iii) to allow isoform-specific binding of target proteins (e.g. enzymes) to modulate activity and (iv) differential expression during stages of development, allowing regulation of the process (see [13] for review). Many independent studies have identified 14-3-3 isoforms having different binding affinities to a number of target proteins, suggesting a requirement for so many isoforms. An alignment of the human isoforms is shown in figure 1.2, with conserved residues in red and conservative substitutions in yellow. This alignment reveals several blocks of highly conserved residues with 48% sequence identity between these 14-3-3 isoforms (gap penalty of 3). Examining the same isoform across different mammalian species can give a sequence identify of 96-100% [13]. The majority of conserved residues are essential for dimerisation and ligand binding, as discussed below. The alignment of 14-3-3 sequences here uses the alternatively processed, longer, 14-3-3 β isoform and also the longer epsilon isoform. This gives consistent numbering allowing more straightforward comparison of residues between isoforms (see figure 1.2). Pertinent residues are indicated in boxes, with the numbering as used in the literature and text here. Many functionally important residues are found in the conserved regions, but there are subtle differences in sequence within the 14-3-3 isoforms, including phosphorylation sites, that may lead to isoform binding specificity, discussed further in section 1.5.

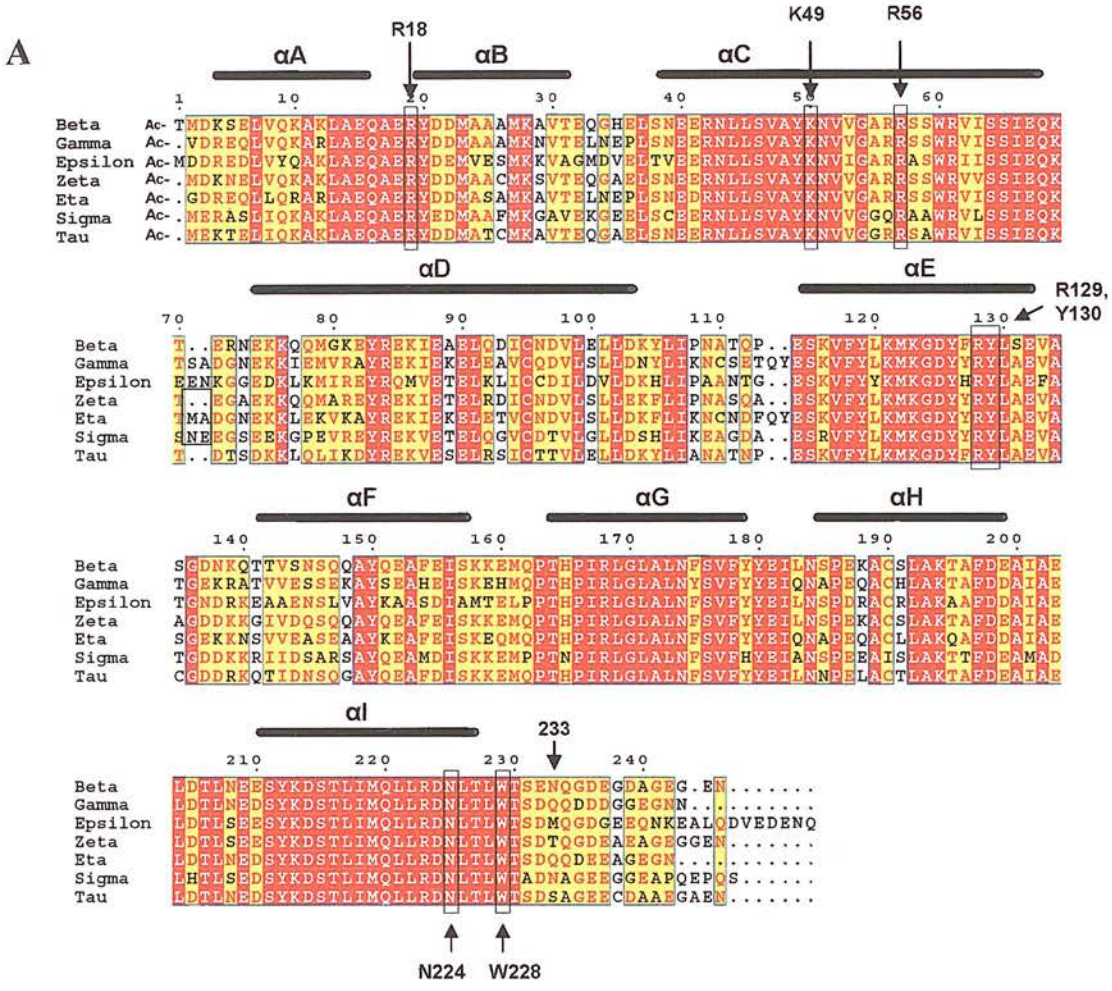

Figure 1.2 Alignment of Human 14-3-3 isoforms

A, Human 14-3-3 sequences were aligned using the ClustalW server at: http://npsa-pbil.ibcp.fr Black bars above sequences indicate α-helices. Residues involved in contacting bound ligands and phosphorylation sites are indicated and explained in the text.

B, shows relationships between 14-3-3 isoforms, produced using the facility at http://pir.georgetown.edu/pirwww/aboutpir/aboutpir.html. Sigma is the most distinct from other 14-3-3 sequences. Gamma and eta are very similar and distinct. These differences may explain different binding affinities to 14-3-3 ligands, as discussed in 1.2.2 and 1.5. Similarity between sequences is shown in arbitary units (0.1 scale bar).

1.2.3. Binding motifs

1.2.3.1. Phosphorylated ligands

Initial investigations into 14-3-3:Raf-1 interaction, using sequences derived from Raf-1, identified 14-3-3 as a specific phospho-serine binding protein, with an apparent K_d of 122nM [14]. To find optimal 14-3-3 binding sites, oriented peptide libraries were screened and identified a general consensus of: RSXpSXP and is called a 'mode 1' motif [14]. This was later refined to RXXXpSXP and is called a 'mode 2 motif', then further refined to RS[+/Ar]pS[L/E/A/M]P and RX[Ar][+]pS[L/E/M]P, where X=any amino acid, + = a positively charged amino acid and Ar = an aromatic amino acid [15]. Arginine at -3 or -4 from pSer is crucial for 14-3-3 interaction, whereas P at +2 is dispensable, although the K_d is decreased [16]. These general consensus motifs have greatly aided the identification of potential 14-3-3 binding partners, allowing computer based searches of protein databases, refinement of known 14-3-3 interactions and identification of candidate binding site(s). However not all proteins conform to this consensus, a list of proteins found experimentally to interact with 14-3-3 is found in table 1.1. For example, examination of the interaction of 14-3-3 with the proto-oncogene Cbl generated a further motif consisting of $RX_{1-2}SX_{2-3}S$, where x is any amino acid and at least one S is phosphorylated [17].

Recently a further motif, pS/TX_{1-2}-COOH dubbed 'mode 3', was discovered in arylalkylamine N-acetyltransferase (AANAT) [18] – a protein already known to contain a mode 1 motif. When doubly phosphorylated, two site binding of 14-3-3 to AANAT lowers the K_m of AANAT for serotonin ~40 fold to ~30μM [19] and see section 1.2.4. This motif is similar to another, atypical binding motif found in the plant H^+-ATPase – $QQYpT^{948}V$-COOH [20], where both motifs require the COOH at the C-terminus. However, phosphorylation does not always increase the association with 14-3-3, for example when p53 is doubly phosphorylated within the 14-3-3 motif ($KGQPS^{376}TpS^{378}RH$) the association is actually reduced, compared to phosphorylated S^{378} alone [21]. Another word of caution is that 14-3-3 does not always bind the optimal motif, even within the same protein. For example, 14-3-3 binds Gem through the two motifs $RWpS^{23}IP$ and $KSKpS^{289}CH$, whereas another, more canonical motif ($RKEpS^{261}MP$) does not. The result of 14-3-3 binding is to increase the half life of Gem [22].

1.2.3.2. Unphosphorylated ligands

14-3-3 has been shown to interact specifically with a number of non-phosphorylated proteins and with a similar affinity to phosphorylated proteins. One set of interactions appears to be through cysteine rich domains (CRD), e.g. the CRD domain of Raf-1 [23, 24] and the platelet GPIα [25]. Other ligands interact through acidic residues, e.g. ExoS ADP-ribosyl transferase [26, 27] and the 43KDa inositol 5-phosphatase [28] see table 1.1 for sequences.

During screens for optimal peptides, a peptide known as R18 (PHCVPRDLWLDLEANMCLP, underlined residues bind in the basic pocket) was found to bind 14-3-3 with an affinity of 70-90nM [29]. It has been demonstrated by Yaffe et al [15] that the combination of two phosphopeptides (RSApSEP), separated by a linker region, had a ~30 fold increased association with 14-3-3 [15]. The result was presumably through bidentate binding, as each peptide can bind into each 14-3-3 monomer. Based on this observation, the laboratory of Fu et al designed a DNA construct that produces two R18 peptides that are separated by a linker region [30]. The purpose of using a peptide that does not require phosphorylation to interact with 14-3-3 was appealing, as it should remain a potent 14-3-3 interactor, when transfected into cells. Transfection of a construct containing these two sequences, known as Difopein (Dimeric fourteen three three peptide inhibitor), induced apoptosis within a few hours, by sequestering all 14-3-3 - placing 14-3-3 as an essential antiapoptotic factor [30]. The mode of interaction of an unphosphorylated ligand may not be that different than that of a phosphorylated one, as the R18 peptide can clearly compete out binding to many ligands. Interaction through non-phosphorylated ligands may confer more isoform binding specificity due to involvement of other residues on 14-3-3 not usually involved in binding phosphorylated ligands.

1.2.4. Interacting partners

The number of binding partners for 14-3-3 is growing rapidly. The group of MacKintosh and colleagues recently identified over 200 binding partners in an *in vitro* binding screen whereby HeLa extracts were passed through an immobilised 14-3-3 column and eluted with a generic mode 1 phospho-peptide (ARAApSAPA) [31]. Of course, whilst direct binding of 200 proteins to 14-3-3 is not claimed in this study, as protein complexes are certain to exist; it does reinforce the large repertoire of 14-3-3 binding proteins identified over the years. Currently more than 100 proteins have been well characterised and the binding motif identified (see section 1.2.3 and table 1.1, below). This table only includes proteins that have been proven experimentally to interact with 14-3-3, where the site(s) have been determined and is not a list of *all* 14-3-3 interacting proteins. It includes interacting proteins with phosphorylated, non-phosphorylated and 'atypical' binding motifs.

Table 1.1 Sequences within mammalian proteins experimentally determined to bind 14-3-3. Adapted and updated from [32].

Target protein by category	binding sequence	Reference
Protein kinases		
Big mitogen-activated kinase 1 (BMK1/ERK5)	ALLKpS^{486}LRS	[33]
Ca^{2+}/calmodulin-dep. myosin light-chain kinase	FLHSPpS^{161}CPA	[34]
CamKII	RKFpS^{74}LQ	[35]
GSK3β (Glycogen synthase kinase 3β)	RPRTTpS^{9}FA	[36, 37]
KIF1C (Kinesin like protein KIF1C)	RRQRS^{1092}AP	[38]
Mei2P (*S. pombe*)	RTEpS^{438}SP, RSLpT^{527}VG	[39]
PCTAIRE-1, protein kinase 1	NKRLpS^{119}LP	[40]
p90 ribosomal S6 kinase 1 (RSK1)	FTRLpS^{154}KEV	[41]
PKCμ (PKD)	RRLpS^{205}NVS^{208}, RTSpS^{219}AELpS^{223}TS	[42]
PKCζ	RHMDpS^{186}VMP	[43]
c-Raf-1 kinase	RSTpS^{259}TP, RSApS^{621}EP	[44]
B-Raf kinase	RSApS^{728}EP	[45]
Testicular protein kinase (TESK1)	RCRpS^{439}LP	[46]
Wee1, cell-cycle Y kinase	RSVpS^{642}LT	[47]
Phosphatases		
PTPH1, tyrosine phosphatase	RSLpS^{359}VE, RVDpS^{853}EP	[48]
Cdc25A, cell-cycle dual-specificity phosphatase	RSPpS^{290}MP	[49]
Cdc25B, cell-cycle dual-specificity phosphatase	RSPpS^{323}MP	[50]
Cdc25C, cell-cycle dual-specificity phosphatase	RSPpS^{216}MP	[51, 52]
Slingshot-1L (SSH1L)	RSSpS^{937}, RSHpS^{978}LA	[53]
α-Chain of interleukin 9 receptor (IL-9R)	KARpS^{519}WpT^{521}F-$_{COOH}$	[54]
β-Chain of GM-CSF, interleukin-3 and -5 receptors	PPHSRpS^{585}LP	[55]

Exoenzyme-S, ADP-ribosylation	DALDL^{428}	[27]
GPIb α subunit of platelet membrane glycoprotein Ib	RLpS^{166}LTDP, RYSGHSL^{610}-$_{COOH}$	[56]

Receptors, G-proteins and related proteins

Adam 22	RSNpS^{857}TE	[57]
Adam22cyt	RSNpS^{834}WQ	[58]
AKAP-lbc	FRRHpS^{1565}WGPGK	[59]
GEF-H1	PRRRpS^{885}LPAG	[60]
Grb10	RSVpS^{428}EN	[61]
Insulin growth factor I receptor S	VPLDPSASSSpS^{1283}LP	[62]
Iip35, major histocompatibility complex-associated	RSRpS^{8}CR	[63]
Insulin receptor substrate 1 (IRS-1)	RSKpS^{270}QS, NHSRpS^{374}IP, PKSVpS^{641}AP	[62]
KCNK3	RRSpS^{393}V-$_{COOH}$	[64]
KCNK9	RRKpS^{373}V-$_{COOH}$	[64]
Kir/Gem	QQRWpS^{22}IP, KLKSKpS^{289}CH	[65]
Na+/H+ exchanger isoform-1 (NEH1)	RIGpS^{703}DP	[66]
Na^+, K^+-ATPase α1-subunit	KKpS^{18}KK	[67]
Nicotinic acetylcholine receptor α 4 subunit	RSLpS^{441}VQ	[68]
Nuclear receptor (Nur77)	RLPpS^{350}KP	[69]
Phosducin (photoreceptor *Gbc*-binding protein)	RQMpS^{54}SP	[70]
prolactin receptor (PrlR)	KCSpT^{391}WP	[71]
RAS effector protein RIN1	RSMpS^{351}AA	[72]
Regulators of G-protein signalling, RGS3, RGS7	EKDpS^{496}YP, KSDpS^{434}YP	[73]
Rem2	RRGpS^{69}M, QRSRpS^{334}C	[74]
Ron	RPLpS^{1394}EP	[75]
p190RhoGEF, guanine nucleotide exchange factor	I^{1370}QAIQNL	[76]

Apoptosis-regulating proteins

c-Abl, tyrosine kinase	RSVpT^{735}LP	[77]
Apoptosis signal-regulating kinase 1 (ASK1)	RSIpS^{967}LP	[78]
BAD, (Bcl-XL/Bcl-2 associated death promoter)	RHSpS^{112}YP,RSRpS^{136}AP,RRMpS^{155}DF	[79, 80]
Cyclin-dependent Kinase 11 (CDK11^{P110})	RHRpS^{118}HS	[81]
TSC2 (tuberin)	RSTpS^{939}LN, KSLpS^{1210}VP	[82-84]

Adaptor proteins

Cbl	RHpS^{619}LPFpS^{623}, RLGpS^{639}TFpS^{642}	[17]
Cofilin	MApS^{3}GVAV, RKSpS^{24}TP	[85-87]
HSP20	RRApS^{16}AP	[88]
KSR (kinase suppressor of Ras)	RSKpS^{297}HE, RTEpS^{392}VP	[89]
p130cas (Crk-associated substrate)	RSTpS^{592}EP	[90, 91]
tau	GSRSRTPpS^{214}LP	[92]

Transcription factors and nuclear proteins

Ataxin-1	RRWpS^{776}AP	[93]
BRF1 (butyrate response factor1)	RDRSFpS^{92}EG	[94]
Cabin1	RAKpS^{2126}RP	[95]
E2F1	RLLDSpS^{31}QIVI	[96]
Forkhead transcription factor (FKHRL1)	RPRSCpT^{32}WP, RRRAVpS^{253}MD	[97, 98]
Histone deacetylase, HDAC4	RKTApS^{246}EP, RTQpS^{467}AP, RAQpS^{632}SP	[99]
Histone deacetylase, HDAC5	RKTApS^{259}EP, RTQpS^{498}SP	[100]
Histone deacetylase, HDAC7	RKTVpS^{178}EP, RTRpS^{344}EP, RAQpS^{479}SP	[101]
TAZ	RSHpS^{89}SP	[102]

Miz1	RSGpT^{291}YG, CGRSFpS^{428}DP	[103]
Nuclear factor of activated T-cells (NFAT3)	RRYpS^{272}pSpS, RRGpS^{289}	[104]
P27^{Kip1} (p27)	RKRPApT^{157}DD	[105]
p53 tumour-suppressor/transcription factor	KGQSTpS^{378}RH/G	[21]
TORC2	RTSpS^{171}DSA, QGSHpS^{369}HP	[106]
YAP (Yes-associated protein)	RAHpS^{127}SPA	[107]

Enzymes and others

43 kDa inositol polyphosphate 5-phosphatase	ELVLRSESEEKVV^{371}	[28]
Endopeptidase 24.15	RTpS^{644}ILRP	[108]
PFK-2	RRNpS^{466}FTP, RNYpS^{483}VGS	[109]
K1F1C, kinesin-like protein	RRQRpS^{1092}AP	[38]
Keratin 18 cytoskeletal component	RPVpSSAApS^{33}	[110]
Middle T antigen, polyoma virus	RSHpS^{257}YP	[111]
Nedd4-2 (E3 ubiquitin ligase)	RSLpS^{468}SP	[112]
NUDEL	APSpS^{198}PT, SLPApT^{219}PV,NTFPpS^{231}PK	[113]
Par1b (EMK1/ MARK2)	VSRSpT^{595}FHAGQ	[114]
xPar-1	RSpT^{593}FHA, RNLpS^{646}FRF	[115]
Par3α	KKSSpS^{814}LES	[116]
Par3β	KKSSpS^{746}LES	[116]
Phosphodiesterase 3B (PDE3B)	PRRRpS^{279}SCVS, FRRPpS^{302}LPC	[117]
Phospholipase A_2	^{127}KEESEK (not phosphorylated)	[118]
Plakophilin 2 (PKP2)	RTSpS^{82}VPE	[119]
Rep68	RGHpS^{535}L	[120]
Rim1(Rab3 interacting molecule α)	RSRpS^{287}EP, RYRpS^{379}DP	[121]
Rim1α (Rab3 interacting molecule α)	RRHpS^{413}DVAL	[122]
Rim2	RYRpS^{315}DP	[121]
Rabphilin 3	RANpS^{274}VQ	[121]
Serotonin N-acetyltransferase (AANAT)	RRHpT^{31}LP, RRNpS^{205}DR-$_{COOH}$	[19, 123]
Stannin (Snn)	RISQpS^{45}EP	[124]
Tyrosine hydroxylase	RRAVpS^{19}ELD, IGRRQpS^{40}LIEDA	[125, 126]

Plant related proteins

RSG (Repression of shoot growth)	NHFRSLpS^{114}VDAD	[127]
Fructose 2,6-bisphosphate (Fru-2,6-P_2)	SLSASGpS^{220}FR, RLVKSLpS^{303}ASSF	[128]
H^+-ATPase (plant plasma membrane)	QSYpT^{946}V-$_{COOH}$	[129]
Nitrate Reductase (NR)	RTApS^{543} TP	[130]

Abbreviations: pS, phosphoserine; pT, phosphothreonine; GM-CSF, granulocyte/macrophage colony-stimulating factor; TNF, tumour necrosis factor. PFK2, 6-phosphofructo-2-kinase/fructose-2,6-bisphosphatase; Sgk1 - serum- and glucocorticoid-inducible protein kinase, KIF1C; TAZ, Transcriptional co-activator with PDZ- binding domain;

Summary of 14-3-3 binding motifs:

There are 25 14-3-3 binding proteins with *no* Arg at pS-3/4, 6 with a pSx-$_{COOH}$ motif, 4 with a non-phosphorylated motif and 15 with an Arg at pS-2.

1.2.5. 14-3-3 structure

The crystal structures of 14-3-3 τ [131] and ζ [132] revealed near identical structures consisting of nine antiparallel alpha helices in each monomer, in a curved arrangement, that form a 'cup shaped' structure (see figure 1.3). From these studies, the size of the amphipathic central groove formed by the dimers was ascertained to be 35Å wide and 35Å long, with a depth of 20Å [131]. Also evident is the different charges clustered along the central groove, forming a hydrophobic patch at one end, with a charged, polar group at the other. It is in this amphipathic groove where binding was predicted to occur. Due to the high sequence conservation, solving the structures of 14-3-3 τ [131] and ζ [132], serves as a good template for other 14-3-3 isoforms.

Residues 5-21 of one monomer, form contacts with residues 58-89 of the opposing monomer, forming an area of 2150Å^2 making up the dimer interface, of which 70% of this area (1520 Å^2) is composed of hydrophobic residues [131], more than the area covered by a typical antibody:antigen interaction [132, 133]. These structural studies help explain biochemical data gathered on 14-3-3. For example, protease digestion of 14-3-3 ε, followed by gel filtration identified a 17KDa region that forms a dimer [10]. Deletion of the N-terminal 26 amino acids, disrupted dimerisation and also was less effective as an inhibitor of PKC [10]. It is clear from the structure that this domain represents the dimer interface.

Whilst the crystal structure of 14-3-3 provides very useful insights, crystallisation with bound ligands is needed for more complete understanding. After identifying optimal binding peptides for 14-3-3 (see section 1.2.3.1) crystallographic studies were performed on 'Mode 1' and 'Mode 2' peptides bound to 14-3-3-3 ζ, identifying key residues involved in binding. A 'mode 1' peptide is shown binding in the 14-3-3 dimer in figure 1.3 and 1.4, the peptide is shown in yellow, with the phosphorylated serine in purple. Here the residues highlighted in red are directly involved in ligand binding; most have been shown experimentally to be essential for binding. There is a basic pocket that binds the phosphorylated serine (seen more clearly in figure 1.4, monomer). Within this pocket, residues K49, R56 and R60 have been shown experimentally to be essential for binding, although to differing degrees [134, 135].

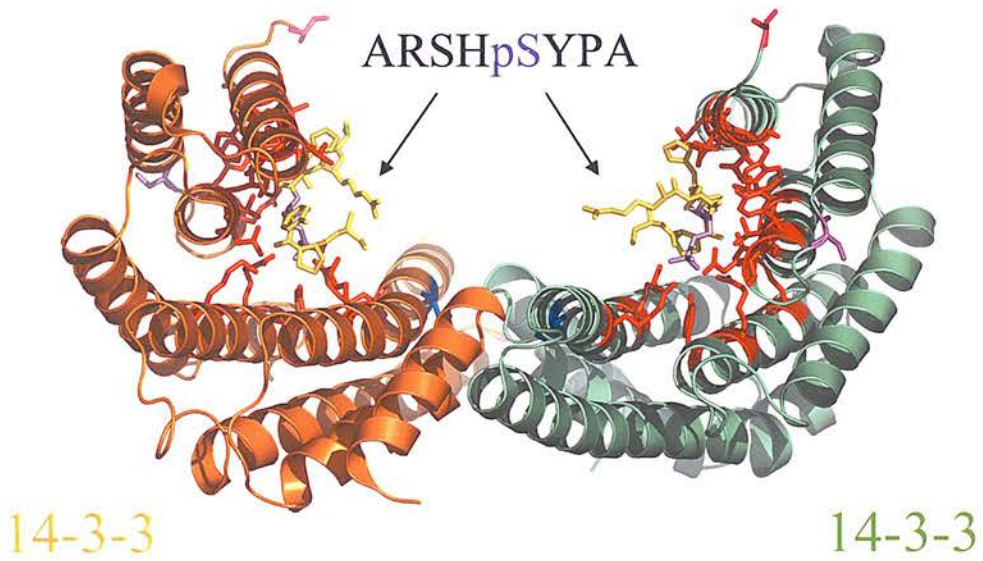

Figure 1.3 14-3-3 in Complex with a 'Mode 1' Peptide
Each 14-3-3 monomer is represented in different colours, one orange, the other green, showing the nine alpha helices that make up each 14-3-3 monomer. The 'mode 1' peptide is coloured yellow, with phosphorylated serine in purple. Red colouring indicates the basic pocket and other residues that make contact with bound peptide [16, 131].

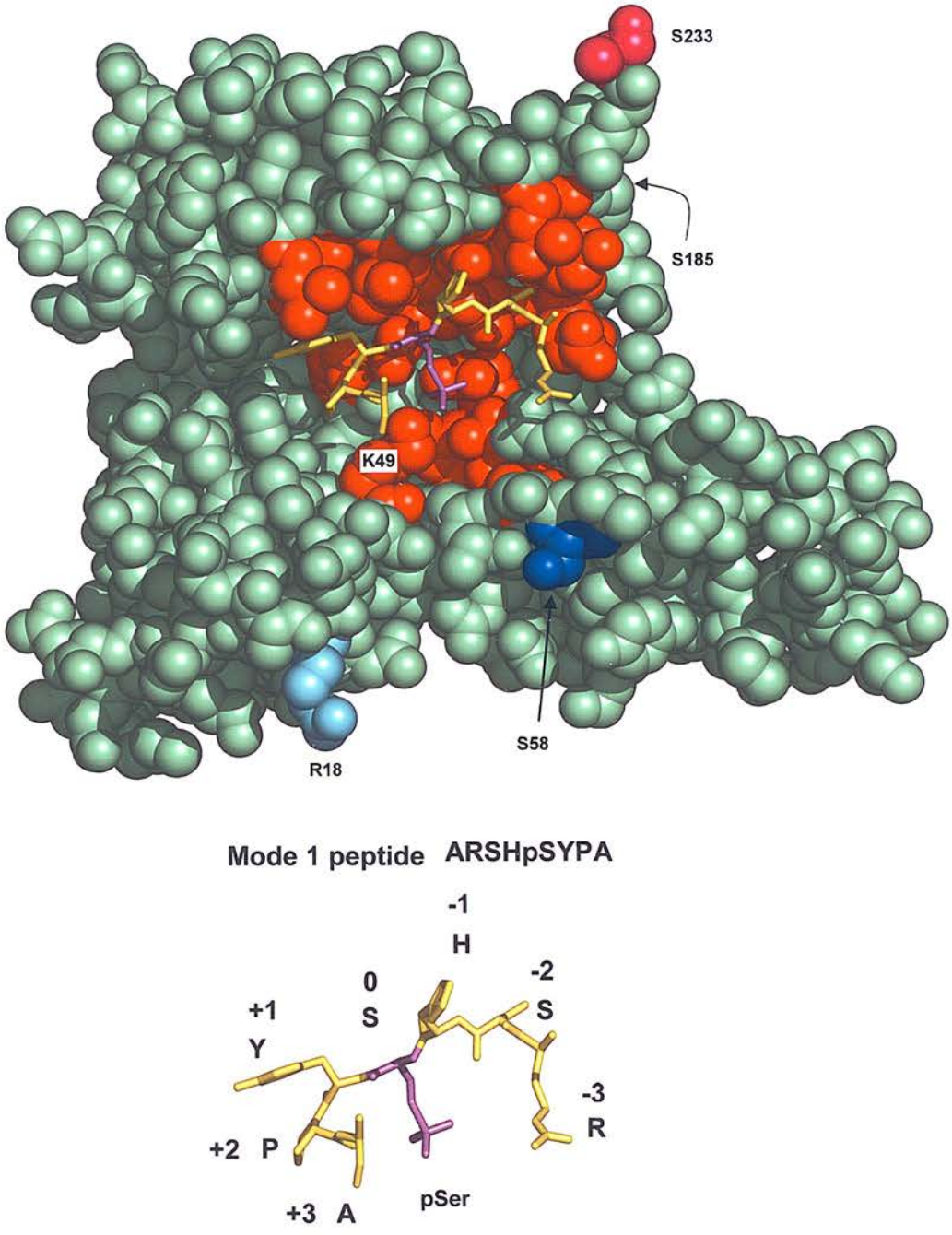

Figure 1.4 14-3-3 monomer bound to a type 1 peptide
One monomer from co-ordinates 1QJB is shown represented with spheres. Key to residue colouring:
Purple: pSER of bound peptide
Blue: S58, involved in dimer formation
Turquoise: R18 juxtaposed to S58 of the second monomer
Yellow: mode 1 phospho-peptide, ARSHpSYPA, with the 14-3-3 mode 1 motif listed.Pink: S185 and S233 phosphorylation site.
Red coloured spheres are residues that have been shown experimentally [16, 131] to contact bound ligands.

Indeed salt bridges are formed from the phosphoserine to each of these residues, with a hydrogen bond to the hydroxyl group of Y128 [15]. Specifically, a charge reversal mutation of Lys49 to Glu leaves 14-3-3 unable to bind Raf-1 kinase and Exoenzyme S both in reticulolysates and in yeast [134]. Charge reversal mutation of R56E partially reduced binding to Raf with R60E having only a subtle difference [134]. Further studies revealed mutations of several hydrophobic residues that also reduce the ability of 14-3-3 to associate with binding partners [135]. Hydrophobic to acidic mutations consisting of: L172D, V176D, and L220D drastically reduced Raf-1, Cbl and BCR binding to 14-3-3 ζ in Jurkat T-cells [135]. More extensive studies where the structure of 14-3-3 was solved with 'mode 1' and mode 2' peptides and a refined structure to 2Å, allowed detailed analysis of electrostatic interactions with bound peptides. Comparing 'mode 1' and 'mode 2' peptides revealed the proline induces a sharp twist, turning the peptide out of the binding pocket and back toward the central groove. The orientation in which 'mode 1' and 2 peptides are bound, however, is quite different. 'Mode 1' peptide is in the cis- conformation, whereas 'mode 2' adopts a trans-conformation, causing the peptides to contact different residues within 14-3-3 [16]. The formation of salt brides and hydrogen bonds with the peptides showed E180, N224, W228 would also be critical for binding ligands [16]. This was later tested, as mutation of Glu180 to Lys allowed 14-3-3 ε to bind a different subset of binding partners, in particular A-, B- and C-Raf could not bind E180K mutant, but IRS-1 could, albeit with lower affinity [16].

In this study a double mutation of R56A/R60A was used with the intention of reducing the necessity of requiring a phosphate, without affecting or repelling binding of ligand per se. This charge reversal mutant has been used before to investigate PKUα localisation and regulation [136] and place 14-3-3 with an anti-apoptotic role increasing JNK and p38MAPK activation [137].

The structure of 14-3-3 is unique and few proteins share homology, however the recent solution of a protein involved in targeted RNA destruction, SMG7, was found to have a region with near identical tertiary structure to 14-3-3 [138]. Interestingly, the sequence identity at the amino acid level is less than 10%, but the positions of the residues that *are* conserved, reside at equivalent positions found in previous 14-3-3:phosphopeptide structures, that make contact with bound peptide

[138]. Indeed mutations of these residues within SMG7 reduced binding, as observed in previous 14-3-3 interaction studies [16] (and see above).

The only crystal structure of 14-3-3 in complex with another protein, is one of the first proteins found to interact with 14-3-3, arylalkylamine N-acetyltransferase (AANAT) [18]. This study used a truncated form of AANAT, lacking the last amino 6 amino acids (due to problems with crystallisation) phosphorylated on T^{31} by PKA [18]. This structure showed the actual region of AANAT, the area around pT^{31}, binding to 14-3-3 in a similar conformation to the crystallised peptide studies of Rittinger et al [16], with the cis- proline at +2 twisting the interacting loop out of 14-3-3 (see figure 1.5). Superimposing the two 14-3-3 structures revealed a very slight change in 14-3-3 structure – about 2Å wider and raising the floor of 14-3-3 by 1.5Å, indicating the rigidity of 14-3-3 [18]. Indeed it is this rigidity that led to the theory of 14-3-3 acting as a 'molecular anvil' by Mike Yaffe [139] – actively forcing bound proteins into a particular conformation. The solution of the co-crystal structure accompanied with previous structural and biochemical knowledge of AANAT [123, 140, 141] revealed that extensive contacts keep AANAT in an active conformation, by restricting movement of the active loop, leaving the active site readily available for substrate binding. The result of which is that on 14-3-3 binding to AANAT, the K_m for serotonin is lowered substantially [123]. Further studies revealed that 14-3-3 can bind another site on AANAT (containing pS^{205}) and 14-3-3 binding to both phosphorylated sites (pT^{31}/pS^{205}) lowers the K_m for arylalkylamine 30 fold compared to unphosphorylated AANAT [19]. 14-3-3 binding to phosphorylated S^{205}, with T^{31} mutated to A, increased the K_m for arylalkylamine 40 fold to 1.2mM [19], indicating a key regulatory mechanism and showing dual binding is required for maximal activity. Binding to 14-3-3 may also protect AANAT from dephosphorylation and/or degradation, prolonging the activation state [19].

14-3-3 σ is quite distinct from other isoforms and the recent elucidation of the 14-3-3 σ structure has revealed residues whose positions and properties explain explicit homo-dimer formation of 14-3-3 σ and distinct binding partner selection [11]. 14-3-3 σ has two extra amino acids between helices α-C and α-D (identified in figure 1.6) creating a more disordered loop and subsequently a helix one turn shorter than in ζ. Also A Phe-Cys substitution at residue 25 alters salt bridge formation such that

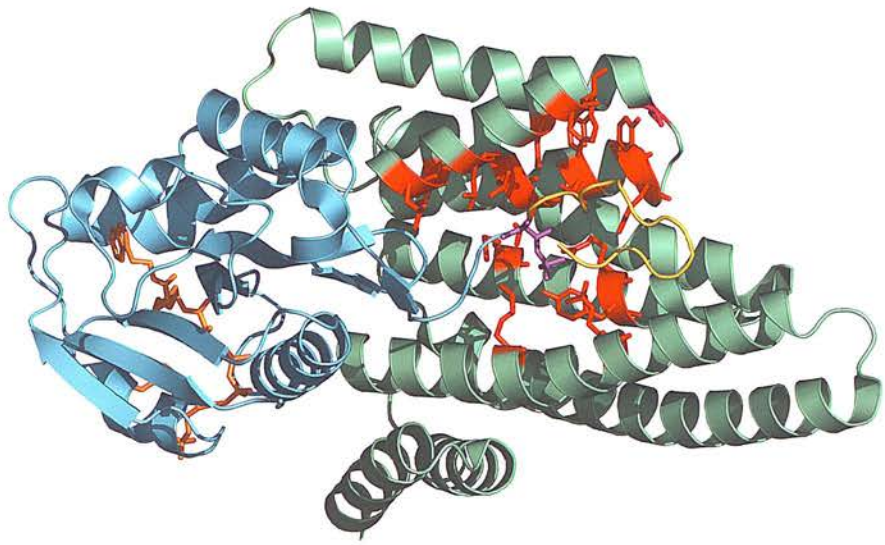

Figure 1.5 Crystal structure of 14-3-3 with AANAT.
Ribbon model of the crystal structure of 14-3-3 complexed to AANAT, from co-ordinates 1IB1.pdb, rendered using Pymol. Only one 14-3-3 monomer (green) and one AANAT (light blue) are shown. Red residues indicate the binding pocket, yellow the interacting region, pT^{32} in purple. The orange molecule is COT (CoA-S-Acetyl tryptamine).

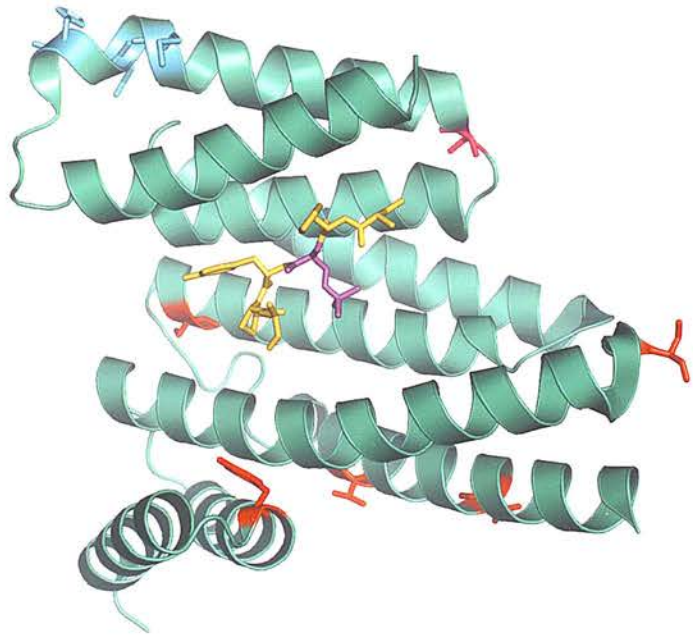

Figure 1.6 14-3-3 σ complexed with phosphopeptide.
Residues recently identified as phosphorylation sites [142] are coloured red, residues found to mediate 14-3-3 σ isoform selectivity (cyan), dark blue indicates an extra amino acid compared to all other 14-3-3 isoforms, pink indicates S185. The peptide is in yellow, pSer in purple. From 1WYT.pdb [11].

there are four stabilising interactions in the homodimer interface that could not occur in heterodimers. Additionally S5 and E80, both unique to σ are juxtaposed, but in other isoforms, E80 would be adjacent to D or E, forming a highly unstable interaction [11]. Another intriguing observation is that, in 14-3-3 σ, mutation of three residues near the C-terminus (M202, D204, and H206) that are only variant in σ, to I, E, D residues in all other isoforms, gives σ the ability to bind cdc25, similar to all other 14-3-3 isoforms [11] and figure 1.6. These data highlight the fact that although the basic pocket may bind phosphorylated ligands, other contacts along the binding groove play an important part in mediating interacitons.

Apparent from the 15 crystal structures of 14-3-3 obtained so far (RCSB database, http://www.rcsb.org/pdb/, August 2005) has been the lack of good quality data to ascertain the structure of the extreme C-terminus (structure to S233 is the furthest achieved yet (1QJB)). This is due to the disordered nature of this region and it has been proposed to function as a regulatory 'pseudo-substrate', binding within the 14-3-3 amphipathic groove itself, therefore blocking interaction with ligands [131]. The authors of one of the first crystal structures noted that it could be modelled to fit quite comfortably within the groove [131], however this has not been observed in any crystal structures. Studies involving a combination of time-resolved fluorescence, FRET and molecular modelling have shown two intriguing features of this region. First, that when 14-3-3 is unbound in solution, this loop does in fact bind in the binding groove [143] and secondly that on phosphorylation of S233, this region adopts an extended conformation, protruding further into the binding groove [144]. These data are in agreement with previous results, as discussed in 1.2.6.3 and [145, 146], that have shown phosphorylation of residue 233 modulates binding.

It is worth noting where the conserved residues reside in the context of tertiary structure. Figure 1.7 shows the structure of 14-3-3 ζ, using the identical colourings as the sequence alignment in figure 1.2, except with divergent residues in green. It is evident that the invariant residues are located in the binding groove of the protein and divergent residues on the outer surface, perhaps explaining how 14-3-3 isoforms can often bind the same protein and also functionally replace each other. For example, 14-

3-3 τ can replace 14-3-3 ζ as an essential cofactor for the ADP-ribosylation activity of exoenzyme S [147] and yeast strains devoid of 14-3-3 genes (BMH1 and BMH2) can be rescued with genes from Arabidopsis [148, 149]. Also, deletion of both BMH1/ BMH2 in yeast is lethal, whereas mutation of either isoform produces a viable phenotype [148], implying a degree of functional redundancy. Other examples of redundancy have been found in genetic analysis of mutants in Drosophila. One study showed 14-3-3 ε with a degree of redundancy, between ε and ζ in the formation of photoreceptors [150].

There also exists preferential expression of isoforms, for example 14-3-3 ζ (Leonardo in Drosophila) [151], indicating the requirement of that particular isoform.

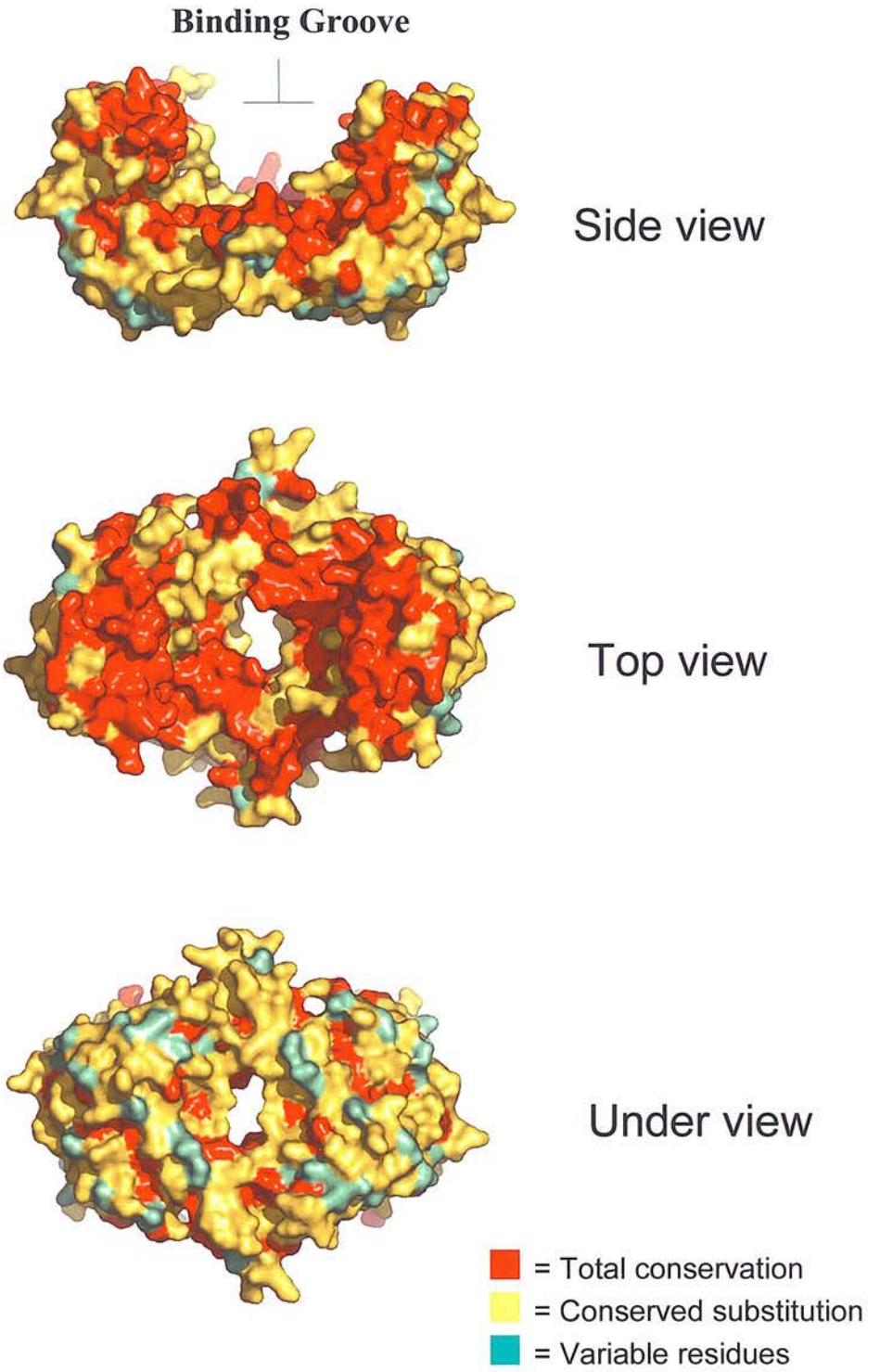

Figure 1.7 Sequence conservation on 14-3-3
Surface rendering of the 14-3-3 structure from 1QJB, created using PyMol, from www.pymol.org. Residues are coloured according to level of conservation as explained in the key. Generally, the most conserved residues are in the central binding groove, with most divergent residues on the opposite side.

1.2.6. Regulation of interactions

Generally 14-3-3 ligands need to be phosphorylated to allow interaction, allowing binding to be controlled by the action of appropriate kinases and phosphatases. Many kinases have a consensus similar to either of the Mode 1 or mode 2 14-3-3 binding motif, see table 1.2 below, for some examples of kinases that have been shown experimentally to phosphorylate within a motif and induce 14-3-3 binding. The similarity of the 14-3-3 binding consensus to the consensus for PKA, PKB and PKC (basic at n-3 or 4), suggest the co-evolution of these signalling systems [15].

Table 1.2 Known kinases that phosphorylate 14-3-3 motifs

Kinase	Consensus motif	14-3-3 ligand	Reference
PKA	RXS/T, RR/KXS/T	AANAT	[19, 123]
PKB (Akt)	RXRXXS	FKHR	[98]
PKC	RXS, RXXS, RXXSXR	Integrin CD18	[152]
PKD (PKCμ)	LXRX(M/L/K/E/Q/A)SXXXX	Par-1b	[114]
P21-activated PK (PAK)	KRXS, RRXS	Bad	[153]
MAPKAPK1	RXRXXpS/T	p27Kip1	[154]
MAPKAPK2	$PX_{1-2}S/TP$	Cdc25B/C	[50]
CamKII	Hyd-XR/KXXS/TXX	Phosducin	[70]
CK2	S/TaaAa*Aa**AaAa	KIF1C	[38]

References for kinases' motif consensus: PKA [155], PKB [156-158], PKC [159], PKD [160], PAK [161], MAPKAPK1 aka Ras-activated PK (RSK1) [156, 157], MAPKAPK2 [162], CamK II [162]. Underlined S/T indicates target residues to be phosphorylated. Aa are acidic residues, Aa* particularly strong if phosphoserine or phosphotyrosine [163].

However, often the kinases responsible are not known and given the increasing diversity of the 14-3-3 binding motif, many other kinases may well phosphorylate within and create 14-3-3 binding motifs. As alluded to earlier, phosphorylation of 14-3-3 directly also has an affect on ligand binding, discussed further below.

1.2.6.1. Phosphorylation of 14-3-3

It has long been postulated that phosphorylation of residues within the dimerisation domain (S59, S64, see figures 1.1, 1.4) would disrupt dimer formation and this in turn could affect the ability of 14-3-3 to bind target ligands [164]. The first report of a kinase capable of phosphorylating S58, on intact 14-3-3, was termed

Sphingosine dependent kinase (SDK1) as phosphorylation occurred only in the presence of sphingosine [164]. This kinase was later identified as a truncated form of PKCδ [165, 166]. The group of Woodcock then showed that phosphorylation of 14-3-3 by SDK1/truncated form of PKCδ on S58 negatively affects dimer formation [167], but did not affect 14-3-3 binding to phosphorylated ligands. This contrasts with findings from the laboratory of Guri Tzvion, who found dimer mutants of 14-3-3 could bind bona-fide ligands (Raf-1 and Fas-16) independently of phosphorylation status [168]. PKB/Akt has also been shown to phosphorylate S58 [169]. Curiously, in that study, the authors found that dimerisation was not affected.

Phosphorylation of S185 on 14-3-3 ζ increased the inhibition of PKC two fold [7], however the mechanism of this inhibition is not clear, presumably a slight structural change in 14-3-3 allows a different orientation of binding to PKC. The kinase responsible for phosphorylation of S185 was identified during the course of these studies, when the group of Gotoh discovered JNK can phosphorylate S185 on 14-3-3 ζ and σ (numbering used in paper is S184 for ζ, 186 for σ; but they are comparable residues, see figure 1.2) in response to cell stress (Actinomycin treatment) [170]. Phosphorylation of S185 leads to the dissociation of Bax, causing translocation to the mitochondrion, leading to apoptosis by cytochrome C release. Phosphorylation of S185 also negatively regulates the interaction with Foxo3a [171]. Phosphorylation of 14-3-3 on S185, also causes release of Bad, the combination of which antagonizes Akt mediated signalling [171].

Phosphorylation of 14-3-3 ζ on S233 by Casein kinase 1 negatively affects the interaction with Raf-1 [145, 172]. As mentioned above, the residue S233 lies in the flexible, unstructured region of 14-3-3, the phosphorylation of which causes a conformational change, negatively affecting binding to ligands.

A recent paper showed that 14-3-3 σ from cultured spontaneously immortalized granulosa cells (SIGCs) is phosphorylated on seven residues and the phosphorylation level was reduced after treatment with Progesterone [142]. The significance of this has yet to be determined, but two of these residues lie between alpha helices (αA-αB, αC;αD, see figure 1.6, red residues), similar to S185, and may well affect binding to ligands. The only other reported phosphorylation of 14-3-3 causing a negative affect on interaction is tyrosine phosphorylation on Y^{127} in the

maize isoform, GF14-6. Phosphorylation reduces the ability to associate with the peptide from plant H^+-ATPase [173].

1.2.7. Isoforms and Dimers.

1.2.7.1. Binding specificity and affinity

Discerning potentially different binding affinities between isoforms for a particular ligand is experimentally challenging. For example, due to the potential for 14-3-3 to form heterodimers, experiments have to been conducted using *in vitro* assays, as 14-3-3 can be produced as pure homodimers, thus allowing one isoform at a time to be examined. Work involving screening of oriented peptide libraries used to identify optimal motifs identified different isoforms had different affinities for certain peptides [15]. These data were confirmed for the η isoform with Biacore experiments involving passing 14-3-3 (termed the ligand in these studies) over an immobilised peptide [15]) and solution assays, where 14-3-3 was pre-bound to peptides, before passing over the Biacore sensor (with bound peptide). From this work, it is clear that there is a distinct preference for any particular isoform, over a given sequence. However, further complication arises from the fact that one 14-3-3 dimer could bind two peptides, as discussed in section 1.2.3.2 [15]. This may explain tight binding to proteins with two 14-3-3 binding sites, for example, Foxo [98, 174, 175], Raf-1 [14, 176] and AANAT [123]. There are also examples of particular isoforms interacting with ligands, with different affinities. For example yeast two hybrid studies on the Zinc finger protein A20 found that out of the several 14-3-3 isoforms that bound, 14-3-3 η bound the most, with ε less and β, ζ the least [177] and see table 1.3. The dual specificity phosphatase CDC25B has been reported to bind 14-3-3 β, ζ and η more strongly than ε and τ [178]. Further experiments suggest that CDC25 has one binding site available to all isoforms, but a high affinity site for ζ and η [178]. See table 1.3, below, for a summary of some isoform specific interactions with 14-3-3. This would go some way as to explain how 14-3-3s may regulate such diverse cellular functions if different isoforms had different functions, but many of these studies have identified the particular isoform through identification by a screen (e.g. yeast two-hybrid), or simply not tested other isoforms. However the structural studies on 14-3-3 σ, show

unambiguous evidence of how this isoform is able to have such specific binding properties [11] and so it is likely other isoforms will have similar regulatory binding mechanisms.

Table 1.3 14-3-3 binding proteins binding in an isoform-specific manner

Protein	Motif	Isoform order	In vivo/in vitro	Ref
A20	unknown	η, ε, β/ζ, not γ	*in vivo*	[177]
Adam 22	RSNpS^{857}TE,	ζ, β, ε, η, not σ and τ	*in vitro*	[57, 58]
AKAP-lbc	FRRHpS^{1565}WGPGK	β, ε, ζ	*in vitro*, β *in vivo*	[59]
Ataxin-1	RRWpS^{776}AP	ε and ζ, not others	*in vitro, in vivo*	[93]
CamKII	RKFpS^{74}LQ	η, γ, not ε or τ, ζ slight	*in vitro*, γ *in vivo*	[35]
Cbl	RHpS^{619}LPFpS^{623}	τ	*in vivo*	[17]
Cdc2/cyclin B		σ		[179]
CDC25B	RSPpS^{323}MP	η, β, ζ, τ, ε slight,	*in vitro*	[50, 178]
CDC25C	RSPpS^{216}MP	all, except σ	*in vivo*	[51, 52]
CLIC4	R^{219}YLpTNAYpS	ζ, ε	*in vitro*	[180]
CDK11^{P110}	RHRpS^{118}HS	β, γ, ε, τ, ζ slight, not σ	*in vitro, in vivo*	[81]
GR	unknown	η	*in vitro*	[181]
IGF-1	VPLDPSASSSpS^{1283}LP	ε	*in vitro*	[62]
NFAT3	RRYpS^{272}pSpS, RRGpS^{289}	τ, 5x more than ζ	*in vitro*	[104]
PMCA4	unknown	ε, not ζ or τ	*in vitro, in vivo*	[182]
P27^{Kip1} (p27)	RKRPApT^{157}D	β, ε, γ; τ, (ζ slight), not σ	*in vitro*	[105]
Par3α	KKSSpS^{814}L	τ, ε, ζ, (β slight)	*in vitro, in vivo*	[116]
PKCζ	RHDMpS^{186}YMP	τ, γ, ζ, ε, β, η	*in vitro, in vivo*	[43]
Raf-1	RSTpS^{259}TP, RSApS^{621}EP	β, ζ	*in vitro*	[183, 184]
B-Raf	RSApS^{728}EP	ζ, η, τ	*in vitro*	[45, 185]

Interactions indicated as *in vitro* include pull down assays, baculovirus system, or yeast two hybrid systems. *In vivo* interactions were demonstrated by co-transfection or single transfection of the 14-3-3 ligand protein and use of isoform specific antibodies. When only one isoform is indicated, that isoform was generally selected from a screen (e.g. yeast two hybrid) or proteomic study (identification by ms). Other isoforms are listed as strongest interaction first. Not all 14-3-3 isoforms are necessarily tested for interaction. Abbreviations: A20, zinc finger protein; CamKII, Calcium and calmodulin-dependent dependent kinase kinase; CDK11, cyclin dependent kinase 11; CLIC4, Chloride intracellular channel protein; GR, glucocorticoid receptor; IGF-1, Insulin growth factor 1 receptor; NFAT3, Nuclear factor of activated T-cells 3; PMCA4, plasma membrane calcium pump; PKC, protein kinase C.

1.2.7.2. Heterodimerisation

The picture is further complicated by the ability of 14-3-3 to preferentially form heterodimers *in vivo* [186]. 14-3-3s produced in bacterial systems will form homodimers, even if there is a preference for a heterodimer, simply because it is energetically more favourable to form a dimer than monomer. Analysis of 14-3-3 in cells shows that many heterodimers exist. Studies in our laboratory using stably transfected PC12 cell lines, found that the gamma isoform formed homo and hetero-

dimers, whereas epsilon formed solely heterodimers, with no homodimers detected [186]. A summary of the findings is shown in table 1.4, below.

Table 1.4 Summary of heterodimerisation of 14-3-3s

Possible combinations from studies involving 14-3-3γ and ε

Monomer 1	β	γ	η	ζ	τ	σ	ε
Monomer 2	ε	γ	ε	ε	ε	ε	β
		ε			ζ		γ
		ζ					ζ
		η					η

Data from [186].

Reading across the table (left to right), 14-3-3 isoforms are listed, with isoform of the possible conjoining monomer listed vertically. As γ and ε could form dimers with other isoforms, the reciprocal is listed in this table. Absolute preference of heterodimer is difficult and not attempted due to different titres of antibodies and large number of 14-3-3 isoforms present in the cells [186]. BMH1 and BMH2, The two 14-3-3 isoforms from *Saccharomyces cerevisiae* were also examined and were found as predominantly heterodimers. Another curious finding was the increase of 14-3-3 γ:η heterodimerisation occurring 48 hours after NGF treatment, an affect not seen for ε:γ heterodimers.

Previous work by the group of Muslin showed stable transfection of a binding mutant of 14-3-3 η formed a heterodimer with native ζ in NIH3T3 cells [137]. The overall effect of transfected binding mutants into cells in culture was to sensitise them to radiation, in contrast to the protective role of normal, wild type 14-3-3.

The ability of 14-3-3 to bind in an isoform-specific manner, and the ability to form heterodimers, suggests two roles: Heterodimers may offer a role of adaptor protein, bringing two different molecules together, whereas the homodimer may be more of a chaperone role that can sequester bound protein to a particular location, for example the cytoplasm. Examples of 14-3-3 exhibiting an 'adaptor function' however has been seen only rarely: BCR kinase with Raf-1 kinase [187], Raf-1 and A20 [177] and Raf-1 and PKCζ [43].

Heterodimers have also been observed in plants, where GFP fusions formed heterodimers with endogenous 14-3-3 in Arabidopsis cells [188]. Isoform specific localisation was also observed for many isoforms.

1.2.7.3. 14-3-3 location and distribution

Spatial and temporal regulation may offer an explanation as to how such a ubiquitous protein is able to have such specific effects on so many different molecules. For example, tissue specific expression or increased expression/repression of 14-3-3 at specific times, during the cell cycle or development, could modulate the activity of a number of proteins, helping shape the required outcome.

14-3-3 is largely found in the cytoplasm, but is also found associated with the plasma membrane [183], the Golgi apparatus and in the nucleus [189]. There are several examples of 14-3-3 sequestering target proteins to the cytoplasm. For example, studies on the transcription factor for cell senescence, Daf-16 in C. elegans and FOXO (FKHR) in mammalian cells, found that after phosphorylation by PKB/Akt, 14-3-3 sequesters the transcription factor in the cytoplasm, inhibiting transcription [98, 190]. A similar role is performed by 14-3-3 for the cell cycle regulator Cdc25 [191] and the cyclin dependent kinase (CDK) inhibitor p27(Kip1) [105, 154]. The tyrosine kinase c-Abl is phosphorylated by an unknown kinase, causing 14-3-3 sequestration of c-Abl to the cytoplasm [77]. DNA damage then causes JNK phosphorylation of 14-3-3, releasing c-Abl to the nucleus, inducing apoptosis [77]. 14-3-3 not only induces nuclear exclusion, although rare, there is one example is nuclear targeting of telomerase, by masking the nuclear export sequence (NES) for CRM1 (also known as exportin) [192]. Another regulatory role recently discovered for 14-3-3 is involvement in the quality control of various receptors, including potassium channels and acetylcholine receptors. In the case of the potassium channel, HCNK3, dibasic motifs located on the receptors are bound by COPI (coatamer I)-coated vesicles, forming a retrograde transport system for the HCNK3 channel back to the ER [64]. Although separated by some distance in linear amino acid sequence, 14-3-3 binds with mutual exclusivity [to the HCNK3 channel],

displacing the COPI vesicle, allowing the HCNK3 channel to escape the ER and locate to the cell membrane [64].

14-3-3 γ has been found as the major isoform at the Golgi apparatus [189]. 14-3-3 ζ is also present at the Golgi and is shown to be a substrate for the Ste20 kinase YSK1 [193], the consequence of which is not known.

Due to the high level of 14-3-3 found in the brain [2], the expression of individual isoforms has been the subject of many studies in particular in response to neurological disorders. For example analysis of 14-3-3 isoform expression within the prefrontal cortex has revealed differing levels at the DNA transcript level – 14-3-3 β and 14-3-3 γ are expressed at higher levels than η and ζ [194]. Examination of the same tissue from patients with Schizophrenia found that14-3-3 η was the only isoform that was significantly down regulated ([194] and references therein). The exact reason for this downregulation is unknown, but the authors do point out that the 14-3-3 η gene is found within an area of chromosome 22 (22q12–q13) that is known to be mutated in the 5' UTR region in schizophrenics [194]. Specific 14-3-3 isoforms are also found in the cerebral spinal fluid (CSF) of patients with CJD (Creutzfeldt-Jakob disease) and is used a clinical marker for the presence of this disease [195]. The location of 14-3-3 isoforms within a murine (murine scrapie) model of CJD changes after infection with scrapie [196, 197]. Combined, these results suggest that 14-3-3 may play a role in the pathogenesis of CJD. However a mouse knockout of 14-3-3 γ (found in greatest abundance in CJD CSF [196]) had no difference in response to inoculation with infectious prion protein [198]. However, 14-3-3 isoform redundancy may have played a role.

Many investigations involving 14-3-3 isoform specific localisation or increased/decreased expression have been centred on 14-3-3 σ (also known as stratafin). 14-3-3 σ has been shown to be up regulated in a number of cell lines and tumours and a number other investigations (discussed above) have suggested 14-3-3 as having an anti-apoptotic role. Despite these antiapoptotic roles, 14-3-3 σ in various cancers is commonly downregulated or silenced by promoter methylation [199, 200]. However this seemingly paradoxical situation remains controversial, as a recent proteomic study by the group of Julio Celis, found that 14-3-3 σ promoter methylation is a sporadic event in primary breast cancers [201]. The proteomic results

were corroborated using specific 14-3-3 σ antibodies for immunohistochemical analysis. There was also no increase in DeltaNp63, a dominant-negative transcriptional regulator of 14-3-3 σ and also no increase in the E3 ubiquitin ligase that targets 14-3-3 σ for destruction [201].

1.3. Breakpoint Cluster Region Kinase (BCR)

The term breakpoint cluster region (bcr) refers to an area of 5.8kb on chromosome 22 that by a reciprocal translocation event with the c-abl gene, from chromosome 9 produces the chimera bcr-abl (figure 1.8). It is this reciprocal translocation event that creates an aberrant chromosome called the Philadelphia chromosome (ph^1) that is the hallmark of chronic myelogenous leukaemia (CML) – found in over 90% of patients with CML [202]. CML is characterised by an abnormal build up of haematopoietic cells in the bone marrow and elevated peripheral white blood cell counts [203]. BCR-ABL proteins can vary in size, depending on the breakpoint within Bcr. The resultant fusion protein, containing different amounts of the bcr gene fused to abl gives rise to different clinical outcomes with ranging severity [204, 205]. For example, the protein fusion of 190KDa ($p190^{BCR/ABL}$) is a more potent transformer of fibroblast cells, compared to the longer, 210KDa ($p210^{BCR/ABL}$) fusion [205, 206]. As well as varying breakpoints, alternative splicing of exons within both Bcr and c-Abl transcripts further increases the variety of BCR-ABL transcripts [207], the exact significance of this is yet to be elucidated. The normal product of c-Abl is intimately involved with regulation of cell death [208] and is usually tightly regulated by an N-terminal inhibitory region. When fused to Bcr, this inhibitory region is lost and the kinase is constitutively active [208]. This, combined with BCR-ABL being predominantly cytoplasmic [209] allows the BCR-ABL fusion to extensively phosphorylate cellular proteins, transforming cells and making them growth factor independent [210]. As an onco-protein BCR-ABL activates several signalling pathways, to achieve transformation of cells, highlighted in table 1.5.

Table 1.5 Pathways activated/affected by BCR-ABL.

Protein	Effect	References
Myc	activates myc through E2F1	[211, 212]
Ras	activates Ras	[213-215]
c-Raf	phosphorylation and activation of Raf	[216, 217]
MAPK/ERK	activates	[213]
SAPK/JNK	5 fold increased c-jun transcription, corresponding JNK activation	[213, 218]
STAT	constitutively activates STAT5, phosphorylates STAT on tyrosine	[219, 220]
NF-κB	activates,	[221]
PI3K	PI3K shown to be essential for transformation	[222, 223]
$p27^{Kip1}$	inhibits expression of $p27^{Kip1}$, signalling through PI3K	[224]
p53	reduces p53 levels	[225]

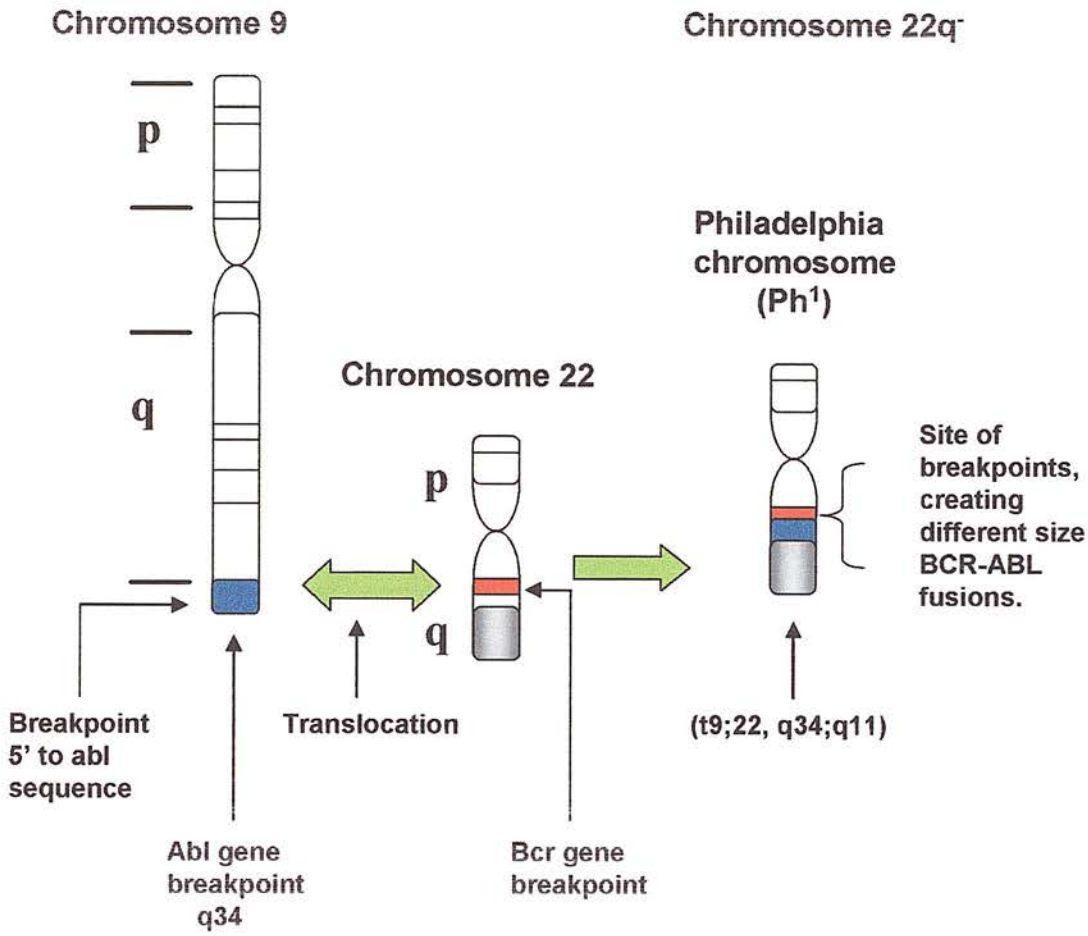

Figure 1.8 Chromosomal translocation of BCR.
The shortened chromosome, known as Philadelphia chromosome (Ph^1) is a hallmark of chronic myelogenous leukaemia (CML). Exchange of genetic material from chromosome 9 (where bcr resides) and chromosome 22 (where abl is found) forms bcr-abl transcripts of variable length. Most studies to date involving bcr have focussed on this chimeric gene and the abl gene alone, but rarely on bcr itself.

The formation of the BCR-ABL fusion protein is thought to occur during late S-phase, where the close proximity of each gene to the other has been highlighted by fluorescence in situ hybridisation (FISH) analysis [226]. The short distance is thought to afford the opportunity for reciprocal recombination [227].

The constitutively active tyrosine kinase activity of BCR-ABL, essential for the progression of CML [228], has been the focus of many studies to find an effective inhibitor, of which a compound known as Gleevec, Imatinib or STI571 (Novartis) has proved to be highly successful [229]. Structural studies have shown Gleevec to bind in the kinase domain of Abl and displace ATP, keeping the kinase in an inactive conformation [230, 231]. However, due to the highly selective nature of this kinase inhibitor, point mutations arise quickly following administration. For example one patient was found to have 19 point mutations in the BCR-ABL kinase domain [232, 233]. Another approach to reduce the effect of overexpressed BCR-ABL, has been the development of siRNAs. They have been shown to decrease transcripts of BCR-ABL, but not BCR in primary cells from patients with CML [234], however the transition of siRNA based technology into a therapeutic agent can be an arduous task [235]. It is due to this clinical relevance that most research has focused on the chimeric BCR-ABL, with few studies on the normal cellular function of BCR. Whilst originally BCR-ABL fusion was thought to be found only in cases of CML, recent highly sensitive PCR techniques have found the presence of BCR-ABL transcripts in healthy individuals [236, 237]. Current opinion is that, in healthy individuals, the immune system is able to monitor cells producing these transcripts and stop proliferation.

1.3.1. BCR Domain organisation

Although Bcr has homology to many proteins involved in cellular signalling, and has been shown to associate with well characterised proteins in cell signalling, it has no known physiological function [207]. Overexpression of Bcr itself inhibits cell proliferation [187] and it has been speculated that it can act as a negative regulator of BCR/ABL protein [238].

The normal Bcr gene gives rise to two major proteins that are 130kDa and a 160kDa in size [239-241] (most studies have centred on the 160kDa protein) and contain a number of domains, see figure 1.9. These include an oligomerisation domain [242], an atypical S/T kinase domain [147, 187, 243], SH2-binding domain [214], guanine nucleotide exchange factor (GEF) domain [244, 245]. and a GTPase activity (GAP) domain [246]. Residues 1-294 of the kinase domain were originally identified (by a series of GST-truncation mutants of BCR) as incorporating the 14-3-3 binding domain [147]. However, with longer exposure, binding can be seen with the other mutants corresponding to regions towards the C-terminus – indicating more then one binding site. There is also PH and C2 domains, identified by homology, that may help targeting of BCR to the membrane. The fact that BCR has demonstrable GEF and GAP activities suggests a dual role in G-protein signalling events.

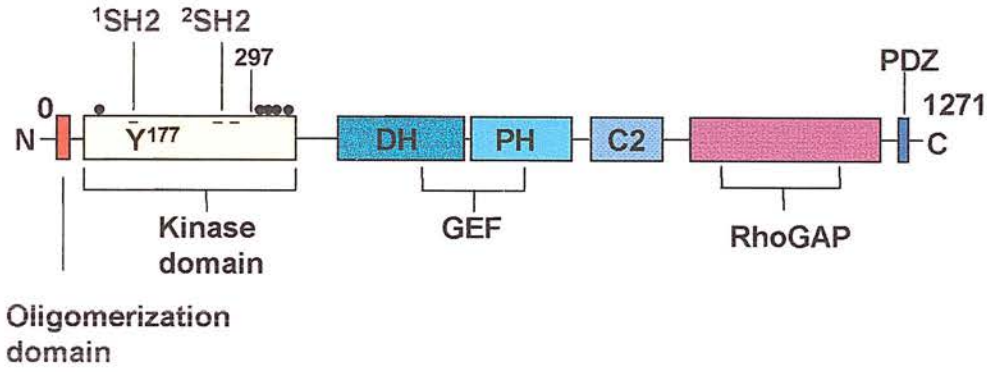

Figure 1.9 Schematic of BCR kinase
[1]SH2 domain that through phosphorylated tyrosine binds Grb-2[247].
[2]SH2 domains essential for oncogenic activation of BCR-ABL, it is unusual in that phosphorylated serine and tyrosine residues are used within this SH2 motif, as opposed to phosphorylated tyrosine. The structure of the oligomerisation domain has been solved [248], defining how the observed tetramer of BCR [243] occurs. Possible 14-3-3 binding motifs are indicated with filled circles, as identified in [249]. '297' indicates amino acids 0-297 identified in [147] that were shown to bind most 14-3-3. The domain marked PH has homology to Cdc24, Dbl, Vav (all GEFs) [244, 245], this domain also binds to XPB protein [250, 251]. PH (pleckstrin homology) and C2 (Ca^{2+}-dependent phospholipid binding) domains may regulate BCR association with the membrane. RhoGAP has demonstrated GTPase activity toward p21rac [246]. A PDZ domain mediates interact with AF6 [252], PDZK1 and Mint3 [253].

The oligomerisation domain of BCR consists of a heptad repeat of hydrophobic residues that allow BCR to purify as a >600kDa oligomer [243] and also form heterotetramers with BCR/ABL in K562 cells [254]. Structural studies into the BCR oligomerisation domain (using amino acids 1-72) have revealed that two N-shaped monomers form a dimer, through formation of an antiparallel coiled coil between alpha helices and domain swapping [255], followed by stacking of the two dimers to form a tetramer [248]. BCR-ABL also self oligomerizes through this domain in vivo in 293 cells [256]. Mutations within this region not only disrupt the oligomerisation [256], but also reduce the tyrosine kinase activity of BCR-ABL [242], reduce the ability to associate with the cytoskeleton [242], reduce its fibroblast transformation potential and increase its sensitivity to STI571 [257]. It has been suggested that the sole function of the BCR oligomerization domain is to reduce autoinhibition of BCR-ABL (by disrupting the SH3 domain of ABL binding) by causing intermolecular autophosphorylation [256].

The kinase domain of BCR has short segments homologous to other protein kinases, such as the GxxxxGK motif and GxGxxG with downstream lysine [243, 258]. However, when originally characterised as having kinase activity [240] BCR had so little in common with other kinases that the possibility remained that a co-associating kinase activity was responsible for the activity observed. This was ruled out four years later, with work including an in-gel kinase assay [243], but the possibility that a kinase could associate with BCR *in vivo* remains a possibility. The group of Witte et al also showed that mutating the cysteine residue Cys^{322} to Lys reduced both the auto and trans-phosphorylation activity of BCR and proposed that it was similar to pyruvate kinase in having essential cysteine residues in the nucleotide binding domain [243]. The possibility remains that removing essential cysteine residues could interfere with binding partners of BCR and therefore the subsequent phosphorylation.

One of the three Src homology 2 (SH2) binding domains of BCR (when phosphorylated on T^{177}) allows it to bind to GRB-2, linking it to the Ras pathway [214]. The SH_2 domains are discussed further below.

The central region of BCR is complex with homology to the three different Guanine exchange factors (GEFs). BCR has homology to the haematopoietically expressed VAV proto-oncogene and the mouse homologue of CDC25 Ras activator [244, 259], but has no demonstrated activity similar to these proteins. There is also homology to the oncogene Dbl, a protein capable of catalysing the guanine nucleotide exchange on Rho and CDC42 from GDP to GTP (a GEF) [245, 260, 261]. This Dbl-homologous region of BCR has been shown *in vitro* to stimulate GTP binding to CDC42, RhoA, Rac1 and Rac2 [262]. This RhoGEF domain has also been shown to activate NF-κB through stimulation of endogenous p38MAPK in COS-7 cells [263]. The authors also identified autoinhibitory flanking regions either side of the DH/PH domain that reduced NF-κB activation *in vitro* and *in vivo* [263].

Interestingly *full length* BCR had GAP activity for CDC42, Rac1 and Rac2, suggesting that BCR could act simultaneously with Rho proteins to coordinate cellular signalling [262]. Indeed the C-terminal of BCR has GAP activity for $p21^{rac}$, see below. This region is also the site of the interaction with Xeroderma pigmentosum group B protein (XPB), which reduces the ATPase and helicase activity of XPB [250].

BCR interacts with the proto-oncogene c-myc through residues 871-910, between the DBL domain and the C2 domain [264]. Next to the DB/PH domain of BCR, is the C2 domain (911-1036) that has no known function, but C2 domains found in many other proteins bind phospholipids in a calcium dependent manner [265].

1.3.2. Regulation

BCR can associate with the proto-oncogene Fes, forming a stable complex in co-transfected Sf-9 cells [266]. BCR is also phosphorylated by Fes tyrosine kinase on Y^{177}, Y^{246} and at least one of a cluster of tyrosine residues: Y^{276}, Y^{279}, Y^{283} [267]. A complete list of known phosphorylation sites on BCR is highlighted in table 1.6. Phosphorylation of Y^{177} by the Fes kinase inactivates the trans-phosphorylation activity of BCR toward 14-3-3 [267]. When Y^{177} is mutated to phenylalanine this abolishes GRB-2 binding and abrogates BCR-ABL induced Ras activation [214, 268].

BCR is also a substrate for BCR-ABL, being phosphorylated on Y^{177}, Y^{283} and Y^{360} *in vitro* [269]. These studies found that Y^{177}F and Y^{283}F mutations had wild type kinase activities, whereas Y^{360}F had markedly reduced kinase activity, indicating Y360 as an essential regulatory site. The authors also found that BCR purified from cells expressing BCR-ABL, in conditions to preserve tyrosine phosphorylation had reduced kinase activity [269]. *In vitro* tyrosine phosphorylation within residues 162-413 of BCR by Fes kinase, however, has been shown to decrease the association with 14-3-3, in contrast to increased binding to Grb-2, PLCγ, 85kDa PI3K subunit and Abl [270]. This is an interesting observation, as 14-3-3 binding to BCR has been shown to be a phospho-dependent interaction *in vitro* [44]. In that study potato acid phosphatase was used to dephosphorylate BCR, which reduced 14-3-3 binding [267]. Whether or not 14-3-3 has to bind BCR with high affinity in order to become a substrate remains to be investigated.

Recently five additional phosphorylation sites (T^{310}, S^{459}, S^{463}, $Y^{591}$and Y^{644}) have been found on BCR, in a study designed to follow changes in tyrosine phosphorylation of BCR-ABL on treatment with the inhibitor Gleevec (STI-571) [271]. Of these residues, T^{310} was identified as a potential 14-3-3- binding site and within a PKA consensus using the protein motif scanning facility (at http://www.scansite.mit.edu) [271, 272]. The phosphorylation level of all these residues decreased on exposure to the inhibitor [271], with tyrosine phosphorylation on BCR being effected more rapidly than serine/threonine phosphorylation. This is due, most likely, to the inhibition of the Abl portion of the BCR-ABl kinase.

Table 1.6 Phosphorylation sites *on* BCR.

Kinase	sequence/residue	*in vitro/vivo*	Ref.
Fes	AEKPF<u>Y</u>[177]VNVEF	*in vitro* and *in vivo*	[247, 271]
	GVDGD<u>Y</u>[246]EDAEL	*in vivo*	[267]
	E<u>Y</u>[276]QP<u>Y</u>[279]QSI<u>Y</u>[283]VG	only one is phosphorylated *in vivo*	
BCR-ABL, Abl	QSI<u>Y</u>[283]VGGM	*in vivo*	[269]
	PSPTT<u>Y</u>[360]RMFRD	*in vivo*	[269]
Unknown	QEKRL<u>T</u>[310]WPRRS	*in vivo* (K562 cells)	[271]
	DCGGG<u>Y</u>[328]TPDCS	*in vivo*	[273]
	LPYIDD<u>S</u>[459]PSS<u>S</u>[463]PHLSS	*in vivo* (K562 cells)	[271]
	SQLGV<u>Y</u>[591]RAFYD	*in vivo* (K562 cells)	[271]
	LETLL<u>Y</u>[644]KPVDR	*in vivo* (K562 cells)	[271]
	DSKRQ<u>S</u>[1264]ILFSTEV	*in vivo* (Jurkat T-cells)	[274]

BCR has a region in the extreme C-terminus typical of PDZ binding ligands (S-T-E-V, figure 1.2) that can bind to the PDZ domain (PSD-95/discs large/ZO-1) of AF-6 (a ras-interacting PDZ-domain containing protein of cell junctions) at the plasma membrane in epithelial cells [252]. Furthermore, a complex of these proteins: BCR, AF-6 and Ras at the cellular junction down-regulates Ras-mediated signalling and cell proliferation [252]. AF-6 is also a substrate for BCR, becoming phosphorylated on T893, which increases the interaction [252].

Recently, BCR has been shown to specifically interact with Mint3 (Munc18-Interacting Protein) [253], a predominantly Golgi-localised protein that is involved in protein processing and vesicular trafficking in the distal secretory pathway. Rho GTPases are involved in vesicular trafficking [275] and they could be affected by the GAP and GEF activities of BCR through association with Mint3, therefore exerting an effect on the secretory pathway. BCR phosphorylates the same site on 14-3-3 as CK1, and now we find that BCR, too, is involved in the secretory pathway (see discussion).

BCR also associates with ERBIN (ERB2 Interacting protein) through its PDZ domain [276]. Interestingly, ERBIN is also known to bind to δ-catenin *in vivo* [277], a protein that we have recently shown to bind 14-3-3 [278].

BCR has been reported to associate through 14-3-3 with all isoforms of Raf kinase (See table 1.1 and 1.3). Significantly in this study, ~10 times more Raf was found in the membrane fraction, than in the cytosol [187], suggesting recruitment of Raf. However there have been many conflicting reports on the regulation of Raf and

the role of 14-3-3 recruitment to the cell membrane (see [279, 280] for review). One recent model is that 14-3-3 binds to the proposed high affinity site, S641, aiding dimerisation and activation of Raf, 14-3-3 can then bind to the low affinity site, S259, that functions to 'lock' C-Raf in the cytosol, attenuating Raf activation [281].

1.3.3. Substrates

BCR kinase can phosphorylate histone and casein *in vitro* [243], but the only known *in vivo* substrates are 14-3-3 [147] and AF-6 [252]. Reuther et al [147] showed that phosphorylation of 14-3-3 τ by BCR (*in vitro*) occurred exlusively on serine residues and produced four spots on thin layer chromatography, suggesting four phosphorylation sites. This point is discussed in chapter 3.

AF-6 is phosphorylated on T893 by BCR, as determined by site directed mutagenesis, that induces binding to AF-6, causing downregulation of Ras –mediated signalling, as mentioned above [252].

1.3.4. Localisation

BCR is ubiquitously expressed, with highest levels in brain and haematopoietic cells [207]. Early studies found BCR to be cytoplasmic in uncycled mouse haematopoietic cells [209, 239]. Studies using the cell-cycle blocker aphidicolin, have identified BCR as largely cytoplasmic during interphase, associating with chromosomes during mitosis [282]. The association was also found with DNA and heterochromatin in quiescent cells, identified using immuno-gold and electron-microscopy [282].

1.4. Casein Kinase 1 (CK1)

The protein kinase 'Casein kinase I' (now termed CK1) is named after the initial discovery that preparations of a kinase from calf muscle could phosphorylate purified casein *in vitro* [283]. It is worth noting that both CK1 and the similarly named, but structurally quite different, CKII (now CK2) protein kinase are not responsible for the physiological phosphorylation of casein in milk (this is achieved by membrane bound casein kinases in the Golgi apparatus) [284]. Among one of the first serine/threonine protein kinases to be characterised, CK1 has since been shown to consist of several isoforms with molecular weight ranging from Mr 23,000 to 60,000. The primary structure consists of a large, conserved kinase domain and variable N and C terminal domains (see figure 1.10, 1.11). CK1 is also a dual specificity kinase, being shown to both autophosphorylate and transphosphorylate tyrosine residues both *in vitro* and *in vivo* [285-287], although it is predominantly a S/T kinase. In higher eukaryotic organisms, the CKI family consists of seven isoforms in mammals, denoted: α, β, $\gamma_{1, 2, 3}$, δ and ε (figure 1.11), four in *Saccharomyces cerevisiae*, denoted: HRR25, YCK1, 2,3 and five in *Schizosaccharomyces pombe* denoted Cki1, 2, 3, Hhp1 and Hhp2 [288]. Alternative splicing can increase the number of isoforms, resulting in different biochemical properties. For example in CK1α there exists potentially four splicing variants [289-291]. A study by Zhang et al into one of these variants found that a 28 amino acid insertion into the catalytic domain (denoted CK1αL) had distinct effects on the kinase activity when compared to CK1α [291]. CK1αL has increased catalytic turnover, compared to CK1α toward some substrates, but not others. In addition, they also found that CK1αL exists at 15% of the level of CK1α in almost all mammalian tissues tested. The insert appears just before the 'hinge' region of CK1, where substrate is recognised and could therefore accommodate larger or different shaped proteins [291] and see figure 1.10 for CK1 crystal structure indicating classical bilobal protein kinase structure. Shorter splice variants of CK1α in goldfish are localised to the nucleus of oocytes and all four isoforms of CK1α are expressed in a tissue dependent manner [292].

1.4.1. Substrate specificity

The wide tissue distribution, large number of isoforms and broad substrate consensus has produced a formidable list of substrates and binding partners that implicate CK1 in a range of diverse cellular processes. To date, at least 60 substrates for CK1 have been identified (table 1.7). However, some proteins identified as *in vitro* substrates have not been shown to be phosphorylated *in vivo*, for example glycogen synthase [293]. The first *in vitro* substrates to have the phosphorylation sites identified after phosphorylation by CK1, were on SV40 large T antigen [294] and glycogen synthase [295], reviewed in [284]. Subsequently, Peter Roach and colleagues discovered that prior phosphorylation of rabbit muscle glycogen synthase by PKA, *in vitro*, allowed CK1 to incorporate much more phosphate [into glycogen synthase] [296]. Refinement of these studies using peptides with varying distance between the phosphorylatable Ser/Thr residues and the pre phosphoprylated residue, determined an optimal distance of two residues N-terminal to the Ser/Thr to be phosphorylated by CK1 to give the form $pS/pTX_{1-2}S/T$, where X is any amino acid [297]. These phosphorylatable ser/thr residues then became known as 'priming' sites. Additionally, blocks of three or four Asp or Glu residues ending at the -3 position can increase a substrates propensity to be phosphorylated by CKI, giving the consensus $D/E_{3-4}XXS/T$, but are still not as good as a phosphorylated serine/threonine at n-3 [298, 299]. Knowledge of these substrate determinants has enabled rapid identification of many CK1 substrates, using computer-based searches of known phosphorylated proteins. In most studies, known canonical motifs recognised by CK1 isoforms have been show to phosphorylate Ser/Thr residues *in vitro* and *in vivo*, however, a growing number of alternative, 'atypical', motifs are being discovered, for example: β-catenin [300] and see table 1.7 for a summary of all published CK1 phosphorylation sites. β-catenin has four acidic residues the 'wrong side', at n+7 downstream from phosphorylatable serine in an SLS motif ([300] and see table 1.7), but peptides used in that study mimicking the β-catenin site are 15-25 fold less efficient that the classical peptides following the $pS/pTX_{1-2}S/T$ consensus motif [300]. With this, it is becoming clear that a general consensus motif for CK1 substrate recognition may not be possible, making substrate speculation less predictable. The

use of tandem mass spectrometry can identify exactly which S/T is phosphorylated on the peptide and therefore help to discover if a priming phosphorylation is required.

The first published report of tyrosine phosphorylation by CK1 was a preparation from erythrocytes that could phosphorylate synthetic polyglutamine/tyrosine peptides [285]. Subsequent studies showed the yeast CK1 isoforms: HRR25p, Hhp1 and Hhp2 and Xenopus CK1α capable of both trans- and auto-tyrosine phosphorylation, although again trans-phosphorylation was only on synthetic peptide substrates and had lower efficiency [286, 287].

Table 1.7 CKI substrates and interacting proteins

Protein	Site(s) of phosphorylation[†]	CK1 isoform[‡]	Reference
cytoplasmic[1]			
Adenomatous polyposis coli protein (APC)	FSRCS***S***^{1276}LS$\underline{S}$^{1279}LSSAED FSRCT***S***^{1389}VS$\underline{S}$^{1392}LDS	CK1δ, ε, C-term Δ* HEK293#	[301, 302]
Aminoacyl-tRNA synthetases	Ser/Thr residues identified	rabbit reticulocytes*	[303]
Acetyl CoA carboxylase	serine phosphorylated Stoichiometry suggests two sites	rat liver	[304]
β-Catenin (Armadillo in *Dm*)	AP$\underline{S}$^{45}LSGKGNPEEEDVD – atypical, priming for GSK phosphorylation of T41, S37, S33	rat liver, CK1α,αL,ε,	[300] [305-309]
DARPP-32	DEEED$\underline{S}$^{137}QAEVL – classical¶ GRATQ$\underline{S}$^{189}EPGEE – atypical*	Calf thymus* rat striata#	[310]
Dishevelled	unidentified in this study	xCK1, 97% similar to CK1ε*	[306]
Elongation factor eIF-4E	ser/thr phosphorylated	rabbit reticulocyte*	[307]
FREQUENCY (FRQ)	PEST1 domain (544-560) by CK-1a only PEST2 domain (843-893) by CK-1a and b* QAVSEK$\underline{S}$^{513}TKFQLS is not phosphorylated in vitro, but is in vivo, along with S^{510} and S^{519}. Possibly hierarchal.	CK-1a, b (*N. crassa*) CK1ε-like	[308, 309]
Galectin-3 (formerly S-type lectin, L-29)	AADSF$\underline{S}$^{6}LNDAL$\underline{S}$^{12}GSGN – S^6 classical, S^{12} minor site	polarised MDCK cells	[311]
Glycogen synthase	TL**S**^{7}VS$\underline{S}$^{10}LPGLE, hierarchal However NOT found *in vivo*	rabbit liver* rabbit#	[296, 312] [293]

Protein	Site(s) of phosphorylation[†]	CK1 isoform[‡]	Reference
cytoplasmic[1]			
Guanine-nucleotide-exchange factor (GEF)	serine phosphorylated*	rabbit reticulocyte	[313]
Inhibitor-2 (regulatory subunit for PP1)	DDDAYS^{86}DTETT* DEEMS^{174}ETADGE*	rat liver, or porcine spleen	[314, 315]
Initiation factor 2B, eIF2B, (ε-catalytic subunit)	DEDDGQFS^{461}DDS^{464}GA S^{464} likely major site *in vivo*	293 cells[#]	[316]
Initiation factors 3, 4B, 5	unidentified in this study	human erythrocytes***	[317]
Insulin receptor 1 (β-subunit)	exclusively serine phosphorylated	HeLa membrane*	[318, 319]
Tumour necrosis factor α (TNFα) p75	exclusively serine phosphorylated	pig spleen*	[320]
mRNP particles	unidentified in this study	rabbit retic.*	[321]
Non-structural protein (NSP5)	RRREDIGPSDSAS^{67}NDPL	CK1α* MA104 cells[#]	[322]
p40 tyrosine kinase	Ser/Thr phosphorylated	rat liver*	[323]
PARKIN	CEREPQS^{101}LTRVDLSSSVL[!!] YHEGECS^{378}AVFEASGTTT	rat CK1δ* HEK293[#]	[324]
Period (mPer1)	CAS^{653}SSSYTASSAS^{663}DDDK AES^{714}VVSVTSQCSFSS^{726}TI T^{902}SVSPATFPSPLVT^{915}P	CK1ε*	[325, 326]
Protein kinase C (PKC)	unidentified residues, but identical peptide pattern as autophosphorylated PKC	rat liver*	[327]
PtdIns(4)P 5-kinase (PIP_2-kinsae)	unidentified in this study inhibits its activity[¶]	CKi *(S. pombe)** ***S. pombe***[#]	[328]
Prolactin	DES^{161}Q – potentially, not definitive	rabbit retic.*	[329]
Smad 1, 2, 3, 5 (TGFβ-activated)	Identify linker region and MH1 domain	CK1ε, with C-terminal Δ*	[330]
Spermidine/ spermine acetyltransferase (SSAT)	identify predominantly Ser phosphorylated	h Erythrocyte*	[331]
Synaptic vesicle-specific Protein (SV2)	unidentified in this study	rat brain*	[332]
Uracil permease (Fur4p)	KEYKSS^{43}QS^{45}NITTEVYEASS^{56}FEEK, SA mutants show S42, 43, 45, 55, 56 are Phosphorylated*, within a PEST region.	YCK1/2[#]	[333, 334]
14-3-3	DNLTLWTSDT^{233}QGDEA - atypical	CK1α, yeast* HEK293[#]	[172]

Cytoskeletal, membrane and sarcoplasmic reticulum - associated proteins, including receptors

Actin	prefers Thr to Ser, also co-purifies	rat liver*	[335, 336]
Ankyrin	identify Ser/Thr phosphorylated	erythrocyte prep.	[337]
α-synuclein	EAYEMP<u>S</u>[129]EEGYQDY	CK1δ, with	
	TVEGAG<u>S</u>[87]IAAATG	C-terminal Δ*	
	major site S129, minor site on S87	HEK293, PC12[#]	[338]
α-and β-tubulin	unidentified in this study	CK1δ, C-term Δ*	[339]
Beta-site APP cleaving	DDL<u>S</u>[498]LLK	COS-7[#]	
enzyme (BACE)			[340, 341]
Calsequestrin (CS)	Ser/Thr phosphorylated	rat liver*	[342]
Connexin 43 (Cx43)	YNKQA<u>S</u>[306]EQNW	CK1δ, C-term. Δ*	
	ANY<u>S</u>[314]AEQNRM	rat kidney cells[#]	[343]
	GQAG<u>S</u>[325]TI<u>S</u>[328]N<u>S</u>[330]HAQ[♦]		

Cytoskeletal, membrane and sarcoplasmic reticulum - associated proteins, including receptors

Connexin 49 (Cx49)	unidentified in this study	eye tissue,	
		likely CK1α[#]	[344]
Erythrocyte band 3	HDTEA<u>T</u>[42]ATDYHT – major site	human	
	YMAQ<u>S</u>[303]RGELLH – minor site	erythrocytes	[345]
Filamin, vinculin	unidentified in this study		[346]
Spectrin	Ser, on –COOH terminal	h erythrocytes[#¶]	[347-350]
m1-muscarinic receptor	unidentified in this study	CK1α, from	
		porcine brain*	[351]
m3-muscarinic receptor	14 potential sites, in clusters	CK1α, from	
	Identify 3[rd] intracellular loop,	293 lysates*	
	Ser[345]–Leu[463]		[352-355]
Myosin (light chain),	Ser/Thr phosphorylated	rabbit skeletal	
troponin		muscle*	[356, 357]
Neurofilaments (IFs)	unidentified in this study	R. reticulocytes*	[358, 359]
Neural adhesion	Ser/Thr phosphorylated	rat forebrain,	
molecules (N-CAM)		R.reticulocytes*	[360]
Neurochordins	serine phosphorylated		[361]
Polyamine transporter	GEGAKYT<u>T</u>[52]ATEGNGGA	yeast[¶]	
Protein (TPO1)	yeast, genetic deletion approach		[362]
Presenelin 1, 2	PEMEED<u>S</u>[327]YD<u>S</u>[330]FGEPSY	CK1δ, C-term. Δ*	
		HEK293, HeLa[#]	[363, 364]
Rhodopsin	DDEA<u>S</u>[334]TTVSK	CK1γ*	[355, 365]
Ror2 (receptor-	identify S/T residues	CK1ε*	
tyrosine kinase)		CK1ε in H293[#]	[366]
Smoothened (Smo)	DLNSSE<u>T</u>[629]NDISS	dm embryonic	

(*Dm*)	SLDSEIS^{673}VSRH VE***S***RRNSVDS^{691}QVS^{694}VK RESSTS^{743}VES^{746}QV QDMSSSS^{820}EEDN$^{\blacklozenge}$	S2 cells stably expressing HhN$^{\#}$	[367, 368]
Tau	SGYSSPGS^{202}PGT^{205}PGS GAEIVYKS^{396}PPVVSGDT^{404}SPPR KVAVVRT^{231}PPPKSPSS prior phosphorylation of S^{39} by PKA, CaMKII or GSK-3 can increase subsequent phosphorylation$^{\#}$	CK1δ, with C-terminal Δ* HEK293$^{\#}$	[339] [369-372]
TGFβ-Type II Receptor (aka p80)	predominantly Ser phosphorylated	CK1 prep* CK1ε, C-termΔ*	[330, 373]
Troponin	unidentified in this study	rabbit skeletal muscle*	[357]
Vesicular monoamine transporters (VMAT2)	GDDEES^{512}ES^{514}D	CK1δ, C-term Δ* CHO, HEK293$^{\#}$	[374]
nuclear[2]			
Cubitus interruptus (Ci-155) transcription factor (*Dm*)	FRRDSQNS^{841}TASTY Q***S***RRSSQSS^{859}QVSSI ***S***RRSSQMS^{895}NGANC	rat CK1δ, with C-terminal Δ*	[375]
CREM	AETDDS^{97}ADS^{100}EVIDS^{105}HKRRE KIEEEKS^{140}EEEGTP S^{97}, S^{100}, S^{105}, S^{140}, after phosphorylation of S^{117} by PKA, PKC, CamK or CDC2	CK1 from porcine spleen* COS$^{\#}$	[376]
Ets-1	unidentified in this study	CK1ε, C-term Δ*	[377]
FOXO1a (formerly FKHR)	RPRTS***S***^{319}NAS^{322}TIS^{325}GRL phosphorylation of S319 by PKB needed for phosphorylation of S^{323}, S^{325} SEEEQSSSS^{228}VKKDE$^{\blacklozenge\blacklozenge}$	CK1δ* HEK293, ES stem cells$^{\#}$ CK1α*	[98, 190]
hnRNP-C	VKMES^{240}EGGADDS^{247}AEE (**S** CK2)		[378]
Iκ-Bα	suggest S^{288} and S^{293}, no data shown	CK1ε, C-term Δ*	[377]
NF-AT1	SRR-1 region CK1δ and ε co-associate	CK1δ, with C-terminalΔ*	[379]
NF-AT4	'A-domain' phosphorylated, undefined. 'Z-domain' phosphorylated peptide: FT^{204}LGS^{207}PLT^{210}S^{211}PGGS^{215}PGGC$^{\blacklozenge}$	CK1δ, with C-terminal Δ* CK1α in BHK$^{\#}$	[380]

nuclear[2]			
Nonhistone chromatin	unidentified in this study	Calf thymus	
Proteins			[381]
SV4O large T-antigen	ADSQHS^{123}TPPKK – hierarchal	bovine and	
	EATADS^{120}QHSTP – atypical	HeLa nuclear	[294]
	QAPQSS^{677}QSVHD – atypical ¶	extracts*	[382-384]
p53	MEES^{4}QS^{6}DIS^{9}LE – classical (murine) ¶	bovine muscle,	[385]
	PPLS^{15}QES^{18}FS^{20}D – hierarchal (human) ¶	CK1δ, ε*	[386, 387]
MDM2	WLDQDS^{240}VS^{242}DQFS^{246}VEFE	CK1δ, with	
	QDKEESVES^{383}SLPLNAI[check again!]	c-terminal Δ*	[388]
RNA Polymerase	RNA Pol II better substrate than RNA	calf thymus*	
I and II	Pol I *In vitro*		[389]
Extracellular			
Fibrinogen	serine phosphorylated	rat liver*	[390, 391]
Virally encoded proteins			
respiratory syncytial	DTSDEVS^{215}LNPTS	rat CK1δ, with	
virus phosphoprotein P	This phosphorylation has no effect on	C-terminal Δ*	
(HRSV)	transcriptional activity	HEp-2 cells#	[392]
Virus Glycoprotein	Ser identified#¶	Calf thymus	[391]

[1] Largely cytoplasmic
[2] Able to transit to the nucleus/largely nuclear, but can also be found in the cytoplasm.
*shown to occur *in vitro*
#shown to occur *in vivo*
¶shown to occur both *in vitro* and *in vivo*
† The phosphorylated serine is underlined, with the type of consensus motif indicated.
Residues *shown* to be phosphorylated by PKA/PKC/'priming kinase' are indicated **S/T** and *potential/suspected* priming residues indicated ***S/T***.
‡The CK1 isoform used is indicated. The tissue sources for biochemical purifications of CK1, where known, are stated - these studies are predominantly early, purely biochemical work, before molecular cloning of CK1, and could thus contain multiple CK1 isoforms.
♦ The study identified these phospho-peptides by ms/mutation analysis of blocks of potential CK1 sites only.
♦♦ Only two of the underlined residues are shown to be phosphorylated.
!! note the SLT, but note the amino acids n+7 downstream

1.4.2. Structure

Crystal structures of CK1 have identified potential binding sites for substrate for phosphorylated substrate recognition, and potential autophosphorylation sites from the binding of tungstate/sulphate ions, see figure 1.10, from [393, 394]. The crystal structure of a truncated CK1δ by Longenecker et al [394], using molecular replacement of the crystal structure of Cki1 from Xu et al [393], identify three possible autophosphorylation sites: Y^{161}, T^{166}, S^{179}, also indicated in figure 1.10, in orange type.

These crystal structures are based on truncation mutants of CK1δ, lacking C-terminal residues for solubility reasons [393, 394]. CK1δ has the last 97 C-terminal amino acids deleted, terminating at H^{317}, with diffraction data accurate only to L^{298} [394]. Cki1 was deleted to N^{298}, deleting the last 148 amino acids [393]. Whilst yielding very useful information on the catalytic nature of CK1, these structures exclude residues implicated in further autophosphorylation and subsequent auto-inhibition (see figure 1.11) [395, 396]. Limited proteolysis and site-directed mutagenesis of CK1δ and ε, in mammalian cell lines and *in vitro* studies have been shown to increase the trans-phosphorylation activity of CK1 by ten-fold for CK1δ [395] and eight-fold for CK1ε [396]. Indeed, many recombinant enzyme preparations used in studies listed in table 1.6 have used a truncated CK1δ for *in vitro* studies – on order to have an active kinase. These findings are concordant with the fact that CK1α (examined here) lacks a C-terminus similar to CK1δ, ε and is constitutively active. A naturally occurring Ser→Asn mutation at the autophosphorylation site S408 in the C-terminus of CK1ε from patients with sleep disorders has increased kinase activity compared to wild type [397]. It has been speculated that dimerisation of CK1 may also play a role in CK1 regulation, as crystal structures of CK1 determined by Longenecker et al appeared as dimers [398]. However, this may be an artefact of the crystalisation procedure.

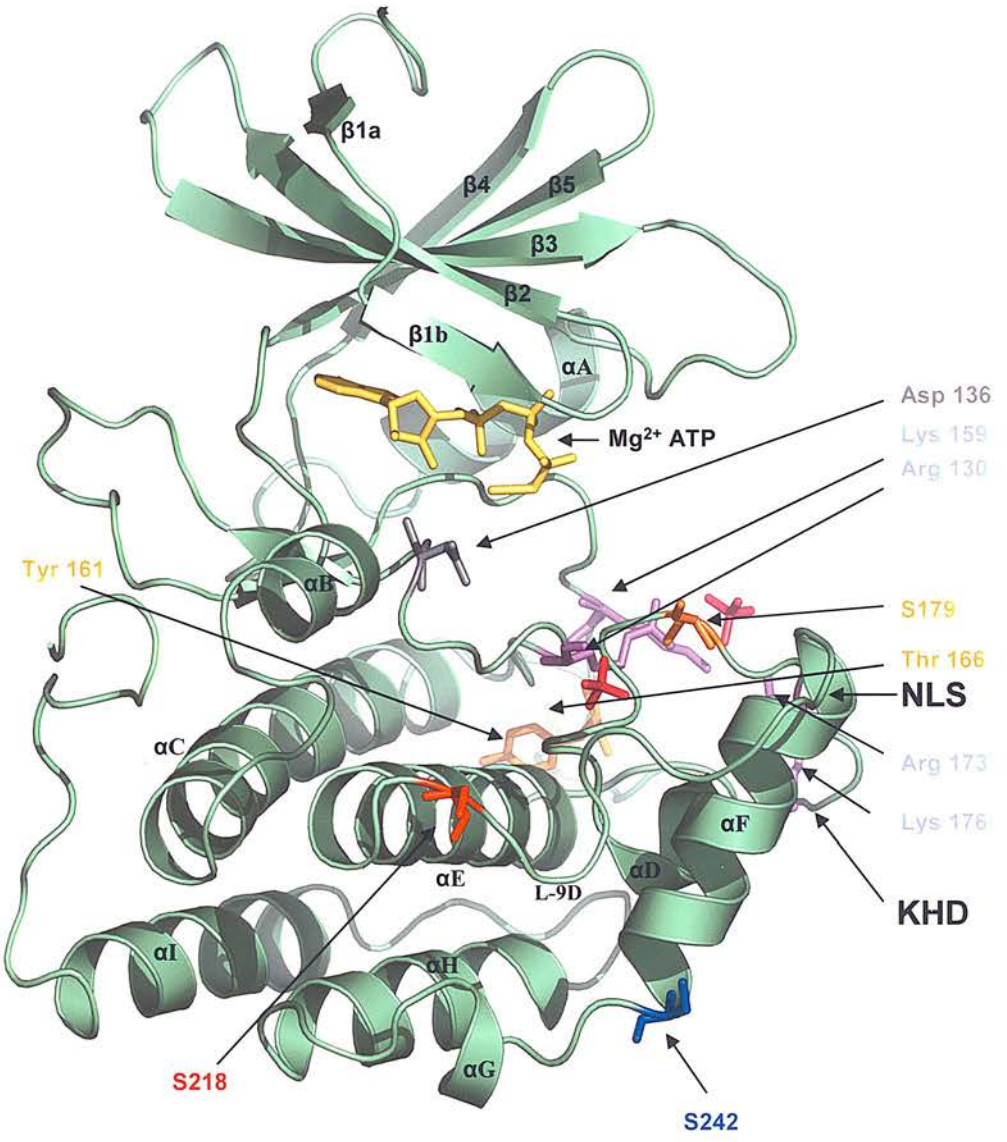

Figure 1.10 Crystal Structure of CK1
Purple residues are possibly involved in phospho-substrate binding, orange residues indicate potential autophosphorylation sites; Mg^{2+} ATP is shown in yellow. Sulphate ions are shown in pink, blue indicates phosphorylation site Ser 242 (CK1α numbering, equivalent to Ser 239 in this crystal structure). Structure rendered using PyMol from 1CSN.pdb.

1.4.3. Regulation of CK1

CK1 is largely second messenger independent [284] and there have been few examples of the enzymatic activity being directly affected by another entity. For example, CK1 has been shown to be inhibited by phosphatidylinositol 4,5-bisphosphate (PIP_2) in solution [399]. This inhibition is increased with a PIP_2:protein mixture, suggesting other factors than PIP_2 alone is/are involved [399]. The CK1 homologue, dmCK1, from Drosophila has been shown to be activated and relocated from a predominantly cytoplasmic to nuclear location, in response to gamma irradiation [400]. The change in kinase activity was most likely due to phosphorylation of the C-terminus, as phosphatase treatment re-activated the kinase [400], in a mechanism similar to CK1 ε and δ described above. Other reports of CK1 levels being elevated include insulin stimulation [401] and viral transformation [402], but more detailed investigations into the nature of these effects have not been reported.

As described above, a major way in which CK1 recognises substrates is by prior or hierarchal phosphorylation. This can indirectly lead to regulation of CK1, by the activation or inhibition of other kinases (that are in turn regulated by their respective second messengers). Hierarchal phosphorylation has been shown to occur in several proteins, including the Adenomatous polyposis coli protein, the transmembrane protein smoothened, transcriptions factors such as FOXO1a (formerly FKHR), Cubitus interuptus (Ci-55), and p53, (see table 1.7). The result of these multiple phosphorylations can have a dramatic effect. For example, in the case of FOXO1a, phosphorylation of S^{319} by PKB creates a consensus for CK1, which increases phosphorylation of S^{322}, which creates a consensus for S^{325}. The result of this phosphorylation, including S^{329} (phosphorylated by DYRK1A) leads to the subsequent exclusion of FOXO1a from the nucleus [98, 190]. Indeed a newly discovered inhibitor of CK1, called D4476 (used in this study), has been shown to reduce the rate of nuclear exclusion of FOXO1a in HEK293 cells [403].

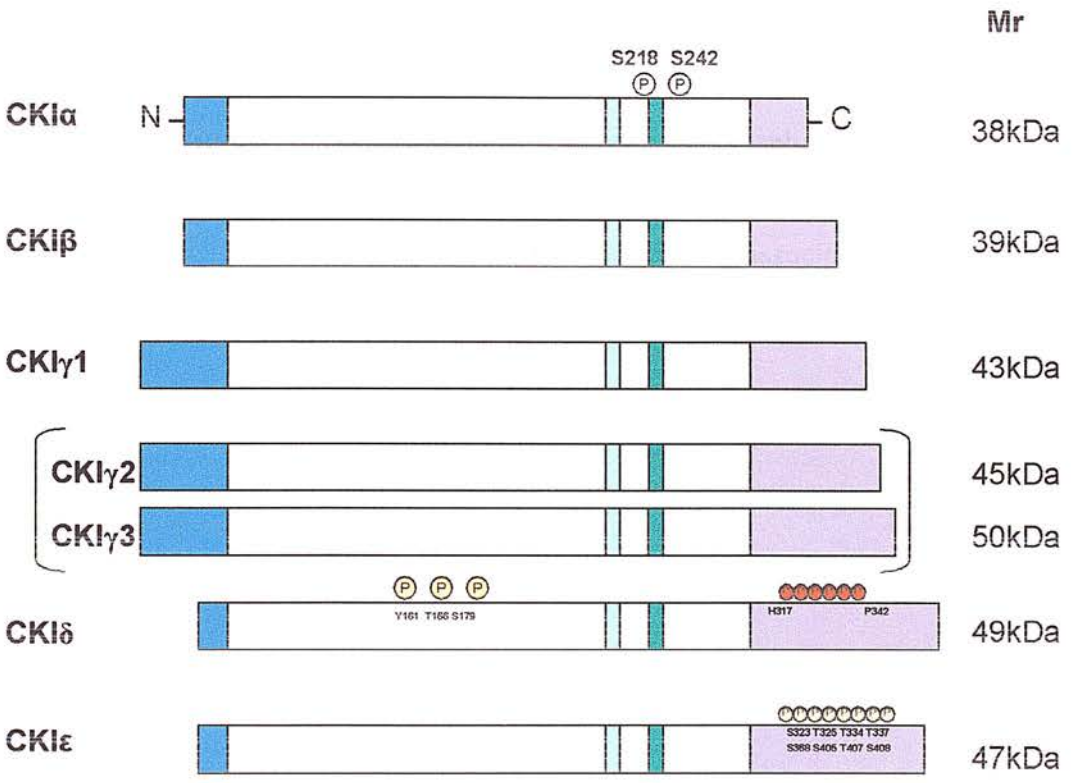

Figure 1.11 Schematic Representation of mammalian CKI Isoforms
The conserved kinase domain is shown in grey, the variable N- and C- terminal regions are shown in blue and purple, respectively. Kinesin homology domains are show in turquoise and nuclear localisation sequences in green. Additionally, phosphorylation sites, where known, are represented with a white circled 'P' and autophosphorylation sites by yellow filled circles. Regions known to undergo autophosphorylation that contain residues that have not been determined specifically are indicated by red filled circles, with amino acids either side of phosphorylatable residues indicated. References: phosphorylation sites on CK1α, this study; CK1δ, Y^{161}, T^{166}, S^{179}, [394]; CK1δ C-terminal phosphorylation [395]; CK1ε, [396].

1.4.4. Sequence conservation between CK1 isoforms

CK1 belongs to a large, evolutionary conserved family of protein kinases. Alignment of CK1 isoforms reveals highest conservation in the kinase domain, with highly divergent residues found at the N- and C-domains (see [288] for review). It is likely the highly divergent residues outwith the kinase domain provide substrate specifity for CK1 isoforms. Figure 1.12 shows an alignment of 16 CK1 isoforms from 6 different organisms, over the region examined in this study (residues 213-247). This reveals a high level of conservation; totally conserved residues are in red, with conserved substitutions in yellow. Interestingly (and relevant to the findings in this thesis), non-phosphorylatable residues comparable to position 218, in CK1α, are only found in two isoforms (in this alignment), whereas non-phosphorylatable residues are found in six isoforms at position 242. This difference in potential 14-3-3 interaction sites may provide a further level of regulation by reducing association with particular isoforms.

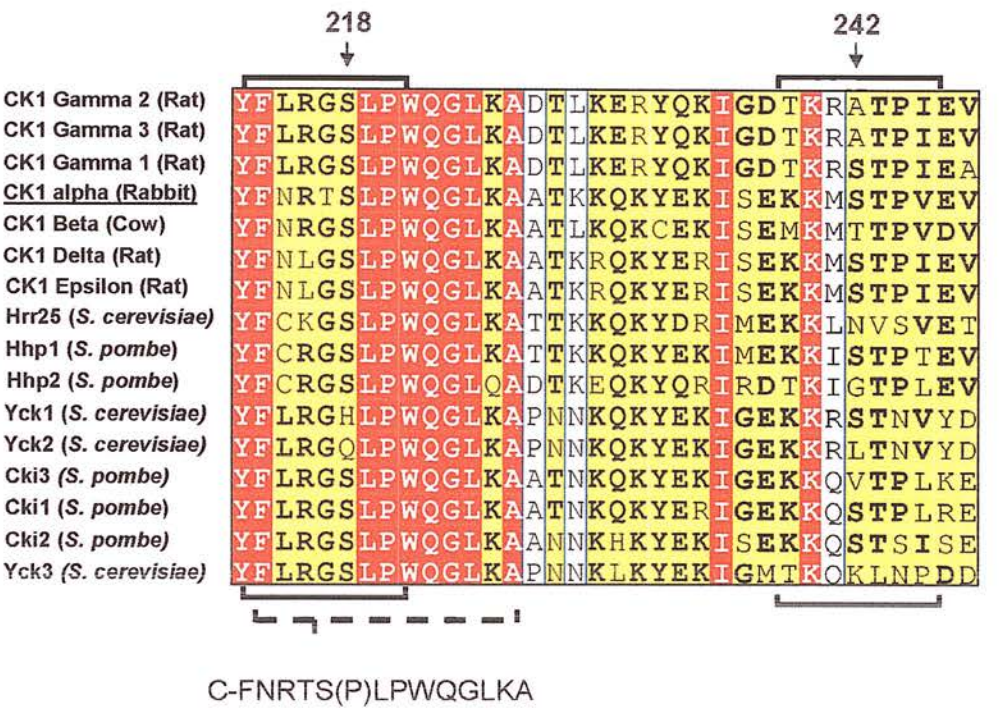

Figure 1.12 Sequence alignment around proposed interaction region
Alignment of higher Eukaryotic CKI isoforms, showing amino acids around the proposed binding region – the flexible loop region, as identified by crystal structure. The peptide used in this study is shown underneath the aligned sequences. The Cys was introduced to allow convenient coupling to agarose beads, via SH groups. Residues 218 and 242 are indicated with arrows, CK1α used in this study is underlined.

1.4.5. Function

Studies on the *saccharomyces cerevisiae* CK1 isoforms, Hrr25, Yck1, Yck2 and Yck3, have revealed a number of common functional themes involving CK1, including cytokinesis, membrane trafficking, cell division and DNA repair [288]. All isoforms apart from Hrr25 have an isoprenylation sequence that locates the kinase to the membrane. The function of mammalian isoforms is less clear, but recent work has identified some common themes. For instance, the mammalian CK1δ and ε isoforms are involved in the regulation of apoptosis through phosphorylation of key components of this process. The human p53 tumour suppressor is phosphorylated on multiple residues in both the N- and C-terminal domains (reviewed in [404-408]). At the N-terminus of p53, CK1δ/ε phosphorylates S^9 and S^{18} - after prior phosphorylation of S^6 and S^{15} respectively. ATM kinase (ataxia telangiectasia mutated) has been shown to phosphorylate S^{15} [409] in response to DNA damage by the radiomimetic drug neocarzinostatin. S^{15} is also phosphorylated by ATR (ataxia-telangiectasia- and Rad3-related) in response to UV radiation [410]. Phosphorylation of S^{18} and/or S^{20} is thought to disrupt binding to MDM2, thereby potentially reducing the destruction/inhibition of p53 [405]. Interestingly, ionising radiation of MCF-7 breast carcinoma cells promoted dephosphorylation of S^{376} (of p53), creating a 14-3-3 consensus around S^{378}, inducing 14-3-3 association and increasing p53 affinity toward DNA [21]. The level of complexity increased recently with the report that CK1δ can phosphorylate key sites on MDM2 (S^{240}, S^{242}, S^{246}, and S^{383}) both *in vitro* and *in vivo*, that regulate p53 turnover [388].

CK1 can also phosphorylate inhibitors of PP1 - DARPP-32 (dopamine- and cAMP-regulated phosphoprotein of 32 kDa) and the regulatory subunit of PP1c, inhibitor-2, see table 1.7. Whilst phosphorylation of inhibitor-2 by CK1 increases its potency as an inhibitor of the phosphatase [315], phosphorylation of DARPP-32 does not [310]. Phosphorylation of DARPP-32 on S^{137} protects dephosphorylation of T^{34} (phosphorylated by PKA/PKG) by calcineurin (PP2B), thus leaving DARPP-32 an efficient inhibitor of PP1 [411]. DARPP-32 phosphorylated by CK1 is dephosphorylated efficiently by PP2Ac and PP2C, but not by PP1c or calcineurin,

leading to a proposed 'phosphatase cascade' to re-activate PP1c after PKA-induced inhibition [412].

1.4.6. Localisation

A focus of study in CK1 biology has been its location within the cell at various points of the cell cycle. CK1α has been shown to associate with cytosolic vesicular structures and the nucleus/centrosome throughout interphase, then associate with the spindle apparatus/kinetochore fibres during mitosis [413]. It is worth noting that CK1 has a kinesin homology domain, conserved throughout all known CK1 isoforms (highlighted in figure 1.10). The kinesin motor proteins are associated with microtubules and are involved in cytokinesis; roles where CK1 has been impicated [288]. To further implicate CK1 in cell-cycle control, antibodies to CK1α injected into mouse oocytes, prevented progression to the first cleavage [414]. It follows that spatial organisation of CK1 would be an essential part of regulation, as alluded to by Gross and Anderson [288]. Concomitant with this idea, CK1 has recently been identified by yeast two-hybrid screen, using 'kinase dead' CK1δ as bait, to interact with CG-NAP/AKAP450 [415] (also now known as AKAP350 [416]) in mammalian cells [415]. This is particularly interesting as CG-NAP/AKAP450 primarily localises to the centrosome [417, 418] and also has an established role of recruiting signalling molecules to the centrosome. This finding may explain why CK1δ and ε have been found localised to centrosomes in the past [339]. CK1 has also been found in membrane preparations [399].

CK1 can associate with a number of proteins, although this does not always seem to affect the kinase activity [419, 420]. Work in our laboratory has identified a number of brain proteins that associated with CK1α by affinity chromatography and co- immunoprecipitation [421]. These include RCC1, High mobility group proteins 1 and 2 (HMG1and HMG2), Erf, Centaurin α-$_1$, synaptotagmin IX and CPI-17 [421]. We have further characterised the interaction of centaurin-α and CPI-17 [419, 422]. Centaurin-α was shown to associate with a loop region within the kinase domain of CK1, using a peptide corresponding to the residues 214-226 [419], a region proposed

to function as an interaction site [393], and conserved across all CK1 isoforms. However centaurin-α was not a CK1 substrate and had no effect on CK1 activity [419]. CK1α has recently been reported to associate with the scaffold protein axin and like centaurin-α, binding did not reduce kinase activity [420].

A new binding motif for CK1 has recently been identified in the transcription factor NF-AT1 as FSILF [379]. The authors report that proteins from the Wnt, Hedgehog, and circadian-rhythm pathways contain the general motif FXXXF, that could be identified as a CK1 binding motif [379].

1.4.7. Centaurin-α_1

Centaurin-α_1 is a soluble 46 kDa phosphatidylinositol-(3,4,5)-inositol (PIP_3) and inositol (1,3,4,5) tetrakisphosphate (IP_4) binding protein that was originally identified in a screen of brain proteins using an IP_4 analog immobilised on a resin support [423]. Also known as $p42^{IP4}$, centaurin-α_1 was identified in our laboratory in a complex with CK1 purified from porcine brain [419]. Centaurin-α_1 contains a zinc finger domain and two plecstrin homology (PH) domains that have been shown to bind PIP_3 and are required for targeting of centaurin to the membrane on PI3K stimulation [424, 425]. Centaurin-α_1 is ubiquitously expressed, with highest expression levels in the brain [423]. Association of centaurin-α_1 has been observed with vesicular presynaptic structures [426] and cell membranes [419]. Our laboratory further identified that CK1α and CK1ε can associate with centaurin-α_1 [419]. The interaction between centaurin-α_1 and CK1 was further examined and is discussed in chapter 4.

1.5. AIMS

The aim of this study was to investigate two 14-3-3 kinases, BCR and CK1. BCR has been shown to both associate with and phosphorylate certain 14-3-3 isoforms, but the phosphorylation sites were undetermined. To understand the physiological significance of the phosphorylation site(s) on 14-3-3, *in vitro* kinase assays were performed using all 14-3-3 isoforms as substrate, followed by Ser-Ala mutants of 14-3-3. This approach identified residue 233 as the site of phosphorylation on 14-3-3 τ and ζ. *In vitro* and *in vivo* binding experiments revealed that BCR can interact with all 14-3-3 isoforms, but to varying degrees.

Our laboratory has shown that CK1α phosphorylates 14-3-3 ζ *in vitro* and *in vivo*. However the interaction of the two had not been fully addressed. Regulation of CK1 activity is largely ill defined; primarily regulation is through being 'phosphate directed', or location dependent. 14-3-3 has been shown to modulate many enzymes, both by direct inhibition/activation and spatial directing. Therefore experiments were designed to investigate if CK1 could bind 14-3-3 and if so, identify any isoform specificity. An established site of interaction on CK1 for other proteins was confirmed as the site of interaction for 14-3-3, although crucially binding was dependent on phosphorylation. Phosphorylation sites on CK1 essential for 14-3-3 association *in vivo* were identified by mutagenesis as S218 and S242. Dephosphorylation of S218 negatively affected interaction with 14-3-3, but increased association with Centaurin-α_1.

These findings open up a possible regulatory mechanism for regulation of CK1 involving 14-3-3.

CHAPTER 2
Materials and methods

2. Materials and methods

Throughout the following section, the manufacturer of all chemicals, reagents and services are given in parenthesis. Where no mention is made, the reagent was from Sigma-Aldrich. All reagents were of analytical grade.

2.1. Molecular biology

2.1.1. Agarose gel electrophoresis of DNA

Agarose gels of 1% were routinely used, dissolved in a 1x solution of TAE buffer containing 40mM Tris-HCl, pH8.0, 20mM Acetic acid, and 1mM EDTA. The DNA was prepared using a 6x loading dye (detailed in table 2.8) to a final concentration of 1x, then subjected to 50V DC until separated. To visualise the DNA, Ethidium bromide (EtBr) was included in both the gel and the buffer at a concentration of 0.5μg/ml, followed by transillumination using ultraviolet light. Interchelation of the DNA fragments with EtBr compared to standards run in parallel revealed the approximate sizes. Markers used were from Roche – VII for large fragments (BCR) and Roche XIV for smaller fragments, see appendix for an example of the sizes produced.

2.1.2. Production of competent *Eschericia coli.*

All DNA manipulations were carried out in *Escherichia coli* strain JM109 or DH5α. JM109 cells were made competent by modification of the Hanahan method [427] and DH5α by modification of the method by Inoue et al [428]. The Hanahan method involves growing a 100ml culture of JM109 in antibiotic free media to an OD_{600} of 0.5. After centrifugation at 4,000g, 5min, 4°C, the cell were re-suspended in 30ml sterile 100mM RbCl, 50mM $MnCl_2$, 30mM Potassium acetate, 10mM $CaCl_2$, 15% glycerol, pH 5.8 and kept at 4°C for 90 min. After further centrifugation at 4,000g, 5 min, 4°C, the cells were re-suspended in 4ml of sterile, ice cold 10mM MOPS, 10mM RbCl, 75mM $CaCl_2$, 15% glycerol, pH 6.8, snap frozen and stored at -70°C in 200μl aliquots. Briefly, DH5α cells were streaked onto LB-agar plates (no antibiotic) and incubated at 37°C overnight. Ten colonies were introduced into 250ml of SOB medium in a 2 litre flask and grown at 18°C

until the absorbance at 600nm reached 0.6.The flask was cooled by incubation on ice for 10 min, then centrifuged at 5000g for 10 min. The supernatant was removed and the pellet re-suspended in 80ml of transformation buffer see table 2.8. The cell suspension was centrifuged as before and re-suspended in 20ml of TB with DMSO at 7% final concentration. After further 10min incubation in an ice bath, the cells were dispensed into 250µl aliquots and snap frozen in liquid nitrogen.

2.1.3. Preparation of plasmid DNA

Plasmid DNA from transformed *E. coli* cultures was either ethanol precipitated or purified using the QIAGEN DNA purification system.

2.1.3.1. Small scale, 'Mini-preps' of plasmid DNA

Small scale preparations of DNA were used at various sub-cloning stages. Briefly 5ml of overnight culture (with selective antibiotic) was spun down and the pellet re-dissolved in 250µl buffer P1. Then addition of 250µl of an alkaline solution, P2, in order to lyse the cells was added for 5 min, with gentle mixing. This was neutralised with buffer 350µl N3 buffer. The cell debris, now a white precipitate was removed by centrifugation and the DNA recovered by binding to the QIAprep membrane. DNA was eluted into 50µl water or TE (10mM Tris-HCl, pH 8.5).

2.1.3.2. Large scale, 'Maxi-preps' of Plasmid DNA

The Quiagen kit for purifying larger amounts of DNA was used to recover amounts of DNA necessary for transfection. The manufacturer's instructions were followed and briefly outlined here. Overnight cultures (200ml) of *E. coli* culture LB were centrifuges and the pellet resuspended in 10ml buffer P1. Buffer P2 (10ml) was then added to lyse the cells. After 5 min, 10 ml of neutralizing buffer N3 was added and left to stand for 10 min at room temp. The lysate was clarified by using the Quiagen filter, the flow through was then passed through the Quiagen resin column, eluted and precipitated isopropanol. The DNA was washed with 70% ethanol, air-dried and dissolved in nuclease free water or TE (10mM Tris-HCl, pH 8.5).

2.2. DNA Manipulation

2.2.1. Prokaryotic vector manipulations – 14-3-3

The cDNAs for all 14-3-3 isoforms were from various sources. All isoforms were produced as GST fusions with the exception of 14-3-3 ε that was produced as an MBP fusion.

2.2.1.1. 14-3-3 β isoform cloning

14-3-3 β, is an IMAGE clone (4843961/gi14060448), and was subcloned from the supplied vector (pOTB7) by PCR with two oligonulcleotides: 5' GATCGAATTCATGACAATGGATAAAAGTGAGCTGGTA and 3' GATCGTCGACTTAGTTCTCTCCCTCCCCAG, creating an *EcoR1* and a *Sal1* restriction site respectively (underlined). The PCR reaction was set up as in the following table:

2.2.1.2. Polymerase chain reaction

Table 2.1 polymerase chain reaciton

Plasmid DNA 25, 50, 75μg	0.5, 1.0, 1.5μl
Primer 1 with a *EcoR1* site (40pmol)	1.5μl
Primer 2 with a *Sal1* site (40pmol)	1.5μl
DNA Polymerase buffer (10X)	5μl
dNTPs (each at 10mM)	1μl
nuclease free water	39.5, 39, 38.5μl
Pfu DNA Polymerase (1U)	1μl
total	50μl

The program that yielded one product of high purity was 1 cycle of 95°C, 2 min; 30 cycles of 95°C for 30 sec, 66°C for 45 sec, 72°C for 10 min; final cycle of 72°C for 10 min.

2.2.1.3. Restriction enzyme digestion

The PCR product was inserted into pGEX-4T1 (Amersham), by ligating under the following conditions: 1μl vector, to 3μl insert and a second reaction of 1μl vector and 6μl insert, 1μl (1U) of DNA ligase, 1μl 10x DNA ligase buffer (see table 2.8) and nuclease

free water to 10µl. The reaction was left overnight at 20°C. This created an N-terminal GST fusion protein with a thrombin cleavage site between the GST moiety and 14-3-3.

2.2.1.4. 14-3-3 σ cloning

14-3-3 σ was a gift from Henrik Leffers, provided in the vector pGPT-delta 6. The insert was produced as a PCR fragment using the oligonucleotides 5' GATCGAATTCATGGAGAGAGCCAGTCTGATC and 3' GATCGTCGACTCAGCTCTGGGGCTCCT creating an *EcoR1* site and *Sal1* site respectively (underlined). Essentially the same PCR reaction was used as for 14-3-3 β. The PCR product was digested with *EcoR1* and *Sal1*, cleaned up and ligated into cut pGEX-4T1 vector, creating an N-terminal GST fusion.

2.2.1.5. 14-3-3 η, γ ζ and τ cloning

14-3-3 η and 14-3-3 γ were a gift from Henrik Leffers. The 14-3-3 η and 14-3-3 γ clones were provided as N-terminal GST-fusions in the vector pGEX-2T (Amersham). 14-3-3 ζ was from a human T-cell cDNA library and has been produced as an N-terminal GST fusion in the pGEX-2T vector [172, 429]. 14-3-3 ε was produced as an N-terminal MBP fusion, from a rat cDNA (accession m84416) [10]. 14-3-3 τ was from a human source and was produced as an N-terminal GST fusion. All cDNAs were checked by sequencing both strands by Cytomyx, Cambridge, UK or in house on an Applied Biosystems 3730 DNA analyser running Big Dye v3.1 and analysed using the programs ChromasPro™ and GeneJockey™.

2.2.2. Eukaryotic vector manipulations

2.2.2.1. *B*reakpoint *C*luster *R*egion (BCR) cloning

A vector containing the bcr sequence was a kind gift from Owen Witte. To create a GST-fusion of BCR, the coding sequence for bcr was amplified by polymerase chain reaction (PCR) using two oligionucleotides 5' GATCGCGGCCGCGCGCCATGGTGGACCCGGTGGGCTT and 3' GATCGAATTCGACTTCGGTGGAGAACAGGATGCTCTGTCT creating the restriction sites *Not1* and *EcoR1* respectively and underlined, ligated into the pEBG-2T

GST vector for mammalian expression (kind gift from Dario Allesi, School of life sciences, University of Dundee) creating an N-terminally fused bcr construct. A C-terminally FLAG tagged fusion of bcr was created with two oligionucleotides: (5'GATCGAATTCATGGTGGACCCGGTGGGCTTCG and 3' GATCGCGGCCGCTTAGACTTCGGTGGAGAACAGGATGCTCTGTCT) were used to produce bcr cDNA, containing the restriction sites *EcoR1* and *Not1* for ligation into the pCMV-4A vector (Stratagene), producing a C-terminal fusion with the FLAG tag.

2.2.2.2. Casein Kinase 1 (CK1) cloning

The cDNA corresponding to casein kinase 1α from rabbit skeletal muscle (from Peter Roach) was cloned into pcDNA 3, using oligonucleotides to create an N-terminal HA tag was created by Thierry Dubois [430]. Site-directed mutagenesis of this clone was used to create ser-ala mutations within possible 14-3-3 binding sites.

2.2.3.
2.2.4. Site-directed mutagenesis of CK1α

To obtain point mutations of CK1α to observe binding requirements to 14-3-3, slight modification of the Quickchange™ site directed mutagenesis protocol (Stratagene) was used. The sense primer used for the S218A mutant was 5' GA TAT GTT TTG ATG TAT TTT AAT AGA ACC AGC CTG CCG TGG CAA GGA CTA AAG GCT GCA ACA 3' and the antisense primer used was 5' GA TAT GTT TTG ATG TAT TTT AAT AGA ACC **GC**C CTG ***CCA TGG*** CAA GGA CTA AAG GCT GCA ACA 3' this created a unique, translationaly silent restriction site: *Nco1*, italic, bold. The changed residues are underlined. The template used for this was an HA-CK1α in pcDNA3 plasmid. The ultra high fidelity enzyme PfuUltra™ was used (in place of the standard polymerase) for the PCR creation of mutant template.

2.2.4.1. Polymerase chain reaction

1μl pcDNA3-HA-CK1α plasmid (2, 5, and10ng), 5μl 10x Pfu Ultra high fidelity reaction buffer, 1μl dNTPs (25mM each dNTP), 1.5μl sense primer, 1.5μl anti –sense

primer, 38.6µl water, 1µl Pfu Ultra high fidelity DNA polymerase to a total volume of 50µl were added together in that order.

Temperature cycling for the PCR consisted of denaturation at 95°C for 2 min, annealing temperature of 68°C for 30sec, extension temperature of 72°C for 13min (2min/Kb) for 1 cycle, followed by 30 cycles of 95°C for 30sec, 68°C for 45sec and 72°C for 13min, with a final 10min of 72°C. The PCR product was treated with Dpn1, an enzyme that digests specifically methylated and hemimethylated DNA [431], in this case the parental DNA. The product was checked by agarose gel electrophoresis, before being transformed into XL-blue supercompetent cells (Stratagene). Mini-preps of at least 8 individual colonies were prepared and treated with *Nco1* to screen for DNAs containing the new and unique restriction site.

The same procedure was used for creation of a S242A mutant and S218A/S242A double mutant of CK1α , using the following primers: sense primer 5' ATA CGA AAG ATT AGC GAA AAG AAG ATG **G**CC ACT CCT GTT GAA GTT TTA T and antisense primer: 5'CCT TAC ATA AAA CTT CAA CAC GAG TGG CCA TCT TCT TTT CGC TAA TCT TCT CGT AT 3'. The underlined base indicates the mutated base. For the S242A mutant, the pcDNA3-CK1α w/t plasmid was used, for the double mutant, the pcDNA3-CK1α S218A plasmid was used. Again, all cDNAs were checked by sequencing both strands in house or by Cytomyx, Cambridge, UK.

2.2.4.2. Site Directed Mutagenesis of 14-3-3

The 14-3-3 ζ-myc mutants S233A, S233D and 14-3-3 τ mutant T233A were created in pcDNA3 vectors by Thierry Dubois using site directed mutagenesis [172] and unpublished.

2.3. Protein assay

Protein concentration was routinely measured using the Bradford method [432]. A concentrated dye (Bio-Rad) was diluted 1:4 with water, to give a 1x solution. Samples were made up to 50µl with water and then 4 volumes (200µl) 1x dye was added and allowed to incubate for 5 min at room temperature. The absorbance was measured at 595 nm and compared to a standard curve assay, constructed with known amounts of BSA.

2.4. Sodium-dodecyl sulphate polyacrylamide electrophoresis (SDS-PAGE)

Table 2.2 Buffers and solutions for SDS-PAGE

Stacking gel (5%)	5% (w/v) 0.125M 0.1% 0.1% 0.1%	29:1 acrylamide:N,N'-ethylenebisacrylamide* Tris-Hcl (pH6.8) SDS Ammonium persulphate TEMED
Resolving gel (8-18%)	8-18% (w/v) 0.375M 0.1% 0.1% 0.1%	29:1 acrylamide:N,N'-ethylenebisacrylamide Tris-Hcl (pH8.8) SDS Ammonium persulphate TEMED
Tri-glycine running buffer	0.2M 25mM 0.1% (w/v)	Glycine Tris SDS
3x SDS loading buffer (Laemmli buffer)	0.15M 30% 9% 15% 0.007%	Tris-Hcl (pH6.8) Glycerol SDS β-mercaptoethanol Bromophenol blue
Coomassie blue stain	10% (v/v) 50% (v/v) 0.2% (w/v)	Glacial acetic acid Methanol Coomasie brilliant blue (G250/R250)
Destain	10% (v/v) 30% (v/v)	Glacial acetic acid Methanol

*referred to as acrylamide in text

Proteins were routinely separated by size under denaturing conditions by polyacrylamide gel electrophoresis, using Tris-glycine gels of varying density of acrylamide, according to the method of Laemmli [433]. Samples were made to 1x final concentration in Laemmli buffer, boiled briefly before storage and/or separation. Samples were applied to a two-phase SDS-PAGE gel consisting of the stacking gel (5% acrylamide, pH 6.8), followed by the resolving gel (8-18% acrylamide and pH 8.8). A vertical slab-gel apparatus from Sigma was used, with the cathode at the top, and anode bottom. For the first, stacking gel phase, a voltage of 100V was applied (typically 20 min), followed by an increase to 150V, variable current for the resolving gel. An 8% gel was used for large proteins, e.g. BCR (160kDa), 10% for 60-100kDa, 12.5% for 30-60kDa (14-3-3), 15% for 10-30kDa and 18% for small peptides (gel recipe from Sambrook [434]). Generally pre-stained protein markers from New England Biolabs were used, with a range of 6.5kDa to 175kDa. Separated proteins were visualised with either staining by coomassie/GelCode® or transferred to nitrocellulose membrane for analysis by western blotting.

2.4.1.

2.4.2. Western blotting

Table 2.3 Transfer buffer

TBS-Tween (TBS-T)	20mM Tris-HCl, pH 7.6 137mM NaCl 0.1% Tween-20
Transfer buffer	192mM Glycine 25mM Tris 0.1% SDS 20% Methanol

After separation by SDS-PAGE, proteins were transferred from the gel to nitrocellulose membranes in the presence of transfer buffer at constant current of 0.2A for 90 min. The membranes were routinely blocked using 5% skimmed milk solution made up using TBS-Tween for 1 h shaking at room temperature. This was followed by incubation with the primary antibody for 1-2 hours at room temperature, or 4°C overnight, in 5% milk solution. After four 10 min washes in TBS-Tween the membrane was incubated with secondary antibody conjugated to horse radish peroxidase in 5% milk solution for 1 hour with shaking. After a final wash regime of four to six washes, the

membrane was incubated with the enhanced chemiluminescence (ECL) system (Amersham Pharmacia, UK) for five minutes. Immediately after this incubation, the membrane was dried and exposed to autoradiographic film (Kodak) for various time intervals from 10 sec to 60 min. For the use of phospho-specific antibodies, the above procedure was repeated exactly as above, except a 1% BSA in TBS-Tween solution was used to reduce cross-reaction with phospho casein present in milk.

Table 2.4 Antibodies used for western blotting and immunoprecipitations

specific for	Name	Raised against peptide or whole protein	Source	Organ-ism/ cell type where produced	Mono clonal poly-clonal	Dilution For western blotting
14-3-3 isoforms:			Alastair Aitken and Harry Martin			
14-3-3β	2042	Ac-TMDKSELV*C*	AA/HM	rabbit	poly	1:3000
14-3-3γ	1005	Ac-VDREQLVQKA*C*	AA/HM	rabbit	poly	1:6000
14-3-3ε C-term	1116	*C*GEEQNKEALQDVEDENQ	AA/HM	rabbit	poly	1:3000
14-3-3ζ	1002	Ac-MDKNELVQKA*C*	AA/HM	rabbit	poly	1:3000
14-3-3η	2043	Ac-GDREQLLQRAR*C*	AA/HM	rabbit	poly	1:3000
14-3-3σ	789	Ac-MERSASLIQKA*C*	AA/HM	rabbit	poly	1:3000
14-3-3τ	197	Ac-MEKTELIQKA*C*	AA/HM	rabbit	poly	1:3000
14-3-3 PAN	1106	Whole protein, KCIP	AA/HM	rabbit	poly	1:3000
14-3-3 S233^{P}	T233L	*C*TLWTSDT^{P}QGDEAEAG	AA/SC	sheep	poly	1:500
14-3-3 S185^{P}	SPEKA	EILNS^{P}PEKA*C*	AA/SC	sheep	poly	1:250
BCR	7C6	SSINEEITPRRQS	Santa Cruz	mouse	mono	1:500
CK1α (C-terminus)	CKIα (C-19)	c-terminus	Santa Cruz	goat	Poly	1:250
CK1α (N-terminus)	CKIα (N19)	n-terminus	Santa Cruz	goat	poly	1:250
CK1γ	CKIγ (R-19)	c-terminus	Santa Cruz	goat	poly	1:250
CK1δ	CKIδ (R-19)	c-terminus	Santa Cruz	goat	Poly	1:250
HA-tagged protein	HA-7	YPYDVPDYA	Sigma	mouse	mono	1:2000
Myc-tagged prtoein	9E10	EQKLISEDL	Sigma	Mouse	mono	1:1000
FLAG-tagged protein	M2	DYKDDDK	Sigma	Mouse	mono	1:1000
GST	Anti-GST	whole protein	Sigma	rabbit	poly	1:1000
Rabbit IgG	Anti rabbit	rabbit whole molecule IgG	Bio-Rad	goat	poly	1:2000
Mouse IgG	Anti mouse	mouse whole molecule IgG	Chemicon	goat	poly	1:2000
Goat IgG	Anti goat	goat whole molecule IgG	Sigma	donkey	poly	1:2000
Sheep IgG	Anti sheep	sheep whole molecule IgG	Sigma	donkey	poly	1:2000
Rat IgG	Anti rat	rat whole molecule IgG	Amer-sham Pharmacia	goat	poly	1:1000

2.5. Generation of antiserum to phospho-14-3-3 S185.

2.5.1. Peptide coupling and Immunisation of the sheep

Approximately 1mg of the peptide EILNpS^{185}PEKAC (for 'pSPEKA' antibody) was coupled to maleimide-activated Keyhole Limpet Hämocyanine (KLH) according to the manufacturers instructions (Pierce, Rockford, IL, USA) using the cysteine introduced at the C-terminus for this purpose. The coupled peptide was injected subcutaneously with Freund's complete adjuvant (FCA), an emulsion containing mycobacteria that generally produces a strong immunogenic response. Three subsequent booster injections were performed, approximately every month, using half as much KLH conjugated peptide and incomplete FCA, lacking mycobacteria. One litre of blood yielded 200-400 ml serum and was stored at -20°C until further use. The animal(s) were not exsanguinated after the immunisation procedure. Immunisation and serum recovery were performed according to Diagnostics Scotland's standard procedures.

2.5.2. Peptide affinity purification of anti-phospho-14-3-3

2.5.2.1. Immobilising the peptide

Table 2.5 binding buffer

Binding buffer	50mM Tris-HCl pH7.5 5mM EDTA
Blocking buffer	50mM Tris-HCl pH7.5 50mM Cysteine 5mM EDTA

The peptides to be used for purification of the antibody were immobilized using the Pierce Sulfolink® gel, essentially as according to the manufactures instructions. Briefly, one milligram each of the peptides used for the immunisation of the sheep, SPEKA and pSPEKA were dissolved at a concentration of 1mg/ml in binding buffer and incubated with 1 ml (bed volume) of Sulfolink® coupling gel (Pierce, Rockford, IL) for 30 min, rotating at room temperature, followed by a further 15 min incubation at room temperature. After washing with binding buffer, the beads were blocked with a 50mM Cysteine solution for 30 min, rotating at room temperature. After extensive washing to

remove Cysteine, the columns were stored in binding buffer with the inclusion of 0.05% sodium azide.

2.5.2.2. Binding and eluting the Antibody

The serum was clarified by ultracentrifugation at 40,000 RPM (125,000g) in a Beckman Type 45Ti centrifuge at 4°C for one hour and then filtered through a 0.45μm low protein binding (PVDF) membrane filter (Millipore, Bedford, MA). The supernatant was diluted ten times in binding buffer and then passed four times through the column containing bound unphosphorylated SPEKA peptide, at 4°C, using gravity flow. The serum was then passed four times through the phosphorylated pSPEKA peptide column, again at 4°C. Each column was washed with 20 column volumes of binding buffer, followed with elution using 10 ml of 200mM acetic acid. Each 1 ml fraction was eluted directly into 220μl of 1.5M Tris pH~10 to neutralise the solution, the pH was checked using pH indicator strips (BDH, UK) and corrected to pH 8, if not already and stored at 4°C.

2.5.2.3. Testing the Antibody

Serial dilutions of the dissolved SPEKA/pSPEKA peptides were spotted onto nitrocellulose membrane and blocked in 1% bovine serum albumin (BSA) in TBS-T for 30 min, followed by three 5 min washes in TBS-T. The first three fractions were tested by incubating with blocked membrane containing either phospho- or unphospho- peptide to observe the specificity. Pre-incubations with either the dephospho- or unphospho-peptide were also performed by incubating approximately 2μg antibody, measured by Bradford, with 1μg peptide – a molar concentration several fold higher of peptide to antibody was used. To observe how the antibodies behaved with whole proteins, brain extracts (containing approx 50% phosphorylated 14-3-3) were subjected to SDS-PAGE alongside recombinant 14-3-3 β and ζ. The gel was transferred to nitrocellulose membrane and cut into strips for testing each fraction. The best fractions were pooled and dialysed overnight at 4°C in the following buffer: 20mM Tris-HCl (pH7.5), 150mM NaCl, 100μg/ml BSA (Added after autoclaving), 50% Glycerol (added after dialysis) and 0.05% NaN_3.

2.6. Purification of antibody to S233 site on 14-3-3 ζ

Essentially the same protocol as outlined above was used, with the following exceptions. First, two peptides were synthesised corresponding to the S233 region of 14-3-3 ζ; one with an N-terminal cysteine: *C*WTSDpT^{233}QGDE and another with a C-terminal cysteine: WTSDpT^{233}QGDE*C*. Each peptide was coupled to KLH, BSA or MAP (multiple antigenic peptides) matrix (Pierce) for injection at differing stages. Peptides coupled to KLH were introduced into the animal first, with subsequent injections coupled with BSA and/or MAP. The reason for this was to try to reduce the immunogenic response to the carrier (KLH, BSA, MAP) whilst maintaining the response to the peptide. However, testing of serum showed a very poor immunogenic response (data not shown). Subsequently, a longer peptide consisting of *C*TLWTSDpT^{233}QGDEAEAG was used as an immunogen, in the hope of getting a stronger antigenic response. Two approaches were used to purify the antibody -one peptide column using an N-terminal cysteine *C*WTSDpT^{233}QGDE and another with a C-terminal cysteine (WTSDpT^{233}QGDE*C*). The serum was passed through columns containing these immobilised peptides, washed, eluted and tested as for the phospho-S185 antibody.

2.7. Cell culture

COS-1 and HEK293 cells were routinely cultured in Dulbecos's modified Eagle's medium (DMEM, Invitrogen) supplemented with 10% Foetal bovine serum (Invitrogen) penicillin, streptomycin and L-glutamine at 1U/ml, 1μg/ml and 0.292mg/ml respectively, at 5% CO_2 and 37°C in a humidified incubator.

2.7.1. HEK293 cells, COS-1, COS-7 cells

On reaching 90-100% confluence, the cells were trypsinized with 2ml trypsin per 175cm^2 flask and split 1/5 for maintenance or plated out at varying densities for further treatment, for example transfection. Cell viability was routinely checked by using the trypan Blue exclusion test, whereby 2mls of an approximately 1x10^6 cells/ml suspension were incubated with 0.1ml of 0.4% trypan blue stain for 5 minutes at room temperature. Exclusion of the dye was observed in a haemocytometer for counting viable cells.

2.7.2. Transfection of cells using electroporation

Cells were grown in flasks until confluent, trypsinised and collected by centrifugation. After washing in DMEM, the cells were re-suspended in 10 mls of HeBS buffer (20mM HEPES pH 7.05, 137mM NaCl, 5mM KCl, 0.7mM Na_2HPO_4, 6mM D(+) glucose, filter sterilised) and counted in a haemocytometer. Approximately $2x10^6$ cells in 250µl HeBs with 5-10µg DNA and 50µg herring sperm carrier DNA were added to an electroporation cuvette and electroporated using a BIO-RAD gene pulser set at 0.25V and 125µF. After a recovery period of 10 minutes, 1 ml of DMEM was added to the cells before being incubated for 24 hours in DMEM with FBS at 37°C, 5% CO_2.

2.7.3. Transfection of cells using Lipids

A number of lipid:DNA complex forming reagents are available for transient transfections. Here Lipofectamine (Invitrogen), Metafectene (Cambio) and FuGene (Roche) reagents were trialled for transfection efficiency. Manufacturers instructions were generally followed, with plating of $2\text{-}3x10^6$ cells per 100mm plate were plated out 24 hours before transfection, using antibiotic-free media and left until 80-90% confluent. Ratios of DNA:lipid mix were ~1:3, for example transfection using Lipofectamine 2000 was achieved by mixing 8µg DNA with 24µl reagent in serum-free DMEM to allow DNA:lipid complexes to form. After 20-30 minutes, this mixture was then added to the plates and left to incubate for 24 hours at 5% CO_2, 37°C.

2.7.4. Transfection of cells by calcium phosphate precipitation

A modified calcium phosphate precipitation method of was used to transiently transfect HEK 293 cells. All solutions were prepared in distilled water and sterile filtered through a 0.22µm pore syringe filters. Confluent cells were trypsinized as described above and $2\text{-}3x10^6$ cells per 100mm plate were plated out 24 hours before transfection, using antibiotic-free media and left until 60-90% confluent. For each 10 cm-diameter plate to be transfected, 10µg of DNA was made up to 0.45 ml with sterile distilled water in a sterile tube. In co-transfection experiments, each plasmid was added to the same tube. To this, 50µl of 2.5 M $CaCl_2$-2H20 was added and the solution mixed by vortexing for 15 sec. 0.5 ml of transfection Buffer (50 mM HEPES-HCl pH 6.96 (pH is critical in

this buffer), 280mM NaCl and 1.5 mM Na2HPO4) was added and mixed thoroughly by vortexing for 60 sec. The resulting solution was left for 30 min at room temp to induce the precipitation of DNA/$CaCl_2$ complexes before pipetting the suspension drop-wise to the plate of cells. The cells were then incubated in a 37°C, 2.5% CO_2 incubator. After 16 hr post-transfection, the media was replaced with fresh media and cells incubated at 37°C in 5% CO_2 for a further 8-24 hours.

2.7.5.

2.7.6. Stimulation of 293 cells with dbcAMP

24 hours after transfection, cells were serum starved by incubating in only DMEM for 16 hours before application of dbcAMP. A stock solution of 100mM dbcAMP in sterile water was prepared immediately before the experiment. 40µl was added to 4mls DMEM for differing times; a timetable was constructed to ensure stimulation times were exact. For control experiment, 20µM PKAi-Myr peptide was incubated with the cells for 30 minutes before dbcAMP addition.

2.7.7. Lysis of mammalian cells

Plates were washed twice with ice cold PBS and lysed on ice with 1ml of ice cold standard lysis buffer using a cell scraper. Standard lysis buffer contained 25mM Tris pH 7.5, 137mM NaCl, .01% NP-40, 10% glycerol, 1mM EDTA, 1mM EGTA, 1mM DTT, 20mM NaFm 20mM β-glycerol phosphate, 20mM Sodium pyrosphosphate and a protease inhibitor cocktail from Roche. Changes to this combination were trialled and are detailed in chapter 3.1.3. The lysate was clarified by centrifugation at 16,000G for 30 min at 4°C, addition of 50µl washed Pansorbin A cells (Calbiochem) for 60 min, to remove endogenous IgG, then a further 30 min at 16,000G, 4°C.

2.8. In vitro BCR kinase assay of 14-3-3

2.8.1. *In vitro* kinase assay using ^{32}P-ATP

Glutathione Sepharose 4B (Amersham Pharmacia) beads were used to pull down the GST fusion of BCR from cell lysates of either COS-1 or HEK293 cells, transfected 24 hours earlier, and lysed in standard lysis buffer. The cell lysates were clarified by centrifugation at 13,000 RPM for 30 minutes at 4°C; then GSH beads added to the supernatant for 2 hours with constant rotation at 4°C before washing three times with lysis buffer. The beads were then washed twice in kinase assay buffer (without ATP and DTT). After the last wash, the beads were re-suspended in a final volume of 25μl kinase assay buffer, with a final concentration of 50mM HEPES (pH 7.05) 10mM mM MgCl, 20μM ATP and 20μM DTT. Between 2-10μg of each 14-3-3 isoform was used for each assay. The reaction was carried out for 30min at 30°C and stopped in Laemmli's buffer [433] prior to SDS PAGE.

Essentially the same procedure was carried out for using the BCR-FLAG construct. The transfected cells were lysed and clarified as before, except that the clarified lysate was cleared of endogenous IgGs using protein AG beads before adding 4μg of anti-M2 antibody and incubating with rotation 4-16 hours. The antibody:BCR-FLAG complex was recovered using a mix of protein AG beads incubated with the lysate for 4 hours, before washing as before in preparation for the kinase assay.

2.9. Casein kinase 1 inhibitors

2.9.1. CKI-7

CKI-7 (Shiegaku, Tokyo, Japan) was dissolved in dimethyl sulphoxide (DMSO) as a 10mM stock. For pre-incubation experiments with CKI-7, BCR-FLAG immunoprecipitates were turned end over end during the last wash of the IP in kinase assay buffer including 100μM CKI-7 (minus ATP). Where stated, CKI-7 was added just prior to addition of the substrate (20-100μM).

2.9.2. D4476

D4476 (gift from Rodolfo Marquez, School of Life sciences, The University of Dundee) inhibitor was dissolved in DMSO to a stock of 1mM and was used at 20μM in the final assay. This was added immediately prior to addition of the substrate. No pre-incubation with D4476 was required to observe an inhibitory effect. 2μl of DMSO was used as a vehicle control. Both inhibitor kinase assays were performed exactly as in 2.8.1.

2.9.3. Phosphorylation of Centaurin-α_1 by all classes of Protein kinase C

Approximately 10μg centaurin-α_1 (GST-removed with Thrombin) was incubated with 1U each of PKCα, μ and ε. The PKC activator - a micelle mixture of Phosphatidylserine (PS) and diacylglycerol (DAG) was made immediately prior to the assay by mixing 30μl PS and 8μl DAG together, reducing the volume by speedvac for 5 min until a glossy pellet formed. This was re-suspended in 50μl 20mM HEPES, pH 7.05 and incubated in a water bath for 30 min. Each assay had the following: PKC kinase assay buffer (40mM HEPES pH7.4, 2mM EGTA, 20mM $MgCl_2$), 0.03mg/ml PS, 8μg/ml DAG (3.62μl micelle mix),100μM ATP, 10μCi (0.37MBq) [^{32}P]-ATP, 10μg centaurin-α_1 and 1U PKC. PKCα had an additional 3mM $CaCl_2$ added. The reactions were made to 60μl, incubated at 30°C for 30 min and stopped in Laemmli buffer. Each reaction was run on a 12% SDS-PAGE gel, an autoradiograph taken and the bands corresponding to centaurin-α_1 cut out and digested with trypsin (see section 2.12). For the GST-centaurin-α_1:CK1α binding assay, intact GST-centaurin-α_1 was phosphorylated exactly as above.

2.10. Recombinant Protein Purification

Table 2.6 Clones used for protein over-expression in *E. coli*

Construct name (vector)	Source	Anti-biotic	Growth temp.	OD to induce	IPTG Conc.	Time for induction
GST (pGEX-4T1)	Amersham Pharmaia	Amp	37°C	0.9	0.5mM	4h
MBP (pMAL)	David Jones	Amp	37°C	0.6	0.5mM	4h
GST-14-3-3β (pGEX-4T1)	IMAGE clone (S Clokie)	Amp	37°C	0.9	0.5mM	4h
GST-14-3-3γ (pGEX-2T)	David Jones	Amp	37°C	0.9	0.5mM	4h
GST-14-3-3γ (pGEX-2TK)	Henrik Leffers	Amp	37°C	0.9	0.5mM	4h
MBP-14-3-3ε* (pMAl)	David Jones	Amp	37°C	0.6	0.5mM	4h
GST-14-3-ζ (pGEX-4T1)	Thierry Dubois	Amp	37°C	0.9	0.5mM	4h
GST-14-3-3η (pGEX-2T)	Henrik Leffers	Amp	37°C	0.9	0.5mM	4h
GST-14-3-3η (pGEX-2TK)	Henrik Leffers	Amp	37°C	0.9	0.5mM	4h
GST-14-3-3σ (pGEX-4T1)	Henrik Leffers (S. Clokie)	Amp	37°C	0.9	0.5mM	4h
GST-14-3-3τ (pGEX-2T)	David Jones	Amp	37°C	0.9	0.5mM	4h
GST-centaurin-α1 (pGEX-4T1)	Kanamarlapudi Venkateswardu	Amp	25°C	0.6	0.5mM	4h
GST-14-3-3τ S233A (pGEX-4T1)	Thierry Dubois	Amp	37°C	0.9	0.5mM	4h
GST-14-3-3ζ S185A (pGEX-4T1)	Thierry Dubois	Amp	37°C	0.9	0.5mM	4h
GST-14-3-3ζ S233A (pGEX-4T1)	Thierry Dubois	Amp	37°C	0.9	0.5mM	4h
GST-14-3-3ζS233D (pGEX-4T1)	Thierry Dubois	Amp	37°C	0.9	0.5mM	4h
GST-14-3-3ζ R5660A (pGEX-4T1)	Shaun Mackie/ (S. Clokie)	Amp	30°C	0.8	0.5mM	4h
GST-14-3-3ζ Dimer mutant (pGEX-4T1)	Shaun Mackie	Amp	25°C	0.9	1mM	4h

*MBP-14-3-3ε had added glucose at 2g/l at all stages.

All GST-14-3-3 fusion cDNAs were transformed into *E. coli* BL21(DE3)pLysS competent cells (Novagen), and selected on agarose plates containing 100μg/ml of the appropriate antibiotic. A 100ml culture was grown overnight from one colony in LB supplemented with Ampicillin at 100μg/ml. A 1/10 dilution of the starter culture was made into the same medium and grown at the temperature indicated in table 2.6 until the OD reached 0.6-0.9. The culture was then induced using isopropyl-beta-D-thiogalactopyanoside (IPTG, from ICN) at 0.5-1mM for 3-4h at 25-37°C, in a shaking incubator (220 RPM). The same procedure was used for the MBP-14-3-3 ε, but with the addition of glucose at 2g/litre at all stages. The purpose of including glucose was to prevent the build up maltose-degrading enzymes, so as not to degrade the amylose resin, used at a later stage, to recover the MBP-fusion. Cell pellets, re-suspended in lysis buffer (PBS, 1mM PMSF, 1mM EDTA, 1mM DTT, protease inhibitor tablet (Roche) and 0.1% Triton), were sonicated 6 times for 30s with an amplitude of 5 microns. The Triton X-100 concentration was increased to 1%, the cell suspensions were rotated for 30 min at 4°C and clarified by centrifugation at 16,000g for 30min. The supernatant was then passed through a 0.22μm filter and the GST fusion protein was recovered from the lysate using glutathione sepharose 4B beads (Amersham/Pharamcia) and the MBP-14-3-3 ε recovered by amylose resin (New England Biolabs). The beads were washed extensively and the 14-3-3 cleaved from the GST moiety using 50U thrombin (Sigma T-7009) for each litre of original culture of GST fusion, or 50U factor Xa/litre for MBP14-3-3ε. The protease was removed by passing the supernatant through a benzamidine sepharose column. Benzamidine sepharose beads were first equilibrated in benzamidine binding buffer (20mM Tris pH 7.4, 500mM NaCl) before the cleaved 14-3-3 protein was then passed through the immobilised benzamidine column twice. The 14-3-3 was then concentrated and buffer-exchanged into PBS and protease inhibitors using a vivaspin 10K MWCO concentrator (Fisher), snap-frozen in liquid nitrogen and stored in small aliquots at -70°C until use.

Intact GST-14-3-3 was eluted off the glutathione beads by incubating GST-14-3-3 bound beads with 10mls of GST elution buffer (50mM Tris pH7.4, 20mM glutathione) for 1 hour at 4°C, with gentle agitation. The eluted protein was dialysed into PBS to remove bound glutathione, concentrated and stored as above. MBP-14-3-

3 ε could not be stored in this way if to be used for 'bait' in future pull down experiments, due to the maltose binding with such affinity that it can not be dialysed off. For these purposes, the MBP-14-3-3 ε was prepared just before use and left on the amylose beads. For reciprocal binding experiments, MBP-14-3-3ε was eluted with maltose and treated as for the GST fusion proteins.

2.11. In Vitro Transcription Translation

Table 2.7 Clones Used for IVTT

δ-catenin-FLAG (pCMV-4A)	Shaun Mackie
BCR-FLAG (pCMV-4A)	This Study
HA-CK1α (pcDNA3)	Frank McKeon
HA-CK1α17-325	Thierry Dubois
HA-CK1α 164-325	Thierry Dubois
HA-CK1α189-325	Thierry Dubois
HA-CK1α217-325	Thierry Dubois
HA-CK1α233-325	Thierry Dubois
HA-CK1α17-287	Thierry Dubois
HA-CK1α164-287	Thierry Dubois
HA-CK1α189-287	Thierry Dubois
(all cloned in pcDNA3)	

One μg of each plasmid GST-Bcr, delta catenin, casein kinase 1α w/t, S218A, S242A, S218A/S242A were incubated with 40μl of a T7 TNT coupled transcription/translation system (Promega Corp., Madison, WI). This rabbit reticulolysate master mix™ includes all amino acids, but lacks methionine. Added separately, 0.37 MBq of [^{35}S]-methionine (Amersham) and nuclease-free water took the volume to 50μl. The transcription/translation reaction was allowed to proceed for 90 min, the lysate was then divided into two, incubated with either GST or GST-14-3-3 and incubated for 15min at 30°C, then 300μl of NP-40 buffer containing 15μl GSH beads was added and this was left with gentle rotation for 1 hour. For phosphorylation stimulation/inhibition experiments, after the 90min transcription/translation period, the lysate was incubated for a further 30min with the inclusion of PKA and 100μM ATP or 5mM NaF. The beads were washed 5 times in NP-40 buffer and subjected to SDS-PAGE. After staining/destaining, the gel was incubated for 30min with Amplify solution (Amersham), effectively a scintillant, to enhance the signal. The gel was dried, and exposed to film at -70°C.

2.12. Protein digestion and mass spectrometry

Proteins separated by SDS-PAGE were stained with either coomassie blue (R250) or the colloidal dye Gelcode™ (Pierce) to reveal bands. Individual bands were excised and treated according to the protocol of Aitken and Learmonth [435]. Briefly, gel pieces were incubated with three changes of 0.2M NH_4HCO_3/50% acetonitrile at 30°C for 30 min to remove SDS. The proteins were reduced by incubation with 20mM DTT/0.2M NH_4HCO_3/50% acetonitrile at 30°C for 1 hr. After several washes to remove DTT, the cysteine residues were alkylated by incubation in 50mM iodoacetamide (made fresh) for 20 min. After further washing the band was cut into small (1 x 2mm) pieces and shrunk with the addition of 100% acetonitrile (gel piece turns opaque white) - the acetonitrile was then removed in a centrifugal evaporator. The gel pieces were then rehydrated with a trypsin solution on ice for 15 min on ice, then enough 0.2M NH_4HCO_3 was added to cover the pieces and incubated overnight at 30°C. The peptides were collected in the supernatant, further extraction was achieved by sonication for 30 min at 35°C, the supernatants collected and lyophilised in a centrifugal evaporator for 30 min. Peptides were stored at -20°C until analysis by mass spectrometry.

2.12.1. Image analysis – Densitometry using AIDA/ImageJ software

Image analysis was performed predominantly on gels with coomassie stained proteins, or autoradiographs of radiolabelled proteins for accurate quantification of binding levels. Briefly, sections were drawn through each band to assess if the signal was too intense for analysis; only sharp peaks were analysed. The area under the peak was then calculated according to the software developers' instructions.

Table 2.8 Media and buffers used

LB (Luria-Bertani) broth	10g tryptone, 5g yeast extract, 10g NaCl, distilled water to 1 litre
LB Agar	10g tryptone, 5g yeast extract, 10g NaCl, 12g agar, distilled water to 1 litre
SOB	20g tryptone, 5g Yeast Extract, 2ml of 5M NaCl, 2.5ml of 1M KCl, 10ml of 1M $MgSO_4$, distilled water to 1 litre.Prior to use add: 10ml of 1M $MgCl_2$
SOC	As SOB media, but with the addition of 20ml of 1M glucose
TE	10mM Tris-Hcl pH 7.5, 1mM EDTA
NZY^+	10g cassamino acids (casein hydrolysate), 5g yeast extract, 5g NaCl, water to 1 litre. Prior to use add: 12.5ml 1M $MgCl_2$, 12.5ml 1M $MgSo_4$, 20ml of 20% (w/v) glucose, filter sterilized
Transformation buffer (TB)	10mM PIPES, 55mM $MnCl_2$*, 15mM $CaCl_2$, 250mM KCl. The media was made to pH 6.7 with KOH, autoclaved, the filter-sterilised $MnCl_2$ was added
TBS	25mM Tris, pH7.5, 137mM NaCl.
DMEM	Invitrogen #2169035
DMEM reduced serum	DMEM as above, but with 0.1% FBS
FBS	Foetal bovine serum, heat inactivated. Invitrogen #10108165
Trypsin	.05% EDTA Invitrogen #25300054
ATP	Preparation of 10mM stock: 2.5g of adenosine-5'-triphosphate MW 605g, dissolved in 400mls ice cold water, adding immediately small lumps of KOH to near pH 8.0, then a concentrated KOH solution to exactly pH 8.0
Cell Culture lysis buffer	50mM Tris (pH 7.5), 10% glycerol, 137mM NaCl, 10mM β-glycerol phosphate, 10mM NaF, 10mM $NaVO_4$, 1mM EDTA, 1mM dithiothreitol (DTT) and protease inhibitor cocktail tablet, EDTA-free (Roche)
Kinase assay buffer	2x stock: 100mM HEPES pH7.0, 20mM $MgCl_2$, 2mM DTT*, 40μM ATP*, 0.37MBq γ-32ATP*. *Added just before use.
NP-40	20mM Tris pH 7.5, 100mM NaCl, 10% glycerol, 1mM DTT*, 0.1% non-idet P40. *Added just before use.
Laemmli Buffer 3x (loading dye)	For 40ml: 7.6ml Tris Hcl pH 6.8 1M, 12ml glycerol, 6ml β-mercaptoethanol, 12ml 20% SD, 1.2ml 1% bromophenol blue, 1.2ml water.

*add just before use

CHAPTER 3.
Identification of phosphorylation site on 14-3-3 by BCR kinase

3. Identification of phosphorylation site on 14-3-3 by BCR kinase.

3.1 Introduction

14-3-3 has been shown to be phosphorylated by the wild type BCR kinase and also the chimeric BCR-ABL kinase [147]. The authors ascertained the phosphorylation to be on serine/threonine residues and on 14-3-3 ζ and τ isoforms, in addition they showed that 14-3-3 zeta was 15 times a poorer substrate for BCR than tau. 14-3-3 τ, ζ and β have also been shown to associate with BCR kinase [147, 187]. 14-3-3 binding to BCR may well be dependent on BCR phosphorylation [44]. Figure 3.1 shows a schematic of kinases that phosphorylate BCR.

To identify which 14-3-3 residue was phosphorylated by BCR kinase, BCR was produced in mammalian cells and incubated with all mammalian 14-3-3 isoforms in an in vitro kinase assay (Figure 3.4). In agreement with Reuther et al [147], only 14-3-3 τ, and to a lesser extent ζ, were phosphorylated. Alignment of all 14-3-3 isoforms shows the only common and unique Ser/Thr to τ and ζ, is residue 233 (Thr in ζ, Ser in τ). This site was previously identified in our laboratory as a phosphorylation site by CK1α [172], the phosphorylation of which reduces the interaction with Raf kinase [145]. Repeating the kinase assay using mutants of this site revealed that residue 233 of 14-3-3 zeta and tau are phosphorylated by BCR kinase (figure 3. 6, 3.7). As BCR phosphorylates the same site on 14-3-3 as CK1α, experiments were performed to rule out the possibility of phosphorylation of S/T233 by a contaminating endogenous CK1.

To investigate the possibility that additional isoforms may also interact with BCR, three approaches were taken. Firstly BCR-FLAG was overexpressed in 293 cells, GST-14-3-3 fusion proteins were incubated with the lysate, glutathione beads added and the 'pull downs' were subjected to SDS-PAGE and western blotted for anti-FLAG antibody (figure 3.17). Secondly, 293 cells were co-transfected with 14-3-3 isoforms and BCR-FLAG, reciprocal immunoprecipitations carried out and binding levels ascertained by western blot (figure 3.18). Thirdly, BCR-FLAG was overexpressed in cells, immunoprecipitated and western blotted to detect interaction with endogenous 14-3-3 isoforms (figure 3.19).

During these investigations it was observed that a PKA-like associating kinase co-precipitated with M2 anti-FLAG antibody from cell lysates.

3.1.1. DNA manipulation and purification of recombinant proteins used for kinase assays and binding experiments.

A clone of BCR from Owen Witte was introduced into the mammalian expression vector pEBG-2T resulting in an N-terminal GST fusion protein. A C-terminal FLAG tagged construct of BCR was also produced by PCR and inserted into the vector pCMV-4A (Stratagene). All recombinant 14-3-3 clones were produced as GST fusions, except 14-3-3 ε that was produced as an MBP fusion. The 14-3-3 proteins were cleaved using thrombin (GST constructs) or factor Xa (MBP) (see Materials and methods).

GST-14-3-3s could be conveniently stored in 30% glycerol at -70°C for several months without aggregation or degradation (data not shown). The MBP-14-3-3ε construct used as 'bait' in pull down experiments had to be used directly after purification from the bacterial lysate. This was due to the maltose binding so tightly to the MBP moiety such that it could not be dialysed off and so could not be re-captured on the amylose resin. GST-14-3-3 ε constructs had been tried before in our laboratory, but resulted in a series of truncations when analysed by SDS-PAGE [10].

3.1.2. GST-BCR and BCR-FLAG transfection in cells

Previous studies centred on BCR have used eukaryotic expression systems when studying *full length* BCR [204], or bacterial systems when truncation mutants of BCR were studied [243]. Correct folding and post translational modifications may well be required for such a large protein. To this end BCR was produced in mammalian cells and purified using immuno-precipitation or glutathione affinity pull-down followed by extensive washing. Different cell lines were tested for their ability to ectopically express BCR. COS-1, COS-7 and HEK293 cell lines were compared for their ability to produce BCR. Overall COS-7 cells gave the best yield, with COS-1 and HEK293, producing less, in that order (figure 3.2 and data not shown).

However, both GST-BCR and BCR-FLAG constructs were consistently difficult to express, with optimal conditions ascertained empirically. Indeed, in cases where other groups have over expressed BCR in HEK293 cells [252] they could only detect BCR by western blot. Briefly, HEK293 cells were most sensitive to plating density (no less than ~80% or $1.8\text{-}2^6$ cells/10cm plate, at time of plating), splitting density during maintenance (no less than 1:4) and number of passages before significantly reduced transfection efficiency (no more than 15-20 passages). Longer than 2-3 minutes incubation with trypsin also reduced transfection efficiency. Several transfection approaches were tested – Cationic lipids (Lipofectamine 2000®, Metafectine®, Fugene®), electroporation and calcium phosphate DNA precipitation (all detailed in Materials and methods). Lipofectamine and metafectine proved the most efficient, as judged by western blotting and monitoring of an empty GFP construct transfected in a parallel (data not shown). The COS-1 and -7 cells were more robust during routine culture and plating densities and responded better to calcium phosphate transfection than other strategies.

BCR transfection in HEK293 cells produced lower levels of BCR compared to COS-1 and COS-7, but still sufficient to assess both kinase activity and 14-3-3 binding without creating a false representation of binding interactions. As COS-1 cells were more robust than HEK293 and gave greater levels of transfection, they were used for routine production of BCR to be used in kinase assays.

BCR produced as a C-terminal FLAG fusion had greater activity than BCR as an N-terminal GST fusion (data not shown). Perhaps due to less steric hindrance near the kinase domain. Also, western blot analysis of GST-BCR pull downs revealed several cross-reacting bands (figure 3.2), perhaps truncated forms of BCR. In addition BCR-FLAG was useful for further studies involving binding experiments with GST-14-3-3.

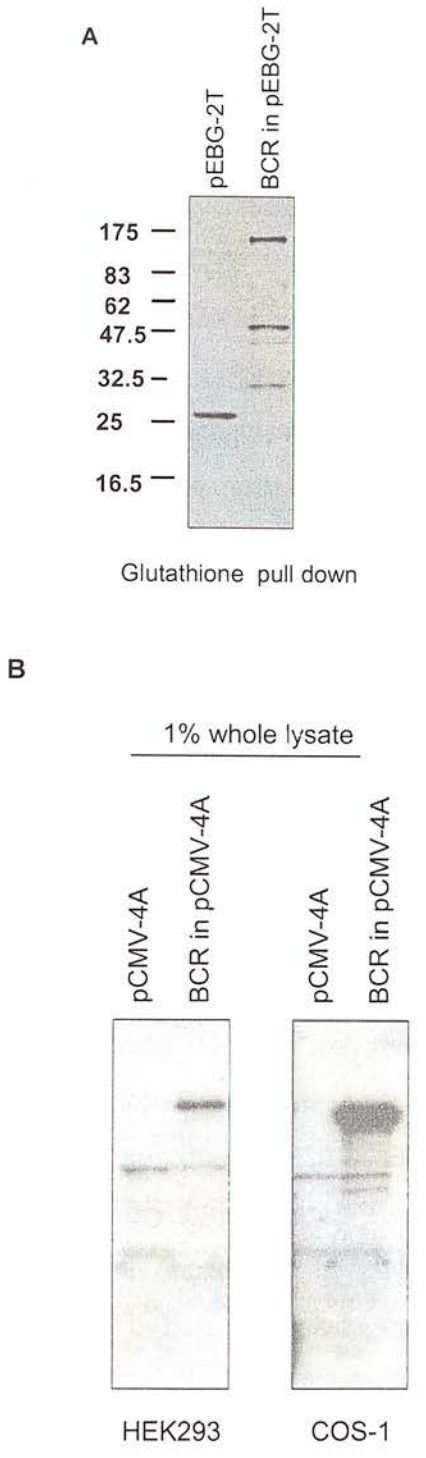

Figure 3.2 Expresion efficiency in COS-1 and HEK293 cell types.
A, COS-1 cells were transfected with either control vector (lane 1) or a GST-BCR construct (lane 2). Glutathione beads were incubated with the cell lysates, washed and western blotted with anti-GST antibodies. **B**, HEK293 or COS-1 cells (indicated) were transfected with empty vector (pCMV-4A) or BCR-FLAG in pCMV-4A, lysed and anti-FLAG immunoprecipitates analysed by western blot using anti-FLAG antibodies.

3.1.3. Optimisation of BCR purification and phosphorylation of 14-3-3 by BCR.

The source of active BCR for most previous studies has been from baculovirus infected insect cell systems (sn2, sf9 cells [44, 243]) or purified from cell types expressing BCR or BCR-ABL such as MDCK or K562 respectively. Composition of lysis buffers used varied in terms of 'phosphate protection' i.e. the inclusion of phosphatase inhibitors, perhaps because at that stage little was known about the intricate regulatory mechanism of BCR. Later studies have shown phosphorylation of Y360 reduces transphosphorylation activity of BCR purified from COS-1 cells [269]. However, previous reports have shown treatment of BCR with phosphatase reduced the interaction with 14-3-3 [44]. So with this in mind, experiments were performed to find optimal conditions where sufficient BCR could be produced in a form able to interact with and phosphorylate 14-3-3. Briefly four plates of HEK293 cells were transfected with equal amounts of BCR-FLAG DNA and each plate was lysed in four different lysis buffers. All buffers had the same basic composition of Tris, salt and detergent (see Materials and methods and table in figure 3.3). The purpose of each buffer is detailed below:

Buffer A – was designed to maintain optimum phosphorylation state

Buffer B – as A, but containing DTT that may reduce the inhibitory activity of $V0_4$ and amount of BCR immunoprecipitated using IgG (by dissociating the light chain), but may improve purification/reduce contaminating proteins

Buffer C to allow dephosphorylation

Buffer D – a buffer similar to one used in an original investigation on BCR [436].

After lysis in the respective buffer, each lysate was clarified by centrifugation and the BCR-FLAG was immunoprecipitated with anti-FLAG antibody. After SDS-PAGE, one IP from each buffer was equilibrated in kinase assay buffer and incubated with 14-3-3 τ and $^{[32]}$P-ATP. 14-3-3 levels in each lysate remained constant, indicating no bias toward lysis efficiency of any buffer (figure 3.3B). Coomassie staining showed that lysing cells in buffer B allowed the most BCR to be immunoprecipitated and therefore, presumably, the highest level of phosphorylation.

Buffer B was chosen for further experiments as it yielded the greatest amount of active BCR.

A

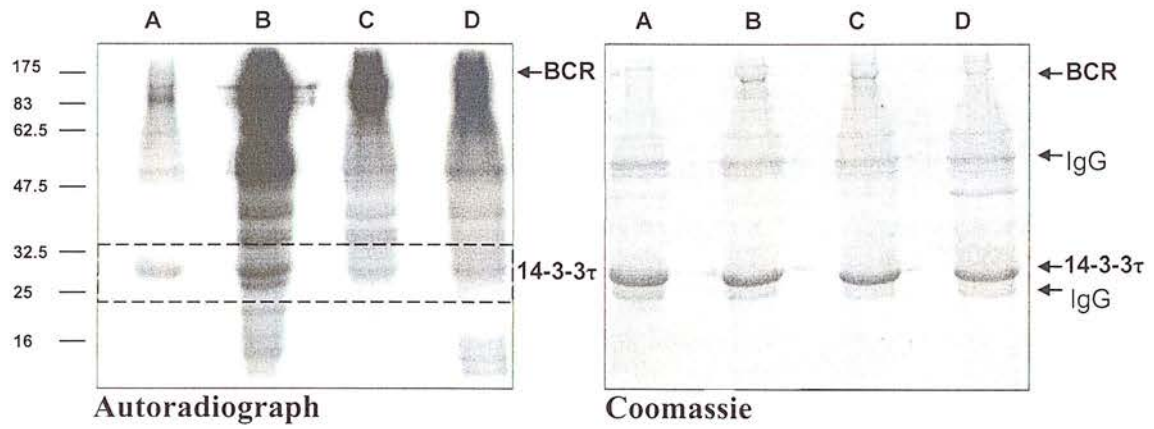

Buffer	DTT	NaF	Na_3VO_4	β-G-P	EDTA	PI
A	0mM	1mM	1mM	5mM	5mM	yes
B	1mM	1mM	1mM	1mM	0mM	yes
C	0mM	0mM	0mM	0mM	0mM	yes
D	0mM	0mM	0mM	0mM	5mM	yes

B

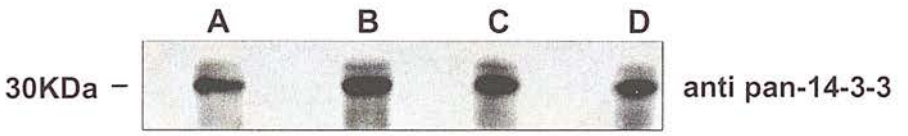

Figure 3.3 Optimisation of lysis buffer for BCR immunoprecipitation and 14-3-3 τ phosphorylation. Equal amounts of bcr-flag DNA were transfected into separate 10cm dishes containing HEK293 cells. After 24 hours, the cells were washed twice in PBS and lysed in buffers A-D containing: Tris (25mM), NaCl (137mM), detergent (NP-40, 0.1% v/v), glycerol (10% v/v), and various other components as listed in the table. The BCR-FLAG was immunoprecipitated using anti-FLAG antibodies, washed extensively and incubated under kinase assay conditions with 5μg of recombinant 14-3-3 τ and [^{32}P]-ATP. The reactions were separated by SDS-PAGE, coomassie stained, dried and exposed to film at -70°C. The autoradiograph on the left shows that that buffer B allowed for the greatest ^{32}P incorporation into 14-3-3 τ compared to other lysis buffers. A coomassie load control is shown in the right hand panel. **B** shows a western blot of 1% of each lysate using a general anti-14-3-3 antibody indicating equal amounts of 14-3-3 present in each lysate. Buffers A-D are indicated.

3.1.4. BCR selectively phosphorylates 14-3-3 isoforms *in vitro*

BCR-FLAG was used for all subsequent kinase assays, due to higher kinase activity. Typically 10μg BCR-FLAG DNA was transfected into HEK293 cells, using Lipofectamine or Calcium phosphate precipitation method (see Materials and methods for details). After 24-36 hours the cells were lysed, incubated with Pansorbin cells, to remove endogenous proteins that may cross-react with protein A, and then clarified by centrifugation. The BCR-FLAG was immunoprecipitated with M2 anti-FLAG antibody conjugated to sepharose beads, washed in lysis buffer followed by equilibration in kinase assay buffer, then incubated with 14-3-3 isoforms in an *in vitro* kinase assay in the presence of $^{[32]}$P-ATP (figure 3.4). The kinase reactions were stopped in Laemmli sample buffer and subjected to SDS-PAGE. Between 2 and 5 μg of 14-3-3 were incubated in the kinase assay, as used in previous reports [147, 187]. Out of the seven 14-3-3 isoforms incubated with BCR kinase, only the 14-3-3 tau and zeta were phosphorylated (figure 3.4). Coomassie load control is shown underneath. The experiment was repeated at least twice for all isoforms assayed in parallel, for other isoforms such as τ and ζ, multiple assays were performed.

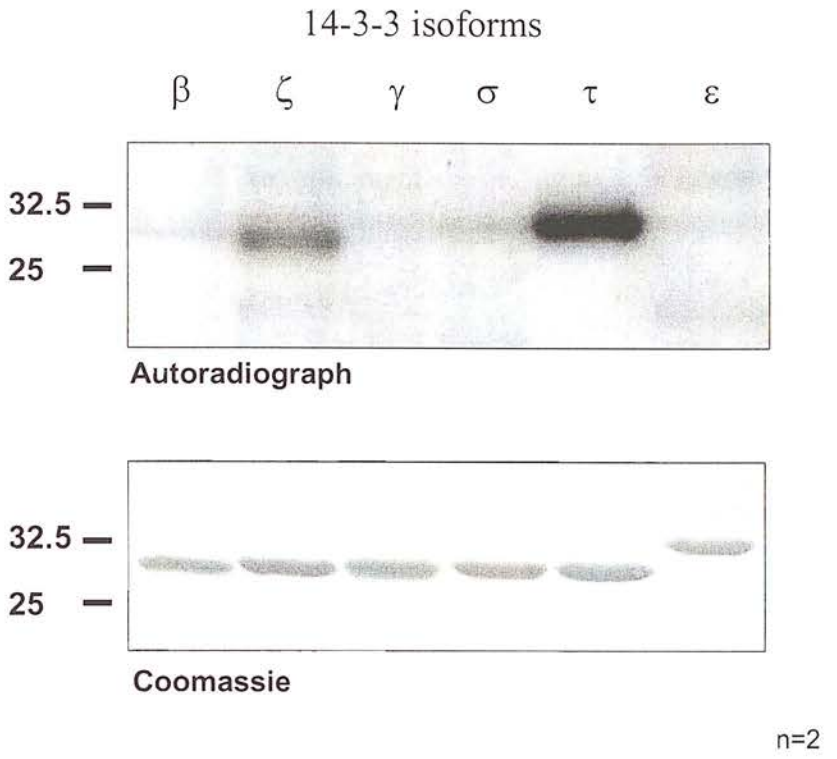

Figure 3.4 BCR kinase phosphorylates only 14-3-3 tau and zeta
All 14-3-3 isoforms were produced and purified as described in materials and methods. Equal amounts of recombinant 14-3-3 were incubated with BCR-FLAG immunoprecipitated from HEK293 cells, under kinase assay conditions. The IPs separated by SDS-PAGE, stained and the autoradiograph shown in the top panel. Coomassie staining shows approximately equal loading.

Figure 3.5 Comparison of the 14-3-3 isoforms around residue 233
14-3-3 τ and ζ share a residue capable of undergoing phosphorylation at reside 233.

3.1.5. BCR phosphorylates 14-3-3 tau and zeta on Ser/Thr 233

Alignment of the mammalian 14-3-3 isoform sequences indicate that the only Ser/Thr residues common to τ and ζ, but not present in the other isoforms, are S233 in 14-3-3 τ and T233 in 14-3-3ζ (see alignment above, figure 3.5). Using Ser/Thr-Ala mutants of these phosphorylation sites, kinase assays were performed as before. Figure 3.6 shows BCR-FLAG incubated with 14-3-3 τ w/t and 14-3-3 τ S233A. Levels of BCR kinase and recombinant 14-3-3 in the assay are approximately equal as judged by coomassie blue staining (right hand panel). Autophosphorylated BCR and phosphorylated 14-3-3 are indicated with arrows. Control immunoprecipitations with empty vector (indicated FLAG in figure 3.6) showing no phosphorylation of 14-3-3. It is clear that BCR kinase only phosphorylates wild type 14-3-3 τ; the S233A mutant shows only a small amount of background phosphorylation, indicating S233 as the phosphorylation site.

14-3-3 ζ and Ser-Ala mutants of the known phosphorylation sites S185 and S233 were next assayed with BCR (figure 3.7). Although phosphorylation of 14-3-3 ζ was low and 14-3-3 τ wt very strong, there is a difference between 14-3-3 ζ w/t and S233 mutant. There is no difference between w/t and S185A, indicating S233 is the site of phosphorylation by BCR. The coomassie stained gel is shown underneath, indicating equal protein loading.

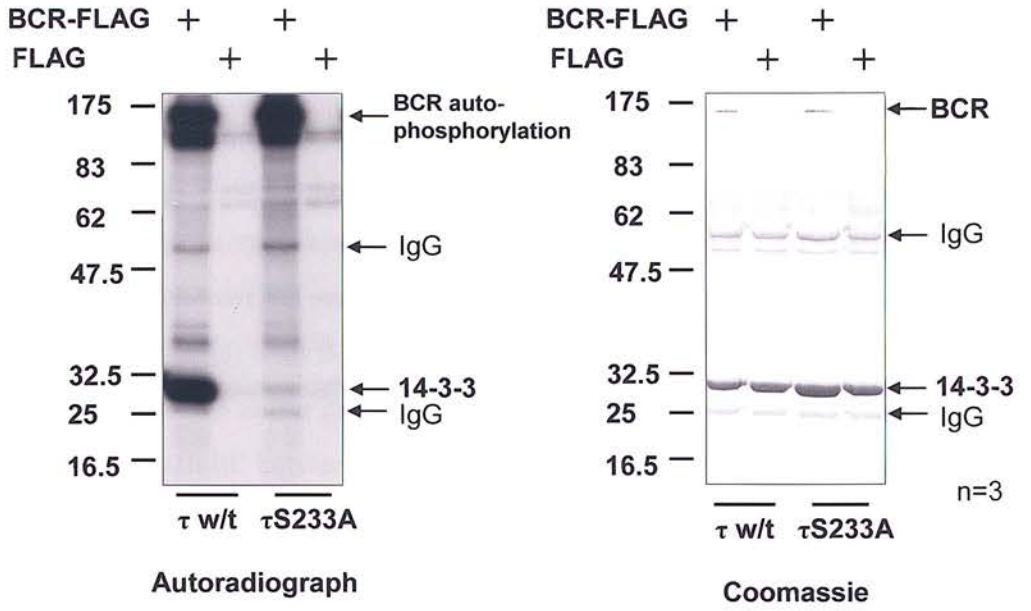

Figure 3.6 A Ser-Ala mutation at residue 233 abolishes phosphorylation of 14-3-3 τ *in vitro*. BCR-FLAG and FLAG vector control transfected cells were immunoprecipitated with anti-FLAG antibodies, washed and incubated with recombinant 14-3-3 τ and τ S233A. An autoradigraph on the left shows phosphorylation of 14-3-3 τ wt, but not τ S233A mutant. A coomassie load control is shown on the right.

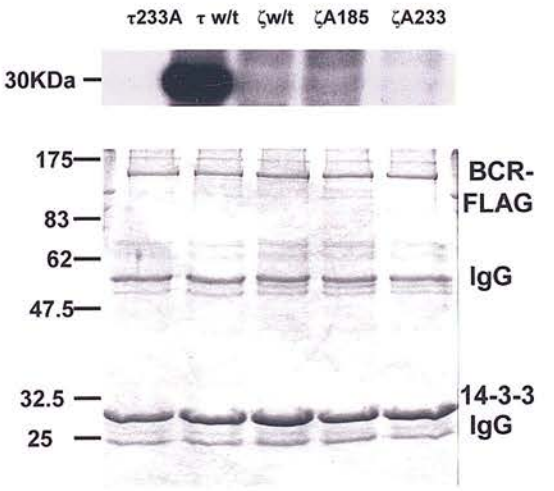

Figure 3.7 A Thr-Ala mutation at residue 233 abolishes phosphorylation of 14-3-3 ζ *in vitro*.
14-3-3 τ and ζ isoforms and mutants were incubated with BCR kinase under kinase assay conditions (see Materials and methods). 14-3-3 τ is clearly phosphorylated more than ζ wt and ζ S185A. ζ S233A mutant is not phosphorylated, indicating that 233 is the site of phosphorylation.

3.1.6. Endogenous CK1 does not co-precipitate and phosphorylate 14-3-3 in BCR-FLAG immunoprecipitations.

Serine 233 was previously identified in our laboratory as a phosphorylation site by CK1α [172]. With the knowledge that CK1α is active toward known substrates at very low concentrations (Thierry Dubois, personal observation), the possibility existed that endogenous CK1 was co-precipitating through endogenous 14-3-3 (in high abundance in cells) with BCR kinase and it was this endogenous CK1 that was phosphorylating 14-3-3 at the 233 site. Additionally, there is reported evidence of 14-3-3 acting as a 'scaffold' between BCR and Raf [187]. Perhaps CK1 could replace Raf in this complex?

To exclude this possibility, two approaches were taken. First, inhibitors of CK1 were used. One is an established CK1 inhibitor, CKI-7, of the isoquinoline sulfonamide family and the other a newly developed ATP-competitive CK1 inhibitor called D4476 (shown in figure 3.11 (from [403]) that was developed in Dundee after these studies had commenced. Secondly BCR was co-transfected into HEK293 cells with CK1α wild type and kinase dead mutant (D136A) and then kinase assayed *in vitro* to see if phosphorylation on 14-3-3 τ could be increased or decreased respectively by out-competing endogenous CK1. The idea being that the transfected kinase dead CK1 would then be 'bridged' to BCR by endogenous 14-3-3.

Figure 3.8 shows BCR incubated with 14-3-3 τ as substrate, with the inclusion of CKI-7 or DMSO as a vehicle control. Positive (14-3-3 τ wt) and negative (14-3-3τ S233A) controls are shown in the two left hand lanes (both without CK1 inhibitor). Using CKI-7 at 100μM did not reduce phosphorylation activity toward 14-3-3, indicating that CK1 is not present in the immunoprecipitation and phosphorylation of 14-3-3 must be due to the BCR kinase. Subsequent experiments using the D4476 inhibitor are shown in figure 3.10.

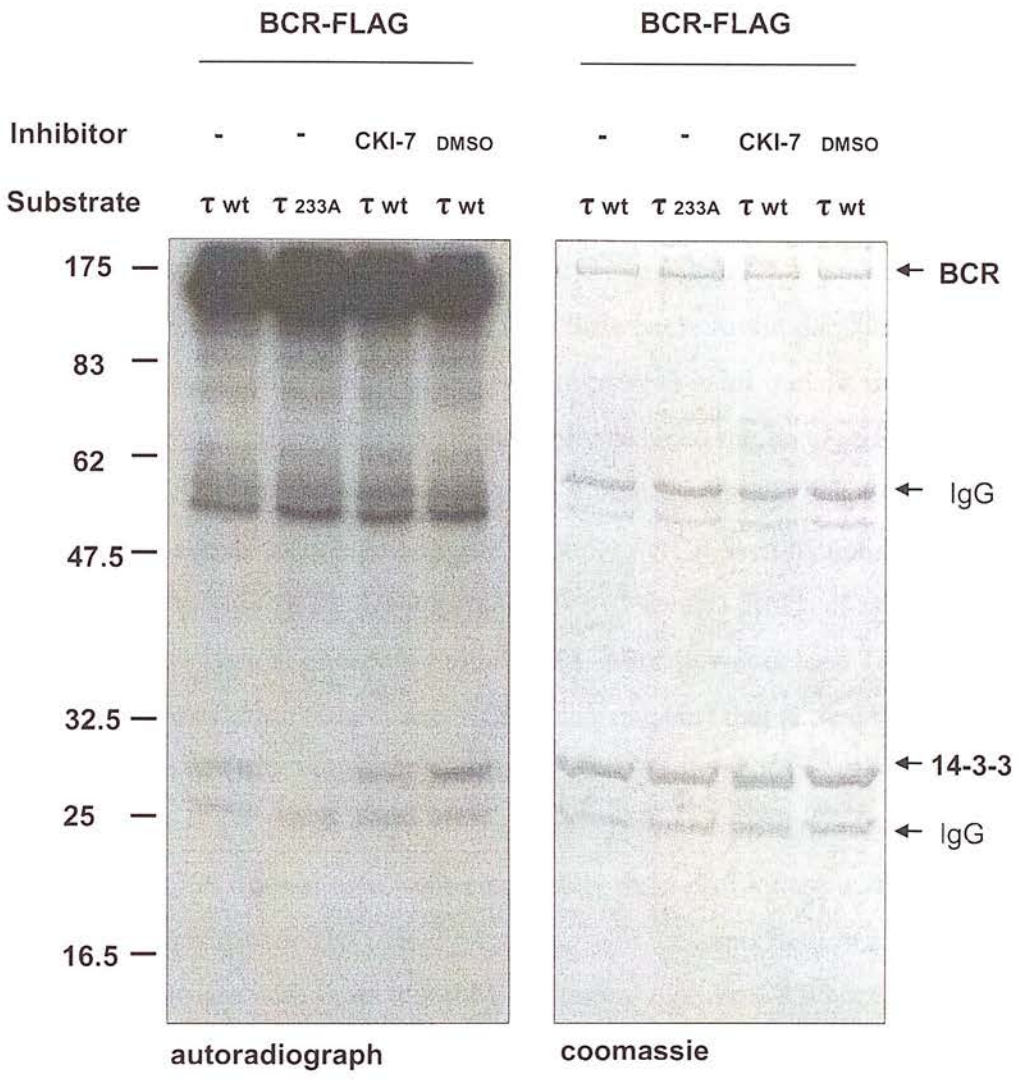

Figure 3.8 CKI-7 has little effect on BCR phosphorylation of 14-3-3.
BCR-FLAG was immunoprecipitated from HEK293 cells as described in Materials and methods. CKI-7 (50μM) was added to the washed immunoprecipitates containing BCR immediately prior to addition of 5μg 14-3-3 τ substrate and [^{32}P]-ATP. 14-3-3 τ S233A was used as a negative control, DMSO was added as a vehicle control. A coomassie load control is shown in the right hand panel.

3.1.7. Overexpression of BCR and CK1

To further investigate the potential CK1:14-3-3:BCR association, BCR-FLAG and HA-CK1α were transfected into HEK293 cells and BCR-FLAG was immunoprecipitated using the M2 α-FLAG antibody. HEK293 cells have plenty of endogenous 14-3-3, so triple transfections with 14-3-3 were not deemed necessary. Equal amounts of BCR, CK1α and empty vector DNA were transfected using Lipofectamine, the cells lysed after 24 hours and then incubated with M2 anti-FLAG antibody. Each washed immunoprecipitate was incubated with 5μg of recombinant 14-3-3 τ with or without the CK1 inhibitor, CKI-7, under kinase assay conditions (figure 3.9). Control transfections using empty FLAG vector (pCMV-4A) only, empty FLAG vector with CK1α wt or kinase dead mutant (lanes 1-5) shows the specificity of the immunoprecipitation, with very little background phosphorylation (lanes 1-5). Although equal amounts of DNA were present in all transfections it seemed co-transfecting CK1 with BCR substantially reduced the level of BCR expressed, as judged by coomassie stain (figure 3.9, bottom panel). The strength of the autoradiograph signal correlated with the amount of BCR seen by coomassie staining, compare lanes 6-10, fig 3.9 (representative of several different assays). Lane 6 of figure 3.9 shows typical phosphorylation of 14-3-3 τ, however lane 7 shows a reduction in phosphorylation (due to less BCR being present) that is then drastically reduced by addition of CKI-7 (lane 8), possibly indicating that CK1 could be phosphorylating 14-3-3 τ. Lanes 9 and 10 show transfection with a kinase dead mutant of CK1 that has been shown to be completely devoid of kinase activity [380]. These kinase assays responded to CKI-7 treatment with the same pattern as with the wild type CK1 (compare with lanes 4 and 5), indicating that the CKI-7 was inhibiting general, background, kinase activity. Interestingly CKI-7 reduces BCR autophosphorylation activity (lanes 8 and 10, figure 3.9); further suggesting that CKI-7 can reduce kinase activity non-specifically. It must be stressed that CKI-7 was used at a high concentration here (100μM) along with pre-incubation of the BCR IP with CKI-7 for one hour. This step was deemed necessary as preliminary experiments showed little effect on inhibition of CK1 at the concentrations published previously e.g. ~9μM in [403, 437] and data not shown. As CKI-7 is an ATP-competitive

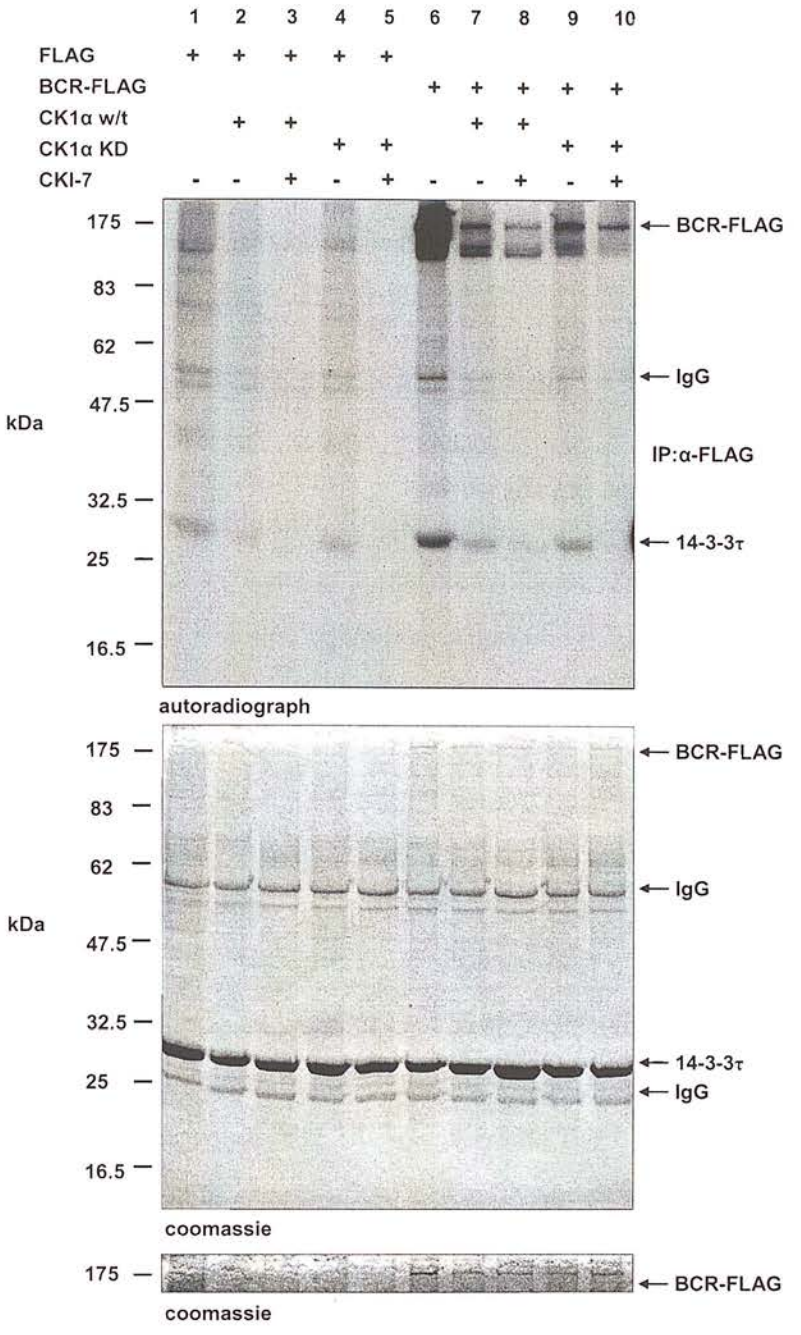

Figure 3.9 Co-expression of BCR and CK1α
BCR-FLAG or empty vector (FLAG) were co-transfected with HA-CK1 and HA-CK1 kinase dead (KD) mutant, BCR immunoprecipitated from lysates using α-FLAG then incubated with/without CK1 inhibitor CKI-7 (100μM), *in vitro* with 5μg 14-3-3 τ and 5μCi [^{32}P]-ATP. Lanes 1-5 are controls with empty vector (FLAG tag only) transfections, lanes 6-10 show immunoprecipitated BCR. Presence or absence of CK1 wt and KD are indicated. BCR levels of transfection can be seen in the coomassie gel and reflected in the autophosphorylation levels in the autoradiograph (top panel). Approximately equal loading of 14-3-3 is also indicated on the coomassie stain, BCR can be seen in the third panel, where the contrast has been increased compared to the middle panel.

inhibitor, concentrations this high may well affect kinases generally. However, CKI-7 has been used at concentrations up to 500μM [438], although no mention of other kinases being affected are mentioned in this study. Although levels of BCR in co-transfection preparations are not equal to BCR transfected alone, if CK1 was capable of co-associating through 14-3-3 with BCR, expression of a kinase dead mutant would be expected to substantially reduce phosphorylation of 14-3-3.

3.1.8. D4476 does not affect BCR kinase auto- or trans-phosphorylation activity.

As previously mentioned, Hidaka and co-workers reported an IC50 of 8.5μM for CKI-7 [437] whilst by Rena et al reported a value of 6μM [403]. In experiments performed here CKI-7 reduced phosphorylation of 14-3-3 only at a high concentration and when pre-incubated for an hour before the kinase assay and at a high concentration (see figures 3.8 with 3.9). D4476 however has recently been shown to be highly specific for CK1 and has an IC_{50} of 0.3μM at 100μM ATP [403]. Therefore the use of D4476 instead of CKI-7 could avoid the unwanted side effect of reducing BCR kinase activity. To this end, separately transfected CK1α and BCR immunoprecipitated from HEK293 cells were assayed for kinase activity in parallel as before, except with the addition of D4476 at 20μM (figure 3.10). The CK1 IPs were included to check the efficacy of the inhibitors. D4476 completely inhibited the ability of CK1α to phosphorylate 14-3-3τ, whereas there was no effect on BCR. CKI-7 was used at 50μM in this experiment and shows no effect on phosphorylation of 14-3-3 by the BCR immunoprecipitate. However partial reduction in phosphorylation of 14-3-3 by CK1 was observed, indicating that the CKI-7 was functioning properly. DMSO alone actually increases phosphorylation compared to kinase assay buffer alone, for both BCR and CK1 – a phenomenon peculiar to DMSO, as occasionally observed previously [439].

These data demonstrate that CK1 was not the 14-3-3 kinase in BCR immunoprecipitates because no reduction in phosphorylation was observed on incubation with 14-3-3 τ under kinase assay conditions, including the highly specific D4476 inhibitor or CKI-7 inhibitor - compare lanes 2, 3 and 4 in each panel, figure 3.10

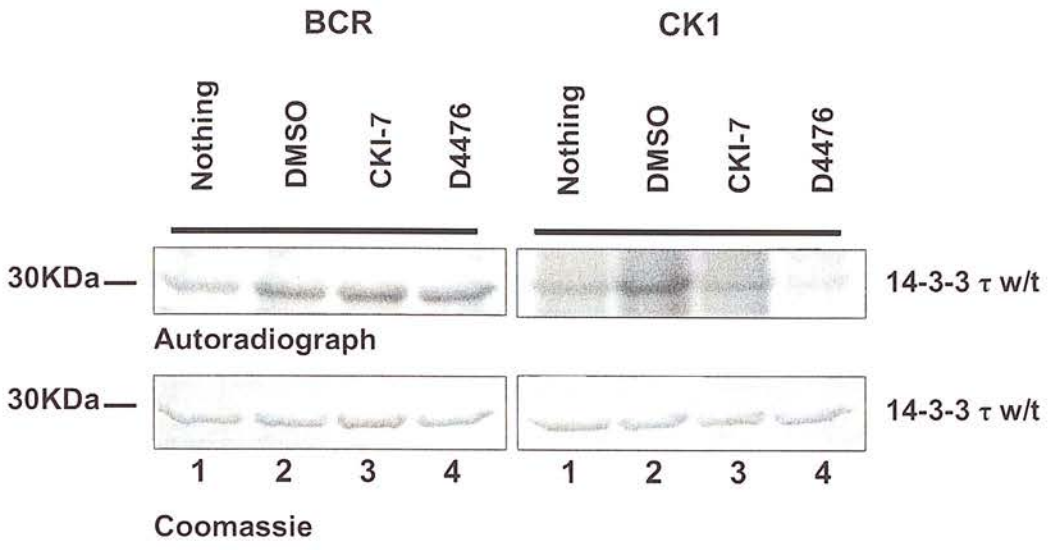

Figure 3.10 CK1 does not co-immunoprecipitate with BCR kinase.
All assays contained 2μg 14-3-3τ and 5μCi [^{32}P]-ATP. Lane **1**, nothing indicates kinase buffer alone; lane 2, DMSO as vehicle control; lane3, CKI-7 in DMSO at a concentration of 50μM and lane 4 contains 20μM D4476 in DMSO. Kinase reactions were stopped in Laemmli buffer, boiled and subjected to SDS-PAGE, coomassie staining and autoradiography as indicated.

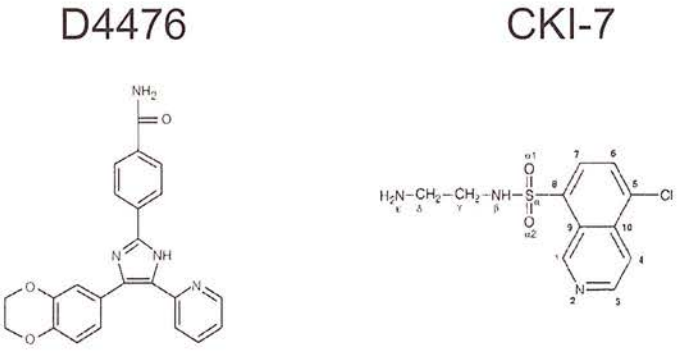

Figure 3.11 Structures of CK1 inhibitors used in this study (from [403] **and** [440]**).** CKI-7 is a well established CK1 inhibitor, whereas D4476 is a newly identified inhibitor, with an IC_{50} approximately ten times lower than CKI-7 [403].

3.2. M2 FLAG antibody precipitates a cyclic A-like kinase: a cautionary tale

During the course of the investigation, constructs of 14-3-3 η and γ in the pGEX-2TK vector (hereafter referred to as '2TKη' and '2TKγ') were used that have the additional motif GSRRASV (a cyclic AMP-dependent kinase phosphorylation site) which remains attached to the recombinant protein, after thrombin cleavage of the GST moiety. The purpose of this is to label recombinant proteins in vitro using ^{32}P and recombinant cyclic A-kinase, allowing easy detection in binding experiments. This vector was not deliberately used for this purpose and was not seen as a potential problem. Specifically, immunoprecipitation with anti-FLAG antibodies has been widely used, shown to be highly specific [441-443] and therefore unlikely to immunoprecipitate protein kinase A. However, M2 α-FLAG immunoprecipitates from BCR-FLAG or FLAG empty vector transfections that had been extensively washed and then incubated with 14-3-3 containing this extra site showed robust phosphorylation of 2TKη an 2TKγ (figure 3.12, lanes 1, 2, 9 and 10). Curiously, BCR-FLAG phosphorylated '2TKη' more than FLAG empty vector alone (compare lanes 1 and 2). This result suggests three possibilities:

(1) BCR phosphorylates a motif similar to PKA and is phosphorylating GSRRASV

(2) BCR phosphorylates a true site on 14-3-3η

(3) PKA associates with BCR and is phosphorylating GSRRASV.

14-3-3 τ, τS233A mutant and 14-3-3 σ were assayed in parallel by way of control and showed predicted results (figure 3.12, lanes 3-8). BCR did not phosphorylate 14-3-3 η or γ when different constructs, devoid of GSRRASV, were used (see figure 3.4).

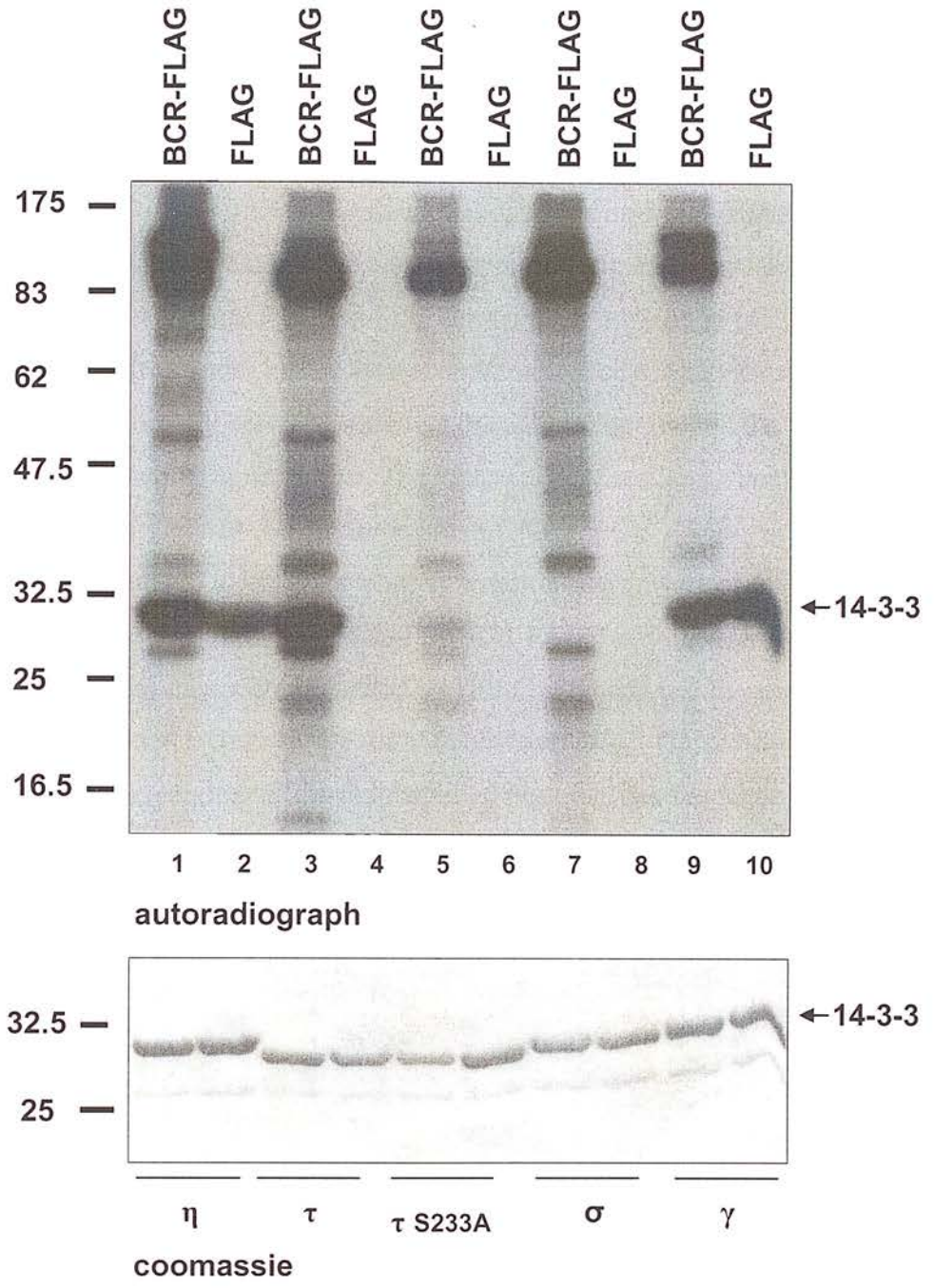

Figure 3.12 M2 FLAG antibody co-purifies with a PKA-like kinase
BCR-FLAG and FLAG empty vector were transfected into COS-1 cells, immunoprecipitated, extensively washed in lysis buffer and incubated with 5μg 14-3-3 protein. 14-3-3 η and γ have a slightly higher molecular weight than 14-3-3 τ due to extra amino acids in the PKA phosphorylation site. Control kinase assays are shown in lanes 3-8, with τ wt as a positive control and τ233A and σ as a negative control. A coomassie load control of recombinant protein is shown in the lower panel.

Pre-conjugated M2 anti-FLAG beads were used to see if the contaminating kinase could be removed, but to no avail (data not shown). Kinase assays of the anti-FLAG beads used to pre-clear lysates with 14-3-3 showed an identical pattern (to figure 3.12) as transfected lysates and for this reason, non-transfected cells were used for further studies. A time course was carried out to establish some kinetic parameters and is shown in figure 3.13A. M2 anti-FLAG antibody and protein A:G beads were added to un-transfected COS-1 cell lysate, centrifuged briefly, washed and divided equally into seven Eppendorf tubes. Equal amounts of 14-3-3γ in pGEX-2TK were added and incubated under kinase assay conditions (excess ATP) for the time indicated. Densitometry was performed on the autoradiogram and the values plotted against time, shown in figure 3.13B. The kinase is very resilient - being able to robustly phosphorylate 14-3-3 for three hours.

Experiments to identify the phosphorylation site(s) were carried out, whereby 14-3-3 γ was phosphorylated, separated by SDS-PAGE and digested with trypsin. The resulting fragments were separated by HPLC and analysed by mass spectrometry and solid phase sequencing (by Dr Andy Cronshaw, EPIC, University of Edinburgh). The peptide corresponding to the radiolabelled peak had the sequence GSRRAS<u>S</u>V, identifying it as the only phosphorylation site (data not shown).

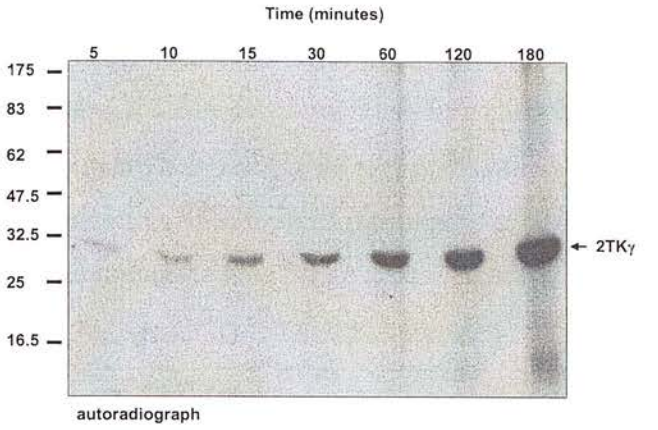

Figure 3.13A Time Course of 14-3-3 γ phosphorylation.
FLAG antibody and protein AG beads from COS-1 lysates were washed and incubated with 14-3-3γ in the pGEX-2TK vector for the indicated times under kinase assay conditions. Reactions were stopped in Laemmli buffer, subjected to SDS-PAGE and the autoradiograph shown.

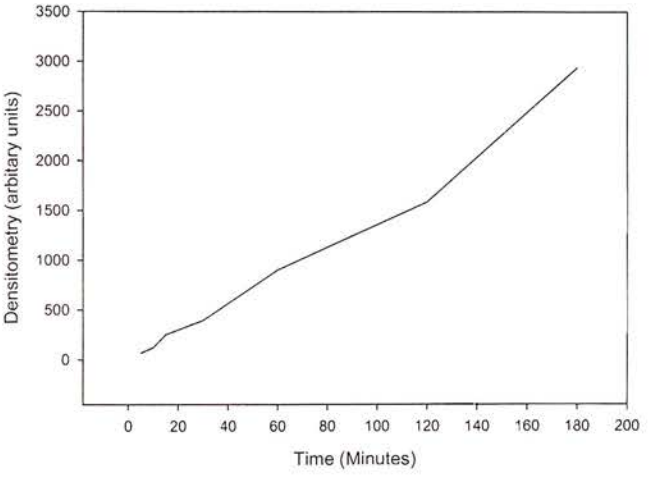

Figure 3.13B Densitometry of 14-3-3 γ phosphorylation.
Each time point of the autoradiograph above was analysed by densitometry using AIDA (see Materials and methods). The values were plotted against time and show no reduction in kinase activity, even after three hours.

3.2.1. PKA co-precipitates with the M2 anti-FLAG antibody from cell lysates

Having established that a PKA motif is phosphorylated by α-FLAG immunoprecipitates, further experiments were performed with the specific, natural inhibitor of cyclic-A kinase, PKAi - a natural inhibitor (this preparation from calf muscle). Empty vector and BCR-FLAG DNA was transfected into cells and immunoprecipitates prepared as before. Both immunoprecipitates were incubated with 2TKγ, either with or without PKAi under kinase assay conditions and the autoradiograph is shown in figure 3.14. The PKA inhibitor eliminates phosphorylation of 2TKγ, suggesting that PKA is the kinase present in the precipitate.

The possibility remained that PKA could be phosphorylating14-3-3 τ on residue 233. This was ruled out by two data: first, no phosphorylation was seen in the empty vector control lane, only in BCR lanes (figure 3.12, compare lanes 3 and 4). Secondly, BCR-FLAG was immunoprecipitated as before and incubated with 14-3-3 τ wt, either with an inhibitor of PKA (PKAi) or PBS (the PKAi solvent). There was no difference in phosphorylation of 14-3-3 τ, on incubation with PKAi, see figure 3.15 top panel.

The only published contaminating, or co-associating protein with the α-FLAG antibody is with a rat Mg^{2+}-dependent phosphatase [444]. Data from this study suggests that a PKA-like kinase can also associate with the M2 α-FLAG antibody.

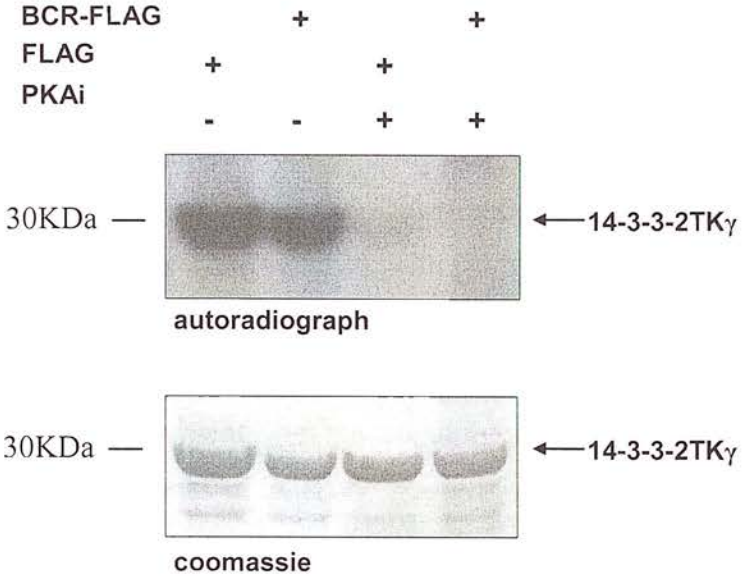

Figure 3.14 PKA co-precipitates with M2-FLAG antibody.
Immunoprecipitates from empty vector (FLAG) and BCR (BCR-FLAG) transfected COS-1 cell lysates were incubated with PKAi under kinase assay conditions for 30 minutes (see Materials and methods). A coomassie load control is shown in the lower panel.

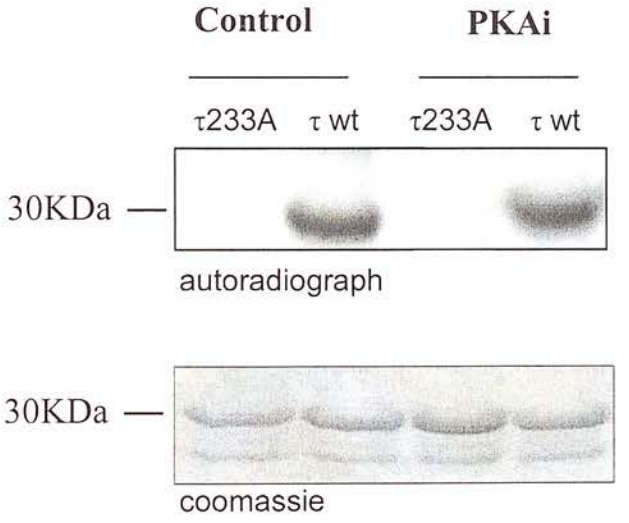

Figure 3.15 co-precipitating PKA does not phosphorylate 14-3-3
BCR-FLAG from COS-1 cells was immunoprecipitated as above and incubate with 14-3-3 τ wt under kinase assay conditions, with the inhibitor PKAi. A coomassie load control is shown in the lower panel.

3.2.2. Investigation of BCR:14-3-3 interaction using an *in vitro* transcription translation system (IVTT)

To investigate the BCR:14-3-3 association, preliminary experiments utilised the IVTT system. BCR was produced in an *in vitro* transcription translation system containing ^{35}S-methionine, the reactions made up to 0.5ml and incubated with GST-14-3-3 ζ (figure 3.16). As a positive control, Delta-catenin was used as it is a similar size to BCR and has been shown to associate with 14-3-3 *in vitro* in our laboratory [445]. Even with a very long exposure, no BCR was seen to associate with 14-3-3 in this system. This could point to the association being phosphorylation dependent as the necessary kinase maybe absent from the reticulolysate, or present in such low abundance that a sufficient level of BCR phosphorylation was not achieved – therefore the interaction was not seen. As this result proved negative, no further 14-3-3 isoforms were tested for association with BCR using this system.

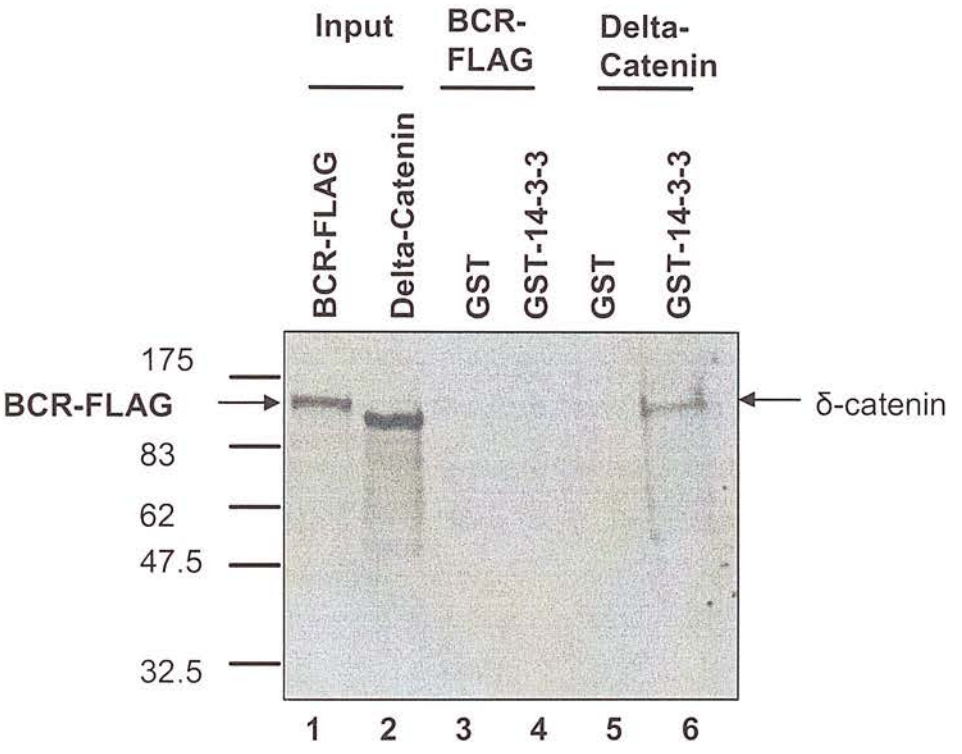

Figure 3.16 *In Vitro* Transcription Translation (IVTT) of BCR-FLAG followed by pull down with GST-14-3-3 ζ

The IVTT product was incubated with GST or GST-Zeta for 4 hours at 4°C. For a positive control, Delta-catenin was also transcribed and incubated with the GST/GST-zeta. BCR-FLAG is apparent as the higher band, δ-catenin as the slightly lower band (compare lanes 1, 2 and 6).

3.2.3. GST-14-3-3 pull down of BCR

Three isoforms of 14-3-3 have been shown to interact with BCR [147, 187]. To investigate if other isoforms can associate, *in vitro* binding assays were performed. To allow for potential post translational modifications, BCR-FLAG was over-expressed in HEK 293 cells and lysed in buffer containing high concentrations of phosphatase inhibitors. The lysate was then clarified by centrifugation, divided equally and incubated with equal amounts of recombinant GST-14-3-3 isoforms. The GST-14-3-3 was recovered by using GSH beads (Amersham) and after extensive washing, the pull downs were subjected to SDS-PAGE followed by western blotting with anti- FLAG antibodies (figure 3.17). As equal amounts of BCR-FLAG transfected lysates were incubated with equal amounts of GST-14-3-3 and the western blots performed at the same time, it is clear that 14-3-3 η and γ 'pull down' more BCR than the other isoforms. It is therefore reasonable to suggest that BCR has higher affinity for 14-3-3 η and γ in this *in vitro* binding experiment.

Phosphorylation of 14-3-3ζ on S233 has been shown to negatively regulate interaction with Raf [145]. A mutant of 14-3-3 ζ, in which Ser233 was mutated to an Asp with the hope of mimicking the phosphorylated residue was also incubated with BCR-FLAG lysate (figure 3.17, lane 9). However, no reduction in binding was seen, indeed a slight increase is apparent. This is due to the fact sometimes the simple introduction of a carboxyl group does not have the same effect as a phosphate group, as, for example, Raf-1 S259D mutation [279].

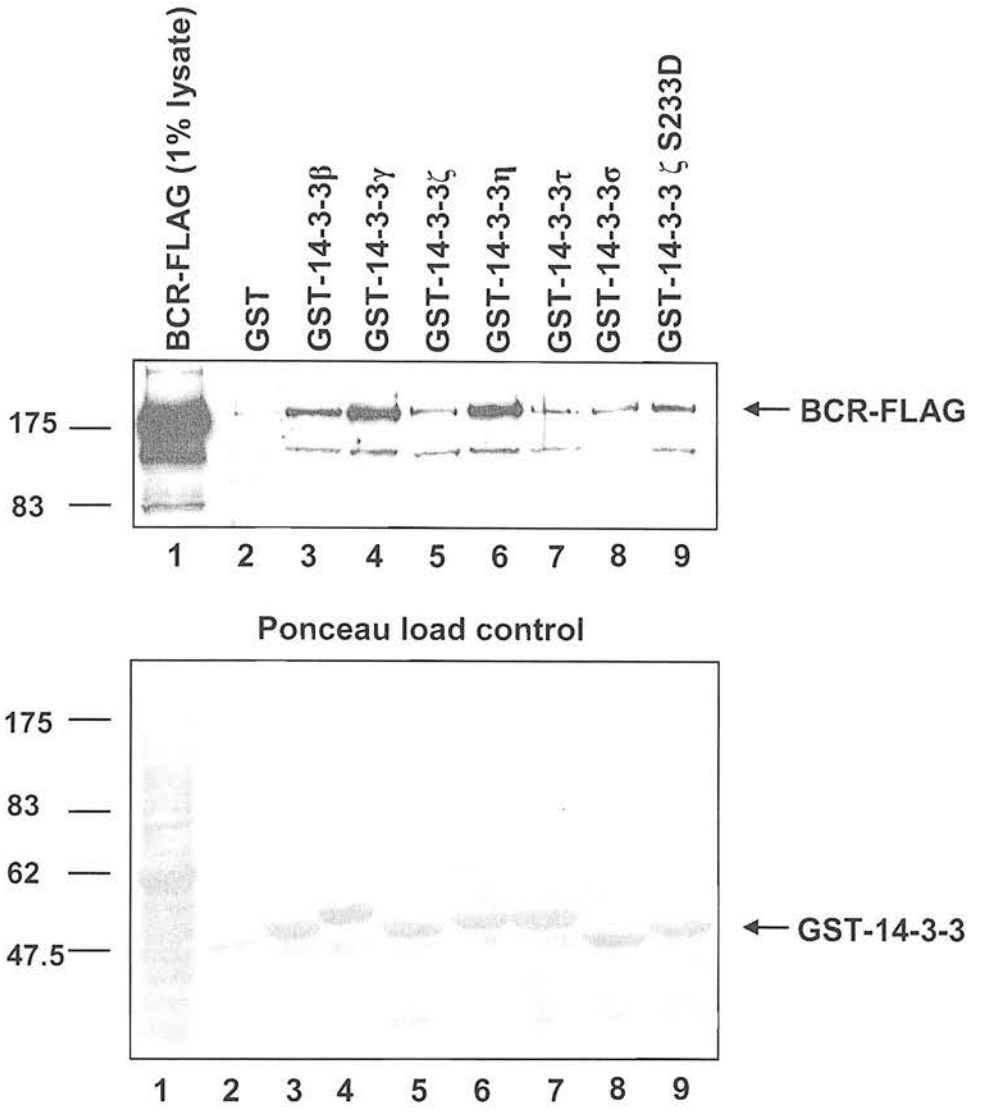

Figure 3.17 BCR interacts with all 14-3-3 isoforms *in vitro*.
HEK 293 cells were transfected with BCR-FLAG, lysed and incubated with the indicated GST-14-3-3 isoform. A loading control for 14-3-3 stained with Ponceau S is shown in the lower panel. The T233D construct was also assayed, lane 9. An equivalent amount of 1% of the BCR-FLAG lysate that used for each incubation is shown in lane 1. A GST-only incubation is shown in lane 2.

3.2.4. Co-expression of BCR and 14-3-3 isoforms in HEK293 cells.

Having shown that 14-3-3 can pull down BCR from a cell lysate, the 14-3-3:BCR interaction was next investigated *in vivo*. BCR-FLAG and 14-3-3 ζ, η, γ (myc tagged) and 14-3-3-τ (HA tagged) constructs were co-transfected into HEK 293 cells. The 14-3-3 was immunoprecipitated with anti-myc or anti-HA antibodies, extensively washed and after SDS-PAGE was western blotted with anti-FLAG antibodies to detect BCR association with 14-3-3. Figure 3.18 shows all 14-3-3 isoforms transfected were able to associate with BCR. Because transfection of 14-3-3 alongside BCR seemed to produce varying levels of both 14-3-3 and BCR in the lysate (compare panels A and B in figure 3.18) interpretation of the data to ascertain preferential binding is difficult. Also 14-3-3 τ was in a different vector and so will be discussed separately (dotted box in figure 3.18). Overall 14-3-3 γ seems to bind more tightly to BCR than 14-3-3 η and ζ, as BCR levels are less in the α-myc-14-3-3 η and ζ immunoprecipitations (panel C, lanes 1, 2, 4). Panel B shows levels of BCR present in the lysate. Although there is less BCR-FLAG in lanes 1 and 2, compared to lane 4, there is significantly more 14-3-3 available for binding BCR (panel A, lanes 1 and 2), further indicating that γ associates with BCR with higher affinity. As 14-3-3 τ is in a different vector and subsequently a different antibody used (α-HA) direct comparisons can't be drawn. However a clear association can be seen, comparing lanes 3 in all three panels in figure 3.18. As the levels of 14-3-3 τ and β in the cell lysates seem more equal, 14-3-3 τ may be binding less tightly than 14-3-3γ. Perhaps, as 14-3-3 τ is a substrate for BCR and as14-3-3 γ is not, BCR phosphorylation may reduce the association with 14-3-3 τ, an observation observed for 14-3-3 ζ:Raf interaction on the equivalent residue after CK1 phosphorylation [172]. 14-3-3 γ on the other hand being non-phosphorylatable may therefore be able to associate without disruption. There is a difference between 14-3-3 ζ and η association with BCR – there is much more 14-3-3 η in the lysate than ζ, yet η still pulls down less BCR, perhaps due to ζ and η binding a different subset of endogenous proteins with different affinities. The data shown in Fig. 3.18 agree with the *in vitro* binding studies (figure 3.17) using recombinant 14-3-3 to capture BCR. As well as verifying that the isoforms ζ and τ, as shown previously, bind BCR [147, 187] the data shown here

indicate that the γ and η isoforms can also associate with BCR *in vivo*, perhaps highlighting a binding preference for 14-3-3 γ.

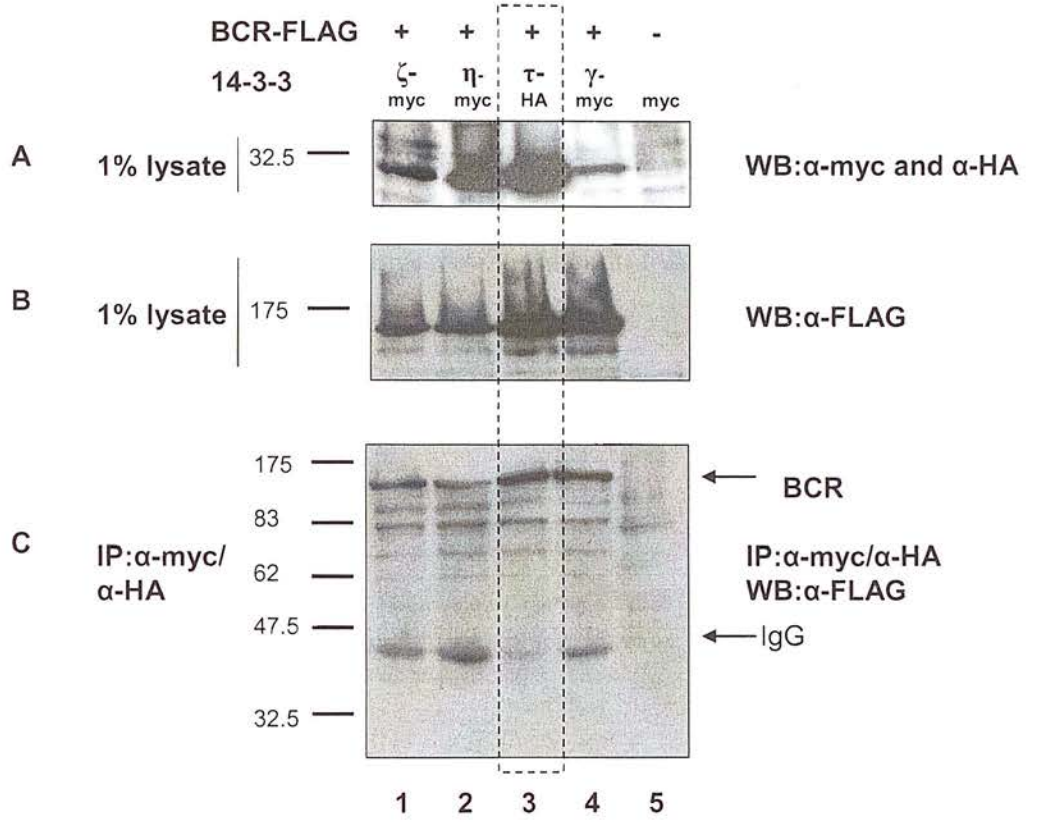

Figure 3.18 Co-transfection of BCR-FLAG with 14-3-3 isoforms.
10μg of each DNA was transfected into HEK293 cells using Lipofectamine 2000 and after 24 hours the 14-3-3 was immunoprecipitated using the indicated antibody. 1% of each lysate was examined by western blot using α-myc, α-HA or α-FLAG antibodies (panels A and B).Western blotting using antibodies to FLAG was used to reveal the association of BCR in the immunoprecipitates (panel C). The dotted box indicates the α-HA immunoprecipitate, for separate analysis from the α-myc IPs.

3.2.5. Endogenous 14-3-3 association with BCR.

Having shown that all recombinant 14-3-3 isoforms examined can pull down BCR *in vitro* and that co-transfection experiments of 14-3-3 with BCR show association *in vivo*, experiments were performed to observe what endogenous 14-3-3 isoforms associate with BCR. To this end, BCR-FLAG from transfected cells was immunoprecipitated and western blotted for *endogenous* 14-3-3 using isoform-specific antibodies (see Materials and methods). This showed that 14-3-3 β, γ, ε, ζ and τ associate with BCR-FLAG (Figure 3.19). 14-3-3 τ is expressed at low levels in 293 cells; nevertheless interaction with this isoform can be seen. The 14-3-3 σ isoform is only expressed at high levels in epithelial cells and is present at such low levels in the 293 cell line that no interaction could be detected. To demonstrate that 14-3-3 isoforms do not bind non-specifically to the IgG:resin, an immunoprecipitation with control IgG was carried out, followed by a western blot with an antibody that recognises all 14-3-3 isoforms (PAN). This highlighted the specificity of immunoprecipitation, as no 14-3-3 was seen (figure 4.19, lower panel, far left lane). Equal amounts of BCR in each immunoprecipitation are indicated by anti-FLAG western (middle panel, figure 3.19).

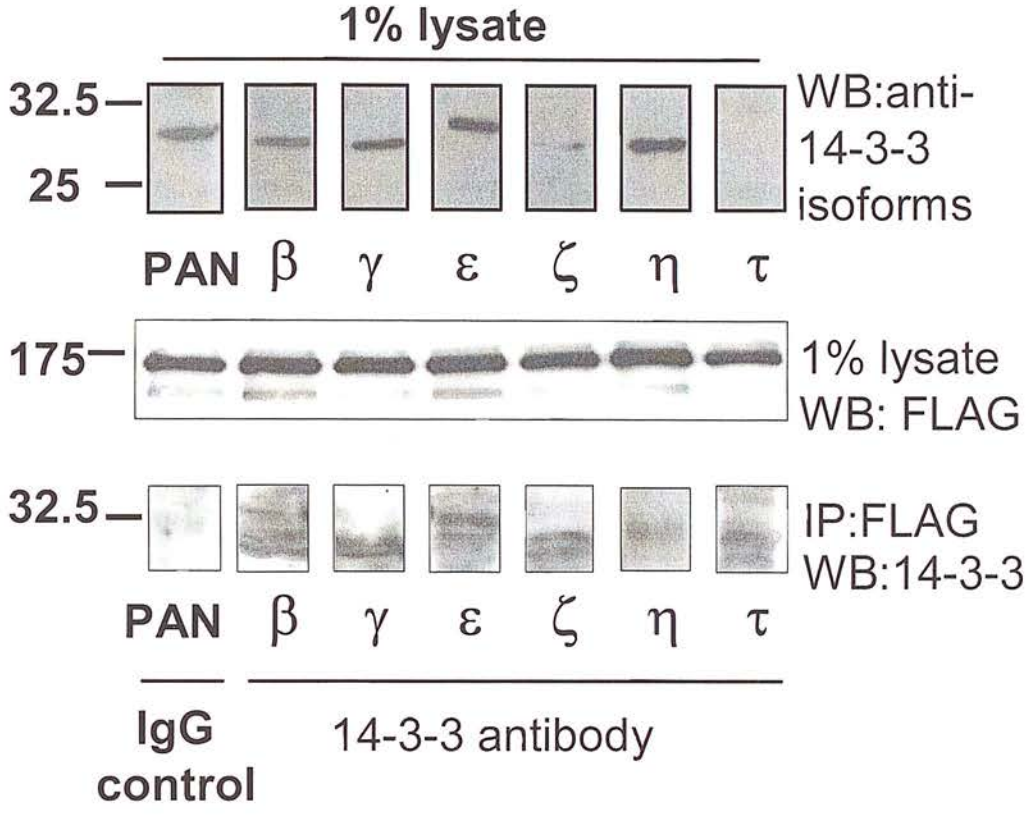

Figure 3.19 BCR interacts with all 14-3-3 isoforms in 293 cells.
293 cells were transfected with BCR-FLAG, the lysates pooled and divided into seven aliquots for immunoprecipitation with anti-FLAG antibody. 1% of the input lysate was western blotted with anti-14-3-3 antibodies to verify levels of endogenous 14-3-3 proteins (top panel). The input lysate (1%) was also western blotted with anti-FLAG antibody (middle panel) to check that BCR-FLAG was expressed and present at an equal level in each IP. The BCR-FLAG was immunoprecipitated with α-FLAG M2 antibody and each α-FLAG IP was western blotted with antibodies specific for a 14-3-3 isoform as indicated (bottom panel).

The two normal genes, bcr and abl, are ubiquitously expressed in normal tissues [207, 208] and their precise role is poorly defined, but aberrant fusion of the two leads to CML as discussed in chapter 1. By exploring the interaction of the normal bcr protein with 14-3-3, data presented here shows an increased repertoire of 14-3-3 isoforms able to interact with the BCR kinase. Also identified was 14-3-3 residue 233 as the site of phosphorylation on the ζ and τ isoforms. This is the same 14-3-3 residue that is phosphorylated by CK1α [172]. Although 14-3-3 η, γ and ε were found to associate with BCR they do not appear to be substrates for the kinase. However, the association of 14-3-3 with BCR may cause a change in sub-cellular location and/or modulate activity of BCR. There is a rational explanation why phosphorylation at Ser233 in this isoform led to the observation by Reuther et al [147] of four phosphopeptide spots on thin layer electrophoresis (TLE). From our own extensive protein sequence analysis ([446] and unpublished) we have shown that tryptic cleavage of 14-3-3 isoforms produces the following two C-terminal peptides: ^{223}(R)DNLTLWTSDS^{233}AGEE<u>C</u>DAAEGAEN^{245} and ^{213}(K)DSTLIMQLL<u>R</u>DNLTLWTSDS^{233}AGEE<u>C</u>DAAEGAEN^{245} . This is due to partial cleavage at arginine223 (underlined). Combined with the unique cysteine residue (underlined) in the tau isoform which may undergoe partial oxidation to cysteic acid under normal conditions of trypsin digestion, phosphorylation at residue 233 would yield two radiolabelled phosphopeptides, multiplied by two due to the partially oxidised cysteine residues (which have a more acidic mobility) producing a total of four spots on TLE.

Several steps were taken to rule out endogenous CK1 phosphorylation of 14-3-3 on residue 233. A kinase dead mutant of CK1 and two CK1 inhibitors were used and the results showed that phosphorylation of 14-3-3 on S233 was solely by BCR. The inhibitors used were CKI-7 (an established CK1 inhibitor) and the other a novel CK1 inhibitor known as D4476 with a ten fold greater IC_{50}. Also shown here is evidence that BCR does not phosphorylate S185 on 14-3-3 ζ any less than wild type, a residue shown recently to be phosphorylated by JNK [170]. The finding that residue 233 on 14-3-3 is phosphorylated by BCR is important, as phosphorylation of this

residue can negatively affect interaction with other signalling molecules [145, 172]. In addition the association of a contaminating kinase, most likely PKA, is reported for the M2 anti-FLAG antibody. The contaminating kinase is most likely PKA based on two pieces of evidence. First, the amino acid sequence of the substrate is known and is a specific PKA phosphorylation motif and, secondly native PKA inhibitor completely wiped out the kinase activity. PKA associating with BCR or, through the M2 antibody (used throughout the study), was also ruled out as the kinase phosphorylating 14-3-3.

CHAPTER 4
CK1α association with 14-3-3.

4. CK1α association with 14-3-3

4.1. Introduction

Previous studies investigating CK1 signalling complexes have revealed a number of interacting proteins with a wide range of functions and localisations (reviewed in [288, 408]. Work in our laboratory found that CK1 co-purified with a number of proteins including the phosphatidylinositol 3,4,5-trisphosphate-binding proteins centaurin-α and -α_1 in brain ([419] and see figure 4.1). The site of interaction on CK1α with centaurin-α and -α_1 was further identified as a loop region contained within the kinase domain comprising residues 217–233 [419]. The original mass spectrometry data that identified CK1α from the co-purifying protein complex showed no indication of phosphorylated CK1α. This was despite identifying the tryptic peptide containing residue S218 in the original data. From crystallographic studies [393, 394], the loop region has been postulated to be a site of interaction with other proteins (see section 1.11). Based on this observation and having identified several other proteins associated with CK1 (figure 4.2), a synthetic peptide was produced corresponding to this region and was shown to bind a number of proteins from brain including: Actin, importin-α1, importin-β, PP2Ac, centaurin α-$_1$ and HMG1 [421]. However, 14-3-3 was not identified during those investigations. This region of CK1 contains a possible 14-3-3 binding motif, if residue S218 were phosphorylated (RTpS^{218}LP). The aim of this study was to examine the possibility that 14-3-3 could interact with this sequence, if phosphorylated within this potential 14-3-3 binding motif. To this end, a similar peptide was synthesised, with the exception of having a phosphorylated S218 residue and an additional N-terminal cysteine: *C*^{213}FNRTpS^{218}LPWQGLKA^{226}. The cysteine was introduced to allow binding to affinity material. This peptide is shown in this chapter (section 4.2) to bind all 14-3-3 isoforms in a phospho-dependent manner whereas dephosphorylation of the peptide actually increased its ability to bind Centaurin-α_1. Similar to many 14-3-3 binding motifs, this sequence contains a reasonable consensus motif for PKA or PKC. To this end, the phosphatase inhibitor, NaF, and/or purified PKA catalytic subunit was added to CK1α produced in an IVTT system and binding assays were performed

using GST-14-3-3 ζ. Binding was shown to increase on treatment with PKA/NaF, indicating a phospho-dependent binding mechanism.

Various CK1α truncation mutants (designed to examine the region around S218 in the interaction) were expressed in an IVTT system and the results suggested that S218 is not the only site essential for 14-3-3:CK1α association. On further inspection of the CK1α sequence, however, another possible 14-3-3 mode 1 binding site is present – at S242. The presence of this site might explain why a CK1α truncation mutant lacking S218, but containing S242 could still bind 14-3-3. In addition, the crystal structure of CK1 reveals that S242 would be accessible for binding (see figure 4.13). To address this possibility, site directed mutagenesis was performed to create both single and double Ser-Ala mutations of residues S218 and S242.

First, experiments designed to see if endogenous 14-3-3 could associate with CK1α in mammalian cells revealed that 14-3-3 η and 14-3-3 γ associated more strongly than other isoforms. Therefore for future binding experiments using cell culture, the association of endogenous 14-3-3 η and γ with CK1α was examined. To try to increase the amount of phosphorylated CK1α present in the cell, HEK293 and COS-7 cells transfected with HA-CK1α in the presence of db-cAMP to (either directly or indirectly) stimulate phosphorylation of sites S218 and S242. This produced a transient increase in binding to 14-3-3 η.

In HEK293 cells, the CK1α mutant S218A had slightly reduced ability to associate with 14-3-3, whereas mutation of S242A reduced the binding almost completely. The double mutation completely abolished binding, indicating that S242 is part of the major binding site. This could be due to different binding affinities of 14-3-3 for these sites or different levels of kinase activity and/or kinase selectivity toward these sites. A further possibility is that the S242 interaction is behaving like a 'gatekeeper', binding 14-3-3 first, then allowing S218 (with presumably lower affinity) to bind into the other binding pocket of the 14-3-3 dimer, according to the 'gatekeeper hypothesis' [139].

Analysis of the crystal structures of 14-3-3 and CK1 using the molecular docking program 'DOT' and 'ZDOCK' through a web-based interface called ClusPro (http://nrc.bu.edu/cluster/) [447] revealed potential insights into the interaction.

Further analysis by Paul Taylor, Edinburgh University, suggested CK1α could only bind one site at any one time, due to steric hindrance. While computer-aided modelling cannot rule out the possibility of CK1α binding into each binding pocket of the 14-3-3 dimer, major conformational changes would have to occur.

The identification of binding partners for CK1α that may affect sub-cellular location is important, as CK1α has few other modes of regulation (see chapter 1.4). The complex with centaurin-α_1 is of particular interest as centaurin-α_1 is predominantly localised at the plasma membrane and so may target CK1 to substrates. A summary of interactions examined in this chapter are shown in figure 4.2.

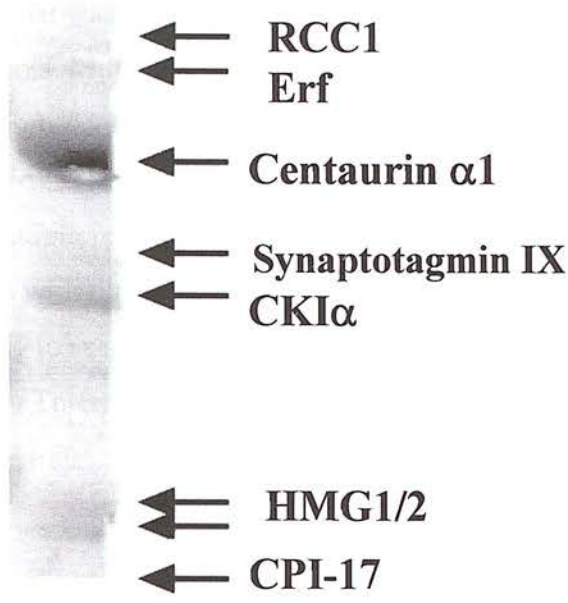

Figure 4.1 Centaurin-α1 co-purifies with CK1α from pig brain.
Other signalling molecules were also discovered, as indicated by arrows. Identification was by mass spectrometry, from Dubois et al, from excision of the coomassie stained bands [419].

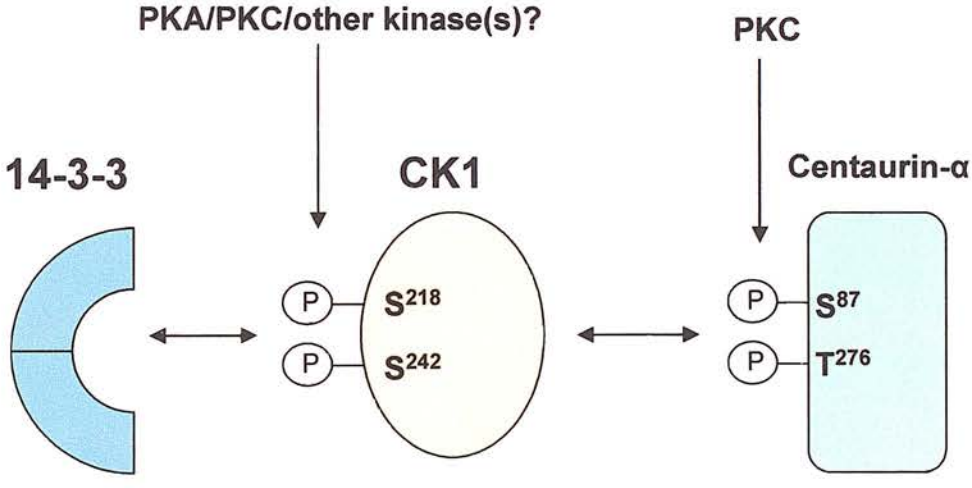

Figure 4.2 CK1 binding partners investigated in this study.
CK1 associates with 14-3-3 in a phospho-dependent manner. Centaurin-α_1 is phosphorylated by PKC on residues S87 and T276.

4.2. Results and Discussion

4.2.1. DNA manipulation and purification of recombinant proteins

A construct of CK1α was obtained from Peter Roach, and cloned into pcDNA3 by Thierry Dubois. Mutants of HA-CK1α were produced according to the Stratagene Quickchange protocol as described in Materials and methods. All recombinant 14-3-3 isoforms were produced as GST-fusions, except epsilon that was produced as a maltose binding protein (MBP) fusion, see Materials and methods section 2.10, and cleaved with thrombin or factor Xa – see appendix A1 for SDS-PAGE/coomassie staining to assess purification). CK1ε was from David Virsup and was cloned into pS752 by Thierry Dubois [419].

4.2.2. Peptide synthesis and clean up of the synthetic peptide by HPLC and coupling of peptide to Sulfolink column.

The synthetic peptide C^{214}FNRTpS^{218}LPWQGLKA^{226} has a high propensity to form inter-peptide disulphide bonds and so was delivered with the inclusion of a large amount of DTT. See Materials and methods for details on synthesis. In order to successfully couple the peptide to Sulfolink beads (Pierce) the DTT was removed by reverse phase HPLC. The peptide was loaded onto a Vydac 'low TFA' column and a gradient of 0% to 100% acetonitrile resulted in the peptide eluting after 26 minutes (see figure 4.3). The fractions were immediately neutralized with Tris base and then incubated with equilibrated Sulfolink beads (see Materials and methods) at a ratio of approximately 1mg peptide per 1ml beads. The amount of peptide bound was assessed by the use of 5,5'-Dithio-bis(2-Nitrobenzoic acid) (DTNB or Ellman's reagent). A binding efficiency of ~90% was calculated (data not shown). A sample of this peptide was checked for integrity using mass spectrometry by Rob Wakefield, University of Edinburgh (data not shown).

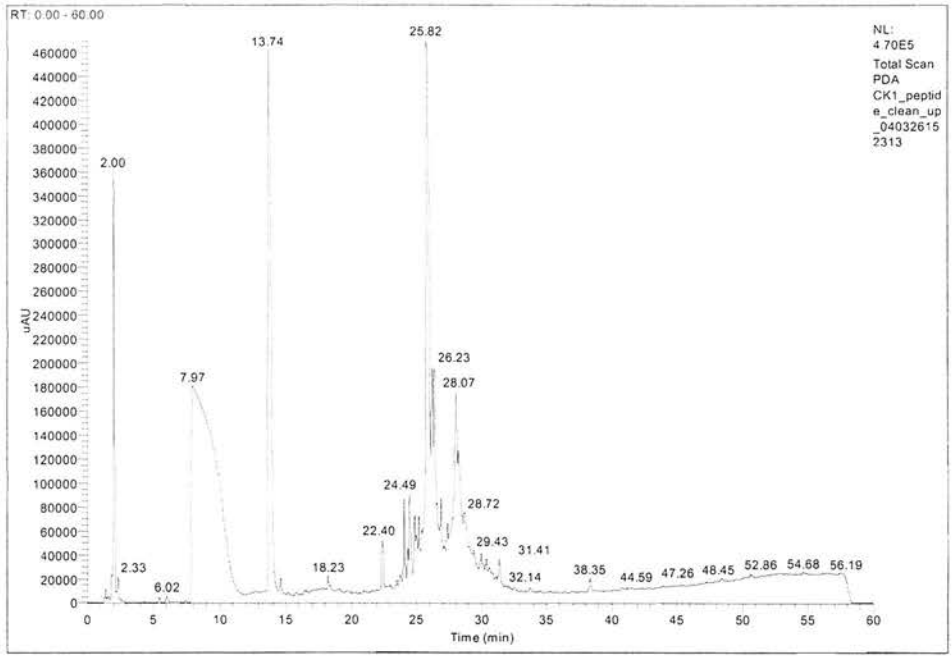

Figure 4.3 HPLC purification of the CK1 peptide corresponding to residues *C*-^{214}FNRTpS^{218}LPWQGLKA^{226}.

A Vydac C18 'low TFA' column was equilibrated with a shallow gradient from methanol to water, then 1mg CK1 peptide (in 500µl water) was injected onto the column, followed by 10 minutes of water. Then a gradient of 100% water to 100% acetonitrile, both with the addition of 0.01% trifluoroacetic acid (TFA) was applied, see Materials and methods for exact details. DTT and other impurities washing through can be seen eluting at time points 2, 7 and 13 minutes. A sample of the eluant at 26min was analysed by mass spectrometry and confirmed to be the phosphopeptide. This fraction was used for the study.

4.2.3. A phospho peptide corresponding to residues 214-226 of CK1α binds all 14-3-3 isoforms.

To investigate whether the peptide corresponding to the proposed 'docking loop' of CK1 could bind 14-3-3, equal amounts of peptide-coupled beads (~20μg/14nmol peptide) were aliquoted into Eppendorf tubes and made up to 0.5ml in binding buffer (see Materials and methods). After incubation with each recombinant 14-3-3 isoform (~15μg) and extensive washing, the bound 14-3-3 was analysed by SDS-PAGE and coomassie blue staining (figure 4.4). This shows that all 14-3-3s associate with the peptide, albeit to different extents. Comparing lanes 1 from all panels, 14-3-3 γ, η, and then β appear to bind most, then τ, ζ and ε all bind to a similar extent, with σ binding to a much lesser extent. Treatment of the beads with λ phosphatase (PPase) almost eliminated binding to 14-3-3 (lanes 2). Control experiments with incubation of the PPase with the inhibitor VO_4 (lanes 4) indicate that the interaction is phospho-dependent and the effect was not due to PPase masking the binding of the peptide to 14-3-3, for example. Lane 3 shows that adding the phosphatase inhibitor VO_4 alone does not affect the interaction. Surface plots of each panel, indicating intensity of each band (created using ImageJ) were created to aid visualisation of the gels. It is worth noting that even if overall binding levels are low (ε and σ) an identical pattern of binding is observed, after the inclusion of phosphatase inhibitor (Na_3VO_4). Two repeat experiments were conducted, the bands were measured by densitometry and the results are summarised in figure 4.5. This shows the intensity of 14-3-3 bands from phosphatase untreated and treated phospho-peptide beads for each isoform. Although the fairly large error bars in figure 4.5 should be noted, the overall binding capacity changed consistently with phosphatase treatment. Confidence that the interaction is phospho-specific can be drawn from the finding that binding of all 14-3-3 isoforms altered in a similar way. It is also worth noting that the phosphopeptide coupled beads used in these binding experiments were dephosphorylated in a large batch and then divided equally for incubation with 14-3-3. As all 14-3-3 isoforms were incubated with identically treated beads, an accurate comparison can be drawn between binding assays.

Figure 4.5B shows the change in 14-3-3 binding, after dephosphorylation of the beads, taking the amount of 14-3-3 bound to phosphorylated beads as 100%. The

difference to dephosphorylated beads was then calculated to show the difference dephosphorylation makes to each isoform. This shows that dephosphorylation of S218 reduces the binding by a relatively similar amount for five of the 14-3-3 isoforms. The binding pattern of 14-3-3 ζ and η are more distinct, with dephosphorylation of ζ creating the biggest change in binding, in other words ζ binds more specifically to the phospho peptide, than the dephospho peptide. On the other hand, the change in η binding shows relatively less discrepancy toward binding dephosphorylated S218 peptide.

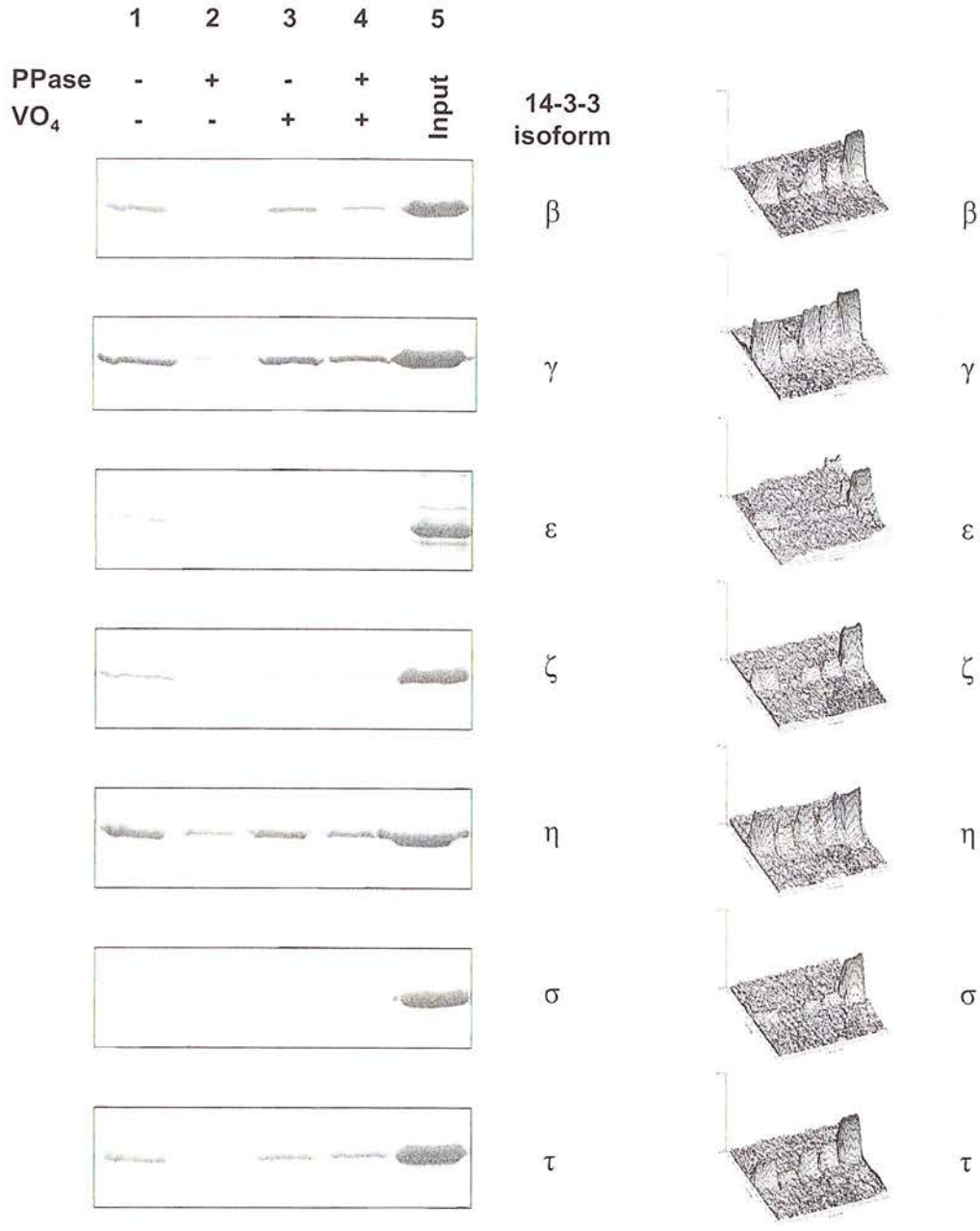

Figure 4.4 A phospho-peptide corresponding to residues 213-226 of CK1α associates with all 14-3-3 isoforms in a phospho-dependent manner. Sulfolink® beads conjugated to ~20μg peptide corresponding to residues 214-226 (C-FNRTS^{P}LPWQGLKA) of CK1α, were incubated with all 14-3-3 isoforms (panels 1-7) washed three times and subjected to SDS-PAGE followed by coomassie blue staining. Lane 1: shows untreated beads; lane 2: beads treated with lambda phosphatase (PPase); lane 3: control whereby beads were incubated with the phosphatase inhibitor sodium orthovanadate (Na_3VO_4); lane 4: control with phosphatase inhibitor (Na_3VO_4) and phosphatase together; lane 5: indicates the amount of 14-3-3 incubated with the peptide beads (input). Surface plots of each panel are shown on the right hand side (performed using ImageJ, from http://rsb.info.nih.gov/ij/).

A

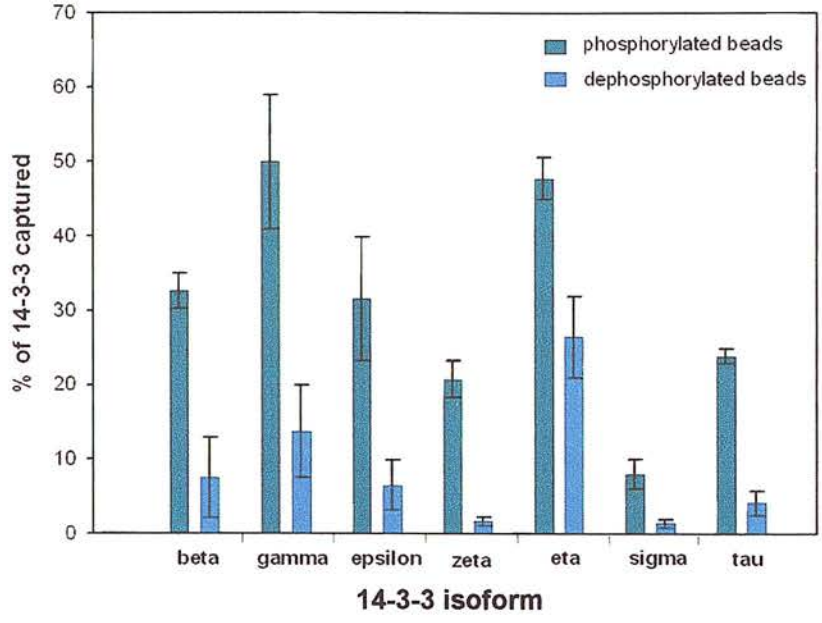

n=3

B

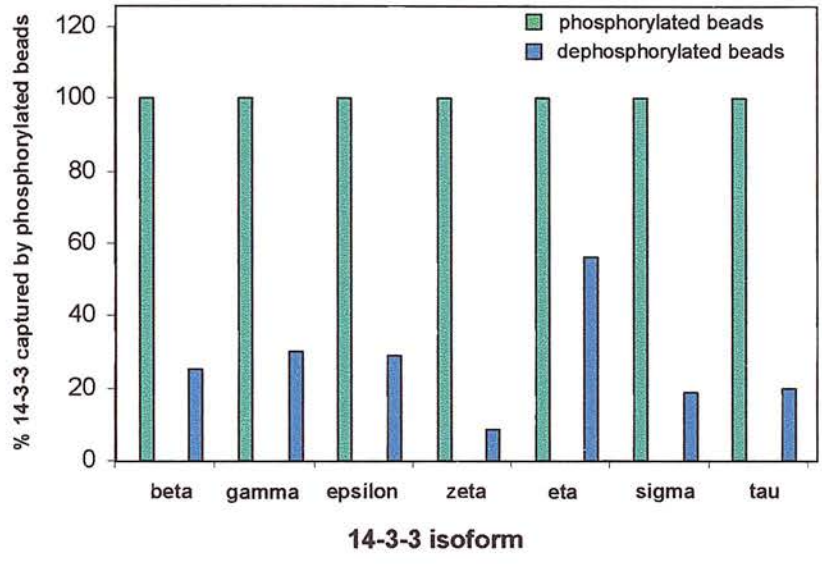

Figure 4.5 Densitometry analysis of CK1 phospho peptide binding to 14-3-3
A, ImageJ software was used to measure the density of bands corresponding to 14-3-3 and the standard deviation plotted using Sigmaplot. Values shown are the percentage of the intensities of 14-3-3 captured compared to the intensity of 14-3-3 applied to the beads. **B**, percentage change in 14-3-3 binding after dephosphorylation of the pS218 peptide, taken from data in **A**. The amount of 14-3-3 captured by phosphorylated beads was taken to 100%, with the amount captured by dephosphorylated beads, multiplied by the same factor, to show comparative binding differences between 14-3-3 isoforms.

4.2.4. The CK1α phosphopeptide binds centaurin-α_1, only when dephosphorylated.

We have previously shown that Centaurin-α_1 associates directly through the domain, shown here to interact with 14-3-3, using a non-phosphorylated peptide [419]. To determine if phosphorylation of S218, within this region, could affect this interaction, GST and GST-Centaurin were incubated with approximately 14nmol phospho-peptide coupled to beads and an equal amount of dephosphorylated peptide-beads. The incubation times and dephosphorylation conditions were identical to those in the previous experiment (4.2.3). The amount of GST-Centaurin-α_1 bound was assessed by SDS-PAGE and coomassie staining (Figure 4.6). Interestingly GST-Centaurin-α_1 showed very little association with the phospho-peptide, but significantly increased association was seen after dephosphorylation of the peptide (compare lanes 2 and 3, left panel). The GST control shows no association with the peptide-beads (right panel, lanes 2 and 3).

This result extends previous findings that centaurin-α_1 associates with CK1 region 214-226 [419] and furthermore reveals that phosphorylation of S218 negatively affects the interaction.

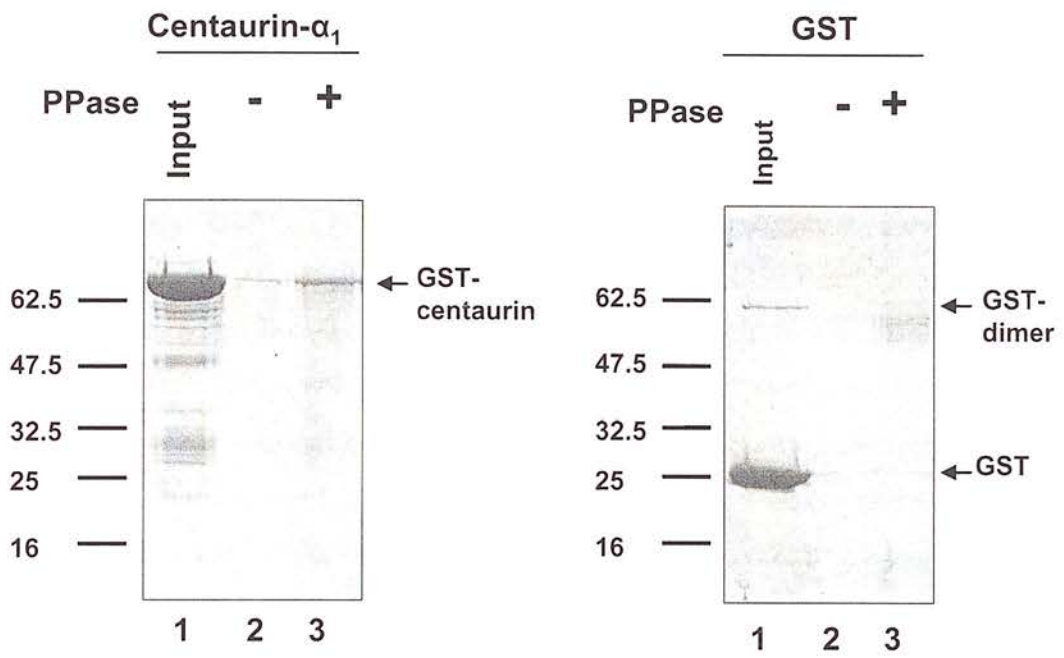

Figure 4.6 Centaurin interacts with region corresponding to CK1 214-226 only if dephosphorylated

Sulfolink® beads conjugated to ~20μg peptide corresponding to residues 214-226 (C-FNRTS^{P}LPWQGLKA) of CK1α, were incubated with GST-centaurin-α_1, washed three times and subjected to SDS-PAGE followed by coomassie blue staining. The left panel in lane 1 shows a representative amount of GST-centaurin-α_1 that was incubated with the peptide-beads; lane 2 shows untreated (phospho-peptide) beads and lane 3 shows beads containing dephosphorylated peptide. Right Panel shows the same conditions, except that GST was incubated with the peptide beads.

4.2.5. CK1 expressed by IVTT associates with 14-3-3, increasing with NaF treatment.

After observing that 14-3-3 can associate with a region of CK1α in a phospho-dependent manner, intact CK1α w/t was produced as a ^{35}S-labelled *in vitro,* transcription, translation (IVTT) product and incubated with GST-14-3-3. Additionally, attempts were made to increase the phosphorylation state of CK1α by kinase(s) present within the reticulocyte lysate, by incubating the lysate with phosphatase inhibitor. To this end, the IVTT reaction was made up to 1mM NaF after the 90 minutes needed to produce CK1α and incubated for a further 30 min. A control reaction was also incubated for an extra 30 min, with 4µl water added (the NaF solvent). A sample of the reaction both with and without NaF treatment is shown in lanes 1 and 2 of figure 4.7. Figure 4.7 shows HA-CK1α w/t incubated with GST-14-3-3 ζ and GST as a control. After incubation with NaF, 2-3 times more CK1α associated with 14-3-3 than a control incubation without NaF (compare lane 4 with 6, left panel). Densitometry was used to quantify the increase (figure 4.7, lower panel). A coomassie stain on the right shows that equal amounts of GST and GST-14-3-3 were incubated with the IVTT reaction. A similar experiment was carried out in which recombinant PKA was added to the assay after IVTT synthesis, along with NaF, however no additional increase was seen (data not shown). These results suggest that a basal level of interaction is possible between 14-3-3 ζ and CK1α, which may be phosphorylation dependent. Certainly conditions to preserve phosphorylated residues further increases the affinity of CK1α toward 14-3-3 ζ.

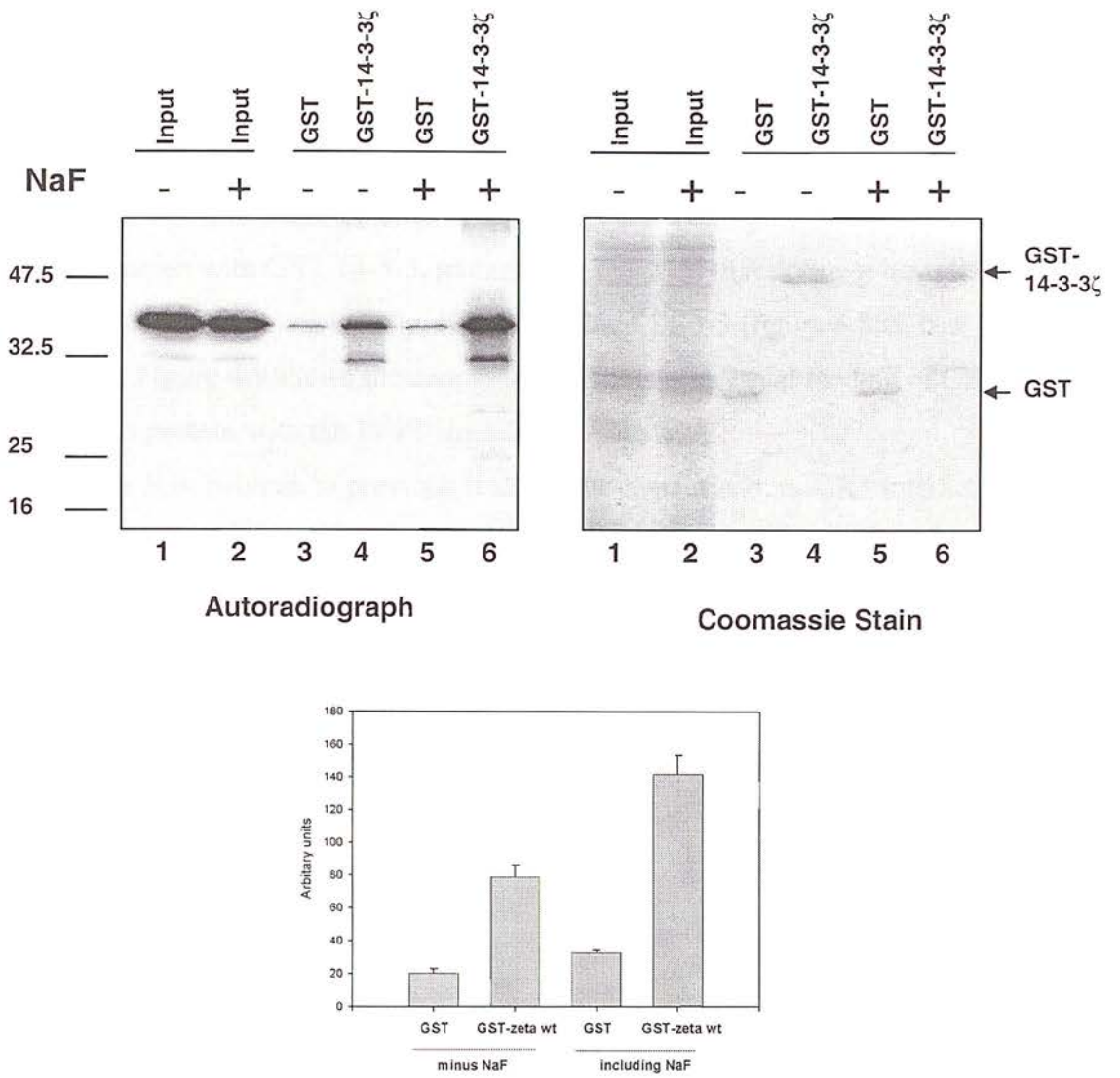

Figure 4.7 14-3-3 binds CK1α in a phospho-dependent manner.
Phosphatase inhibitor (NaF) treatment of CK1α produced in an IVTT system increases its ability to bind 14-3-3. CK1α was produced in the reticulolysate for 90 minutes, then incubated with NaF for an additional 30 minutes at 30°C. Lanes 1 and 2 show 2% of the lysate used for the untreated and phosphatase inhibitor treated (NaF) IVTT reactions. Lanes 3 and 5 show GST controls; lanes 4 and 6 show GST-14-3-3 ζ associating with HA-CK1α. Densitometry analysis of three binding experiments shows a consistent increase in binding with phosphatase inhibitor treatment.

4.2.6. All CK1α truncation mutants associate with 14-3-3.

To further investigate whether residues 214-226 of CK1 are involved in binding to 14-3-3, truncation mutants of CK1α were produced by IVTT (^{35}S-labelled) and incubated with GST or GST-14-3-3 ζ (as in figure 4.7). The truncation mutants were designed to eliminate the region around S218 and a schematic is shown in figure 4.8A, indicating predicted molecular weights. Two percent of the IVTT reaction was analysed by SDS-PAGE (figure 4.8B) to assess the expression level of each mutant. Mutants 4 and 5 yielded much smaller amounts compared to the other truncation mutants, but could be detected after a longer exposure (indicated in separate panel). After incubation with GST-14-3-3, mutant m5 (233-325) that does not have the region 214-226 was, unexpectedly, still able to bind 14-3-3 (figure 4.8.C, lane 12, asterisked). Figure 4.9 shows the coomassie gel indicating equal loading of GST and GST-14-3-3 protein with the IVTT reactions.

This is in contrast to previous findings for centaurin-α, α_1:CK1 interaction [419]. One explanation is another possible 14-3-3 binding site in this region, consisting of KKMpS^{242}TP where pS242 would be phosphorylated for 14-3-3 binding. From the tertiary structure, S242 appears to be more structurally constrained in comparison to S218 (figure 4.12.) and hence had not been considered in initial investigations. However, residue S242 would still be accessible for both phosphorylation and 14-3-3 binding, see figure 4.12.

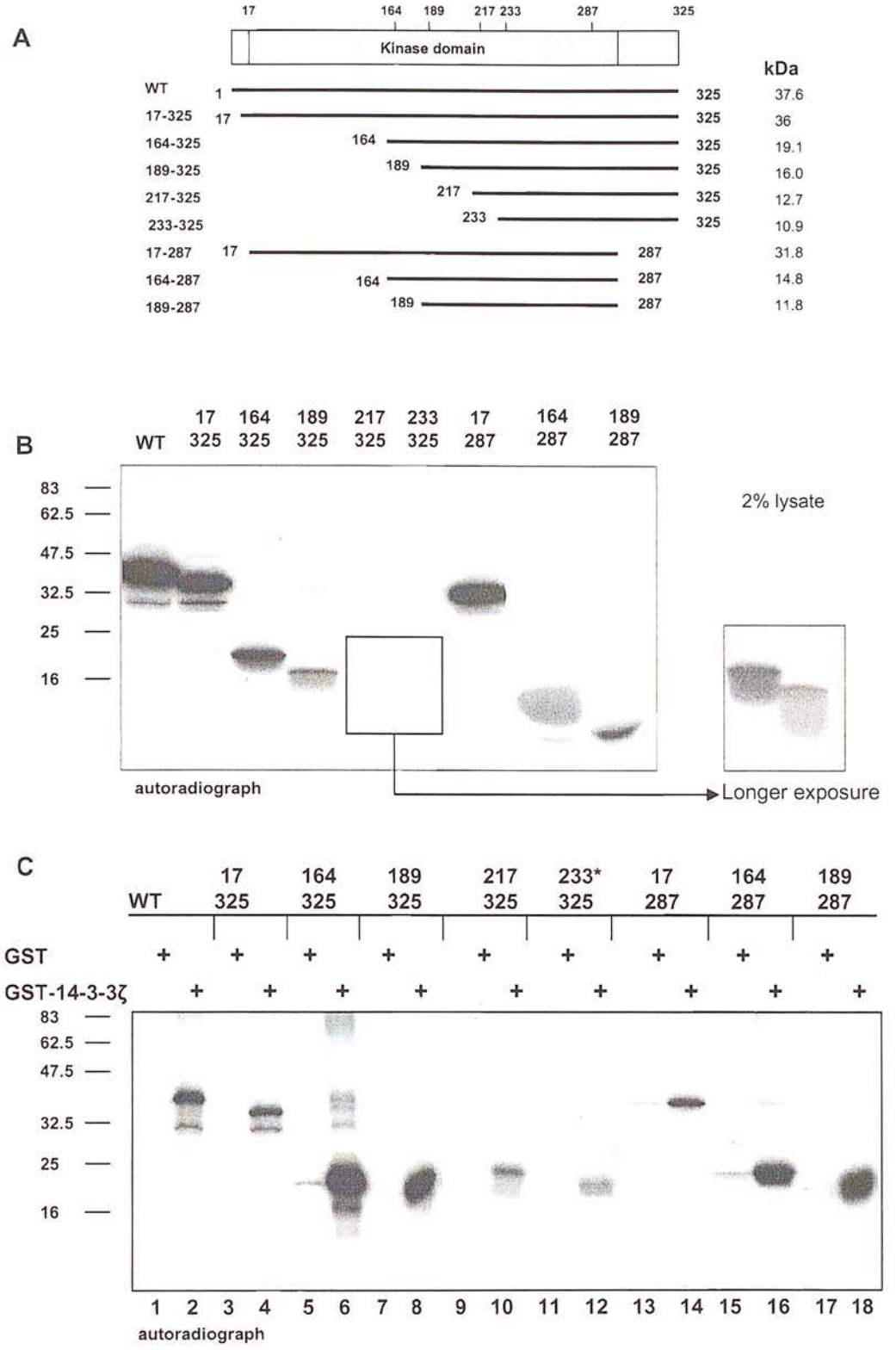

Figure 4.8 14-3-3 associates with all truncation mutants of CK1α.
A, schematic of truncation mutants; **B**, autoradiograph of 2% ^{35}S-labelled IVTT reaction; **C**, autoradiograph of a GST pull down from the reticulocyte lysate, using 10μg GST or 10ug GST-14-3-3 ζ, as in figure 4.7., separated by 15% SDS-PAGE.

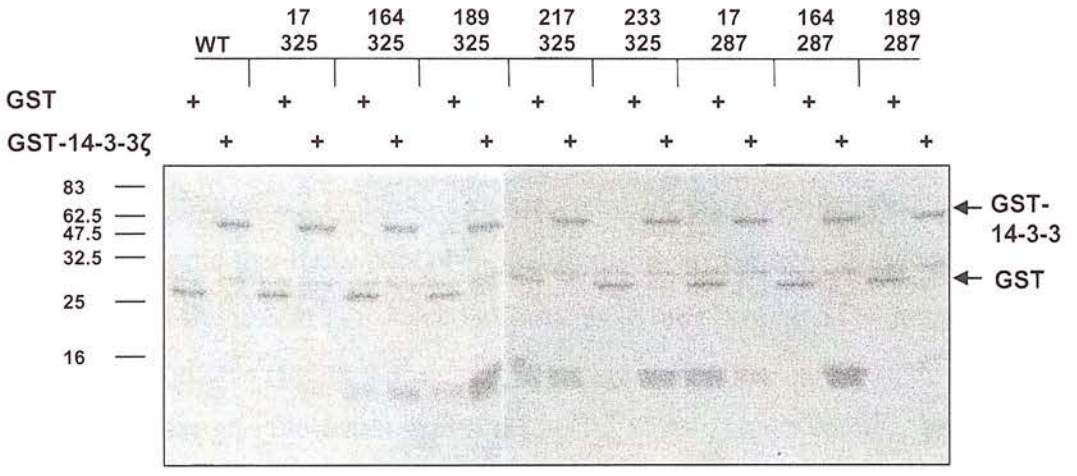

Figure 4.9 Coomassie stain of figure 4.9, showing equal loading of GST and GST-14-3-3 ζ.
This figure refers to the autoradiograph in figure 4.8.

4.2.7. CK1α associates predominantly with 14-3-3 η and γ in un-stimulated HEK 293 cells.

To analyse the possible 14-3-3:CK1 interaction *in vivo*, a screen of CK1α binding affinity to the five 14-3-3 isoforms present in abundance in HEK293 cells was performed. HEK293 cells were transfected with 10μg HA-CK1α wt for 24 hours in the presence of serum and lysed in buffer containing high concentrations of phosphatase inhibitors (see Materials and methods). The HA-CK1α was then immunoprecipitated using HA antibody-conjugated agarose beads (Roche) for three hours at 4°C, washed three times in lysis buffer, re-suspended in Laemmli buffer, subjected to SDS-PAGE and transferred to nitrocellulose membrane. The use of pre-conjugated anti-HA beads allowed clear detection of 14-3-3, as using protein AG Sepharose produced unsatisfactory high levels of cross reaction with the secondary antibody (data not shown). The membranes were then probed with anti-14-3-3 antibodies (figure 4.10A), stripped and re-probed with anti-HA to check similar levels of CK1α were present in each binding assay (4.10B). A control IP is shown in lanes 2 in which a non-HA-immune IgG was incubated in the cell lysate.

This established that, in unstimulated cells, native endogenous 14-3-3 η and γ gave the strongest signal. Although it is not possible to discern quantitatively the binding affinity for the η and γ isoforms, due to the differing titres of the antibodies (discussed in chapter 1.2.7), there is still a clear difference between the isoforms. It is interesting to note that these two 14-3-3 isoforms identified here as associating to a greater degree in vivo, are the same isoforms as in the phospho S218 peptide:14-3-3 binding experiments (figure 4.4).

Interestingly, these two isoforms (14-3-3 η and γ) have recently been identified as being able to bind CaMKK, whereas 14-3-3 ζ and ε were not [35] and in so doing, protect it from dephosphorylation in HEK293 cells. The sequence similarity between these two isoforms, at the amino acid level, could explain the similar binding characteristics (see section 1.1.2) and [448].

4.10A

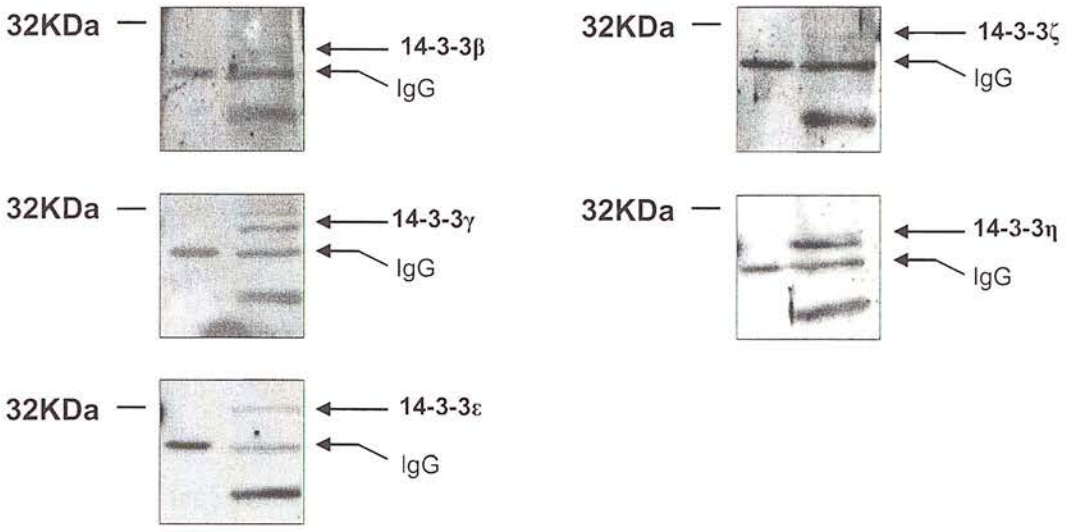

4.10B

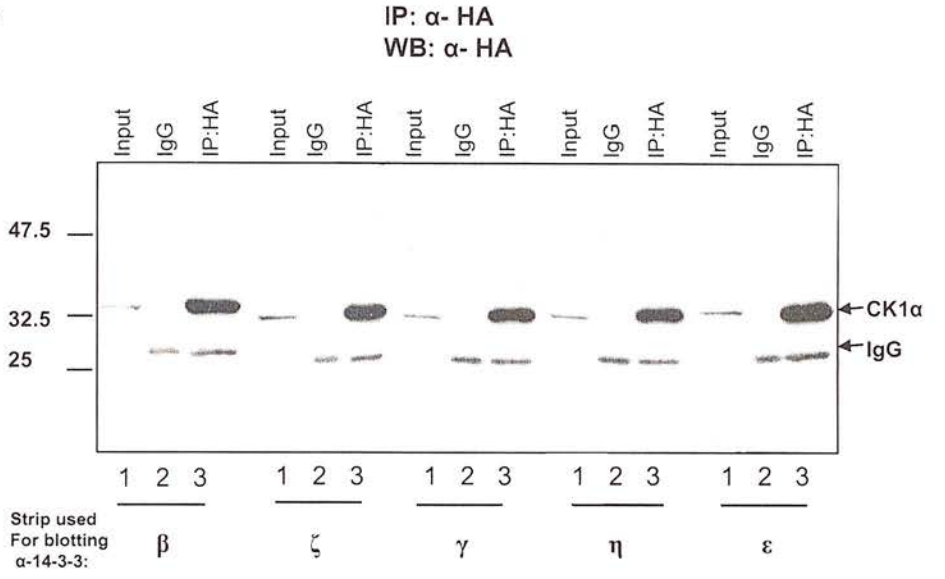

Figure 4.10 14-3-3 isoforms bind CK1α *in vivo*.
A, Unstimulated HEK293 cells were transfected with HA-CK1α and immunoprecipitated with anti-HA-conjugated beads. After extensive washing in lysis buffer, the immunoprecipitates were subjected to SDS –PAGE and western blotted with antibodies specific to 14-3-3 isoforms. Left hand lanes show a non-immune IgG control and right lanes show the α-HA IP. **B,** Equal amounts of CK1 were present for assessment of 14-3-3 immunoprecipitations. Re-probe of figure **4.10A** with anti-HA antibody, showing in lanes 1: 1% of the lysate in unstimulated HEK293 cells transfected with HA-CK1, lanes 2 anti-HA-conjugated agarose beads and in lanes 3 immunoprecipitated HA-CK1 using anti-HA-conjugated agarose beads.

4.2.8. 14-3-3 isoforms associate with CK1α *in vitro*

To confirm the 14-3-3 isoform specificity of the 14-3-3:CK1α interaction, a reciprocal experiment was performed, whereby recombinant 14-3-3 was added to lysates from cells transfected with HA-CK1α. Recombinant GST and GST-14-3-3 protein were incubated with the cell lysate, pulled down and western blotted for CK1α using α-HA antibodies. The results are very similar to the CK1α immunoprecipitations shown in figure 4.10, with GST-14-3-3 η and γ pulling down the most CK1α, followed by β and ζ (figure 4.11). A GST control lane is shown in the far left hand lane and, in the far right hand lane, 1% of the lysate that was incubated with each 14-3-3 isoform. Densitometry analysis of the blot was performed to determine binding levels between 14-3-3 isoforms. The amount of CK1α pulled down by each 14-3-3 isoform was compared to the amount of CK1 present in 1% of the lysate. This is the amount of HA-CK1α available for binding and values for 14-3-3 isoform binding are plotted as a percentage of this (figure 4.11C). It is clear that 14-3-3 η interacts substantially more strongly than other isoforms, followed by γ, β, τ, ζ and σ does not interact at all. Equal amounts of recombinant protein were added as judged by ponceau staining (figure 4.11, panel B).

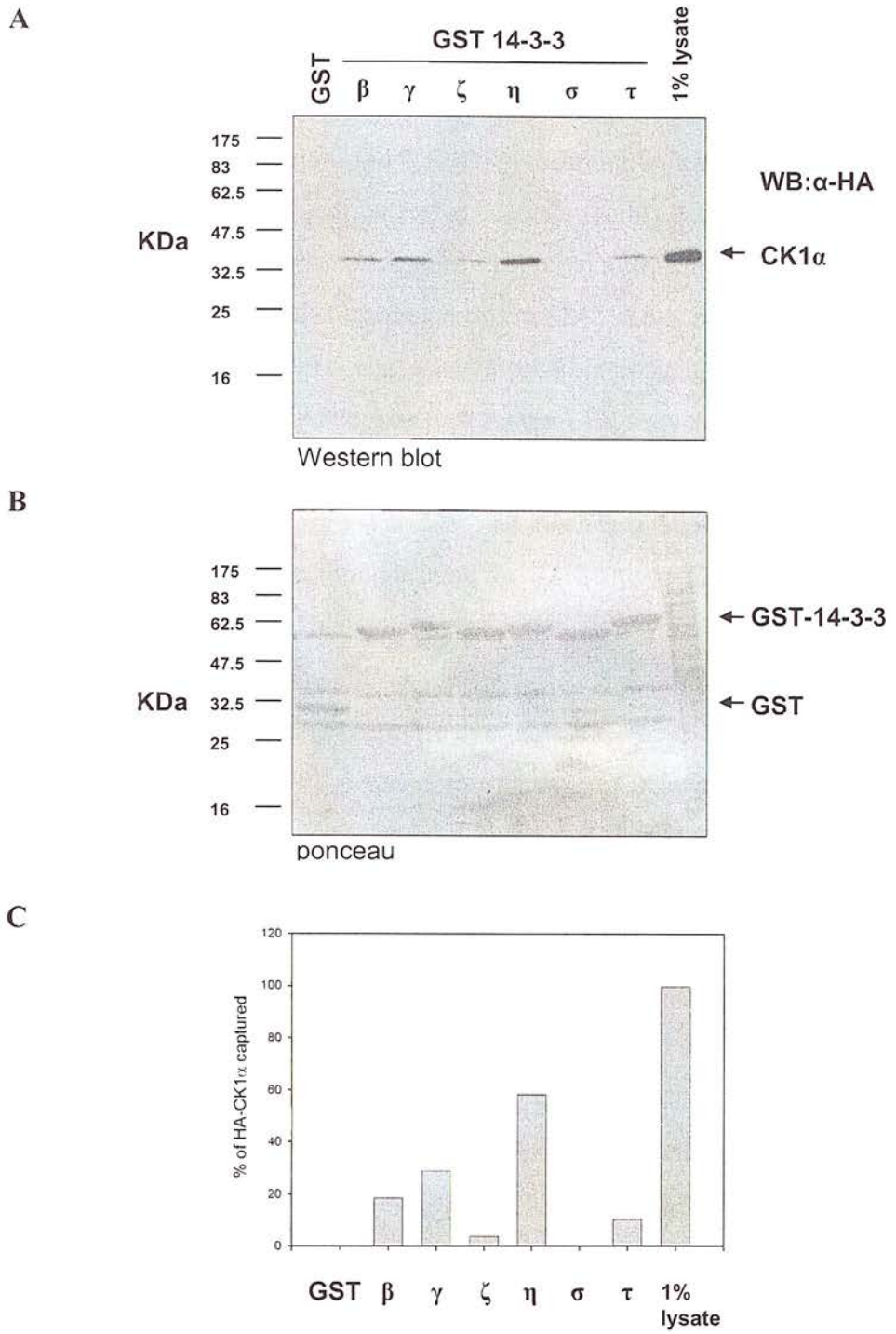

Figure 4.11 14-3-3 isoforms associate with CK1 *in vitro.*
A, COS-1 cells were transfected with HA-CK1α, the lysates were then clarified before addition of 10μg recombinant GST-14-3-3. Each sample was rotated at 4°C for 1 hour before addition of glutathione beads. After two hours, each pull down was washed 3 times in lysis buffer before separation by SDS-PAGE. The gel was transferred and western blotted with α-HA. **B**, Ponceau staining shows equal loading of recombinant 14-3-3 isoforms. **C,** Densitometry analysis of the blot in A, shows 14-3-3 associating with CK1 to varying degrees.

4.2.9. Activation of PKA causes increased association of 14-3-3 with CK1α in HEK 293 cells.

The 14-3-3 binding motif R(S)$X_{1,2}$pSX(P) is, in general, a good consensus for a number of kinases including PKA, Ca2+-calmodulin kinase II and PKC (see chapter 1.2.5 and table 1.2). Indeed, using the Scansite facility (at http://scansite.mit.edu) to analyse the CK1α amino acid sequence revealed a PKA or PKC phosphorylation site around the possible 14-3-3 binding motif at S242. Also, by examining the sequence around residue 218, there is also another possible phosphorylation site for PKA/PKC, although not detected by Scansite (see figure 4.12, sequence). From the manually curated database of phosphorylation sites phospho base at EMBL (http://phospho.elm.eu.org/) it is clear that more than 50% of PKA substrates have a consensus similar to that found around the S218 site on CK1 i.e. just one basic residue at n-1.

It is clear from the CK1 crystal structure that both serine residues would be accessible to kinase(s) and therefore available for 14-3-3 binding (figure 4.12).

To determine if PKA could phosphorylate CK1α on either of these residues and thus induce association with 14-3-3, HA-CK1α was transfected into cells and PKA then activated with the addition of dibutyryl-cAMP. A time dependent increase in 14-3-3 binding could be seen with addition of db-cAMP (figure 4.13); with maximal binding seen after 10 minutes. Loading controls are shown in the lower panels of figure 4.13, indicating equal amounts of 14-3-3 η and β-actin present in the lysate and equal amounts of CK1α being present in each IP (bottom panel). A repeat of this experiment with shorter time points showed maximal binding at an even earlier time point of 5 minutes (data not shown). This time scale broadly agrees with the group of Roger Tsien who were able to observe PKA activation by Forskolin or db-cAMP in real time using FRET and a specially created construct containing 14-3-3 fused to a flexible loop region containing a perfect PKA phosphorylation site within a 14-3-3 binding motif [449]. Binding of 14-3-3 to CK1α decreased, even below the level of original binding, after 60 minutes, possibly due to indirect activation of phosphatases and or translocation of CK1 after 14-3-3 binding.

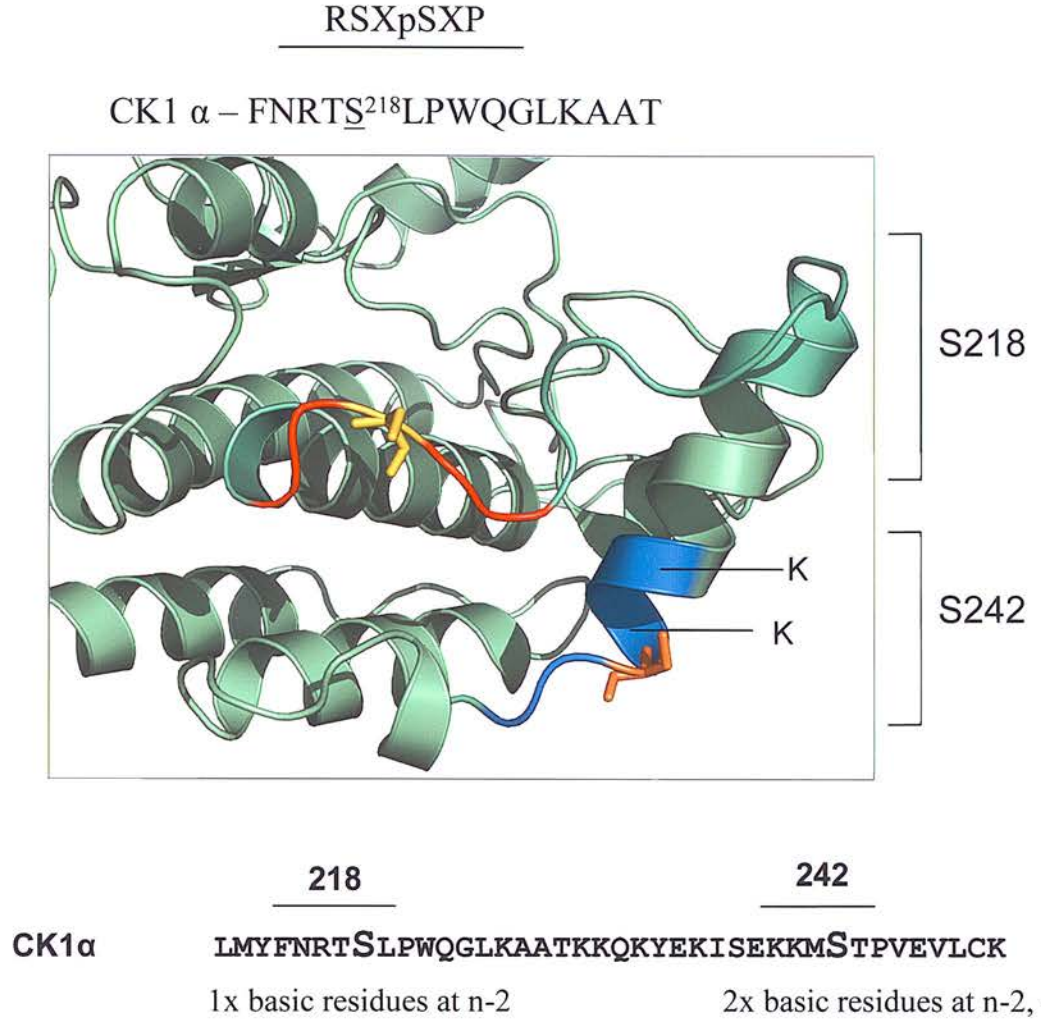

Figure 4.12 Proposed interaction region within CK1α.
The upper red coloured strand shows the flexible, unstructured region of CK1 proposed by Xu et al [393] (who first solved this structure) to act as an interaction loop with other proteins on account of its flexible nature. S218 is shown in yellow, with the proposed 14-3-3 binding region in red. The loop could also theoretically function as an autoinhibitor of CK1, binding into the ATP binding region just above (and shown in figure 1.9.), but this remains a postulation [393]. The lower region in blue indicates the second proposed 14-3-3 binding region around S242 (in orange). The two lysine residues, indicated, start to form part of the alpha helix, potentially making a poorer binding site. However, the pSLP residues would be easily accessible for binding. Created with Pymol, using coordinates from 1CK1.pdb in the Brookhaven database.

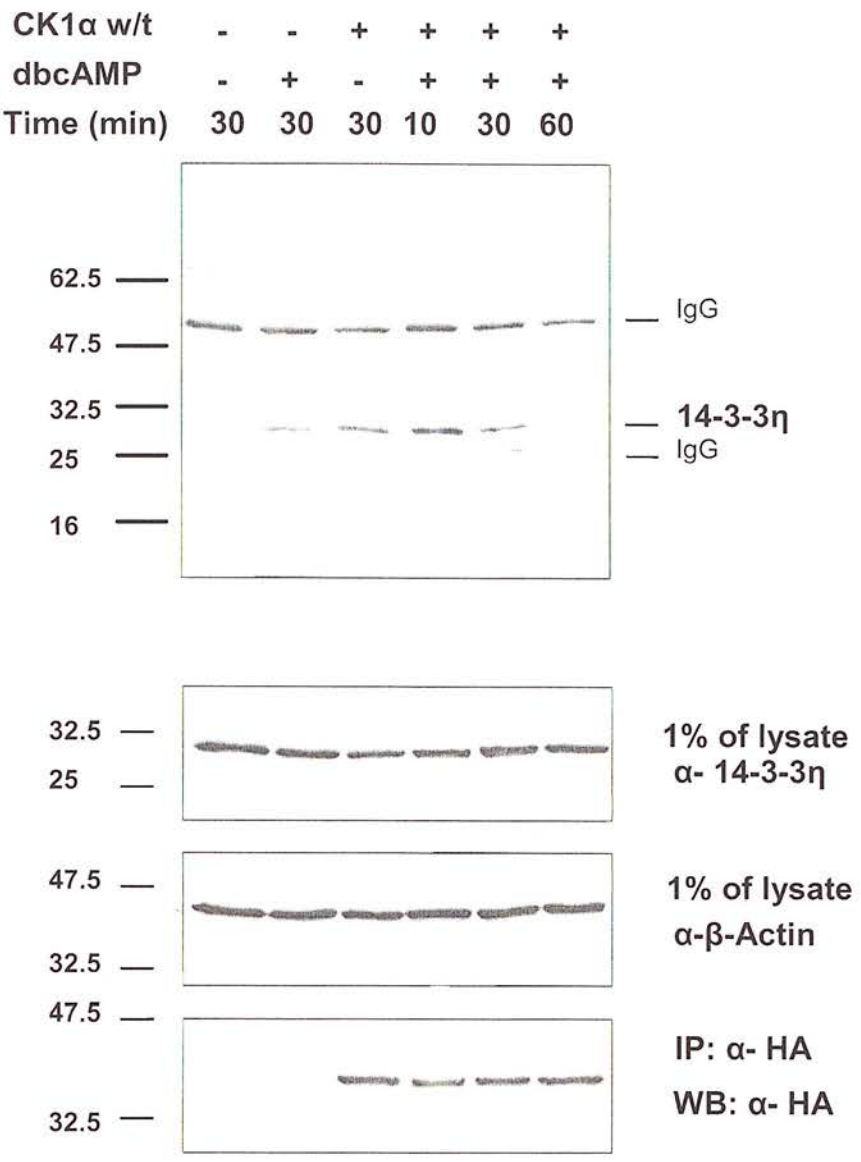

Figure 4.13 Stimulation of PKA in 293 cells causes increased association of endogenous 14-3-3 with CK1α w/t.
HEK293 cells, transfected with CK1α were serum starved for 18 hours, then stimulated with dibutyryl cAMP (db-cAMP) for the indicated times. Lanes 1and 2 are control lanes with no CK1α, with and without db-cAMP. A small amount of 14-3-3 was detected in these control lanes, indicating that the effect of PKA stimulation may not be reproducible. Lane 3 shows unstimulated cells transfected with CK1α as a control; lanes 4, 5 and 6 show increasing time with db-cAMP. 1% of the lysate was western blotted for α-β-actin and α-14-3-3 η. The immunoprecipitated HA-CK1α blot was striped and re-probed with α-HA after blotting with α-14-3-3 η (lower panels). Ten minutes stimulation of PKA induced the greatest amount of 14-3-3:CK1α association, thereafter the association reduced. A Repeat experiment showed a similar result.

4.2.10. Phosphorylation dependent binding of 14-3-3 η to CK1α

Site directed mutagenesis was then carried out to produce S218A, S242A and a S218A/S242A double mutant of CK1α, to reveal if these residues are essential for association with 14-3-3. Having established that PKA activation increases the association with 14-3-3 η and CK1α in 293 cells, subsequent binding experiments involving mutants of CK1 were carried out using cells stimulated with db-cAMP. HA-CK1α wt and SA mutants were transfected into HEK293 cells, stimulated with db-cAMP, lysed and the washed anti-HA immunoprecipitates analysed by western blot for the presence of endogenous 14-3-3 η (figure 4.14). The S218A mutation caused a slight reduction in 14-3-3 binding compared to wild type CK1α, whereas S242A and double 218/242 mutation reduced 14-3-3 binding almost entirely (figure 4.14, top panel). A 1% sample of the lysate was western blotted for 14-3-3 and the IP blot stripped and re-probed with anti-HA antibodies (lower panels) to check protein loading. As the double S218A/S242A mutation had the same affect as the single S242A mutation, two possibilities are apparent. One is that S242 is the major site of 14-3-3 phospho-dependent interaction and the other is that a SA mutation at this position changes the local structure, or conformation of CK1, in such a way as to decrease the binding affinity. The fact that S218A decreases the binding substantially, but not completely, suggests it does play a role in 14-3-3 binding. A possible scenario could be that each 14-3-3 monomer of the 14-3-3 dimer could bind a phosphorylated residue of S218 and S242 simultaneously, after phosphorylation by PKA/PKC or other kinase. Such 'bidentate' binding has previously been observed for molecules such as Raf, BAD, and Cbl [15, 17], this concept is explored later (section 4.2.18 – CK1:14-3-3 modelling).

Although treatment of cells with db-cAMP has been well documented in the literature to increase PKA activity, it cannot be concluded that activating PKA will directly induce phosphorylation at the residues 218 and 242. Indeed it would also not prove that it is the physiological kinase, but would open up possibilities for future studies into the regulation of CK1:14-3-3 association. Further experiments treating cells with the PKA inhibitor peptide (myristoylated for entry into cells) showed a reduction in binding (figure 4.15). There remains the possibility that PKA could

activate another kinase by phosphorylation, or inactivate a phosphatase (by phosphorylation of a phosphatase inhibitor, e.g. DARPP-32), thus leading to increased phosphorylation of CK1.

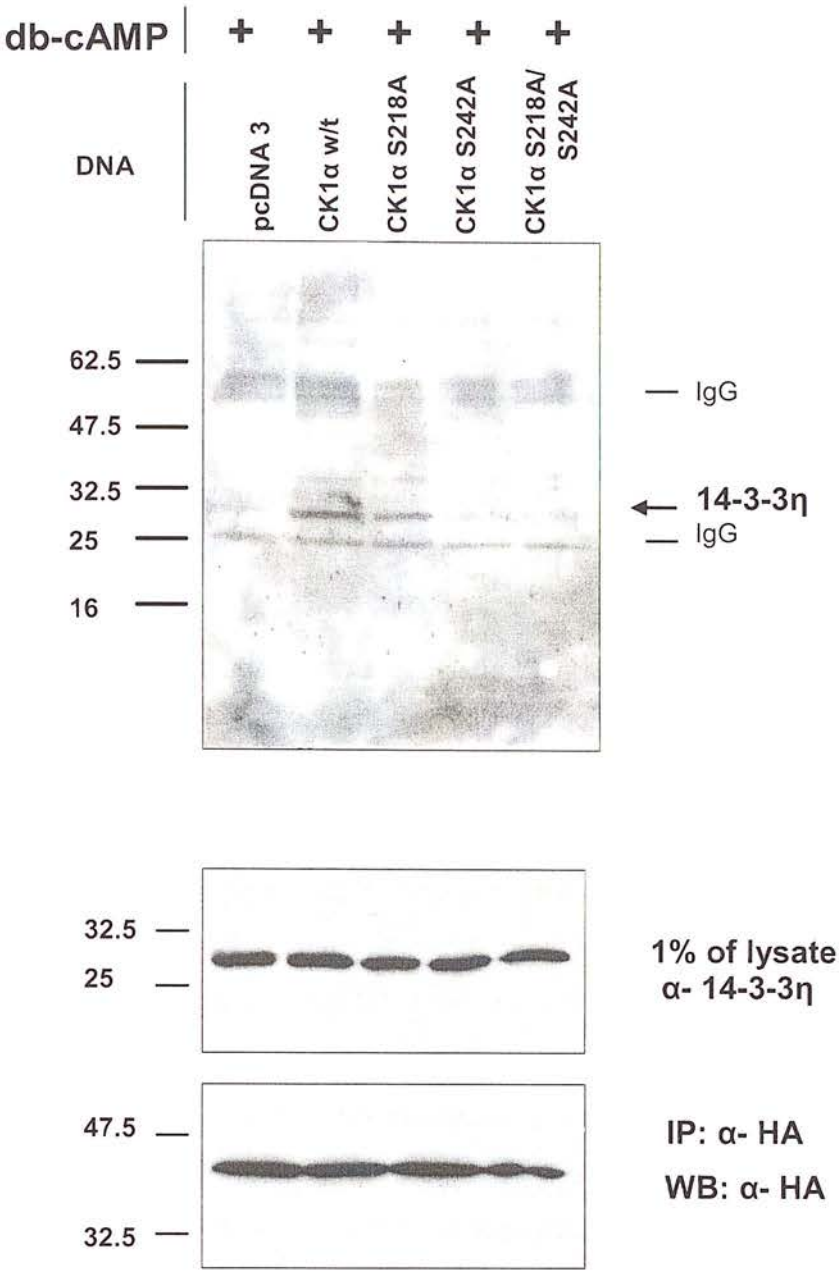

Figure 4.14 Residues S218 and S242 of CK1α are required for 14-3-3 association. Transfected HEK293 cells with point mutations of HA-CK1α were serum starved, then stimulated with db-cAMP for 10 minutes. The cells were lysed and HA-CK1α immunoprecipitated with anti-HA antibodies (clone HA-7 conjugated to agarose beads). The lysates were extensively washed and western blotted with anti 14-3-3 antibodies. Control blots showing 14-3-3 levels and equal amounts of CK1α in each IP are shown in the lower two panels. Lane 1 shows empty vector control; lane 2, wild type CK1α; lane 3, CK1α S218A; lane 4, CK1α S242A; lane 5, CK1α 218A/S242A. The blots are representative of three separate experiments.

4.2.11. Inhibition of PKA reduces CK1α:14-3-3 association

After establishing that PKA stimulation of cells increases 14-3-3 association with CK1α, experiments were performed to investigate if the interaction could be disrupted by inhibiting PKA activity. PKA activity was 'knocked down' by use of a myristoylated PKA inhibitor peptide: Myr-GRTGRRNAI (Myr-PKAi) and the consequent 14-3-3 association with CK1α observed by western blotting. This peptide corresponds to the inhibitor region of protein kinase A inhibitor, with a myristoylated N-terminus to allow entry into cells. For these studies the reciprocal experiment was performed whereby HEK293 cells were co-transfected with 14-3-3 and CK1α, then 14-3-3 immunoprecipitated, followed by analysis of CK1α by western blot. Panel A in figure 4.15 shows that stimulation of PKA with db-cAMP in this experiment caused a negligible increase in CK1α association (compare lanes 1 and 2, panel A). However, pre-incubation with 20μM of the peptide: Myr-GRTGRRNAI (Myr-PKAi) for 30 minutes reduced the CK1:14-3-3 interaction even below that of unstimulated cells (panel A, compare lanes 1 and 3). Control lanes are shown on the right hand side of the panels, with no CK1 present, but identical stimulations (lanes 4-6). Control panels B and C show equal amounts of 14-3-3 and CK1 in each treatment, apart from lane 3. Lane 3 has lower levels of 14-3-3, but it also has lower CK1α. Inhibition of PKA would be expected to interfere with many cell signalling processes and so may be causing either reduced transfection efficiency, degradation of both proteins or change of location, resulting in lower levels of 14-3-3 and CK1. The overall binding level of CK1 in this experiment was low, perhaps due to high passage number of the HEK 293 cells. Experiments using HeLa cells provided increased transfection efficiency of CK1 and 14-3-3; but did not show a difference in binding between the Ser-Ala mutants (data not shown). Although this may be because the amount of 14-3-3 immunoprecipitated is so high, it may mask the phosphorylation-dependent binding. Also 14-3-3 ζ was used that does not bind as tightly as other isoforms. The reason 14-3-3 ζ was chosen was to potentially continue to investigate the role phosphorylation of ζ on Thr 233 and interaction with CK1.

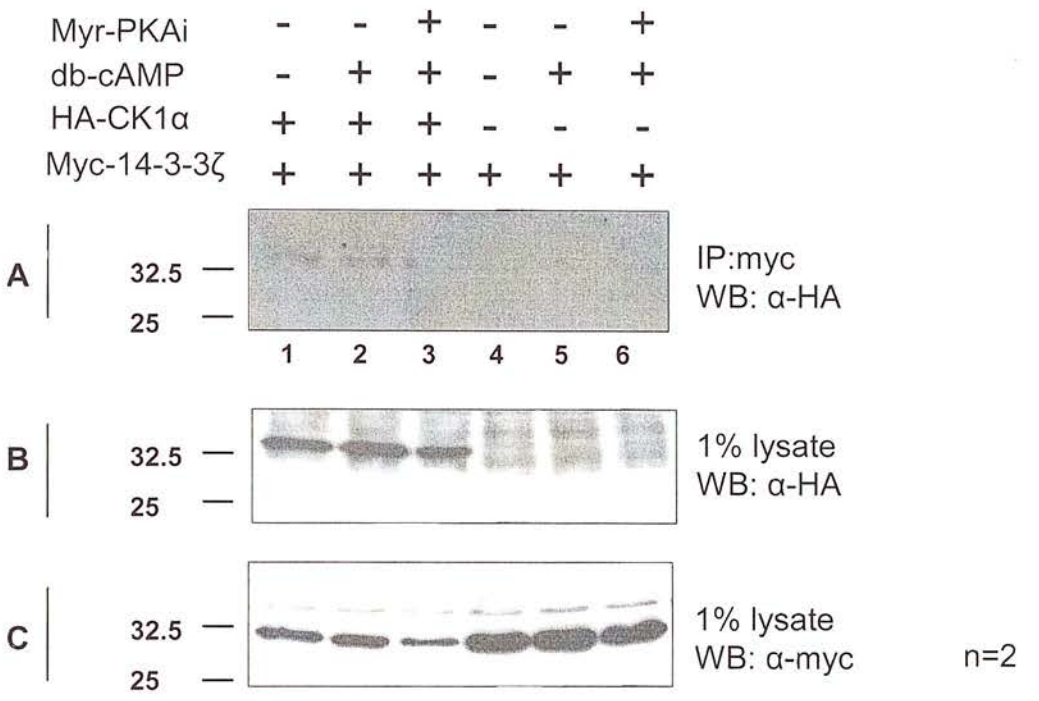

Figure 4.15 Incubation of an inhibitor of PKA reduces association of CK1α with 14-3-3 ζ.

HA-CK1α and 14-3-3-myc constructs were co-transfected into HEK293 cells as indicated above panel A. Lanes 3 and 6 were incubated with 20μM Myr-PKAi for 30 min before addition of 1mM db-cAMP (lanes 2, 3, 5 and 6) for 30 min. After lysis, 14-3-3 was immunoprecipitated using pre-conjugated anti-myc-agarose beads, washed, separated by SDS-PAGE and western blotted using anti-HA antibody (panel A). Panels B and C show 1% of lysate blotted for α-HA and α-myc.

4.2.12. 14-3-3 ζ binding mutant

A mutant of 14-3-3 ζ – R56A, R60A was designed to remove the phosphate requirement for ligand binding, but which unlike the charge reversal mutant K49E, as used by Fu et al [134] might not exclude all interaction (see chapter 1). The R5660A mutant has been used by the group of Muslin, who found that it decreased the interaction with phospho-ERK [137]. Work in our laboratory also found this 14-3-3 mutant to abrogate interaction with δ-catenin [450]. Casein kinase 1α was produced by IVTT and further incubated with NaF to increase phosphorylation status of the CK1α, as described in 4.2.6. After removing 2μl (5%) of the lysate, the remaining 38μl was made up to 200μl binding buffer, divided in two and incubated with either GST or GST-14-3-3 ζ. A parallel incubation was performed, substituting wild type GST-14-3-3 ζ, for GST-14-3-3 ζ R5660A (figure 4.16).

Surprisingly, mutation of these residues made no difference in the ability of 14-3-3 ζ to associate with CK1α. It is likely that only a small fraction of CK1α would be phosphorylated in the reticulocyte, providing a small amount of phospho-CK1α available to associate through the classical phospho-peptide binding pocket in 14-3-3. It is therefore possible that intact CK1α associates with 14-3-3 not solely in a phosphorylation dependent manner, and a low affinity interaction with unphosphorylated CK1 is obscuring the effect of the binding mutant in figure 4.16. To test the possibility that unphosphorylated CK1 interacts with 14-3-3 ζ with relatively low affinity, while phosphorylated CK1 interacts at higher affinity, repeat experiments were performed using 10- and 50-fold less 14-3-3 ζ wt to capture CK1α from the IVTT lysate, in an attempt to selectively capture phosphorylated CK1α. However, using less 14-3-3 showed an identical amount of CK1α being captured as in figure 4.16A (shown in figure 4.16B).

Mutational analysis of 14-3-3 η or γ isoform would be ideal, as perhaps with a larger binding capacity, it would be more sensitive to mutations in the 14-3-3 binding groove. Perhaps some 14-3-3 isoforms have a binding preference for phosphorylated proteins and others are not as selective. Compare η with ζ, in binding single, phosphorylated peptide S218, for example (figure 4.4). Also it would be interesting to see the effect of the K49E mutation on 14-3-3:CK1 binding.

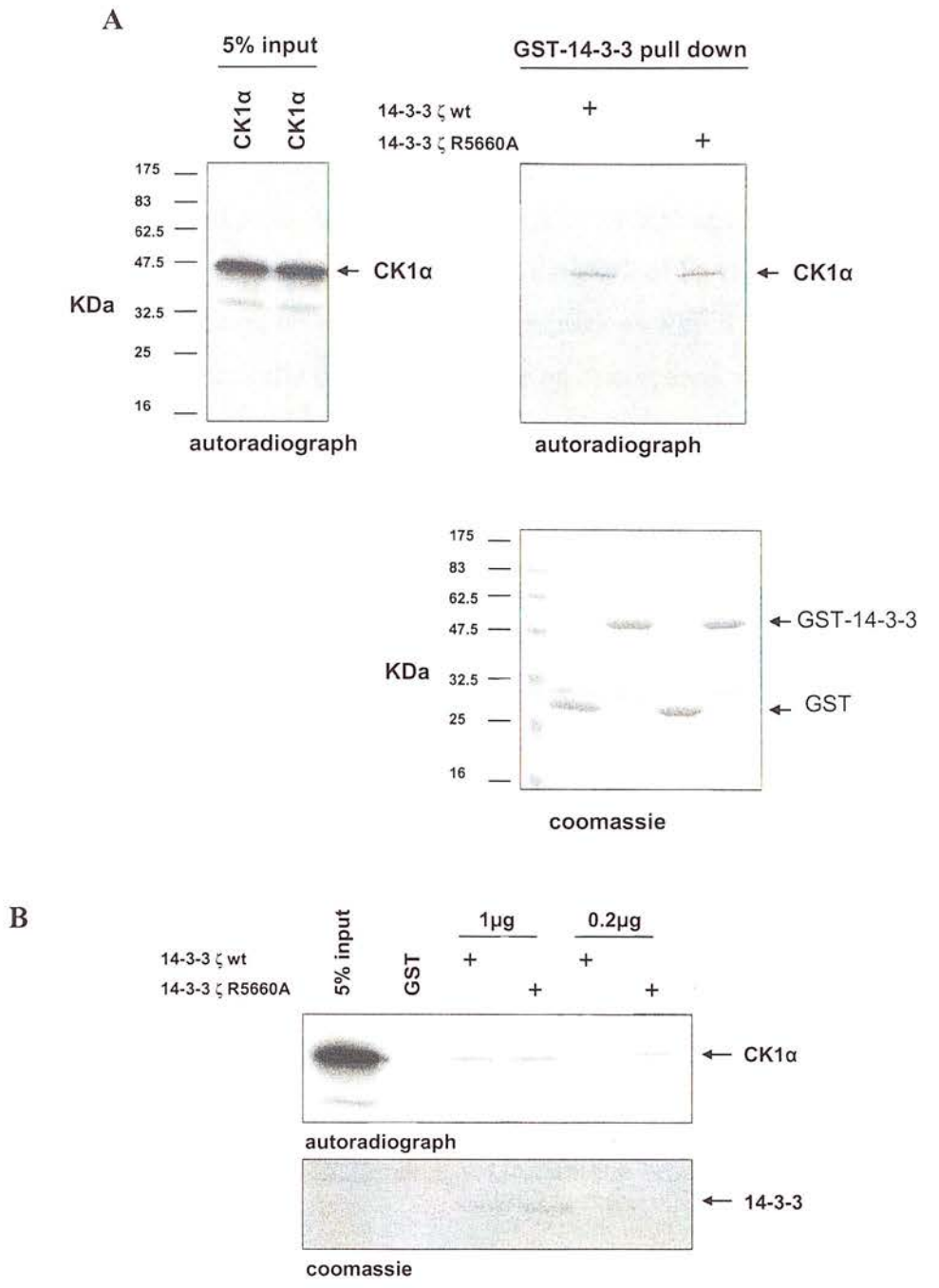

Figure 4.16 Mutation of R5660A has no effect on CK1α association with 14-3-3 ζ
A, HA-CK1α was produced by IVTT, using ^{35}S, with extra incubation with 5mM NaF and incubated with 10μg GST-14-3-3 ζ wt or GST-14-3-3 ζ R5660A protein. The GST-14-3-3 was then captured with the addition of GSH beads. After washing 5 times with 1ml NP-40 binding buffer, the bound CK1α was separated by SDS-PAGE, stained/destained, dried and exposed to film. Top left panel shows a representative 5% of the lysate incubated with each of the GST-14-3-3s. The top right panel shows equal amounts of CK1α binding to both the wt and R5660A 14-3-3s. A coomassie load control is shown underneath. **B**, Repeat experiment using 1μg and 0.2μg, as indicated, of GST-14-3-3 to pull down CK1α. Coomassie could not detect the 0.2μg 14-3-3 loaded.

4.2.13. Inhibition of CK1 binding to 14-3-3 using 14-3-3 antagonists

Results from the previous section suggest that CK1α may interact with 14-3-3 through regions different from the amphipathic groove and thus through contact of residues different from R56 and R60. Mutation of R56 and R60 to alanine, may not preclude binding to all molecules, indeed the work of Fu et al have shown that a range of both charge reversal and neutral mutations within the amphipathic groove can have a dramatically different outcome on interactions with the same protein [134, 135] (and see figures 1.2, 1.3 and 1.4 for location of residues involved in ligand contact).

In order to firmly establish if CK1α binds in the 14-3-3 groove, two established antagonists of 14-3-3 binding were used in an attempt to disrupt the interaction. One is a 14mer peptide corresponding to the region of Raf kinase incorporating pSer259, with a reported binding affinity to 14-3-3 of 120nM [451]. The other is a hybrid of two R18 peptides, known as Difopein (Dimeric fourteen three three peptide inhibitor) originally described in [30] and produced as a GST fusion for thrombin cleavage by Carolyn Brechin, The University of Edinburgh. The R18 peptide was derived from a phage display screen and has a k_D of 7-9 nM [29]. Combination of two R18 peptides is likely to have a synergistic effect on 14-3-3 binding, as a peptide with a tandem phosphorylated 14-3-3 motif decreased the k_D from 730 to ~20nM (30 fold) [15]. The 14-3-3 'inhibitors', R18 and difopein, were incubated with CK1α (produced by IVTT, using ^{35}S) and 14-3-3 ζ wt, ζ R5660A or 14-3-3 η wt at a 10 fold molar excess. Glutathione beads were used to capture the GST-14-3-3, after a two hour binding period and after four washes in NP-40 buffer, the CK1 was visualised by SDS-PAGE, coomassie staining and autoradiography (see figure 4.17). The IVTT lysate used to produce CK1α was also incubated with the phosphatase inhibitor NaF to attempt to increase the level of phospho-CK1α.

Figure 4.17 (lanes 3 and 4) demonstrates that 14-3-3 ζ wt and ζ R5660A mutant bind in a fashion very similar to that shown in figure 4.16, but in comparison, 14-3-3 η binds with higher affinity (see lane 5). This is in agreement with previous findings outlined in this chapter, from data using peptide binding experiments (figure 4.4), *in vitro* assays using intact CK1α (4.11) and *in vivo* binding assays from

transfected cells (4.10). Inclusion of the Raf peptide curiously increased the binding of 14-3-3 ζ wt and ζ R5660A to CK1α (compare lane 3 and 4 to lane 6 and 7), but reduced the interaction with η wt to background levels (compare lane 5, to lane 8). Parallel incubation using the difopein peptide, again, had a similar effect on 14-3-3 ζ wt and R5660A binding (lanes 9, 10); but almost completely removed 14-3-3 η interaction with CK1α (lane 11).

These data indicate that CK1α binds to 14-3-3 η through the amphipathic groove, but this experiment, in itself, does not confirm it is a phospho-specific interaction. The interaction with 14-3-3 ζ appears more complex in light of these data. Results presented in figures 4.16 and 4.17 suggests, for two reasons that CK1α does not bind in the central groove of the 14-3-3 ζ dimer. First, mutation of residues involved in coordinating contact with phosphorylated Ser/Thr residues had no affect on binding (figure 4.16). Secondly, 14-3-3 'binding inhibitors' did not reduce either wt or mutant 14-3-3 (figure 4.17) binding to CK1α. Blocking all possible interaction with the amphipathic groove by using the Raf peptide and difopein, shows 14-3-3 ζ interaction with CK1α must be mediated through other regions of 14-3-3. Perhaps phosphorylation of residues 218 and 242 cause a structural change in CK1α that increases the affinity to 14-3-3, through regions outwith the binding groove, explaining the lack of requirement of the binding groove.

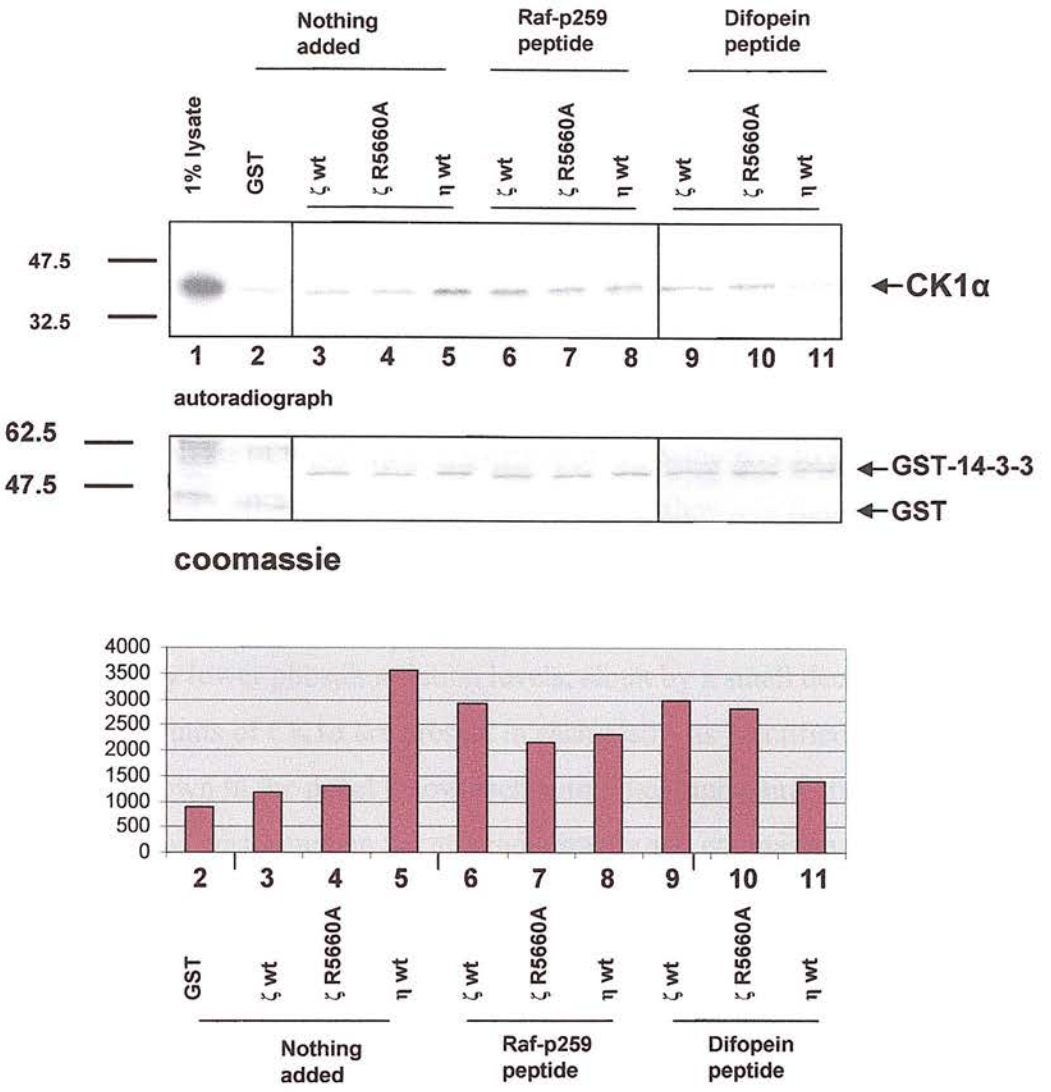

Figure 4.17 Inhibition of CK1 binding to 14-3-3 using 14-3-3 antagonists
CK1α was produced by IVTT, and incubated with the indicated 14-3-3 isoforms in binding buffer alone (nothing added), phosphorylated Raf peptide (Raf-p259), or a double R18 peptide, known as Difopein (Difopein peptide). The GST-14-3-3 was captured by GSH beads, extensively washed and separated by SDS-PAGE. The bound CK1 was visualised by coomassie staining and autoradiography.
Binding of CK1a to GST-14-3-3 was similar to control lanes (compare lanes 3 and 4 with 2), possibly reflecting general binding to the GST moiety.

4.2.14. CK1α mutants retain autophosphorylation and catalytic activity

To ascertain if the mutations of S218A and S242A altered normal enzymatic function of CK1α, *in vitro* kinase assays were preformed. First was to assess autophosphorylation activity and then transphosphorylation activity. To this end, CK1α w/t and mutants were overexpressed in parallel in HeLa cells, immunoprecipitated, washed and incubated with radiolabelled [^{32}P]-ATP and excess cold ATP (100μM) under kinase assay conditions. Transfected HeLa cells were chosen as the kinase source due to higher transfection efficiency (data not shown). Figure 4.18, top left panel shows an autoradiograph of CK1α and mutants incubated in the presence of [^{32}P]-ATP. Compared to wild type CK1α, S218A shows a slightly lower level of autophosphorylation, whereas CK1α S242A (with a Ser at 218) has a level similar to wild type. The S218A/S242A double mutant has a level similar to S218A mutant; suggesting that S218 is autophosphorylated in this assay. However, densitometry analysis of three repeat experiments show there is no significant change in phosphorylation of the mutants S218A and S242A, shown in figure 4.18, top left panel. It appears that mutation of these residues individually introduces more variation between experiments, whereas the double mutation S218A/S242A seems to have consistently lower phosphorylation levels, albeit by a small decrease of ~15% ±1.4. Equal amounts of CK1α are present in each assay, as identified by coomassie blue staining shown in the panel below each autoradiograph panel, figure 4.18. Densitometry was performed on the autoradiographs and coomassie gel whereby each band was measured using ImageJ software (http://rsb.info.nih.gov/ij/) and the density of each mutation in CK1α calculated as a percentage of wild type CK1α in each experiment, therefore allowing a comparison between experiments to be made.

To assess whether or not PKA could phosphorylate CK1α in vitro, and if so on the sites 218/242, CK1α was transfected and immunoprecipitated identically as described above, then incubated under kinase assay conditions with the inclusion of 1U of recombinant PKA (New England Biolabs, USA). This had no appreciable effect on wild type CK1α or on any of the mutants (figure 4.18, right hand panels). In fact these data most resemble the assay without PKA addition (left panels). Densitometry analysis of the autoradiographs from figure 4.18 and two repeat

experiments are shown in figure 4.19. Identical analysis of the coomassie stained gels showed very little difference between each IP, indicating accurate loading and allowing a fair comparison of CK1α wild type and mutants (lower panels, figure 4.19).

These data suggest that PKA may not be the direct kinase that phosphorylates CK1.

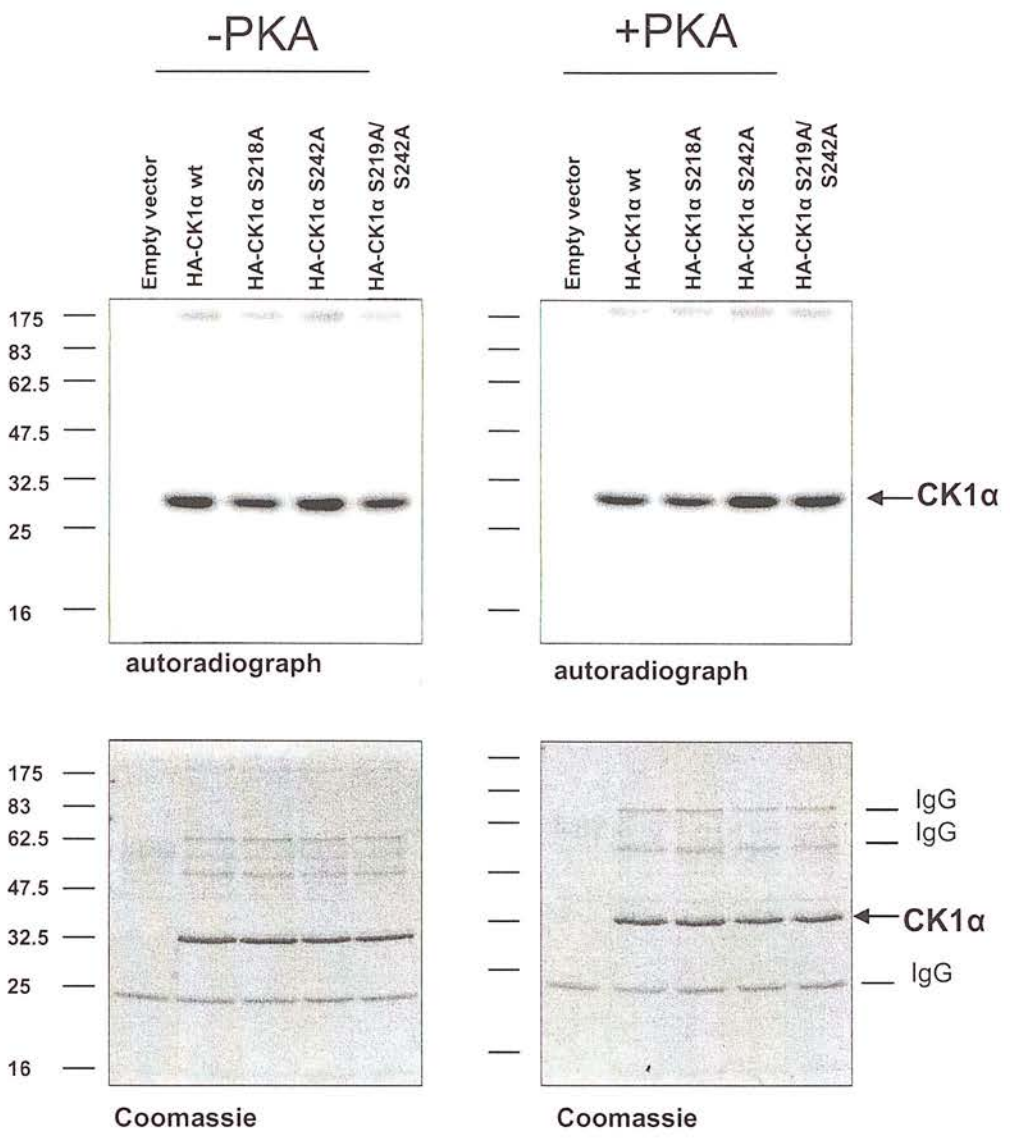

Figure 4.18 Site-directed Mutagenesis of CK1 has little effect on autophosphorylation activity; Protein kinase A is unlikely to be the direct kinase responsible for phosphorylation of S218 and/or S242.
15μg pcDNA3 (empty vector) or CK1α DNA was transfected into HeLa cells and lysed after 24 hours, immunoprecipitated with anti-HA pre-conjugated beads, washed in lysis buffer and equilibrated in kinase assay buffer, then incubated with [^{32}P]-ATP for 30 min at 30°C, with and without PKA (left and right panels), stopped in sample buffer, separated by SDS-PAGE, stained, dried and exposed to film. Autoradiographs are shown in the top panels and coomassie blue stained gels in the lower panels.

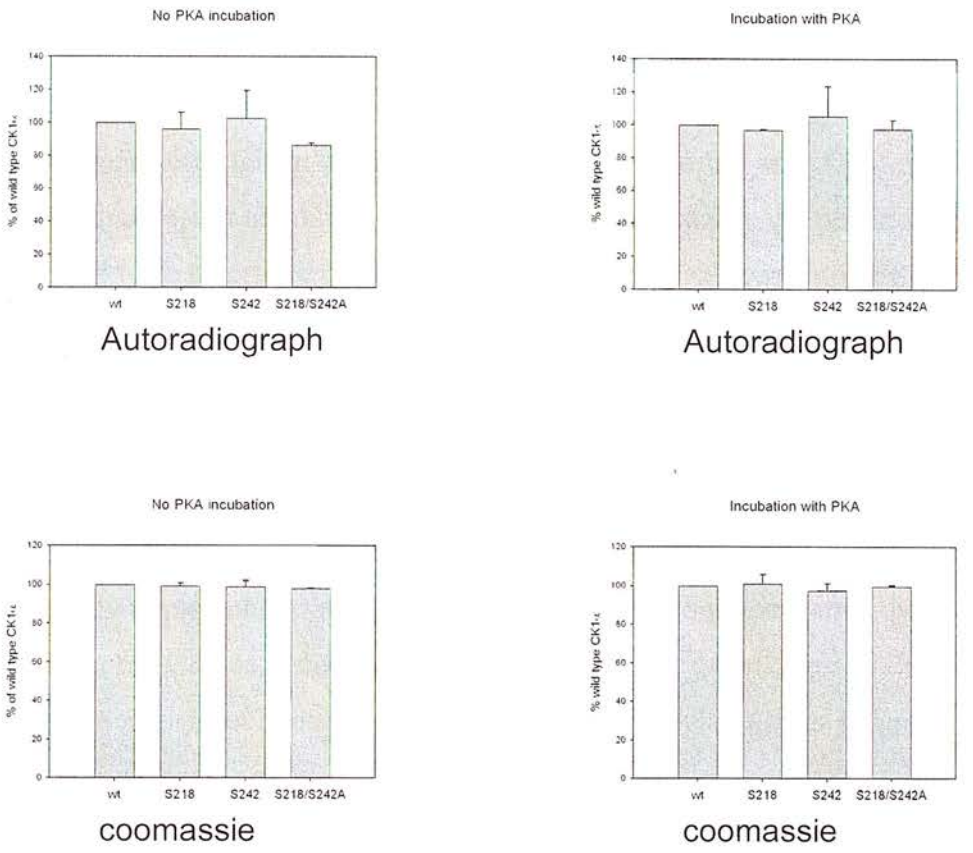

Figure 4.19 Densitometry of PKA incubation with CK1α.
Autoradiographs from separate experiments were scanned and analysed using ImageJ software from http://rsb.info.nih.gov/ij/. Upper and lower error bars indicate standard deviation from the mean of three identical experiments, plotted using Sigmaplot 9.0. No significant difference is observed between mutants and wild type CK1. Lower panels indicate intensity of coomassie staining from each immunoprecipitation.

4.2.15. CK1 site directed mutants phosphorylate a CK1-specific peptide with similar kinetics

To assess transphosphorylation activity of CK1 mutants a similar experiment to that described in the previous section was performed, where HA-CK1 and mutants were incubated with a phospho-peptide substrate that is specific for CK1 - DDDEEpSITR, where pS is phosphorylated and which has a reported K_m for CK1 of 0.5-1mM [452]. The purpose was to monitor if the mutations affect trans-phosphorylation by CK1 towards substrate, as the location of S218 in particular has been postulated from the crystal structure to become autophosphorylated and potentially inhibit the enzyme [393]. The top left panel in figure 4.20 shows an autoradiograph of CK1α wt and mutants in the same order as in figure 4.18, incubated under kinase assay conditions with [^{32}P]-ATP. To visualise the peptides, the kinase reactions were stopped by boiling in Laemmli buffer and separated by 18% SDS-PAGE. Autophosphorylation of CK1 is visible near the top of the gel and it appears that S218/242A double mutation decreases autophosphorylation, consistent with the previous result (figure 4.18). Mutation of S218, S242 and double S218/S242 mutation appear to allow increased phosphorylation of peptide substrate. The right panel shows densitometry analysis of three identical experiments that report a slight increase, in the ability to phosphorylate the phospho-peptide. A coomassie stain did not reveal the peptides, but CK1 is visible, as indicated (bottom left panel, figure 4.20). These data suggest a slight, but consistent increase in kinase activity against a peptide substrate.

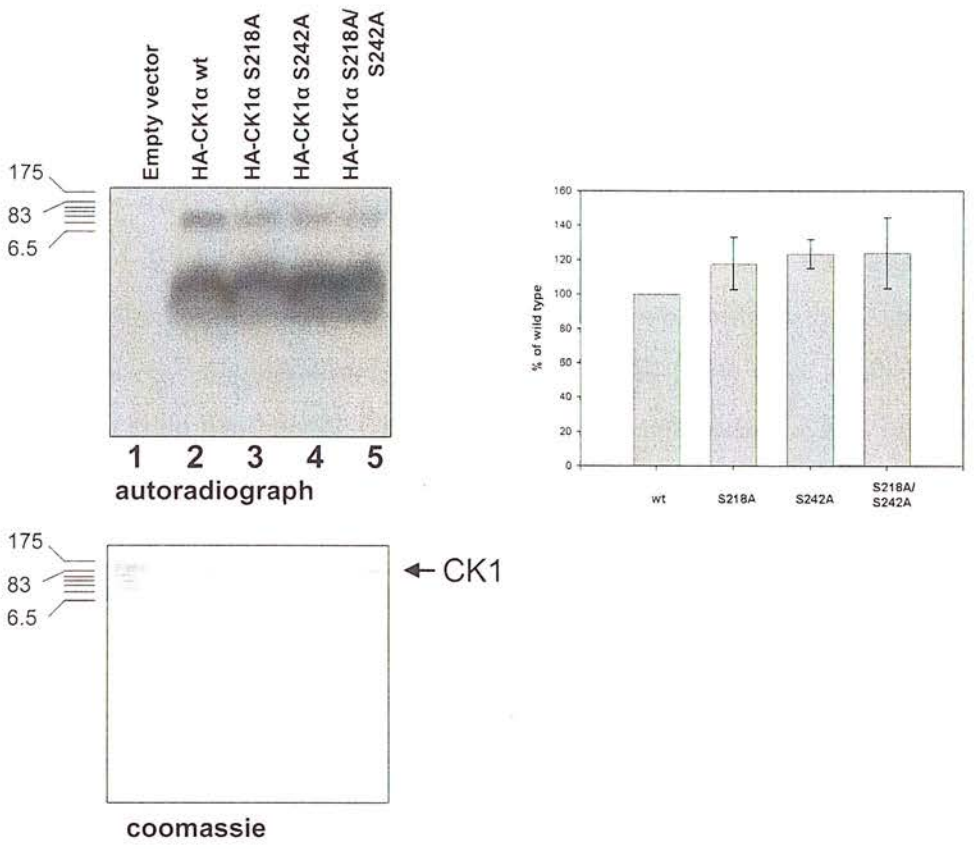

Figure 4.20 Effect of CK1 mutants on the ability of CK1 to phosphorylate a CK1-specific peptide substrate.

CK1a w/t and mutants were immuno-precipitated from non-stimulated HeLa cells using anti-HA Abs, washed in lysis buffer, then incubated with a CK1 specific phospho-peptide and $^{[32]}$P-ATP for 30 minutes at 30°C. Analysis of three separate experiments revealed no significant change in the ability of CK1 to phosphorylate substrate. Peptides could not be revealed by coomassie staining. Approximate positions of the markers are shown, although they are not widely separated on the 18% gel.

4.2.16. 14-3-3 binds to other CK1 isoforms.

To investigate the possibility of 14-3-3 binding to other CK1 isoforms, COS-7 cells were transfected with HA-CK1ε isoform and incubated with the GST-14-3-3 η isoform, as previous experiments showed it to be the isoform that interacted with the highest affinity to CK1α. The left hand panel in figure 4.21A shows a representative sample of 1% of transfected COS-7 lysate transfected with HA-CK1ε. The middle panel shows a GST-14-3-3 η pull down from the cell lysate. Equal amounts of GST or GST-14-3-3 η were incubated in the cell lysate for 2 hours, then after extensive washing, the bound CK1ε was revealed by western blotting to the α-HA tag. Ponceau staining reveals equal amounts of GST and GST-14-3-3 η were incubated with the lysate (far right hand panel, figure 4.21A). The C-terminus of CK1ε becomes hyperphosphorylated, causing autoinhibition of the enzyme [289] presumably by binding in or obscuring the active site such that it cannot access substrate. A similar regulatory mechanism has been observed for CK1δ [395]. CK1ε contains an almost identical sequence around S218 compared to CK1α and a totally conserved sequence around S242. The fact that CK1ε binds 14-3-3 shows that the extended C-terminal in CK1ε does not interfere with binding. As mentioned before, this region is highly conserved through CK1 isoforms, see alignment in figure 4.21B; it is likely therefore that other CK1 isoforms will also interact through the region around S218.

A

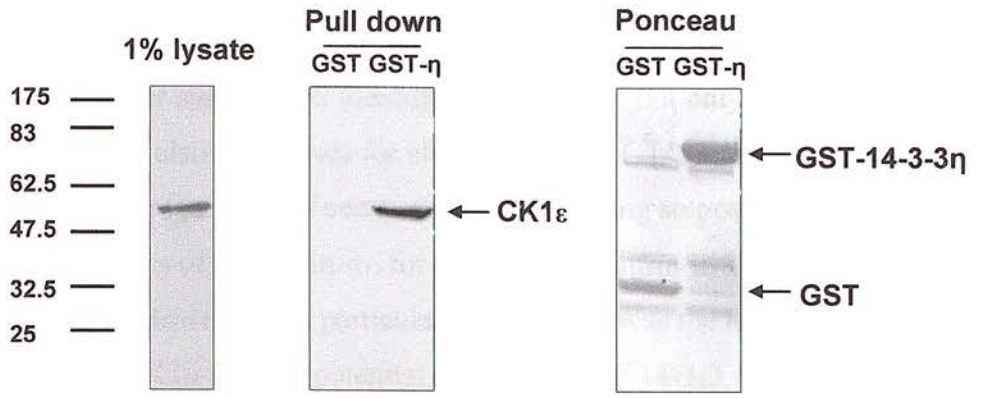

B

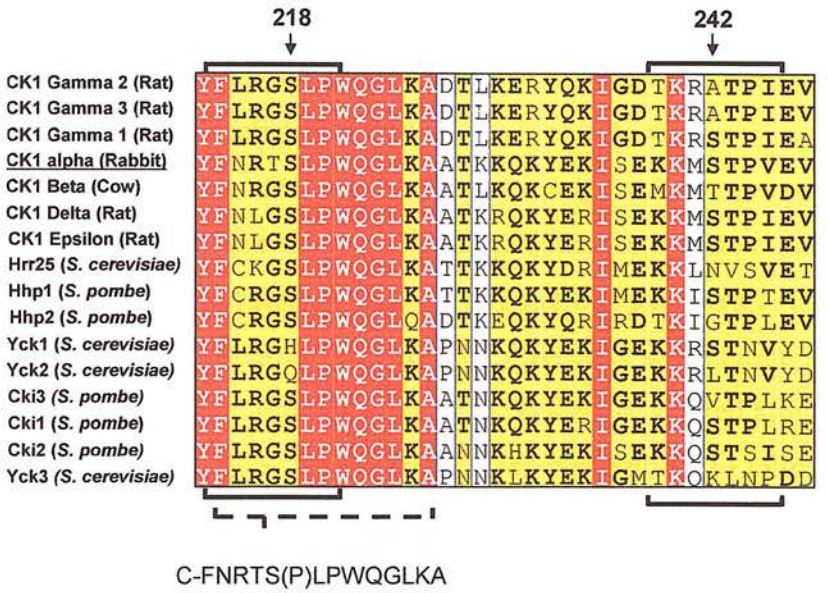

Figure 4.21 A, 14-3-3 η binds to the CK1 ε isoform *in vitro*.
HA-CK1ε was transfected into COS-7 cells, lysed and clarified by centrifugation. A sample of 1% of the lysate is shown in the left hand panel. Equal amounts of GST or GST 14-3-3 η were incubated with the lysate for 2 hours, the GST/GST-14-3-3 η recovered by GSH beads and separated by SDS-PAGE. Western blotting with α-HA antibody revealed the presence of CK1ε in the GST-14-3-3 pull down, but not the GST control (middle panel). Protein loading control is shown in the right hand panel. **B**, Sequence alignment around potential 14-3-3 binding region - showing conserved residues at positions 218 and 242.

4.2.17. PKC Phosphorylates Centaurin-α_1 on residue S87 and T276.

Intrigued by the behaviour of Centaurin-α_1 and its inability to bind phosphorylated CK1α, experiments were designed to further investigate this interaction. Work in our laboratory by Thierry Dubois showed that centaurin-α_1 could associate with CK1 through the same nonphosphorylated region, shown here to bind 14-3-3 [419]. Further studies then identified centaurin-α_1 not only as a binding partner of PKC, but also a substrate for all classes of PKC [453]. Phosphorylation may well affect the regulation of centaurin-α_1 and in doing so possibly perturb some of the important roles of centaurin-α_1, for example, centaurin-α_1 is a PIP_3 dependent ARF6 GAP [454]. However, the particular interest here was the interaction of centaurin-α_1 with CK1α and the potential involvement of 14-3-3 in this binding process. For example, if 14-3-3 binds phosphorylated CK1α, could this block the ability to bind centaurin? If centaurin was phosphorylated, could this affect the interaction with CK1α?

Identification of the phosphorylation site(s) was therefore undertaken to determine which domain of centaurin-α_1 may affected by phosphorylation. To this end centaurin-α_1 was incubated with PKC in vitro, followed by trypsin digestion, separation of peptides by HPLC and solid phase sequencing. Figure 4.22A shows that Centaurin-α_1 was phosphorylated by PKCα, μ and ε. As PKCα phosphorylated centaurin-α_1 with highest stoichiometry, this band was excised and digested with trypsin as outlined in Materials and methods. Cerenkov scintillation counting showed $\geq$50,000cpm in the band originally, with $\geq$20,000cpm recovered after trypsin digestion/peptide extraction. This provided plenty of activity to follow the elution profile over HPLC. After separation of the peptides by reverse phase HPLC (figure 4.22B), the fractions containing the activity were first analysed by mass spectrometry (by Rob Wakefield to identify the peptides: (fractions 6 and 7) - FESK and ARFESK) and (fractions 43 and 46) - WFTMDDR and WFTMDDRR. Automated solid phase Edman degradation (by Alastair Aitken and Andy Cronshaw) further showed radioactivity released during cycle 3 and 5 in the first peptide and cycle 3 in the second peptide, corresponding to FES^{87}K/ARFES^{87}K and WFT^{276}DDR respectively (figure 4.22C). The locations of these phosphorylation sites within the centaurin-α_1 primary structure are shown in figure 4.23C.

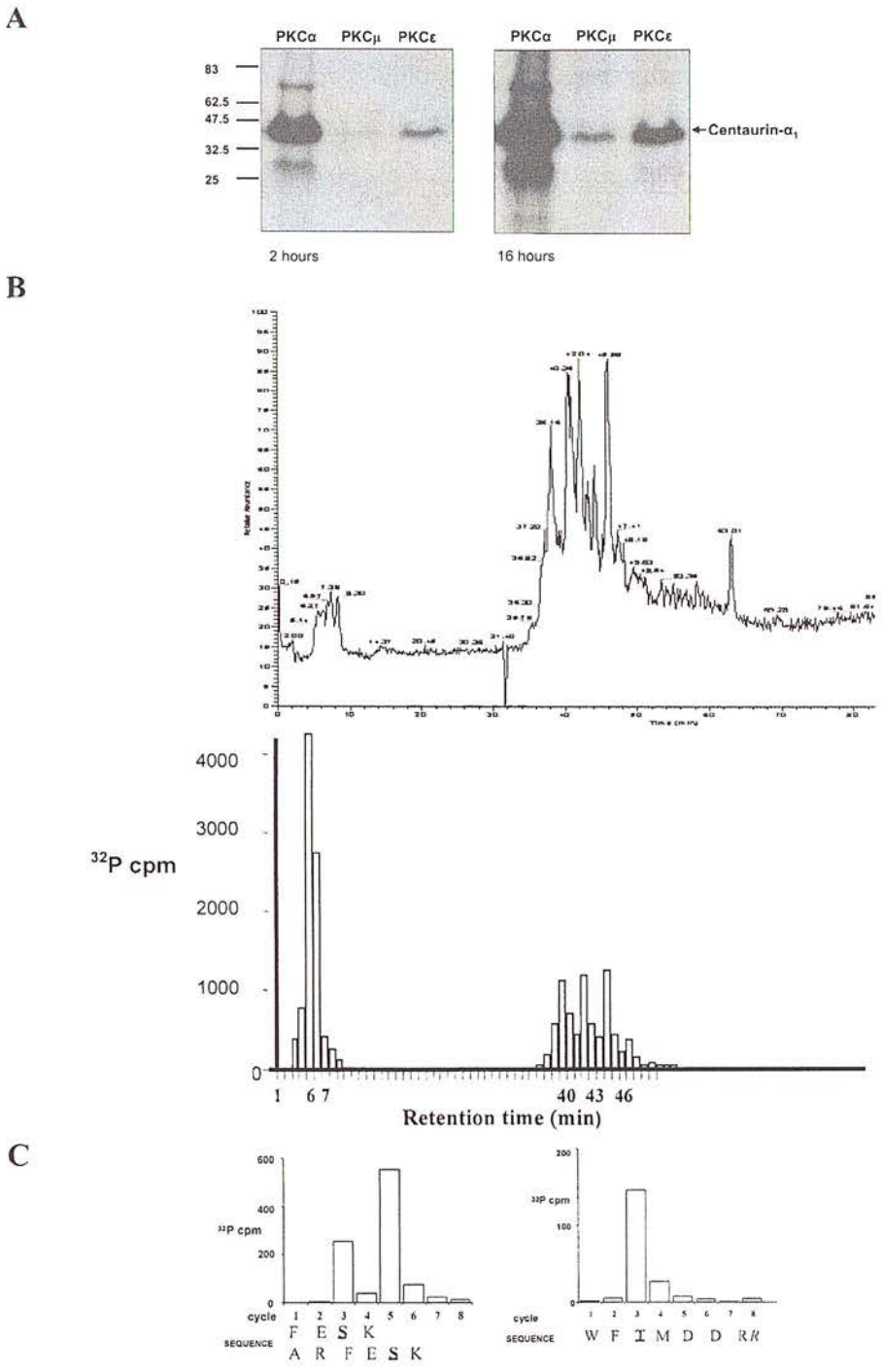

Figure 4.22 PKC phosphorylates Centaurin-α1 on residues S87 and T276
A, Recombinant PKC from all classes was incubated with recombinant centaurin-α_1 in the presence of [^{32}P]-ATP. **B** After excision and tryptic digestion of the bands from A, the peptides were separated by reverse phase HPLC and the fractions counted by Cerenkov counting. Online ms analysis identified the peptides FESK, ARFESK in fractions 6/7 and WFTMDDR in fractions 43 /46. **C**, Solid phase sequencing revealed which residue was phosphorylated. Figure published in [453].

4.2.18. Phosphorylation of Centaurin-α_1 by PKC negatively affects interaction with CK1α

Having established the phosphorylation sites on centaurin-α_1, binding assays were performed on phosphorylated centaurin-α_1 to assess the effect of phosphorylation on the interaction with CK1α. To this end, CK1α was produced by IVTT, using ^{35}S incorporation, followed by incubation with GST or GST-centaurin-α_1 that had been phosphorylated (prior to binding) by PKCε. Controls incubations were preformed whereby the bait proteins, GST and GST-centaurin-α_1, were incubated under kinase assay conditions for 30 minutes prior to incubation with the CK1α lysate. After incubation at 4°C for 2 hours and extensive washing in NP-40 buffer, the pull downs were analysed by SDS-PAGE, coomassie staining and autoradiography. The top panel in figure 4.23A shows an autoradiograph of CK1α captured to varying degrees by GST-centaurin-α_1. A representative 5% of the CK1α lysate is shown in lane 1. A GST control is shown in lane 2, followed by GST-centaurin-α_1, also incubated under kinase assay conditions, but lacking PKC and lane 3 shows GST-centaurin-α_1 incubated with PKCε. PKCε phosphorylation of centaurin-α_1 reduces association with CK1α, by a small, but reproducible amount, as demonstrated in densitometry analysis of three separate experiments, shown in the right hand panel.

Further studies are required to ascertain if phosphorylation of one or both residue(s) S87/T276 is required to abrogate the interaction with CK1α. The residue S87 lies outwith any recognised functional domain and T276 lies N-terminal of the second PH domain (figure 4.23C). However, phosphorylation on T276 is unlikely to perturb binding to phosphoinositides, as the alignment of several PH domains places T276 a considerable distance from the residues that contact bound phosphoinositides (see figure 4.23B). Of course, the three dimensional structure of the intact protein may well position the other phosphorylation site (S87) near the phosphoinositide binding site. The data shown here suggests that CK1α could bind close to either phosphorylation site, or that phosphorylation creates a larger structural change in centaurin-α_1, obscuring another CK1 binding site.

A

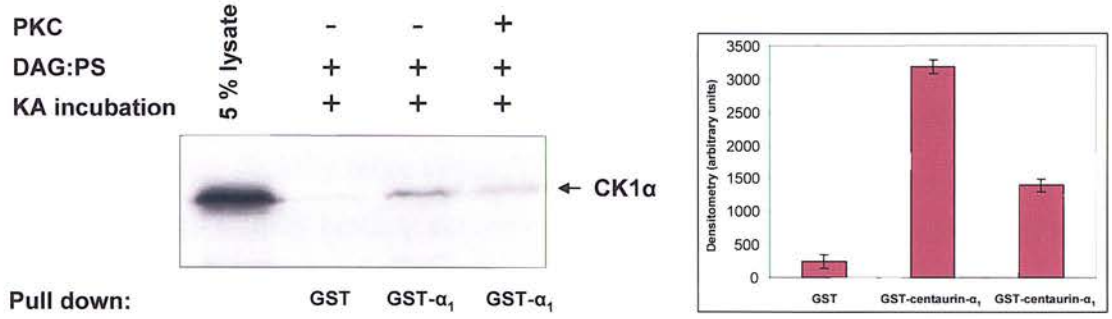

B

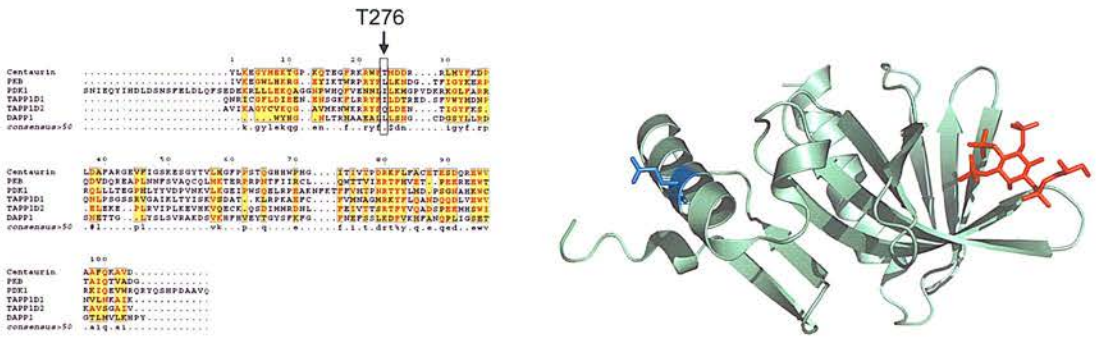

C

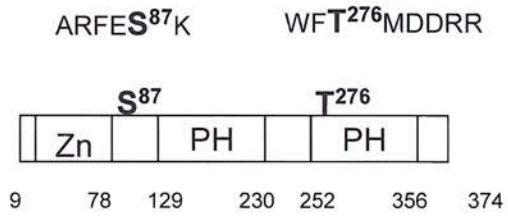

Figure 4.23 Phosphorylation of centaurin-α_1 by PKCε impairs association with CK1α.

A, HA-CK1α was produced in an IVTT system and incubated with GST and GST-centaurin-α_1 that had been previously phosphorylated by PKCε. Mock assays lacking PKCε showed that the kinase assays conditions (DAG mimetic/PS and 30ºC for 30 minutes) did not affect binding. Densitometry of three repeat experiments is shown in the right panel. **B,** Left panel, Sequence alignment of PH domains from crystal structures complexed with phosphoinositides, including the second PH domain in centaurin-α_1 (top sequence). T276 is indicated by the arrowed box. Right panel shows the crystal structure of the PH domain from PDK1, bound to Ins(1, 3, 4, 5)P_4 in red and the relative position of the phosphorylation site at T276 in blue. **C**, location of centaurin-α_1 phosphorylation sites in the primary structure.

4.2.19. Computer modelling of 14-3-3 and CK1α

14-3-3 has been shown to be a substrate for CK1α and the fact that 14-3-3 binds to CK1α in a phospho-dependent manner from data presented here suggests the possibility of simultaneous binding and phosphorylation of 14-3-3. A possible explanation for the result of CK1α binding 14-3-3 in figure 4.15 where S242A mutation had significantly more impact than S218A on 14-3-3 binding, could be that S242 is the high affinity binding site, followed by S218 binding as the low affinity site, suggested as a general binding mechanism by Yaffe [139]. As the crystal structure of a truncated CK1 and 14-3-3 are known [131, 393], computer docking simulations were performed to identify a possible binding conformation and see if (at least *in silico*) 14-3-3 could bind CK1 in a conformation where each 14-3-3 monomer contacts a phospho-S218 and phospho-S242. The structure co-ordinates 1QJB.pdb and 1CKI.pdb were manually edited to remove water molecules, before being uploaded to the ClusPro site ([447] and http://nrc.bu.edu/cluster/) and modelled using the ZDOCK program under standard parameters. Figure 4.24 shows one of the most probable conformations between the two molecules. In figure 4.24A and B are shown wire mesh representations of the modelled interaction. When residues 218/242 are binding into the binding groove (purple and orange residues, respectively) it can be seen that S233 (marked in pink) would be unlikely to reach residue D136 of the active site, marked in dark blue. Panels C and D show the close proximity of the CK1 218/242 regions to the 14-3-3 binding pocket; with S218 considerably further from the binding pocket compared to S242. Distances were calculated using PyMol and are shown between residues corresponding to S218/S242 peptide backbone and residues within the phosphate binding pocket of 14-3-3 (panels E and F, figure 4.24) and are summarised in the table in figure 4.24. For comparison, distances between a phospho peptide bound to 14-3-3 are shown in panel G. In this orientation, the distances appear to be too great for a pS218 and a pS242 to bind in the phospho-binding pockets of the same 14-3-3 dimer, i.e. the CK1 molecule would have to undergo large conformational changes to reach both pockets simultaneously. The rigid structure of 14-3-3 would be unlikely to change conformation to accomadate simultaneous binding of these two residues. Another combination (not shown) placed S218 of CK1 near a 14-3-3 binding pocket, but concordantly S242 was moved out of reach of the

other binding pocket. Further manual analysis was performed by Paul Taylor (The University of Edinburgh) who also found the likelihood of two site binding unlikely without large structural changes. As always with computer modelling, these results must be interpreted with caution, but they do suggest that CK1 could comfortably bind either of the S218 or S242 residues, but perhaps not at the same time.

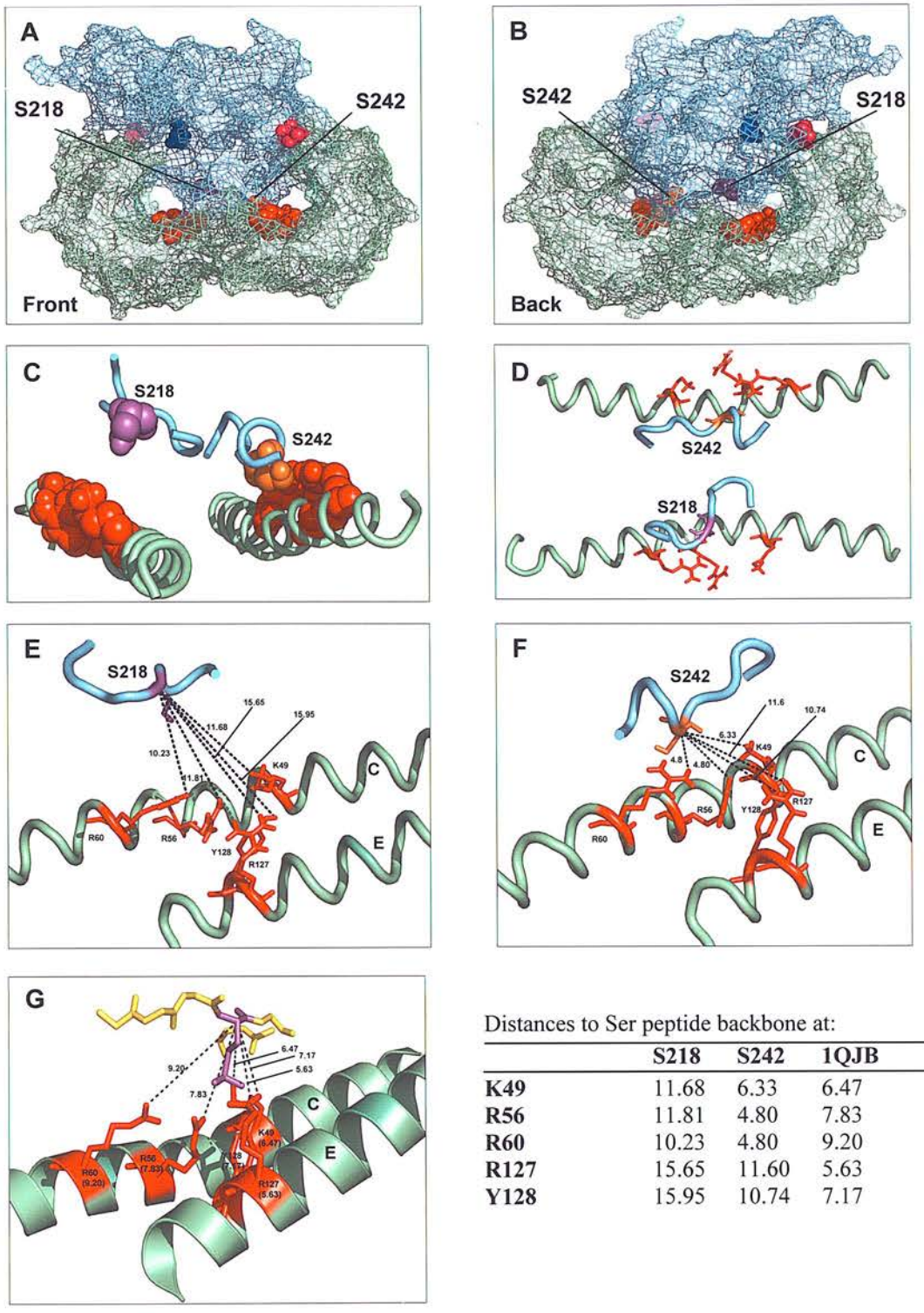

Distances to Ser peptide backbone at:

	S218	S242	1QJB
K49	11.68	6.33	6.47
R56	11.81	4.80	7.83
R60	10.23	4.80	9.20
R127	15.65	11.60	5.63
Y128	15.95	10.74	7.17

Figure 4.24 A-F Predicted CK1:14-3-3 interaction. CK1 is represented in blue, 14-3-3 in green; residues that co-ordinate ligand binding to 14-3-3 are in red; D136 in the active site of CK1, dark blue; S218 of CK1, purple; S242 of CK1, orange; S233 of 14-3-3, pink. Produced using PyMol from coordinates from 1QJB.pdb (14-3-3 zeta) and 1CKI.pdb, using ZDOCK, on the ClusPro server [447], see text for further details. Measurements in table are in Angstroms.

4.2.20. Discussion

In this chapter, several approaches were used to examine the interaction between 14-3-3 and CK1. CK1α was shown to bind all 14-3-3 isoforms, but to differing degrees and also depending on assay type. Initial experiments showed a phosphorylated peptide corresponding to 214-226 (*C*FNRTpS^{218}LPWQGLKA) of CK1α preferentially bound 14-3-3 isoforms η, γ, β, τ, ε, ζ and σ sigma, in a phosphorylation dependent manner, in that order. This region is conserved among CK1 isoforms (see figure 4.21B). In other experiments, the binding varied slightly, see table 4.1, but *in vivo* binding studies were in broad (except ε, see below) agreement with the *in vitro* experiments (using intact 14-3-3 and CK1α) in identifying 14-3-3 η and γ as the strongest interacting proteins. 14-3-3 ε binding seemed of higher affinity in vivo (figure 4.10). Another result that suggested isoform specificity is that the isoform 14-3-3 σ was unable to bind intact CK1α from cell extracts (figure 4.11).

Table 4.1 summary of 14-3-3:CK1 interactions

Experiment	***in vitro/in vivo***	**isoform preference**
Phospho-peptide	*in vitro*	η, γ, β, τ, ε, ζ and σ*
GST-14-3-3 pull down	*in vitro*	η, γ, β, τ, ζ, σ*
CK1α IP, WB 14-3-3	*in vivo*	η, γ, ε, β, ζ^{+}

* 14-3-3 σ was barely detectable
$^{+}$ 14-3-3 τ or σ were not detected in HEK293 cell lysates used, therefore they are not included.

There are many examples in the literature of 14-3-3 binding in an isoform-specific manner, for example: Cbl, CLIC4, IGF-1, NFAT3, PKCζ and Par3α, as discussed in section 1.2.6 and see table 1.3, although the issue of isoform binding specificity is often not fully addressed in the literature. Data presented here suggests a binding preference exists for CK1α, listed in the table above. Binding experiments using a phosphorylated peptide incorporating residue S218 revealed not only differences in 14-3-3 isoform binding, but also differences in phospho-dependent binding. Further analysis of the data revealed a difference in sensitivity toward phosphorylation, represented in figure 4.4B. After dephosphorylation, most 14-3-3

isoforms displayed a very similar reduction in binding (~70-80% reduction). 14-3-3 ζ showed the biggest reduction (~92%) of binding and 14-3-3 η showed the smallest change in binding (~43% reduction). Of course these data are only for one interaction site on CK1α; presence of another binding site would be expected to alter overall interaction of 14-3-3 and CK1.

The interaction with intact CK1 appears to be phospho-specific, as inhibition of phosphatases in the IVTT lysate (figure 4.7) led to a decrease and an increase in binding respectively; in agreement with the phosphopeptide studies. However, the use of CK1 truncation mutants identified at least one other binding site on CK1α (figure 4.8C). The truncation mutants of CK1α were all produced by IVTT and incubated with phosphatase inhibitors to maximise phosphorylation of the CK1 fragments.

To assess the *in vivo* binding characteristics of intact 14-3-3 and intact CK1, HA-tagged CK1α was immunoprecipitated from cells and western blotted for 14-3-3 isoforms (figure 4.10). These data showed an isoform binding preference very similar to the phospho S218 peptide binding results, although β and ζ were substantially lower. *In vitro* binding studies in which GST-14-3-3 isoforms were incubated with a cell lysate enriched with CK1α (figure 4.11) produced a similar result (see table 4.1). Confidence that the pS218 region is a valid interaction site was drawn from these results as it has very similar binding preferences as the phosphorylated peptide experiment, indicating involvement of this site.

To try to identify further binding sites on 14-3-3, as suggested by the truncation mutant data, site directed mutagenesis of residues S218 and another serine (S242) within a potential 14-3-3 binding site was performed. S242 was detected as the only other canonical 14-3-3 consensus, using the scansite facility [272]. Before transfecting these mutants into cells, preliminary experiments designed to increase phosphorylated CK1α *in vivo* were performed on wild type CK1α. To this end, cells that had been transfected with HA-CK1α were stimulated with the cAMP mimetic dibutyryl cAMP (db-cAMP) and α-HA-CK1α immunoprecipitates were then probed with α-14-3-3 η antibody to assess binding. A time-dependent increase in binding was observed and for further studies a stimulation time of 10 minutes was used – identified as the time point that showed maximal binding. Mutagenesis of S218 to alanine reduced binding to 14-3-3, a S242→A mutant dramatically reduced 14-3-3

interaction and the double S218/S242 double mutation completely abrogated binding in cells (figure 4.14). A further experiment was performed using an inhibitor of PKA, which was shown to reduce the interaction with 14-3-3 (figure 4.15). Modulation of PKA activity in HEK293 cells affected the amount of 14-3-3 association with CK1, suggesting the interaction can be regulated *in vivo*, even if not directly by PKA. Experiments were performed to check the integrity of the CK1α S→A mutants by way of *in vitro* kinase assay. Although unlikely, mutations to alanine could alter the local structure of CK1α in such a way as to decrease binding to 14-3-3, not just due to removal of a phosphorylatable residue. *In vitro* kinase assays of CK1 S→A mutants revealed that the region responsible for phospho-specific binding to 14-3-3 may play a role in substrate recognition, as a double S218/S242A mutation increased the ^{32}P incorporation into a CK1-specific substrate. After these experiments had been performed, the group of Pinna et al showed various point mutations (Q→K), near the S218/S242 region altered the specificity of CK1α towards pre-phosphorylated substrates [455], discussed further in chapter 6.

To investigate exactly how CK1α interacts with 14-3-3, a mutant of 14-3-3 ζ was employed whereby residues known to contact phosphorylated residues within 14-3-3 ligands had been mutated to alanines. The mutant, known as R5660A, showed surprisingly little difference in its ability to bind CK1α from an IVTT system, which had been incubated with phosphatase inhibitor. Even repeating the experiment with 50 times less 14-3-3, in a bid to remove 'background' binding, resulted in no difference between wild type and mutant.

Further experiments using established inhibitors of 14-3-3 binding were used for *in vitro* binding assays. One was a phospho-peptide corresponding to residues around Raf pS259 and the other a tandem repeat of the peptide 'R18', called difopein. Both 14-3-3 antagonists abrogated binding to 14-3-3 η, but had the curious affect of increasing binding with 14-3-3 ζ wt or ζ R5660A mutant (figure 4.17); firmly indicating that CK1α binds into the central groove of 14-3-3 η, but creating a complex picture of how 14-3-3 ζ binds.

The highly conserved nature of 14-3-3, in particular within the binding pocket, suggests very subtle binding differences must exist - to explain exactly how the same ligand can preferentially bind different 14-3-3 isoforms. The interaction of

CK1α occurs, most probably, through contact with the basic pocket within 14-3-3 η, and is potentially further mediated through different contacts within the 14-3-3 dimer, perhaps aiding the observed isoform binding specificity.

One rationale to explain 14-3-3 η binding to CK1α in a phospho dependent manner within the amphipathic groove, in contrast to 14-3-3 ζ, must be that phosphorylation of CK1α causes an unknown structural change that increases its affinity toward 14-3-3 ζ.

Further experiments to investigate other CK1 isoform binding 14-3-3 showed that CK1ε bound 14-3-3 η. 14-3-3 may interact with all CK1 isoforms, as the region ~214-226 is highly conserved. However this region may well have a specific repertoire of binding molecules, as recent studies have found this region in CK1δ could not interact with MAP1A [456], suggesting it is not the only interaction region within CK1. The region around S242 is slightly less conserved (figure 4.21B) and may help to confer more 14-3-3 isoform binding specificity.

Computer modelling of CK1 and 14-3-3 produced a feasible model as to how the two may interact. It placed S242 within binding distance of one binding pocket and S218 close to the other, but with a fairly large structural movement required to accomadate simultaneous binding (figure 4.24).

Centaurin-α_1 was shown to bind only the dephosphorylated sequence around S218 on CK1 (figure 4.6). Phosphorylation of CK1 could therefore modulate the interaction with centaurin-α_1 and thus its localisation. Further experiments using mass spectrometry and solid phase sequencing identified the PKC phosphorylation sites on centaurin-α_1. In addition, preliminary data suggest PKC phosphorylation of these sites negatively affects the interaction with CK1α. The location of the phosphorylation sites within centaurin-α_1 suggests phosphorylation is unlikely to interfere with phosphatidylinositol binding (see figure 4.23).

CHAPTER 5
Antibody Purification

5. Phospho-specific antibodies against 14-3-3

5.1. Introduction

14-3-3 binding can be regulated by phosphorylation of 14-3-3 itself, as discussed in chapter 1. We have previously shown that α and δ were phosphorylated forms of β and ζ respectively and are more than 50% phosphorylated on Ser185 in brain 14-3-3 [7], but we have found no evidence for phospho-forms in a wide range of other tissue types and cell lines. 14-3-3 β, η and ζ isoforms of 14-3-3 (but not ε and γ although they also contain serine at the equivalent site) are phosphorylated by a sphingosine-dependent kinase, SDK1, now identified as the kinase domain of PKCδ produced after caspase-3 cleavage [166]. Phosphorylation on Ser58 may disrupt dimer formation, but has had different reported outcomes in regard to binding partners (see chapter 1). Phosphorylation of 14-3-3 by BCR could affect the ability of 14-3-3 to bind other signalling proteins, for example our laboratory has shown that phosphorylation of 14-3-3 by CK1 negatively regulates binding to Raf *in vivo* [172]. Phosphorylation of S185 increases the efficacy of 14-3-3 as an inhibitor of PKC [7]. Serine 185 is located in the tertiary structure adjacent to residue 233 [421] and the group of Gotoh [170] have recently shown that activated JNK promotes Bax translocation to the mitochondria through phosphorylation of 14-3-3 σ and ζ at sites equivalent to Ser185 which led to dissociation of Bax. Expression of phosphorylation defective mutants of 14-3-3 blocked JNK-induced Bax translocation to mitochondria, cytochrome C release and apoptosis.

To further examine the functional consequence of 14-3-3 phosphorylation, attempts were made to produce phospho-specific antibodies to the S185 and S233 sites of 14-3-3 ζ, as outlined in this chapter.

5.2. Purification of Phospho S185 antibody using peptide affinity chromatography

The peptide EILNpS[185]PEKA*C* ('SPEKA' peptide) was coupled to maleimide activated KLH and injected subcutaneously into three sheep, carried out by Diagnostic Scotland (see Materials and methods for details). The serum from the one animal that responded well was clarified by centrifugation at 40,000RPM (125,000g) for 1 hour and then passed through a 0.2 micron filter. The SPEKA peptide was coupled to sulfolink beads in the same way as in chapter 4 and detailed in Materials and methods. A separate peptide was synthesised with exactly the same sequence, but without a phosphorylated serine. The clarified serum was passed first through the dephospho SPEKA column four times, before being passed through the phospho-SPEKA column four times. After extensive washing of each column, the antibodies were eluted with 200mM acetic acid directly into Tris base to neutralise each fraction immediately. Each fraction was checked to ensure that pH 7-8 had been reached, before being incubated with dot blots onto nitrocellulose paper that had either the phospho or dephospho peptide spotted onto it. Figure 5.1 shows the scheme for purification and representative dot blots from fraction 3. The antibody seemed very specific toward the phospho peptide (compare bottom panels, left versus right). Also, the dephospho peptide elution had a preference for the dephospho peptide (compare top panels, left with right, figure 5.1).

However, to see how the antibody performed on intact proteins, each elution was incubated by western blot with recombinant 14-3-3 β, ζ and homogenised sheep brain (figure 5.2). Fraction 3 gave the clearest difference between sheep brain (where approximately 50% of the 14-3-3 is phosphorylated [7]) and recombinant 14-3-3 (unphosphorylated). Considering the molar amount of 14-3-3 in the recombinant protein lanes compared to whole brain lysate, the specificity seemed good. However many cross-reacting bands can be seen, especially in fractions 3-6, so this would limit the use of the antibody to western blotting.

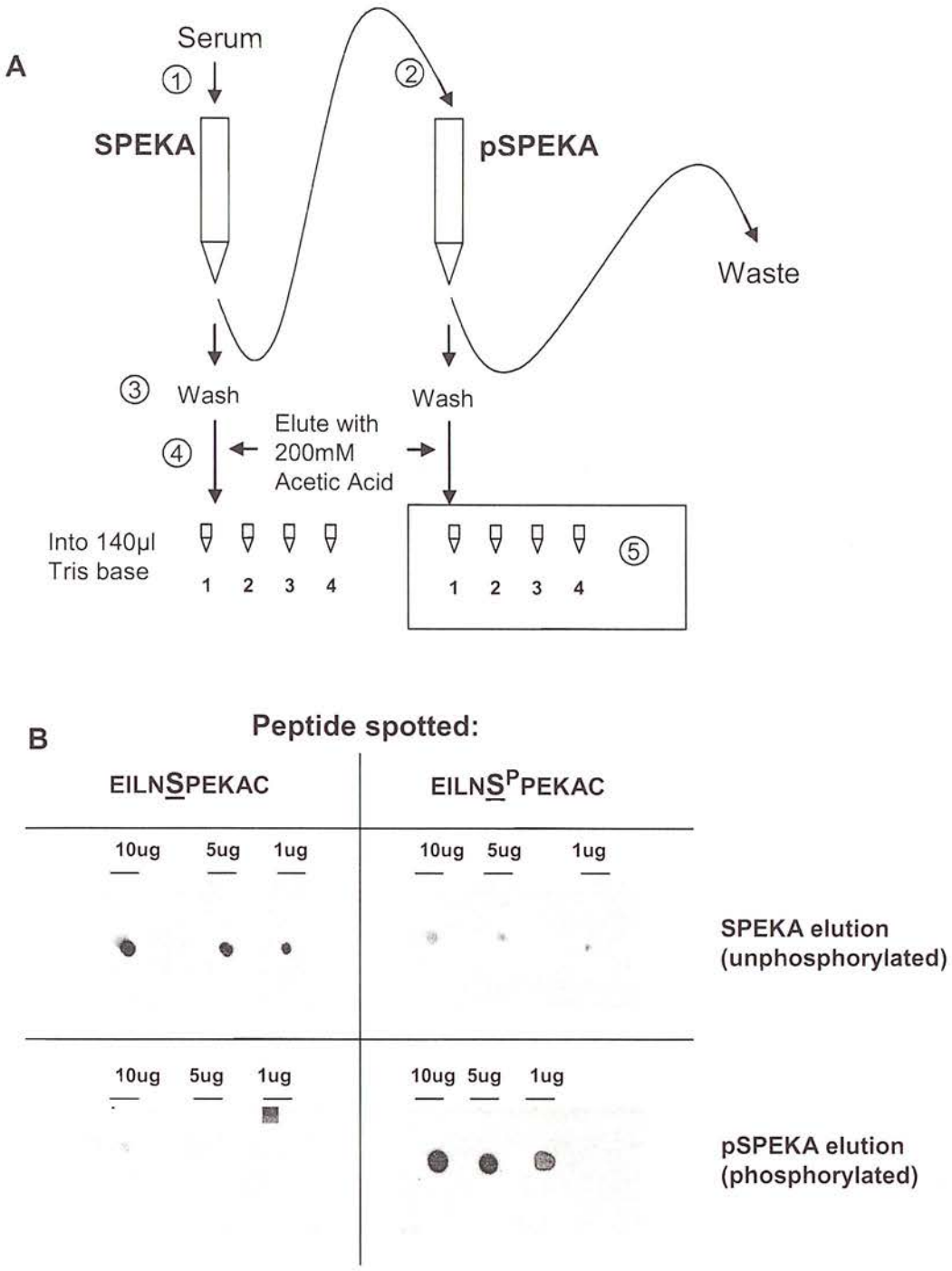

Figure 5.1 A Scheme showing stages of antibody purification. After passing serum through each peptide column (1 and 2), 4 Column columns of wash buffer was passed through (3), finally the antibody was eluted using acetic acid (4) into Tris base (5). **B.** Dot blots of SPEKA/pSPEKA peptides. Each peptide was dissolved in water at a concentration of 1mg/ml and the indicated amount spotted onto nitrocellulose. After blocking, each nitrocellulose strip was incubated with fraction 3 at a dilution of 1:500. HRP conjugated anti-sheep antibody was used at 1:2000, before being developed with ECL

A

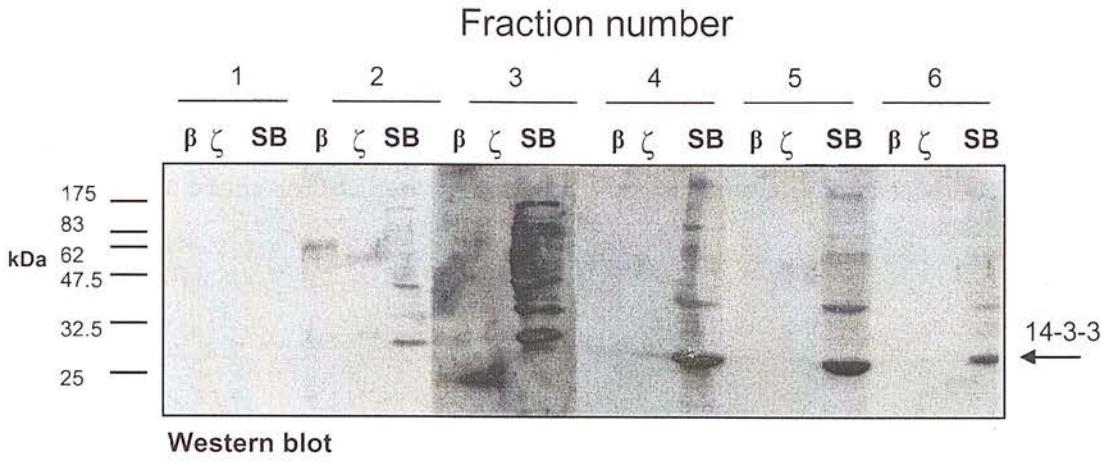

B

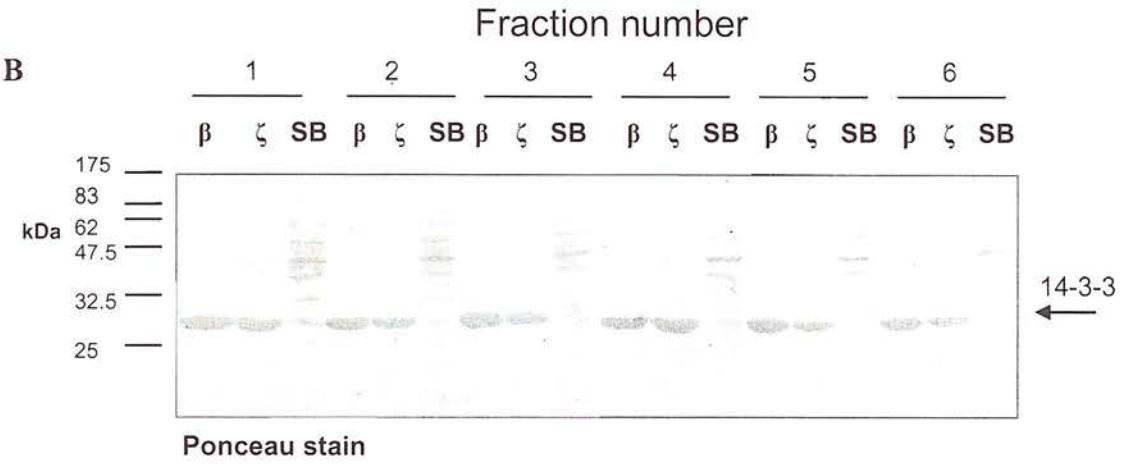

Figure 5.2 A. Western blotting of recombinant 14-3-3 β, ζ and sheep brain extract. 10μg of recombinant protein and 20μg total protein from a sheep brain lysate was loaded, as indicated onto an SDS-PAGE gel and transferred to nitrocellulose. After ponceau staining, the nitrocellulose was cut into strips, blocked and incubated with antibody elutions 1 to 6. The strips were re-aligned, incubated with ECL and exposed for the same length of time. A ponceau load control panel is shown in **B**.

5.2.1. Sensitivity of the pSPEKA antibody

To ascertain the lower detection limit of the antibody, serial dilutions of brain homogenate were separated by SDS-PAGE, transferred to nitrocellulose membrane and blotted with the same concentration of pSPEKA antibody. Figure 5.3 shows the pSPEKA antibody incubated with increasing amounts of sheep brain homogenate and recombinant 14-3-3 ζ. A ponceau stain is shown as a load control underneath. As little as 2μg total brain homogenate, is sufficient to provide a strong signal at 30kDa, however more bands are recognised as the amount of protein is increased, see the right hand lanes.

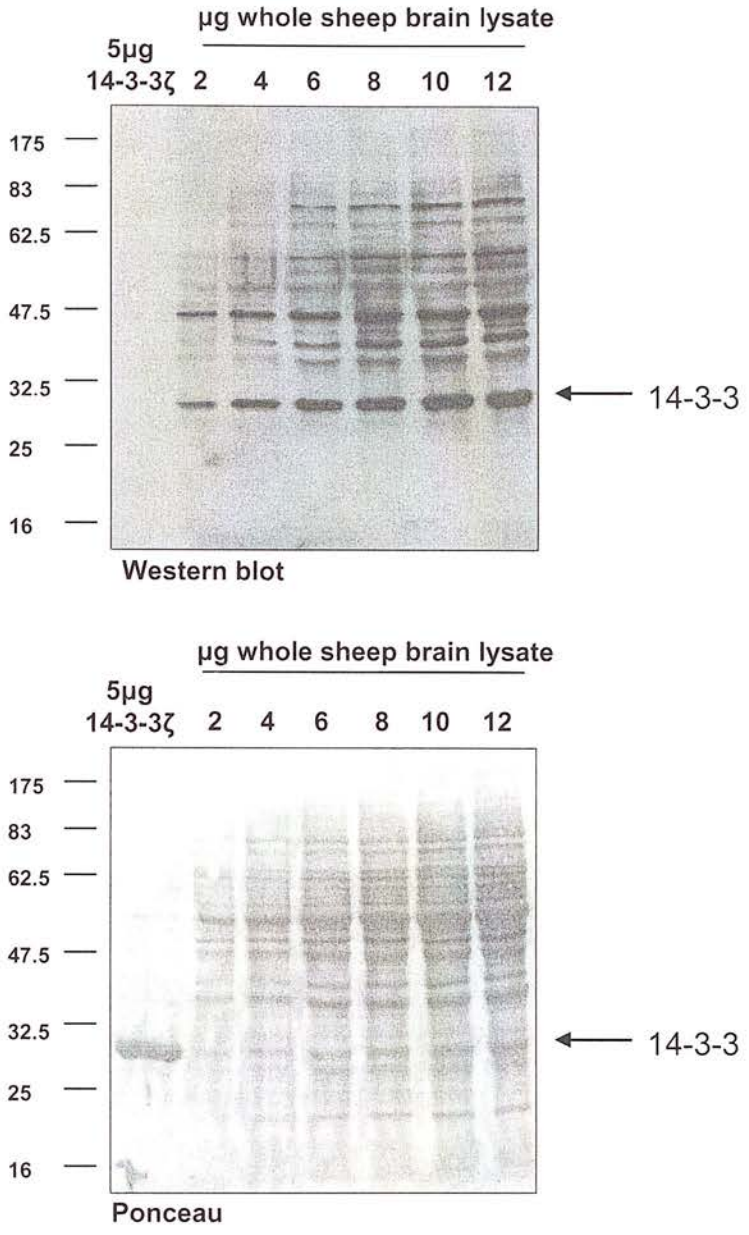

Figure 5.3 Serial dilutions of sheep brain, incubated with pSPEKA antibody. Fraction 3 was diluted 1:1000 into a 1% BSA solution, in TBS-T and incubated as described in Materials and methods. A ponceau stain of the western blot is shown in the lower panel, indicating overall protein loading.

5.2.2. Purification of Phospho S233 antibody

Phosphorylation of S233 on 14-3-3 isoforms has important regulatory consequences as discussed above and in chapter 1. In an attempt to produce antibodies against phosphorylated (pS233) 14-3-3 ζ two phospho peptides were used, corresponding to the region around S233, as described in Materials and methods. One peptide had a cysteine at the N-terminus (*C*WTSDpT^{233}QGDE), the other at the C-terminus (WTSDpT^{233}QGDE*C*); however these peptides did not elicit an immunogenic response from the animal, despite using a number of strategies. This included multiple antigenic peptides (MAPs) that were used to immunise the sheep. The MAP system [457] allows a large number of peptides to be chemically coupled directly onto radially branched lysine side chains, allowing significantly increased exposure of the antigen. Different combinations of boost immunisation using BSA and MAP linked peptides were used, but no serum collected from these animals produced a good immunogenic response.

In a bid to circumvent this problem, a longer peptide corresponding to this region (*C*TLWTSDTpT^{233}QGDEAEAG) was produced for the production of a phospho-specific antibody. This relatively long peptide was chosen with the intention of creating a good antigenic response, although the large size may trigger production of several different, non-pS233 specific antibodies. To try and purify specific antibodies from the serum, two shorter peptides used for the original immunisation were used to affinity purify the antibodies. The peptides were immobilised using the sulfolink beads and binding efficiency estimated using Ellman's reagent (see Materials and methods). The serum was clarified by centrifugation and passed through each N- or C- terminal linked peptide column in the same manner as in figure 5.1, except without a dephospho peptide column first. Figure 5.4 shows each antibody elution incubated against recombinant 14-3-3 ζ and 20μg sheep brain homogenate. The antibody clearly recognises 14-3-3 from both sources, indicating little phosphorylation specificity. However the amount of 14-3-3 used was, in molar terms, very high compared to that found in 20μl total sheep brain. The antibody however does recognise 14-3-3 with very little or no background.

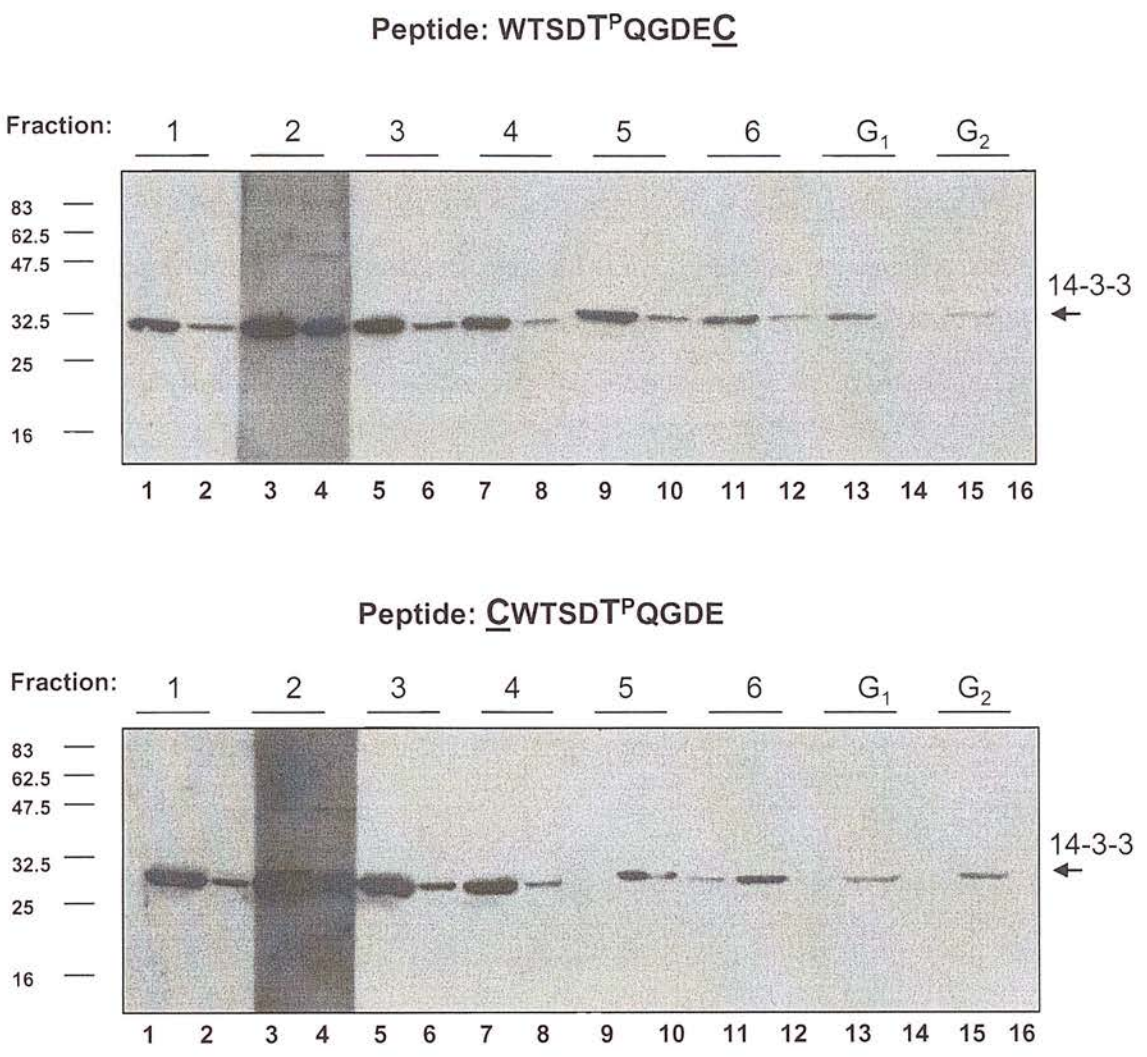

Figure 5.4 Testing of anti S233 antibody
Odd numbered lanes show 5μg of recombinant 14-3-3 ζ. Even numbered lanes show 20μg whole brain lysate. Fractions 1-6 are acetic acid elutions, G1 and G2 are 2M guanidine elutions. Ponceau stain confirmed equal loading as in 5.2 (data not shown).

5.2.3. Cross reactivity of the 233L antibody

The sequence used to create the antibody corresponds to a relatively variable region of 14-3-3, with mainly conserved substitutions around residue 233. A sequence alignment around this region, between all 14-3-3 isoforms, is shown in figure 5.5C, with the zeta sequence in bold, underlined. Experiments were therefore performed to ascertain which isoforms would cross react with the 233L antibody. Recombinant 14-3-3 isoforms were prepared as described in Materials and methods, separated by SDS-PAGE and western blotted using the 233L antibody as shown in figure 5.5A. Two exposure times are shown, for each N- and C-terminal peptide elution (upper and lower panels in 5.5.A), ponceau load controls are shown in 5.5B. The antibody did predominantly recognise 14-3-3 ζ, but was not specific; other isoforms are visible on the longer exposure (60 min) - the cross reactivity with γ, η, ε is summarised in figure 5.5C.

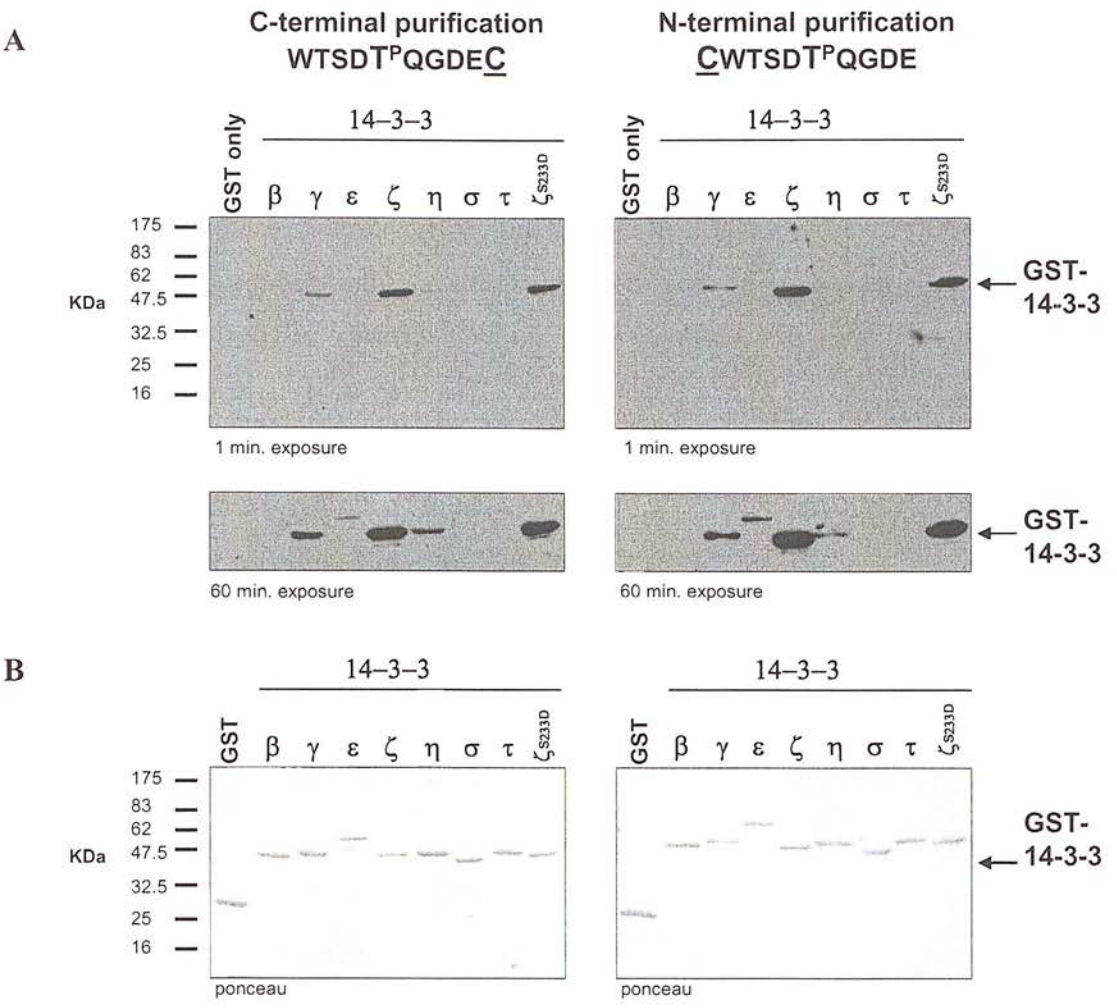

C

		Cross reaction with C233L
γ	DNLTLWTSDQQDDDG--GE	yes
τ	DNLTLWTSDSAGEECDAAE	no
ζ	DNLTL**WTSDTQGDE**AEAGE	yes
β	DNLTWTSENQGDEGDAGEG	no
η	DNLTLWTSDQQDEE–AGE	yes (faint)
σ	DNLTLWTADNAGEEGGEAP	no
ε	DNLTLWTSDMQGDGEEQNK	yes (faint)

Figure 5.5 Cross reactivity of T233L antibody with other 14-3-3 isoforms. **A,** All GST-14-3-3 isoforms were purified as described in Materials and methods. Approximately equal amounts of protein were separated by SDS-PAGE, transferred to nitrocellulose and western blotted using a 1:500 dilution of each (N- or C-) elution of the T233L antibody. A longer exposure (60 min.) is shown in the lower panel. **B,** Ponceau stain shows equal 14-3-3 loading. **C,** sequence alignment of 14-3-3 isoforms around the sequence used to raise the T233L and a summary of the findings in **A,** indicating cross reactivity between isoforms.

5.2.4. Immunoprecipitation of 14-3-3 using T233L antibody.

Immunoprecipitation of endogenous 14-3-3 from cell or tissue lysates would be an advantageous method for studying 14-3-3 binding partners. However many antibodies are not suitable for this purpose, perhaps due to most being raised to sequences that are inaccessible in the tertiary structure. A good example is our N-terminal 14-3-3 antisera where the epitope is in the dimer interface. The use of an epitope that corresponds to an exposed region may be poorly immunogenic. The mechanism that prevents animals from recognising 'self' would be unlikely to produce significant amounts of Ig against an antigen found within the animal itself. As this antibody was raised to a sequence within the C-terminal region of 14-3-3, that is an exposed, unstructured region [131], experiments were performed to determine if the antibody could immunoprecipitate 14-3-3 from cell lysates. A cell lysate was prepared fresh from HEK293 cells and also a rat brain was homogenised as described in Materials and methods. Approximately 2.5mg of each lysate was incubated first with ~10μg of the T233L antibody, overnight at 4°C, with gentle rotation, followed by addition of protein A:G sepharose beads to capture the antibody. After extensive washing, the immunoprecipitations were separated by SDS-PAGE and stained with coomassie blue (figure 5.6). Control immunoprecipitations were performed with an antiserum raised against a non-cognate peptide (control IgG). It is apparent that the control antibody consists of a different class of Ig molecules, as observed by coomassie staining (middle lanes of each panel). A 20μg sample of the cell/brain lysate incubated with the antibodies is shown in the left hand lane of each panel. Immunoprecipitated 14-3-3 is indicated with an arrow and was purified from both cell lysates. This does not suggest that 14-3-3 is phosphorylated in these cell lines.

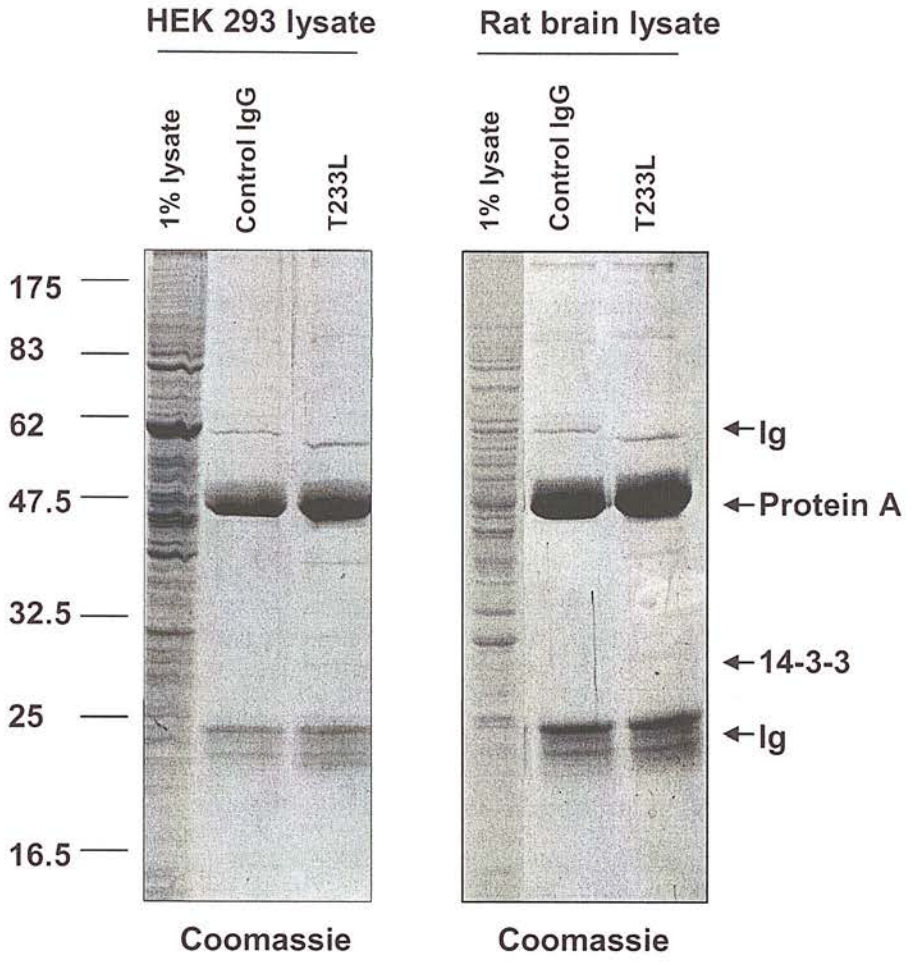

Figure 5.6 Immunoprecipitation of 14-3-3 from cell and tissue lysates
100µl of the 233L antibody from fraction 3 was incubated with either clarified HEK293 lysate or rat brain lysate overnight at 4°C, with gentle rotation. Equal amounts of protein A:G beads were added to capture the antibodies, the beads were extensively washed, boiled and visualised by SDS-PAGE and coomassie blue staining.

5.2.5. Discussion

The production and purification of phospho-specific antibodies is an extremely useful, if not essential, process to fully understanding protein phosphorylation events in biological systems. The characterisation here of an antibody specific for phosphorylated S185 on 14-3-3 ζ will greatly aid future work regarding 14-3-3 regulation. The discovery during these studies of the kinase capable of phosphorylation of 14-3-3 on S185 [170] also opens up many possibilities for future work.

Although the pSPEKA antibody recognises proteins of different molecular sizes (see figure 5.3) it is worth noting that even monoclonal antibodies against pSer/pThr motifs have broad sequence specificity. For example, the Biomol (Exeter, UK) antibody 16B4 recognises pSK as well as the pSP motif [458]; other monoclonal antibodies recognise similarly variable sequences [458]. Therefore, it is likely to be impossible to purify the antibody further, as removal of the Ig class that recognise other bands in the lysate (not at 30K), would be the very antibodies that recognise phosphorylated 14-3-3.

Attempts to produce a phospho-specific antibody to phosphorylated S233 on 14-3-3 ζ were unsuccessful, but did produce a very clean antibody, that would be useful for *in vivo* staining of 14-3-3 by indirect immunofluorescence or immunoprecipitation, as suggested in figure 5.6. The antibody does show cross-reactivity to other isoforms that would preclude its use for identifying specific 14-3-3 isoforms.

CHAPTER 6
General Discussion

6. General Discussion

The aim of this investigation was to further characterise the interactions between 14-3-3 and other signalling molecules, in particular kinases that phosphorylate 14-3-3. 14-3-3s have a history of regulating enzyme activity through molecular constraints or directing the sub-cellular distribution of bound enzymes (see chapter 1). The interaction of BCR and CK1 with 14-3-3 was examined in separate studies using a number of methods including *in vitro* binding assays, peptide affinity assays, kinase assays, site directed mutagenesis and immunoprecipitation from cell lysates. The use of antibodies specific to 14-3-3 isoforms and purified recombinant 14-3-3 protein allowed the identification of isoform binding specificity to be determined for both BCR and CK1, discussed in chapters 3 and 4 respectively.

This chapter provides a summary of results presented in this thesis and potential roles for association of BCR and CK1 with 14-3-3 are discussed.

6.1. BCR

The number of 14-3-3 isoforms known to bind BCR is herein increased to six: β, ζ, τ, η, γ and ε, with σ shown not to interact *in vitro*. The fact that only τ and ζ are substrates for BCR (figure 3.4) suggests that all the isoforms may be binding for reasons other than for the purpose of phosphorylation, perhaps to modulate kinase activity or alter subcellular location. The isoforms that are not phosphorylated do not possess a Ser/Thr residue at position 233. This, combined with site directed mutagenesis firmly proved residue 233 as the site of phosphorylation. It is pertinent to note that the isoforms η and γ are not substrates, yet have the highest binding affinity to BCR. Phosphorylation of the 14-3-3 β, ζ, and σ isoforms, on S185, reduces the binding capacity of 14-3-3 [145, 170, 172]. Phosphorylation of S233 also reduces interaction with ligands [145, 172], therefore the binding of unphosphorylatable 14-3-3 isoforms could allow a longer association time. For example, the binding of the η, γ, ε, and β isoforms to BCR could allow a more stable interaction with Raf-1 kinase [187]. Indeed the tertiary complex observed in COS cells for BCR, 14-3-3 and Raf-1 was with the 14-3-3 β isoform [187]. No functional consequence has been reported for the association of BCR with Raf-1 through 14-3-3, but 10 times more BCR/Raf complex was found in the membrane fraction compared to the cytosolic fraction [187]. Raf-1 kinase can associate with a great number of proteins and the activation and regulation is therefore particularly complex [279]. Recently, BCR has been found localised at the cell membrane in polarised Calu-3 (lung epithelial) cells [253]. The authors also found BCR co-localising with proteins associated with coated vesicles and the trans-Golgi network [253], indicating a potential role for BCR in these processes. BCR was also shown to associate with two PDZ domain containing proteins called PDZK1 and Mint3 [253]. Both interact through the C-terminal 'STEV' domain of BCR at intracellular junction of cultured epithelial cells [253]. It is interesting to note that BCR does not interact with 14-3-3 σ, as shown in this study (figure 3.5), when considering that 14-3-3 σ is highly expressed in this cell type [2, 189]. That the two cannot interact, suggests the potential outcome of binding would be highly deleterious to the cell, perhaps by 14-3-3 σ recruiting another protein which would affect BCR activity.

BCR has been shown to negatively affect Raf activation by phosphorylating and binding to AF-6, leading to increased affinity of AF-6 for Ras, preventing the interaction between Raf and Ras [252]. The proposed model, in quiescent cells, involves the formation of a trimeric complex of BCR, Ras and AF-6. This causes downregulation of Ras-mediated signalling, maintaining cells in a non-proliferative state at points of cell to cell contact [252]. Tyrosine phosphorylation [of BCR] inactivates BCR kinase activity, leading to release of AF-6, therefore eliminating competition for Ras, resulting in activation of the Raf signalling cascade [252]. The binding of 14-3-3 could add an extra layer of complexity to this sequence of events, by potentially recruiting other molecules to these locations, or altering kinase activity of BCR. As another substrate of BCR, AF-6 and 14-3-3 both play a role in modulation of the Raf/MEK/ERK pathway; AF-6 by altering Ras levels and 14-3-3 by interaction with Raf.

BCR has both PH and C2 domains (see figure 1.9) that could aid targeting to the membrane, perhaps explaining the observed location, by Malmberg et al [253], of BCR at the membrane of Calu-3 cells. Additionally, BCR was shown to reside at the same location as β-COP vesicles in non-polarised BHK cells [253]. In a different study, 14-3-3 β mediated retrograde transport of HCNK3 channels by binding to a non-canonical 14-3-3 binding motif, displacing binding of β-COP (that was bound to a distinct, dibasic motif) allowing HCNK3 to escape to the membrane [64]. In another study, 14-3-3 ζ and ε were shown to bind the (ATP) channel alpha subunit, Kir6.2, in a similar mechanism, displacing COPI and allowing release of Kir to the membrane [459]. It is tempting to speculate on the existence of a ternary complex, involving BCR, 14-3-3 and COP vesicles based on the observation that 14-3-3 associates with BCR and the latter is predominantly in the same location as β-COP.

During this investigation, it was hypothesised that endogenous CK1 may bind to endogenous 14-3-3, forming a trimeric complex with BCR. This tertiary complex could have explained the phosphorylation of residue 233 on τ and ζ, a known phosphorylation site of CK1 [172]. The use of two highly specific inhibitors of CK1 ruled out this possibility. Combined with site directed mutagenesis, I identified that BCR is directly responsible for phosphorylation of 14-3-3 on residue 233 [460].

In a preliminary experiment to ascertain the best lysis buffer for preparation of BCR kinase, it was found that preservation of tyrosine phosphorylation had a positive effect on the ability of BCR to phosphorylate 14-3-3 τ (figure 3.3). This is generally contradictory to previous work [267, 269], although the tyrosine residue(s) phosphorylated in the preparation used here, were not determined. Phosphorylation of BCR by Fes kinase on residue Y177 reduced the ability of BCR to phosphorylate 14-3-3 [267]. A similar result was reported for the phosphorylation of Y360 [269]. The authors showed expression and purification of BCR in cells co-expressing BCR and BCR-ABL under conditions designed to preserve tyrosine phosphorylation, had reduced kinase activity toward casein and histone [269]. However, experiments described in chapter 3 were from cells expressing only BCR, therefore it is unlikely that the residues Y177 and Y360 are phosphorylated by these kinase(s) and thus data shown in figure 3.3 indicated phosphorylation on distinct tyrosine residues. Interestingly, tyrosine phosphorylation did not seem to affect 14-3-3 association in BCR-FLAG immunoprecipitations (figure 3.3).

This investigation also revealed that a PKA-like kinase, from cell lysates, can associate with the M2 α-FLAG antibody (see chapter 3). The discovery was accidental due to the use of recombinant protein with an incorporated PKA motif, which was not thought to be relevant. Use of a specific PKA inhibitor further implicated the kinase as PKA. The specific PKA inhibitor had no effect on BCR-FLAG immunoprecipitates, ruling out PKA as a contaminating kinase phosphorylating 14-3-3 on residue 233. This may not be a problem with α-FLAG antibodies generally, as the substrate used in this kinase assay had an optimal PKA motif, thereby making the assay very sensitive.

6.2. CK1

Chapter 4 explores the interaction of CK1 with 14-3-3, identifying a specific and direct interaction both *in vitro* and *in vivo*. Previous work in our laboratory identified CK1 as a 14-3-3 S/T 233 kinase [172], but the interaction had not been further investigated. A physiological consequence of 14-3-3 ζ T233 phosphorylation is to negatively affect interaction with Raf [145, 172] (and perhaps other ligands), therefore by phosphorylating 14-3-3 ζ on residue 233, it is possible that CK1 could negatively affect its own interaction. Considering this, observations outlined in chapter 4 suggest that CK1 has a greater affinity for 14-3-3 isoforms other than ζ, irrespective of this possibility. Firstly, *in vitro* binding experiments using a phospho peptide incorporating residue pS218 of CK1α showed that 14-3-3 isoforms η, γ, β, ε and τ bound with considerably more affinity than ζ (figure 4.5). Using a peptide corresponding to CK1 interacting region eliminates the possibility of CK1 phosphorylating 14-3-3 and thus negatively affecting the interaction. Secondly, performing binding experiments from cell lysates at 4°C would be expected to inhibit all enzymatic activity. 14-3-3 τ has a phosphorylatable residue at position 233 and although no published data has shown that phosphorylation of this residue negatively affects the interaction with other proteins; the sequence and structure conservation of 14-3-3 isoforms suggests phosphorylation would have a similar outcome. It is interesting to note from figure 4.12 that 14-3-3 τ binds intact CK1 with a similar affinity as ζ.

Truncation mutants of CK1α suggested another 14-3-3 binding site and further experiments identified S242 as an essential residue for interaction with 14-3-3 in HEK293 cells (figure 4.15). Analysis of 14-3-3 isoform specificity was also addressed *in vivo* by immunoprecipitating transfected HA-CK1α from cultured cells and analysing the precipitates with isoform specific antibodies. Although the antibodies have very similar titres, firm conclusions cannot be drawn for a particular isoform binding with greater affinity. Aside from the titre variation, heterodimerisation (discussed in 1.2.6.) will preclude definitive analysis *in vivo*. Nevertheless, from these data it is clear that η and γ give a much better signal than the other isoforms tested; β, ζ and ε. The low abundance of 14-3-3 σ and τ in cell lysates precluded analysis, see figure 4.11. For the reason of highest affinity, antibodies to

14-3-3 η were used predominantly throughout these studies. The interaction could potentially be regulated though PKA activation, as the use of the PKA stimulant db-cAMP caused an increase in 14-3-3:CK1 association in HEK293 cells. Antagonising PKA activity by a myristoylated PKA inhibitor peptide also reduced CK1:14-3-3 interaction.

CK1 and 14-3-3 are both ubiquitous, abundant proteins and the exact mode of interaction is complex. The ubiquitous nature of CK1 and large number of substrates recorded for the kinase (see table 1.7), suggests changes in local concentrations of the enzyme as a way of regulation. In the next part of this chapter the findings outlined above and in chapter 4 will be discussed. The results support a role for 14-3-3 in regulation of CK1 activity, with the involvement of centaurin-α_1.

CK1 associates with several molecular scaffold-type proteins, including axin [420], CG-NAP/AKAP450 [415] and centaurin-α. -α_1 [419] with little or no effect on kinase activity. In this study, the interaction of centaurin-α_1 with CK1α was shown to be negatively affected by two mechanisms. One is phosphorylation of S218 on CK1α (figure 4.6) and the other, by phosphorylation of centaurin-α_1 by PKC (figure 4.24). CK1 associates with centaurin-α and -α_1 in cells [419] and because centaurin-α_1 associates with PIP_3 [425], it has been suggested as a mode of recruiting CK1α to the plasma membrane [419]. CK1 may well play a role at the membrane, despite being largely cytoplasmic, as immunocytochemistry has identified CK1δ localising with membranous structures [339]. Also, in *S. cerevisiae*, three out of the four isoforms (YCKI, YCK2, YCK3) carry a consensus for isoprenylation at the C-terminus and are indeed found tightly associated with the membrane [461]. The fourth isoform, HRR25, does not contain this sequence and is found predominantly in the nucleus [461]. Interestingly, results from our laboratory have shown that HRR25 associates with the yeast 14-3-3 isoform BMH1 and is the principal 14-3-3 kinase in yeast (manuscript under revision). CK1α has no isoprenylation consensus and so association with membrane bound proteins would be one method of bringing CK1 in contact to substrates at the membrane. Centaurin-α and –α_1 associate through a region containing S218 and the interaction does not affect CK1 kinase activity [419]. Continued CK1 activity at the plasma membrane would most probably be detrimental to the cell; therefore one mode of regulation would be

to limit CK1 access to the membrane. The finding here that centaurin-α_1 can only associate with the dephosphorylated S218 peptide suggests phosphorylation of CK1, potentially through a protein kinase A regulated pathway, would prevent association and remove CK1 from the membrane. A further consequence of CK1 phosphorylation would be the association with 14-3-3. Data presented in chapter 4 suggests CK1α associates with 14-3-3 in a phosphorylation dependent manner, mediated through two phosphorylated Ser residues: S218 and S242, although the mode of binding of CK1α to specific 14-3-3 isoforms is distinct, for the following reasons. Point mutations designed to disrupt phosphorylation dependent binding through the binding groove of 14-3-3 ζ (R5660A) had no effect on CK1α binding (figure 4.17). Similarly, competition experiments using high affinity 14-3-3 binding peptides, which bind into the binding groove of 14-3-3, did not disrupt binding to 14-3-3 ζ (figure 4.18). In contrast, the data obtained using high affinity 14-3-3 binding peptides and 14-3-3 η, showed that CK1α does interact through the 14-3-3 η binding groove (figure 4.18). Therefore to explain the fact that 14-3-3 ζ does bind CK1α in a phosphorylation dependent manner (figure 4.4, 4.8, 4.14 and 4.15) suggests the interaction must be by an uncharacterised mechanism. This binding mechanism may be conserved for kinases that phosphorylate 14-3-3. Indeed, it is worth noting that BCR binds a similar pattern of 14-3-3 isoforms as CK1α; with both kinases binding the phosphorylatable 14-3-3 isoforms, ζ and τ, with low affinity (compared to the other isoforms).

Association of 14-3-3 with CK1 would likely prevent association with centaurin-α_1, as they share the same interaction site, thereby providing another mode of removing CK1 from the membrane. Association with 14-3-3 may also reduce CK1 activity; a mode of action often attributed to 14-3-3, for example 14-3-3 reduces the kinase activity of PKC [462], CamKII [35], MAPKAPKII [41], PKD (PKCμ) [42], PDK1 [463] and BMK1/ERK5 [33].

In the later part of chapter 4, the PKC phosphorylation sites on centaurin-α_1 were determined (figure 4.23) [453]. Analysis of the primary structure of centaurin-α_1 shows that S87 is outwith any known functional domain and S276 is N-terminal to the second PH domain. Additionally, comparison of the location of this residue, with other PH domain crystal structures, shows it is unlikely to affect PtsIns binding.

Phosphorylation does, however, reduce the affinity to CK1α *in vitro* (figure 4.24). This potentially defines another regulatory mechanism to reduce CK1 presence at the cell membrane (figure 6.1).

Mutation of S218/S242 reduced the amount of ^{32}P incorporated (figure 4.19), suggesting that these are autophosphorylation sites. Therefore autophosphorylation could provide another mechanism to reduce CK1 localisation to the membrane.

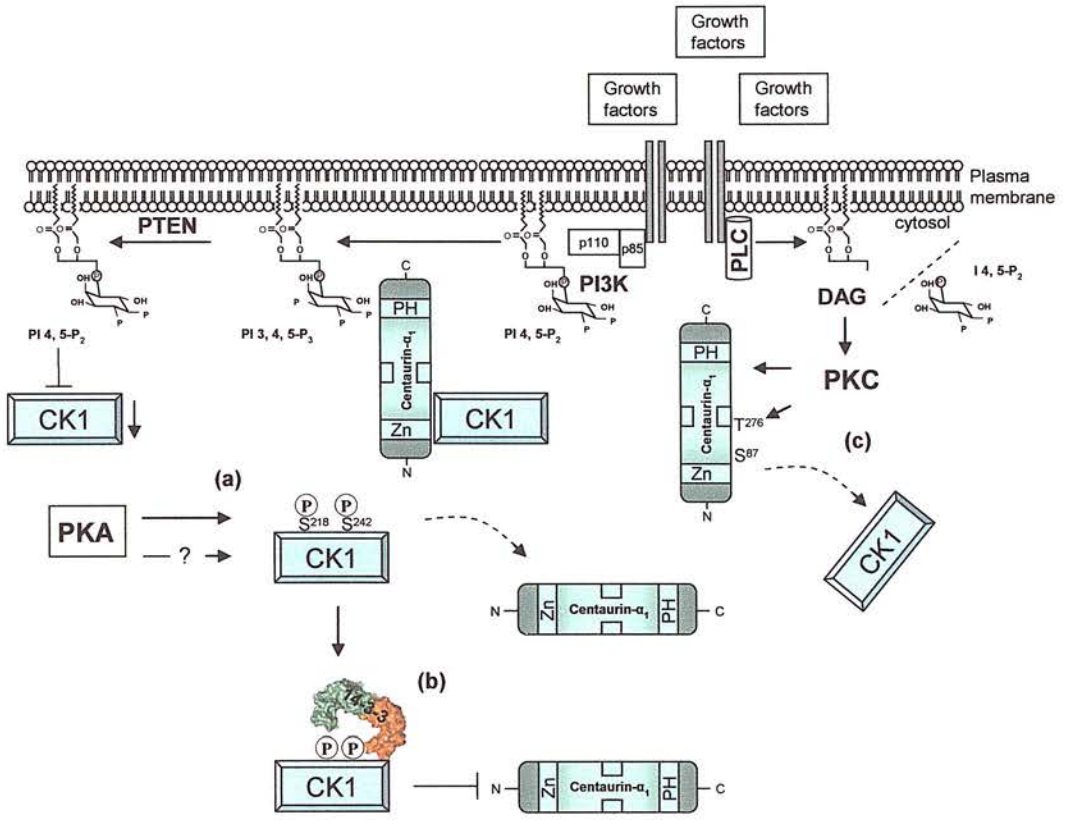

Figure 6.1 Proposed model for CK1α recruitment to the cell membrane
Growth factors induce activation of tyrosine kinase receptors and activation of PI3K. Generation of PIP3 recruits centaurin-α_1 to the membrane, CK1 binds centaurin-α_1; localising to the membrane. CK1 activity at the membrane is attenuated by phosphorylation through a PKA mediated system, by two routes. One is phosphorylation which blocks interaction directly (a) and the second is phosphorylation to create a binding site for 14-3-3, also blocking interaction (b). Recruitment of CK1 to membrane is also impaired by PKC phosphorylation of centaurin (c). PKA activity can also be phosphorylated and activated by PDK1 [464], the net effect on recruitment of CK1α could therefore be either increased or decreased by growth factors.

Immobilised peptide columns are a useful way of identifying proteins that interact with a specific region. An additional benefit is the large binding capacity, enabling the capture of sufficient protein for accurate determination of proteins by mass spectrometry, an approach that led to this study [419, 421]. The region around S218 is clearly important for 14-3-3 association (figure 4.4, 4.15) and may well be important for catalytic activity of CK1 (figure 4.21). A basic region immediately C-terminal from residues 228-231 has recently been shown to be essential for association with axin [420]. Binding of axin to CK1α did not affect kinase activity of CK1α toward casein or a specific peptide substrate [420]. A further paper, using the same K→A mutants, suggested that the ability of CK1 to discern between phosphate primed substrates and non-canonical substrates was lost [455]. Mutation of the basic region increased the k_m up to 40 fold for a ps-4 peptide, 6 fold for ps-3 primed peptide[1], however a single mutation of K232→A had the same detrimental effect as mutation of the whole basic region [455]. The authors also noted that a peptide from β-catenin containing a 'non-canonical' consensus motif was phosphorylated regardless of the mutation carried in CK1. In summary, the lysine residue 232 is essential for recognition of phosphorylated substrates. This region is very near the site of proposed 14-3-3 interaction (see figure 6.1). If 14-3-3 was interacting through this region, this could interfere with substrate recognition and therefore activity of the enzyme.

Also indicated in figure 6.2 is a residue corresponding to T44 in CK1δ. A missense mutation (T44→A) of which causes Familial advanced sleep phase syndrome (FASPS) [465]. Analysis of kinetic parameters of the T44A mutant CK1 showed the V_{max} to be 60 % of wild type CK1δ, and the k_m was 82% [465]. The overall effect on catalytic efficiency (V_{max}/K_m) is therefore decreased (to 73% of wild type). The mutant also showed variable levels of phosphorylation depending on substrate, suggesting that residue Thr 44 is involved in substrate recognition. This residue is some distance from the active site (see figure 6.2), yet the T44A mutation clearly exerts an effect on CK1δ activity, implying extensive contacts are made between CK1 and binding partners. Incubation of CK1α with phosphatase inhibitors, as described in chapter 4, may well result in phosphorylation of residues other than

[1] pS-n refers to a 'primed' substrate, where n is the position of the pre-phosphorylated residue, N-terminal to the target Ser/Thr, for example: pS-3 = pSXXS/T, underlined residue is the target residue.

S218 and S242. Phosphorylation of residue T44, or other residues, could cause a structural change in CK1, increasing the affinity toward 14-3-3, explaining how 14-3-3 binding mutants of 14-3-3 and blocking peptides had no effect on 14-3-3 ζ binding.

A

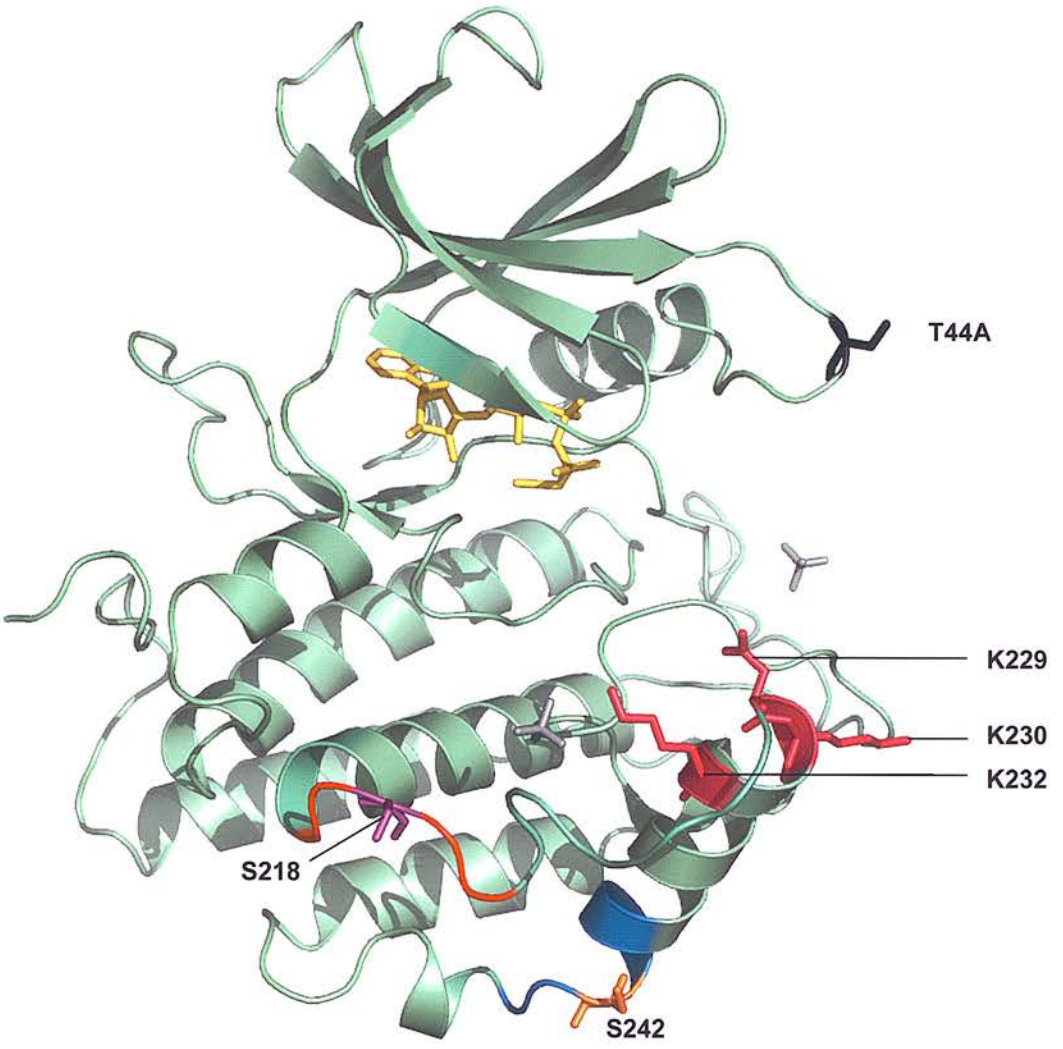

B

```
                                S218                                S242
Zebra fish   CK1α   210 LMYFNRTSLP WQGLKAATKK KKYEKISEKK MSTPVEVLCK
Human        CK1α   210 LMYFNRTSLP WQGLKAATKK QKYEKISEKK MSTPVEVLCK
Rabbit       CK1α   210 LMYFNRTSLP WQGLKAATKK QKYEKISEKK MSTPVEVLCK
                        ********** ********** -********* **********
                                   KAATKK QKYEK
```

Figure 6.2 crystal structure of CK1, indicating interaction sites

A, S218 is shown in purple, with surrounding binding motif in red. S242 is coloured orange, with binding motif in blue. Lysines required for co-ordinating recognition of canonical substrates as demonstrated by Bustos et al [455] are coloured pink. Mg^{2+}-ATP is shown in yellow, sulphate ions are in grey. The residue corresponding to T44 of CK1δ is shown in black. **B**, alignment of CK1α sequence around region 210-240. Lysines 229, 230 and 232 are indicated in pink, lysine 231 (peculiar to the zebra fish) was mutated to glutamine (sequence below alignment) for the study in [420, 455], see separate sequence, below; other colourings are the same as in **A**.

The crystal structures of CK1 and 14-3-3 have been known for some time [131, 393] and allow for computer modelling to suggest how the two might interact. Biochemical evidence gathered in this investigation suggested S218 and S242 as the prime interaction sites and the computer modelling carried out in chapter 4.25 was centred on these residues. The residues 218/242 were placed very near the 14-3-3 binding pocket, by an automated web based interface, using the molecular modelling software ZDOCK (figure 4.25) [447], suggesting an energetically favourable conformation. The orientation of 14-3-3:CK1 binding predicted by the ZDOCK program (figure 4.23) suggests that the residue S/T233 on 14-3-3 could not undergo phosphorylation when bound to S218 on CK1. The modelling does, however, suggest a rationale for results obtained in figure 4.17 and 4.18, where 14-3-3 is shown to interact outwith the central 14-3-3 binding groove. If 14-3-3 ζ were to interact with CK1α through this groove, whilst in contact with residues S218 and/or S242, unfeasibly large structural changes would have to occur to allow S233 access to the active site on CK1 and subsequent phosphorylation. Therefore 14-3-3 ζ must interact with CK1α elsewhere, presumably in a conformation that allows phosphorylation.

6.3. CONCLUSION

The interaction of 14-3-3 with two well studied kinases was examined. BCR phosphorylates 14-3-3 on an important, known, phosphorylation site, S233. Thus providing an explanation of results obtained in the original identification of 14-3-3 as a BCR substrate [147]. This kinase associated preferentially with the 14-3-3 η and γ isoforms. CK1α was shown to interact with 14-3-3 η through the classical amphipathic binding groove in a phosphorylation dependent and isoform specific manner. The interaction provides an attractive model for regulating a highly ubiquitous and second messenger independent kinase.

Chapter 7
Future work

7. Future work

The present study has identified the phosphorylation site on 14-3-3 by the BCR kinase as residue 233. Further studies are required to examine, *in vivo*, when 14-3-3 is phosphorylated, or what cellular conditions induce the phosphorylation. Few studies have addressed the physiological role of BCR [207] and the physiological effect of 14-3-3 interaction with BCR also remains to be studied. The identification of the 14-3-3 binding site(s) on BCR would provide a basis for further study of the interaction. This could be accomplished by the generation of point mutations within putative 14-3-3 binding sites on BCR - of which there are many candidates, see figure 1.9. Cell localisation studies on such mutants of BCR after cell stimulation could shed light on the involvement of 14-3-3.

An interaction between CK1 and 14-3-3 was investigated and a number of insights into the interaction have been discussed in chapter 4, however, further studies would be needed to fully understand the nature of the interaction. Firstly, it would be useful to produce a phospho-peptide corresponding to the region around pS242 – to compare binding affinity to the S218 peptide. Secondly, production of phospho-specific antibodies to S218 and S242 would allow intricate examination of how and when CK1 becomes phosphorylated. Identification of the CK1 kinase(s) would allow *in vitro* phosphorylation of CK1 and subsequent analysis of binding kinetics using techniques such as surface plasmon resonance. Immunoprecipitation of CK1 S218A/S242A mutants, which may act like pseudosubstrates, may allow sufficient levels of kinase(s) to bind for identification by mass spectrometry. Use of different cell stimulators/inhibitors, known to activate specific kinases would also lead to clues as to the identity of the kinase. Mutation of other phosphorylation sites (possibly Y161, T164 and S179 proposed by Xu et al [393]) could potentially help to remove background phosphorylation, aiding observation of phosphorylation by other kinase(s).

The finding that 14-3-3 ζ and η bind to CK1α in a different manner, and different affinity, warrants further investigation. Generation of both neutral and charge reversal mutations within the 14-3-3 η and γ isoform binding pockets would allow further characterisation of the interaction with CK1α.

Colocalisation studies involving CK1α, centaurin-α_1 and 14-3-3 following cell stimulation would be a useful approach to observe subcellular location, perhaps after cell stimulation with growth factors.

8. Appendix

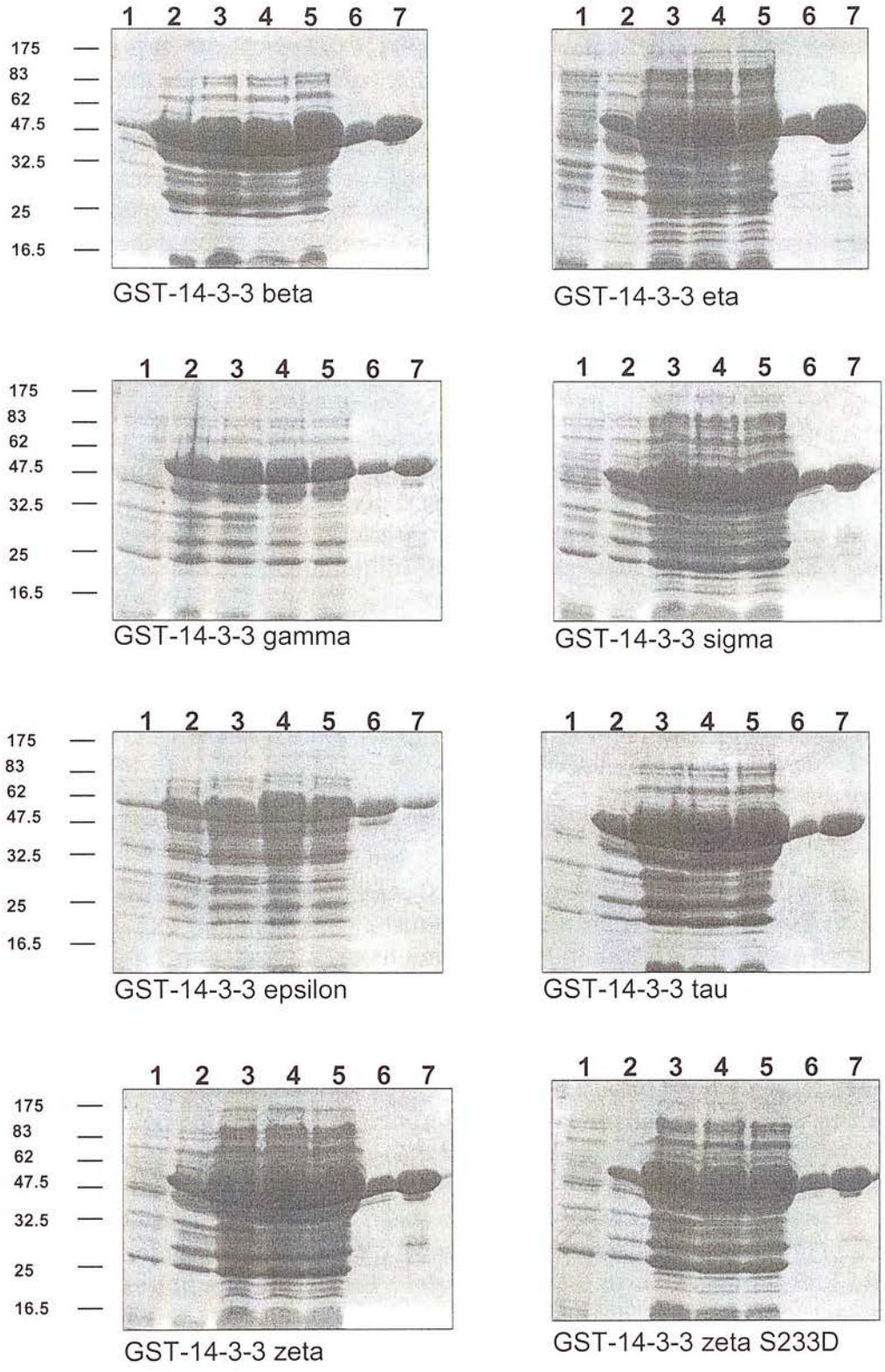

Appendix figure A1
Purification of recombinant GST-14-3-3 isoforms from bacterial lysates.

9. References

1 Moore, B. W., Perez, V. J. (1967) In: Physiological and Biochemical Aspects of Nervous Integration (ed. Carlson, F. D.), Prentice hall, Englewood Cliffs, N.J., 343-359

2 Celis, J. E., Gesser, B., Rasmussen, H. H., Madsen, P., Leffers, H., Dejgaard, K., Honore, B., Olsen, E., Ratz, G. and Lauridsen, J. B. (1990) Comprehensive two-dimensional gel protein databases offer a global approach to the analysis of human cells: the transformed amnion cells (AMA) master database and its link to genome DNA sequence data. Electrophoresis 11, 989-1071

3 Yamauchi, T., Nakata, H. and Fujisawa, H. (1981) A new activator protein that activates tryptophan 5-monooxygenase and tyrosine 3-monooxygenase in the presence of Ca2+-, calmodulin-dependent protein kinase. Purification and characterization. J Biol Chem 256, 5404-5409

4 Ichimura, T., Isobe, T., Okuyama, T., Yamauchi, T. and Fujisawa, H. (1987) Brain 14-3-3 protein is an activator protein that activates tryptophan 5-monooxygenase and tyrosine 3-monooxygenase in the presence of Ca2+,calmodulin-dependent protein kinase II. FEBS Lett 219, 79-82

5 Ichimura, T., Isobe, T., Okuyama, T., Takahashi, N., Araki, K., Kuwano, R. and Takahashi, Y. (1988) Molecular cloning of cDNA coding for brain-specific 14-3-3 protein, a protein kinase-dependent activator of tyrosine and tryptophan hydroxylases. Proc Natl Acad Sci U S A 85, 7084-7088

6 Aitken, A., Collinge, D. B., van Heusden, B. P., Isobe, T., Roseboom, P. H., Rosenfeld, G. and Soll, J. (1992) 14-3-3 proteins: a highly conserved, widespread family of eukaryotic proteins. Trends Biochem Sci 17, 498-501

7 Aitken, A., Howell, S., Jones, D., Madrazo, J. and Patel, Y. (1995) 14-3-3 alpha and delta are the phosphorylated forms of raf-activating 14-3-3 beta and zeta. In vivo stoichiometric phosphorylation in brain at a Ser-Pro-Glu-Lys MOTIF. J Biol Chem 270, 5706-5709

8 Nielsen, P. J. (1991) Primary structure of a human protein kinase regulator protein. Biochim Biophys Acta 1088, 425-428

9 Prasad, G. L., Valverius, E. M., McDuffie, E. and Cooper, H. L. (1992) Complementary DNA cloning of a novel epithelial cell marker protein, HME1, that may be down-regulated in neoplastic mammary cells. Cell Growth Differ 3, 507-513

10 Jones, D. H., Martin, H., Madrazo, J., Robinson, K. A., Nielsen, P., Roseboom, P. H., Patel, Y., Howell, S. A. and Aitken, A. (1995) Expression and structural analysis of 14-3-3 proteins. J Mol Biol 245, 375-384

11 Wilker, E. W., Grant, R. A., Artim, S. C. and Yaffe, M. B. (2005) A structural basis for 14-3-3 sigma functional specificity. J Biol Chem

12 Wang, W. and Shakes, D. C. (1996) Molecular evolution of the 14-3-3 protein family. J Mol Evol 43, 384-398

13 Rosenquist, M., Sehnke, P., Ferl, R. J., Sommarin, M. and Larsson, C. (2000) Evolution of the 14-3-3 protein family: does the large number of isoforms in multicellular organisms reflect functional specificity? J Mol Evol 51, 446-458

14 Muslin, A. J., Tanner, J. W., Allen, P. M. and Shaw, A. S. (1996) Interaction of 14-3-3 with signaling proteins is mediated by the recognition of phosphoserine. Cell 84, 889-897

15 Yaffe, M. B., Rittinger, K., Volinia, S., Caron, P. R., Aitken, A., Leffers, H., Gamblin, S. J., Smerdon, S. J. and Cantley, L. C. (1997) The structural basis for 14-3-3:phosphopeptide binding specificity. Cell 91, 961-971

16 Rittinger, K., Budman, J., Xu, J., Volinia, S., Cantley, L. C., Smerdon, S. J., Gamblin, S. J. and Yaffe, M. B. (1999) Structural analysis of 14-3-3 phosphopeptide complexes identifies a dual role for the nuclear export signal of 14-3-3 in ligand binding. Mol Cell 4, 153-166

17 Liu, Y. C., Liu, Y., Elly, C., Yoshida, H., Lipkowitz, S. and Altman, A. (1997) Serine phosphorylation of Cbl induced by phorbol ester enhances its association with 14-3-3 proteins in T cells via a novel serine-rich 14-3-3-binding motif. J Biol Chem 272, 9979-9985

18 Obsil, T., Ghirlando, R., Klein, D. C., Ganguly, S. and Dyda, F. (2001) Crystal structure of the 14-3-3zeta:serotonin N-acetyltransferase complex. a role for scaffolding in enzyme regulation. Cell 105, 257-267

19 Ganguly, S., Weller, J. L., Ho, A., Chemineau, P., Malpaux, B. and Klein, D. C. (2005) Melatonin synthesis: 14-3-3-dependent activation and inhibition of arylalkylamine N-acetyltransferase mediated by phosphoserine-205. Proc Natl Acad Sci U S A 102, 1222-1227

20 Svennelid, F., Olsson, A., Piotrowski, M., Rosenquist, M., Ottman, C., Larsson, C., Oecking, C. and Sommarin, M. (1999) Phosphorylation of Thr-948 at the C terminus of the plasma membrane H(+)-ATPase creates a binding site for the regulatory 14-3-3 protein. Plant Cell 11, 2379-2391

21 Waterman, M. J., Stavridi, E. S., Waterman, J. L. and Halazonetis, T. D. (1998) ATM-dependent activation of p53 involves dephosphorylation and association with 14-3-3 proteins. Nat Genet 19, 175-178

22 Ward, Y., Spinelli, B., Quon, M. J., Chen, H., Ikeda, S. R. and Kelly, K. (2004) Phosphorylation of critical serine residues in Gem separates cytoskeletal reorganization from down-regulation of calcium channel activity. Mol Cell Biol 24, 651-661

23 Winkler, D. G., Cutler, R. E., Jr., Drugan, J. K., Campbell, S., Morrison, D. K. and Cooper, J. A. (1998) Identification of residues in the cysteine-rich domain of Raf-1 that control Ras binding and Raf-1 activity. J Biol Chem 273, 21578-21584

24 McPherson, R. A., Harding, A., Roy, S., Lane, A. and Hancock, J. F. (1999) Interactions of c-Raf-1 with phosphatidylserine and 14-3-3. Oncogene 18, 3862-3869

25 Du, X., Fox, J. E. and Pei, S. (1996) Identification of a binding sequence for the 14-3-3 protein within the cytoplasmic domain of the adhesion receptor, platelet glycoprotein Ib alpha. J Biol Chem 271, 7362-7367

26 Fu, H., Coburn, J. and Collier, R. J. (1993) The eukaryotic host factor that activates exoenzyme S of Pseudomonas aeruginosa is a member of the 14-3-3 protein family. Proc Natl Acad Sci U S A 90, 2320-2324

27 Henriksson, M. L., Francis, M. S., Peden, A., Aili, M., Stefansson, K., Palmer, R., Aitken, A. and Hallberg, B. (2002) A nonphosphorylated 14-3-3 binding motif on exoenzyme S that is functional in vivo. Eur J Biochem 269, 4921-4929

28 Campbell, J. K., Gurung, R., Romero, S., Speed, C. J., Andrews, R. K., Berndt, M. C. and Mitchell, C. A. (1997) Activation of the 43 kDa inositol polyphosphate 5-phosphatase by 14-3-3zeta. Biochemistry 36, 15363-15370

29 Wang, B., Yang, H., Liu, Y. C., Jelinek, T., Zhang, L., Ruoslahti, E. and Fu, H. (1999) Isolation of high-affinity peptide antagonists of 14-3-3 proteins by phage display. Biochemistry 38, 12499-12504

30 Masters, S. C. and Fu, H. (2001) 14-3-3 proteins mediate an essential anti-apoptotic signal. J Biol Chem 276, 45193-45200

31 Mackintosh, C. (2004) Dynamic interactions between 14-3-3 proteins and phosphoproteins regulate diverse cellular processes. Biochem J 381, 329-342

32 Aitken, A., Baxter, H., Dubois, T., Clokie, S., Mackie, S., Mitchell, K., Peden, A. and Zemlickova, E. (2002) Specificity of 14-3-3 isoform dimer interactions and phosphorylation. Biochem Soc Trans 30, 351-360

33 Zheng, Q., Yin, G., Yan, C., Cavet, M. and Berk, B. C. (2004) 14-3-3beta binds to big mitogen-activated protein kinase 1 (BMK1/ERK5) and regulates BMK1 function. J Biol Chem 279, 8787-8791

34 Haydon, C. E., Watt, P. W., Morrice, N., Knebel, A., Gaestel, M. and Cohen, P. (2002) Identification of a phosphorylation site on skeletal muscle myosin light chain kinase that becomes phosphorylated during muscle contraction. Arch Biochem Biophys 397, 224-231

35 Davare, M. A., Saneyoshi, T., Guire, E. S., Nygaard, S. C. and Soderling, T. R. (2004) Inhibition of calcium/calmodulin-dependent protein kinase kinase by protein 14-3-3. J Biol Chem

36 Agarwal-Mawal, A., Qureshi, H. Y., Cafferty, P. W., Yuan, Z., Han, D., Lin, R. and Paudel, H. K. (2003) 14-3-3 connects glycogen synthase kinase-3 beta to tau within a brain microtubule-associated tau phosphorylation complex. J Biol Chem 278, 12722-12728

37 Yuan, Z., Agarwal-Mawal, A. and Paudel, H. K. (2004) 14-3-3 binds to and mediates phosphorylation of microtubule-associated tau protein by Ser9-phosphorylated glycogen synthase kinase 3beta in the brain. J Biol Chem 279, 26105-26114

38 Dorner, C., Ullrich, A., Haring, H. U. and Lammers, R. (1999) The kinesin-like motor protein KIF1C occurs in intact cells as a dimer and associates with proteins of the 14-3-3 family. J Biol Chem 274, 33654-33660

39 Sato, M., Watanabe, Y., Akiyoshi, Y. and Yamamoto, M. (2002) 14-3-3 protein interferes with the binding of RNA to the phosphorylated form of fission yeast meiotic regulator Mei2p. Curr Biol 12, 141-145

40 Graeser, R., Gannon, J., Poon, R. Y., Dubois, T., Aitken, A. and Hunt, T. (2002) Regulation of the CDK-related protein kinase PCTAIRE-1 and its possible role in neurite outgrowth in Neuro-2A cells. J Cell Sci 115, 3479-3490

41 Cavet, M. E., Lehoux, S. and Berk, B. C. (2003) 14-3-3beta is a p90 ribosomal S6 kinase (RSK) isoform 1-binding protein that negatively regulates RSK kinase activity. J Biol Chem 278, 18376-18383

42 Hausser, A., Storz, P., Link, G., Stoll, H., Liu, Y. C., Altman, A., Pfizenmaier, K. and Johannes, F. J. (1999) Protein kinase C mu is negatively regulated by 14-3-3 signal transduction proteins. J Biol Chem 274, 9258-9264

43, V. D. H., P. C., Van Der Wal, J. C., Ruurs, P., Van Dijk, M. C. and Van Blitterswijk, J. (2000) 14-3-3 isotypes facilitate coupling of protein kinase C-zeta to Raf-1: negative regulation by 14-3-3 phosphorylation. Biochem J 345 Pt 2, 297-306

44 Michaud, N. R., Fabian, J. R., Mathes, K. D. and Morrison, D. K. (1995) 14-3-3 is not essential for Raf-1 function: identification of Raf-1 proteins that are biologically activated in a 14-3-3- and Ras-independent manner. Mol Cell Biol 15, 3390-3397

45 Qiu, W., Zhuang, S., von Lintig, F. C., Boss, G. R. and Pilz, R. B. (2000) Cell type-specific regulation of B-Raf kinase by cAMP and 14-3-3 proteins. J Biol Chem 275, 31921-31929

46 Toshima, J. Y., Toshima, J., Watanabe, T. and Mizuno, K. (2001) Binding of 14-3-3beta regulates the kinase activity and subcellular localization of testicular protein kinase 1. J Biol Chem 276, 43471-43481

47 Honda, R., Ohba, Y. and Yasuda, H. (1997) 14-3-3 zeta protein binds to the carboxyl half of mouse wee1 kinase. Biochem Biophys Res Commun 230, 262-265

48 Zhang, S. H., Kobayashi, R., Graves, P. R., Piwnica-Worms, H. and Tonks, N. K. (1997) Serine phosphorylation-dependent association of the band 4.1-related protein-tyrosine phosphatase PTPH1 with 14-3-3beta protein. J Biol Chem 272, 27281-27287

49 Conklin, D. S., Galaktionov, K. and Beach, D. (1995) 14-3-3 proteins associate with cdc25 phosphatases. Proc Natl Acad Sci U S A 92, 7892-7896

50 Manke, I. A., Nguyen, A., Lim, D., Stewart, M. Q., Elia, A. E. and Yaffe, M. B. (2005) MAPKAP kinase-2 is a cell cycle checkpoint kinase that regulates the G2/M transition and S phase progression in response to UV irradiation. Mol Cell 17, 37-48

51 Dalal, S. N., Schweitzer, C. M., Gan, J. and DeCaprio, J. A. (1999) Cytoplasmic localization of human cdc25C during interphase requires an intact 14-3-3 binding site. Mol Cell Biol 19, 4465-4479

52 Peng, C. Y., Graves, P. R., Ogg, S., Thoma, R. S., Byrnes, M. J., 3rd, Wu, Z., Stephenson, M. T. and Piwnica-Worms, H. (1998) C-TAK1 protein kinase phosphorylates human Cdc25C on serine 216 and promotes 14-3-3 protein binding. Cell Growth Differ 9, 197-208

53 Nagata-Ohashi, K., Ohta, Y., Goto, K., Chiba, S., Mori, R., Nishita, M., Ohashi, K., Kousaka, K., Iwamatsu, A., Niwa, R., Uemura, T. and

Mizuno, K. (2004) A pathway of neuregulin-induced activation of cofilin-phosphatase Slingshot and cofilin in lamellipodia. J Cell Biol 165, 465-471

54 Sliva, D., Gu, M., Zhu, Y. X., Chen, J., Tsai, S., Du, X. and Yang, Y. C. (2000) 14-3-3zeta interacts with the alpha-chain of human interleukin 9 receptor. Biochem J 345 Pt 3, 741-747

55 Stomski, F. C., Dottore, M., Winnall, W., Guthridge, M. A., Woodcock, J., Bagley, C. J., Thomas, D. T., Andrews, R. K., Berndt, M. C. and Lopez, A. F. (1999) Identification of a 14-3-3 binding sequence in the common beta chain of the granulocyte-macrophage colony-stimulating factor (GM-CSF), interleukin-3 (IL-3), and IL-5 receptors that is serine-phosphorylated by GM-CSF. Blood 94, 1933-1942

56 Andrews, R. K., Harris, S. J., McNally, T. and Berndt, M. C. (1998) Binding of purified 14-3-3 zeta signaling protein to discrete amino acid sequences within the cytoplasmic domain of the platelet membrane glycoprotein Ib-IX-V complex. Biochemistry 37, 638-647

57 Zhu, P., Sun, Y., Xu, R., Sang, Y., Zhao, J., Liu, G., Cai, L., Li, C. and Zhao, S. (2003) The interaction between ADAM 22 and 14-3-3zeta: regulation of cell adhesion and spreading. Biochem Biophys Res Commun 301, 991-999

58 Zhu, P., Sang, Y., Xu, H., Zhao, J., Xu, R., Sun, Y., Xu, T., Wang, X., Chen, L., Feng, H., Li, C. and Zhao, S. (2005) ADAM22 plays an important role in cell adhesion and spreading with the assistance of 14-3-3. Biochem Biophys Res Commun 331, 938-946

59 Diviani, D., Abuin, L., Cotecchia, S. and Pansier, L. (2004) Anchoring of both PKA and 14-3-3 inhibits the Rho-GEF activity of the AKAP-Lbc signaling complex. Embo J 23, 2811-2820

60 Zenke, F. T., Krendel, M., DerMardirossian, C., King, C. C., Bohl, B. P. and Bokoch, G. M. (2004) p21-activated kinase 1 phosphorylates and regulates 14-3-3 binding to GEF-H1, a microtubule-localized Rho exchange factor. J Biol Chem 279, 18392-18400

61 Urschel, S., Bassermann, F., Bai, R. Y., Munch, S., Peschel, C. and Duyster, J. (2005) Phosphorylation of grb10 regulates its interaction with 14-3-3. J Biol Chem 280, 16987-16993

62 Craparo, A., Freund, R. and Gustafson, T. A. (1997) 14-3-3 (epsilon) interacts with the insulin-like growth factor I receptor and insulin receptor substrate I in a phosphoserine-dependent manner. J Biol Chem 272, 11663-11669

63 Kuwana, T., Peterson, P. A. and Karlsson, L. (1998) Exit of major histocompatibility complex class II-invariant chain p35 complexes from the endoplasmic reticulum is modulated by phosphorylation. Proc Natl Acad Sci U S A 95, 1056-1061

64 O'Kelly, I., Butler, M. H., Zilberberg, N. and Goldstein, S. A. (2002) Forward transport. 14-3-3 binding overcomes retention in endoplasmic reticulum by dibasic signals. Cell 111, 577-588

65 Beguin, P., Mahalakshmi, R. N., Nagashima, K., Cher, D. H., Takahashi, A., Yamada, Y., Seino, Y. and Hunziker, W. (2005) 14-3-3 and calmodulin control subcellular distribution of Kir/Gem and its regulation of cell shape and calcium channel activity. J Cell Sci 118, 1923-1934

66 Lehoux, S., Abe, J., Florian, J. A. and Berk, B. C. (2001) 14-3-3 Binding to Na+/H+ exchanger isoform-1 is associated with serum-dependent activation of Na+/H+ exchange. J Biol Chem 276, 15794-15800

67 Efendiev, R., Chen, Z., Krmar, R. T., Uhles, S., Katz, A. I., Pedemonte, C. H. and Bertorello, A. M. (2005) The 14-3-3 protein translates the NA+,K+-ATPase {alpha}1-subunit phosphorylation signal into binding and activation of phosphoinositide 3-kinase during endocytosis. J Biol Chem 280, 16272-16277

68 Jeanclos, E. M., Lin, L., Treuil, M. W., Rao, J., DeCoster, M. A. and Anand, R. (2001) The chaperone protein 14-3-3eta interacts with the nicotinic acetylcholine receptor alpha 4 subunit. Evidence for a dynamic role in subunit stabilization. J Biol Chem 276, 28281-28290

69 Masuyama, N., Oishi, K., Mori, Y., Ueno, T., Takahama, Y. and Gotoh, Y. (2001) Akt inhibits the orphan nuclear receptor Nur77 and T-cell apoptosis. J Biol Chem 276, 32799-32805

70 Thulin, C. D., Savage, J. R., McLaughlin, J. N., Truscott, S. M., Old, W. M., Ahn, N. G., Resing, K. A., Hamm, H. E., Bitensky, M. W. and Willardson, B. M. (2001) Modulation of the G protein regulator phosducin by Ca2+/calmodulin-dependent protein kinase II phosphorylation and 14-3-3 protein binding. J Biol Chem 276, 23805-23815

71 Olayioye, M. A., Guthridge, M. A., Stomski, F. C., Lopez, A. F., Visvader, J. E. and Lindeman, G. J. (2003) Threonine 391 phosphorylation of the human prolactin receptor mediates a novel interaction with 14-3-3 proteins. J Biol Chem 278, 32929-32935

72 Wang, Y., Waldron, R. T., Dhaka, A., Patel, A., Riley, M. M., Rozengurt, E. and Colicelli, J. (2002) The RAS effector RIN1 directly competes with RAF and is regulated by 14-3-3 proteins. Mol Cell Biol 22, 916-926

73 Benzing, T., Yaffe, M. B., Arnould, T., Sellin, L., Schermer, B., Schilling, B., Schreiber, R., Kunzelmann, K., Leparc, G. G., Kim, E. and Walz, G. (2000) 14-3-3 interacts with regulator of G protein signaling proteins and modulates their activity. J Biol Chem 275, 28167-28172

74 Beguin, P., Mahalakshmi, R. N., Nagashima, K., Cher, D. H., Kuwamura, N., Yamada, Y., Seino, Y. and Hunziker, W. (2005) Roles of 14-3-3 and calmodulin binding in subcellular localization and function of the small G protein Rem2. Biochem J

75 Santoro, M. M., Gaudino, G. and Marchisio, P. C. (2003) The MSP receptor regulates alpha6beta4 and alpha3beta1 integrins via 14-3-3 proteins in keratinocyte migration. Dev Cell 5, 257-271

76 Zhai, J., Lin, H., Shamim, M., Schlaepfer, W. W. and Canete-Soler, R. (2001) Identification of a novel interaction of 14-3-3 with p190RhoGEF. J Biol Chem 276, 41318-41324

77 Yoshida, K., Yamaguchi, T., Natsume, T., Kufe, D. and Miki, Y. (2005) JNK phosphorylation of 14-3-3 proteins regulates nuclear targeting of c-Abl in the apoptotic response to DNA damage. Nat Cell Biol 7, 278-285

78 Zhang, L., Chen, J. and Fu, H. (1999) Suppression of apoptosis signal-regulating kinase 1-induced cell death by 14-3-3 proteins. Proc Natl Acad Sci U S A 96, 8511-8515

79 Fang, X., Yu, S., Eder, A., Mao, M., Bast, R. C., Jr., Boyd, D. and Mills, G. B. (1999) Regulation of BAD phosphorylation at serine 112 by the Ras-mitogen-activated protein kinase pathway. Oncogene 18, 6635-6640

80 Lizcano, J. M., Morrice, N. and Cohen, P. (2000) Regulation of BAD by cAMP-dependent protein kinase is mediated via phosphorylation of a novel site, Ser155. Biochem J 349, 547-557

81 Feng, Y., Qi, W., Martinez, J. and Nelson, M. A. (2005) The cyclin-dependent kinase 11 interacts with 14-3-3 proteins. Biochem Biophys Res Commun 331, 1503-1509

82 Liu, M. Y., Cai, S., Espejo, A., Bedford, M. T. and Walker, C. L. (2002) 14-3-3 interacts with the tumor suppressor tuberin at Akt phosphorylation site(s). Cancer Res 62, 6475-6480

83 Shumway, S. D., Li, Y. and Xiong, Y. (2003) 14-3-3beta binds to and negatively regulates the tuberous sclerosis complex 2 (TSC2) tumor suppressor gene product, tuberin. J Biol Chem 278, 2089-2092

84 Li, Y., Inoki, K., Vacratsis, P. and Guan, K. L. (2003) The p38 and MK2 kinase cascade phosphorylates tuberin, the tuberous sclerosis 2 gene product, and enhances its interaction with 14-3-3. J Biol Chem 278, 13663-13671

85 Edwards, D. C., Sanders, L. C., Bokoch, G. M. and Gill, G. N. (1999) Activation of LIM-kinase by Pak1 couples Rac/Cdc42 GTPase signalling to actin cytoskeletal dynamics. Nat Cell Biol 1, 253-259

86 Maekawa, M., Ishizaki, T., Boku, S., Watanabe, N., Fujita, A., Iwamatsu, A., Obinata, T., Ohashi, K., Mizuno, K. and Narumiya, S. (1999) Signaling from Rho to the actin cytoskeleton through protein kinases ROCK and LIM-kinase. Science 285, 895-898

87 Gohla, A. and Bokoch, G. M. (2002) 14-3-3 regulates actin dynamics by stabilizing phosphorylated cofilin. Curr Biol 12, 1704-1710

88 Dreiza, C. M., Brophy, C. M., Komalavilas, P., Furnish, E. J., Joshi, L., Pallero, M. A., Murphy-Ullrich, J. E., von Rechenberg, M., Ho, Y. S., Richardson, B., Xu, N., Zhen, Y., Peltier, J. M. and Panitch, A. (2005) Transducible heat shock protein 20 (HSP20) phosphopeptide alters cytoskeletal dynamics. Faseb J 19, 261-263

89 Cacace, A. M., Michaud, N. R., Therrien, M., Mathes, K., Copeland, T., Rubin, G. M. and Morrison, D. K. (1999) Identification of constitutive and ras-inducible phosphorylation sites of KSR: implications for 14-3-3 binding, mitogen-activated protein kinase binding, and KSR overexpression. Mol Cell Biol 19, 229-240

90 Garcia-Guzman, M., Dolfi, F., Russello, M. and Vuori, K. (1999) Cell adhesion regulates the interaction between the docking protein p130(Cas) and the 14-3-3 proteins. J Biol Chem 274, 5762-5768

91 Briknarova, K., Nasertorabi, F., Havert, M. L., Eggleston, E., Hoyt, D. W., Li, C., Olson, A. J., Vuori, K. and Ely, K. R. (2005) The serine-rich domain from Crk-associated substrate (p130cas) is a four-helix bundle. J Biol Chem 280, 21908-21914

92 Chun, J., Kwon, T., Lee, E. J., Kim, C. H., Han, Y. S., Hong, S. K., Hyun, S. and Kang, S. S. (2004) 14-3-3 Protein mediates phosphorylation of

microtubule-associated protein tau by serum- and glucocorticoid-induced protein kinase 1. Mol Cells 18, 360-368

93 Chen, H. K., Fernandez-Funez, P., Acevedo, S. F., Lam, Y. C., Kaytor, M. D., Fernandez, M. H., Aitken, A., Skoulakis, E. M., Orr, H. T., Botas, J. and Zoghbi, H. Y. (2003) Interaction of Akt-phosphorylated ataxin-1 with 14-3-3 mediates neurodegeneration in spinocerebellar ataxia type 1. Cell 113, 457-468

94 Schmidlin, M., Lu, M., Leuenberger, S. A., Stoecklin, G., Mallaun, M., Gross, B., Gherzi, R., Hess, D., Hemmings, B. A. and Moroni, C. (2004) The ARE-dependent mRNA-destabilizing activity of BRF1 is regulated by protein kinase B. Embo J 23, 4760-4769

95 Pan, F., Means, A. R. and Liu, J. O. (2005) Calmodulin-dependent protein kinase IV regulates nuclear export of Cabin1 during T-cell activation. Embo J 24, 2104-2113

96 Wang, B., Liu, K., Lin, F. T. and Lin, W. C. (2004) A role for 14-3-3 tau in E2F1 stabilization and DNA damage-induced apoptosis. J Biol Chem 279, 54140-54152

97 Brunet, A., Bonni, A., Zigmond, M. J., Lin, M. Z., Juo, P., Hu, L. S., Anderson, M. J., Arden, K. C., Blenis, J. and Greenberg, M. E. (1999) Akt promotes cell survival by phosphorylating and inhibiting a Forkhead transcription factor. Cell 96, 857-868

98 Rena, G., Prescott, A. R., Guo, S., Cohen, P. and Unterman, T. G. (2001) Roles of the forkhead in rhabdomyosarcoma (FKHR) phosphorylation sites in regulating 14-3-3 binding, transactivation and nuclear targetting. Biochem J 354, 605-612

99 Wang, A. H., Kruhlak, M. J., Wu, J., Bertos, N. R., Vezmar, M., Posner, B. I., Bazett-Jones, D. P. and Yang, X. J. (2000) Regulation of histone deacetylase 4 by binding of 14-3-3 proteins. Mol Cell Biol 20, 6904-6912

100 McKinsey, T. A., Zhang, C. L. and Olson, E. N. (2000) Activation of the myocyte enhancer factor-2 transcription factor by calcium/calmodulin-dependent protein kinase-stimulated binding of 14-3-3 to histone deacetylase 5. Proc Natl Acad Sci U S A 97, 14400-14405

101 Kao, H. Y., Verdel, A., Tsai, C. C., Simon, C., Juguilon, H. and Khochbin, S. (2001) Mechanism for nucleocytoplasmic shuttling of histone deacetylase 7. J Biol Chem 276, 47496-47507

102 Kanai, F., Marignani, P. A., Sarbassova, D., Yagi, R., Hall, R. A., Donowitz, M., Hisaminato, A., Fujiwara, T., Ito, Y., Cantley, L. C. and Yaffe, M. B. (2000) TAZ: a novel transcriptional co-activator regulated by interactions with 14-3-3 and PDZ domain proteins. Embo J 19, 6778-6791

103 Wanzel, M., Kleine-Kohlbrecher, D., Herold, S., Hock, A., Berns, K., Park, J., Hemmings, B. and Eilers, M. (2005) Akt and 14-3-3eta regulate Miz1 to control cell-cycle arrest after DNA damage. Nat Cell Biol 7, 30-41

104 Chow, C. W. and Davis, R. J. (2000) Integration of calcium and cyclic AMP signaling pathways by 14-3-3. Mol Cell Biol 20, 702-712

105 Sekimoto, T., Fukumoto, M. and Yoneda, Y. (2004) 14-3-3 suppresses the nuclear localization of threonine 157-phosphorylated p27(Kip1). Embo J 23, 1934-1942

106 Screaton, R. A., Conkright, M. D., Katoh, Y., Best, J. L., Canettieri, G., Jeffries, S., Guzman, E., Niessen, S., Yates, J. R., 3rd, Takemori, H., Okamoto, M. and Montminy, M. (2004) The CREB coactivator TORC2 functions as a calcium- and cAMP-sensitive coincidence detector. Cell 119, 61-74

107 Basu, S., Totty, N. F., Irwin, M. S., Sudol, M. and Downward, J. (2003) Akt phosphorylates the Yes-associated protein, YAP, to induce interaction with 14-3-3 and attenuation of p73-mediated apoptosis. Mol Cell 11, 11-23

108 Carreno, F. R., Goni, C. N., Castro, L. M. and Ferro, E. S. (2005) 14-3-3 epsilon modulates the stimulated secretion of endopeptidase 24.15. J Neurochem 93, 10-25

109 Pozuelo Rubio, M., Peggie, M., Wong, B. H., Morrice, N. and MacKintosh, C. (2003) 14-3-3s regulate fructose-2,6-bisphosphate levels by binding to PKB-phosphorylated cardiac fructose-2,6-bisphosphate kinase/phosphatase. Embo J 22, 3514-3523

110 Ku, N. O., Liao, J. and Omary, M. B. (1998) Phosphorylation of human keratin 18 serine 33 regulates binding to 14-3-3 proteins. Embo J 17, 1892-1906

111 Cullere, X., Rose, P., Thathamangalam, U., Chatterjee, A., Mullane, K. P., Pallas, D. C., Benjamin, T. L., Roberts, T. M. and Schaffhausen, B. S. (1998) Serine 257 phosphorylation regulates association of polyomavirus middle T antigen with 14-3-3 proteins. J Virol 72, 558-563

112 Ichimura, T., Yamamura, H., Sasamoto, K., Tominaga, Y., Taoka, M., Kakiuchi, K., Shinkawa, T., Takahashi, N., Shimada, S. and Isobe, T. (2005) 14-3-3 proteins modulate the expression of epithelial Na+ channels by phosphorylation-dependent interaction with Nedd4-2 ubiquitin ligase. J Biol Chem 280, 13187-13194

113 Toyo-oka, K., Shionoya, A., Gambello, M. J., Cardoso, C., Leventer, R., Ward, H. L., Ayala, R., Tsai, L. H., Dobyns, W., Ledbetter, D., Hirotsune, S. and Wynshaw-Boris, A. (2003) 14-3-3epsilon is important for neuronal migration by binding to NUDEL: a molecular explanation for Miller-Dieker syndrome. Nat Genet 34, 274-285

114 Suzuki, A., Hirata, M., Kamimura, K., Maniwa, R., Yamanaka, T., Mizuno, K., Kishikawa, M., Hirose, H., Amano, Y., Izumi, N., Miwa, Y. and Ohno, S. (2004) aPKC acts upstream of PAR-1b in both the establishment and maintenance of mammalian epithelial polarity. Curr Biol 14, 1425-1435

115 Kusakabe, M. and Nishida, E. (2004) The polarity-inducing kinase Par-1 controls Xenopus gastrulation in cooperation with 14-3-3 and aPKC. Embo J 23, 4190-4201

116 Izaki, T., Kamakura, S., Kohjima, M. and Sumimoto, H. (2005) Phosphorylation-dependent binding of 14-3-3 to Par3beta, a human Par3-related cell polarity protein. Biochem Biophys Res Commun 329, 211-218

117 Onuma, H., Osawa, H., Yamada, K., Ogura, T., Tanabe, F., Granner, D. K. and Makino, H. (2002) Identification of the insulin-regulated interaction of phosphodiesterase 3B with 14-3-3 beta protein. Diabetes 51, 3362-3367

118 Sribar, J., Sherman, N. E., Prijatelj, P., Faure, G., Gubensek, F., Fox, J. W., Aitken, A., Pungercar, J. and Krizaj, I. (2003) The neurotoxic phospholipase A2 associates, through a non-phosphorylated binding motif, with 14-3-3 protein gamma and epsilon isoforms. Biochem Biophys Res Commun 302, 691-696
119 Muller, J., Ritt, D. A., Copeland, T. D. and Morrison, D. K. (2003) Functional analysis of C-TAK1 substrate binding and identification of PKP2 as a new C-TAK1 substrate. Embo J 22, 4431-4442
120 Han, S. I., Kawano, M. A., Ishizu, K., Watanabe, H., Hasegawa, M., Kanesashi, S. N., Kim, Y. S., Nakanishi, A., Kataoka, K. and Handa, H. (2004) Rep68 protein of adeno-associated virus type 2 interacts with 14-3-3 proteins depending on phosphorylation at serine 535. Virology 320, 144-155
121 Sun, L., Bittner, M. A. and Holz, R. W. (2003) Rim, a component of the presynaptic active zone and modulator of exocytosis, binds 14-3-3 through its N terminus. J Biol Chem 278, 38301-38309
122 Simsek-Duran, F., Linden, D. J. and Lonart, G. (2004) Adapter protein 14-3-3 is required for a presynaptic form of LTP in the cerebellum. Nat Neurosci 7, 1296-1298
123 Ganguly, S., Gastel, J. A., Weller, J. L., Schwartz, C., Jaffe, H., Namboodiri, M. A., Coon, S. L., Hickman, A. B., Rollag, M., Obsil, T., Beauverger, P., Ferry, G., Boutin, J. A. and Klein, D. C. (2001) Role of a pineal cAMP-operated arylalkylamine N-acetyltransferase/14-3-3-binding switch in melatonin synthesis. Proc Natl Acad Sci U S A 98, 8083-8088
124 Davidson, C. E., Reese, B. E., Billingsley, M. L. and Yun, J. K. (2005) The protein stannin binds 14-3-3zeta and modulates mitogen-activated protein kinase signaling. Brain Res Mol Brain Res
125 Itagaki, C., Isobe, T., Taoka, M., Natsume, T., Nomura, N., Horigome, T., Omata, S., Ichinose, H., Nagatsu, T., Greene, L. A. and Ichimura, T. (1999) Stimulus-coupled interaction of tyrosine hydroxylase with 14-3-3 proteins. Biochemistry 38, 15673-15680
126 Kleppe, R., Toska, K. and Haavik, J. (2001) Interaction of phosphorylated tyrosine hydroxylase with 14-3-3 proteins: evidence for a phosphoserine 40-dependent association. J Neurochem 77, 1097-1107
127 Ishida, S., Fukazawa, J., Yuasa, T. and Takahashi, Y. (2004) Involvement of 14-3-3 signaling protein binding in the functional regulation of the transcriptional activator REPRESSION OF SHOOT GROWTH by gibberellins. Plant Cell 16, 2641-2651
128 Kulma, A., Villadsen, D., Campbell, D. G., Meek, S. E., Harthill, J. E., Nielsen, T. H. and MacKintosh, C. (2004) Phosphorylation and 14-3-3 binding of Arabidopsis 6-phosphofructo-2-kinase/fructose-2,6-bisphosphatase. Plant J 37, 654-667
129 Wurtele, M., Jelich-Ottmann, C., Wittinghofer, A. and Oecking, C. (2003) Structural view of a fungal toxin acting on a 14-3-3 regulatory complex. Embo J 22, 987-994
130 Moorhead, G., Douglas, P., Morrice, N., Scarabel, M., Aitken, A. and MacKintosh, C. (1996) Phosphorylated nitrate reductase from spinach

leaves is inhibited by 14-3-3 proteins and activated by fusicoccin. Curr Biol 6, 1104-1113
131 Xiao, B., Smerdon, S. J., Jones, D. H., Dodson, G. G., Soneji, Y., Aitken, A. and Gamblin, S. J. (1995) Structure of a 14-3-3 protein and implications for coordination of multiple signalling pathways. Nature 376, 188-191
132 Liu, D., Bienkowska, J., Petosa, C., Collier, R. J., Fu, H. and Liddington, R. (1995) Crystal structure of the zeta isoform of the 14-3-3 protein. Nature 376, 191-194
133 Cohen, G. H., Sheriff, S. and Davies, D. R. (1996) Refined structure of the monoclonal antibody HyHEL-5 with its antigen hen egg-white lysozyme. Acta Crystallogr D Biol Crystallogr 52, 315-326
134 Zhang, L., Wang, H., Liu, D., Liddington, R. and Fu, H. (1997) Raf-1 kinase and exoenzyme S interact with 14-3-3zeta through a common site involving lysine 49. J Biol Chem 272, 13717-13724
135 Wang, H., Zhang, L., Liddington, R. and Fu, H. (1998) Mutations in the hydrophobic surface of an amphipathic groove of 14-3-3zeta disrupt its interaction with Raf-1 kinase. J Biol Chem 273, 16297-16304
136 Zhang, S., Xing, H. and Muslin, A. J. (1999) Nuclear localization of protein kinase U-alpha is regulated by 14-3-3. J Biol Chem 274, 24865-24872
137 Xing, H., Zhang, S., Weinheimer, C., Kovacs, A. and Muslin, A. J. (2000) 14-3-3 proteins block apoptosis and differentially regulate MAPK cascades. Embo J 19, 349-358
138 Fukuhara, N., Ebert, J., Unterholzner, L., Lindner, D., Izaurralde, E. and Conti, E. (2005) SMG7 Is a 14-3-3-like Adaptor in the Nonsense-Mediated mRNA Decay Pathway. Mol Cell 17, 537-547
139 Yaffe, M. B. (2002) How do 14-3-3 proteins work?-- Gatekeeper phosphorylation and the molecular anvil hypothesis. FEBS Lett 513, 53-57
140 Hickman, A. B., Namboodiri, M. A., Klein, D. C. and Dyda, F. (1999) The structural basis of ordered substrate binding by serotonin N-acetyltransferase: enzyme complex at 1.8 A resolution with a bisubstrate analog. Cell 97, 361-369
141 Hickman, A. B., Klein, D. C. and Dyda, F. (1999) Melatonin biosynthesis: the structure of serotonin N-acetyltransferase at 2.5 A resolution suggests a catalytic mechanism. Mol Cell 3, 23-32
142 Peluso, J. J. and Pappalardo, A. (2004) Progesterone regulates granulosa cell viability through a protein kinase G-dependent mechanism that may involve 14-3-3sigma. Biol Reprod 71, 1870-1878
143 Silhan, J., Obsilova, V., Vecer, J., Herman, P., Sulc, M., Teisinger, J. and Obsil, T. (2004) 14-3-3 protein C-terminal stretch occupies ligand binding groove and is displaced by phosphopeptide binding. J Biol Chem 279, 49113-49119
144 Obsilova, V., Herman, P., Vecer, J., Sulc, M., Teisinger, J. and Obsil, T. (2004) 14-3-3zeta C-terminal stretch changes its conformation upon ligand binding and phosphorylation at Thr232. J Biol Chem 279, 4531-4540

145 Rommel, C., Radziwill, G., Lovric, J., Noeldeke, J., Heinicke, T., Jones, D., Aitken, A. and Moelling, K. (1996) Activated Ras displaces 14-3-3 protein from the amino terminus of c-Raf-1. Oncogene 12, 609-619
146 Dubois, T., Howell, S., Amess, B., Kerai, P., Learmonth, M., Madrazo, J., Chaudhri, M., Rittinger, K., Scarabel, M., Soneji, Y. and Aitken, A. (1997) Structure and sites of phosphorylation of 14-3-3 protein: role in coordinating signal transduction pathways. J Protein Chem 16, 513-522
147 Reuther, G. W., Fu, H., Cripe, L. D., Collier, R. J. and Pendergast, A. M. (1994) Association of the protein kinases c-Bcr and Bcr-Abl with proteins of the 14-3-3 family. Science 266, 129-133
148 van Heusden, G. P., Griffiths, D. J., Ford, J. C., Chin, A. W. T. F., Schrader, P. A., Carr, A. M. and Steensma, H. Y. (1995) The 14-3-3 proteins encoded by the BMH1 and BMH2 genes are essential in the yeast Saccharomyces cerevisiae and can be replaced by a plant homologue. Eur J Biochem 229, 45-53
149 van Heusden, G. P., van der Zanden, A. L., Ferl, R. J. and Steensma, H. Y. (1996) Four Arabidopsis thaliana 14-3-3 protein isoforms can complement the lethal yeast bmh1 bmh2 double disruption. FEBS Lett 391, 252-256
150 Chang, H. C. and Rubin, G. M. (1997) 14-3-3 epsilon positively regulates Ras-mediated signaling in Drosophila. Genes Dev 11, 1132-1139
151 Philip, N., Acevedo, S. F. and Skoulakis, E. M. (2001) Conditional rescue of olfactory learning and memory defects in mutants of the 14-3-3zeta gene leonardo. J Neurosci 21, 8417-8425
152 Fagerholm, S., Morrice, N., Gahmberg, C. G. and Cohen, P. (2002) Phosphorylation of the cytoplasmic domain of the integrin CD18 chain by protein kinase C isoforms in leukocytes. J Biol Chem 277, 1728-1738
153 Schurmann, A., Mooney, A. F., Sanders, L. C., Sells, M. A., Wang, H. G., Reed, J. C. and Bokoch, G. M. (2000) p21-activated kinase 1 phosphorylates the death agonist bad and protects cells from apoptosis. Mol Cell Biol 20, 453-461
154 Fujita, N., Sato, S. and Tsuruo, T. (2003) Phosphorylation of p27Kip1 at threonine 198 by p90 ribosomal protein S6 kinases promotes its binding to 14-3-3 and cytoplasmic localization. J Biol Chem 278, 49254-49260
155 Pinna, L. A. and Ruzzene, M. (1996) How do protein kinases recognize their substrates? Biochim Biophys Acta 1314, 191-225
156 Alessi, D. R., Caudwell, F. B., Andjelkovic, M., Hemmings, B. A. and Cohen, P. (1996) Molecular basis for the substrate specificity of protein kinase B; comparison with MAPKAP kinase-1 and p70 S6 kinase. FEBS Lett 399, 333-338
157 Vanhaesebroeck, B. and Alessi, D. R. (2000) The PI3K-PDK1 connection: more than just a road to PKB. Biochem J 346 Pt 3, 561-576
158 Obata, T., Yaffe, M. B., Leparc, G. G., Piro, E. T., Maegawa, H., Kashiwagi, A., Kikkawa, R. and Cantley, L. C. (2000) Peptide and protein library screening defines optimal substrate motifs for AKT/PKB. J Biol Chem 275, 36108-36115

159 Nishikawa, K., Toker, A., Johannes, F. J., Songyang, Z. and Cantley, L. C. (1997) Determination of the specific substrate sequence motifs of protein kinase C isozymes. J Biol Chem 272, 952-960
160 Doppler, H., Storz, P., Li, J., Comb, M. J. and Toker, A. (2005) A phosphorylation state-specific antibody recognizes Hsp27, a novel substrate of protein kinase D. J Biol Chem 280, 15013-15019
161 Tuazon, P. T., Spanos, W. C., Gump, E. L., Monnig, C. A. and Traugh, J. A. (1997) Determinants for substrate phosphorylation by p21-activated protein kinase (gamma-PAK). Biochemistry 36, 16059-16064
162 Stokoe, D., Caudwell, B., Cohen, P. T. and Cohen, P. (1993) The substrate specificity and structure of mitogen-activated protein (MAP) kinase-activated protein kinase-2. Biochem J 296 (Pt 3), 843-849
163 Marin, O., Meggio, F., Sarno, S., Andretta, M. and Pinna, L. A. (1994) Phosphorylation of synthetic fragments of inhibitor-2 of protein phosphatase-1 by casein kinase-1 and -2. Evidence that phosphorylated residues are not strictly required for efficient targeting by casein kinase-1. Eur J Biochem 223, 647-653
164 Megidish, T., Cooper, J., Zhang, L., Fu, H. and Hakomori, S. (1998) A novel sphingosine-dependent protein kinase (SDK1) specifically phosphorylates certain isoforms of 14-3-3 protein. J Biol Chem 273, 21834-21845
165 Hamaguchi, A., Suzuki, E., Murayama, K., Fujimura, T., Hikita, T., Iwabuchi, K., Handa, K., Withers, D. A., Masters, S. C., Fu, H. and Hakomori, S. (2003) A sphingosine-dependent protein kinase that specifically phosphorylates 14-3-3 (SDK1) is identified as the kinase domain of PKCdelta: a preliminary note. Biochem Biophys Res Commun 307, 589-594
166 Hamaguchi, A., Suzuki, E., Murayama, K., Fujimura, T., Hikita, T., Iwabuchi, K., Handa, K., Withers, D. A., Masters, S. C., Fu, H. and Hakomori, S. (2003) Sphingosine-dependent protein kinase-1, directed to 14-3-3, is identified as the kinase domain of protein kinase C delta. J Biol Chem 278, 41557-41565
167 Woodcock, J. M., Murphy, J., Stomski, F. C., Berndt, M. C. and Lopez, A. F. (2003) The dimeric versus monomeric status of 14-3-3zeta is controlled by phosphorylation of Ser58 at the dimer interface. J Biol Chem 278, 36323-36327
168 Shen, Y. H., Godlewski, J., Bronisz, A., Zhu, J., Comb, M. J., Avruch, J. and Tzivion, G. (2003) Significance of 14-3-3 self-dimerization for phosphorylation-dependent target binding. Mol Biol Cell 14, 4721-4733
169 Powell, D. W., Rane, M. J., Chen, Q., Singh, S. and McLeish, K. R. (2002) Identification of 14-3-3zeta as a protein kinase B/Akt substrate. J Biol Chem 277, 21639-21642
170 Tsuruta, F., Sunayama, J., Mori, Y., Hattori, S., Shimizu, S., Tsujimoto, Y., Yoshioka, K., Masuyama, N. and Gotoh, Y. (2004) JNK promotes Bax translocation to mitochondria through phosphorylation of 14-3-3 proteins. Embo J 23, 1889-1899

171 Sunayama, J., Tsuruta, F., Masuyama, N. and Gotoh, Y. (2005) JNK antagonizes Akt-mediated survival signals by phosphorylating 14-3-3. J Cell Biol

172 Dubois, T., Rommel, C., Howell, S., Steinhussen, U., Soneji, Y., Morrice, N., Moelling, K. and Aitken, A. (1997) 14-3-3 is phosphorylated by casein kinase I on residue 233. Phosphorylation at this site in vivo regulates Raf/14-3-3 interaction. J Biol Chem 272, 28882-28888

173 Giacometti, S., Camoni, L., Albumi, C., Visconti, S., De Michelis, M. I. and Aducci, P. (2004) Tyrosine phosphorylation inhibits the interaction of 14-3-3 proteins with the plant plasma membrane H+-ATPase. Plant Biol (Stuttg) 6, 422-431

174 Brunet, A., Kanai, F., Stehn, J., Xu, J., Sarbassova, D., Frangioni, J. V., Dalal, S. N., DeCaprio, J. A., Greenberg, M. E. and Yaffe, M. B. (2002) 14-3-3 transits to the nucleus and participates in dynamic nucleocytoplasmic transport. J Cell Biol 156, 817-828

175 Obsil, T., Ghirlando, R., Anderson, D. E., Hickman, A. B. and Dyda, F. (2003) Two 14-3-3 binding motifs are required for stable association of Forkhead transcription factor FOXO4 with 14-3-3 proteins and inhibition of DNA binding. Biochemistry 42, 15264-15272

176 Dumaz, N. and Marais, R. (2003) Protein kinase A blocks Raf-1 activity by stimulating 14-3-3 binding and blocking Raf-1 interaction with Ras. J Biol Chem 278, 29819-29823

177 Vincenz, C. and Dixit, V. M. (1996) 14-3-3 proteins associate with A20 in an isoform-specific manner and function both as chaperone and adapter molecules. J Biol Chem 271, 20029-20034

178 Mils, V., Baldin, V., Goubin, F., Pinta, I., Papin, C., Waye, M., Eychene, A. and Ducommun, B. (2000) Specific interaction between 14-3-3 isoforms and the human CDC25B phosphatase. Oncogene 19, 1257-1265

179 Chan, T. A., Hermeking, H., Lengauer, C., Kinzler, K. W. and Vogelstein, B. (1999) 14-3-3Sigma is required to prevent mitotic catastrophe after DNA damage. Nature 401, 616-620

180 Suginta, W., Karoulias, N., Aitken, A. and Ashley, R. H. (2001) Chloride intracellular channel protein CLIC4 (p64H1) binds directly to brain dynamin I in a complex containing actin, tubulin and 14-3-3 isoforms. Biochem J 359, 55-64

181 Wakui, H., Wright, A. P., Gustafsson, J. and Zilliacus, J. (1997) Interaction of the ligand-activated glucocorticoid receptor with the 14-3-3 eta protein. J Biol Chem 272, 8153-8156

182 Rimessi, A., Coletto, L., Pinton, P., Rizzuto, R., Brini, M. and Carafoli, E. (2005) Inhibitory interaction of protein 14-3-3 epsilon with isoform 4 of the plasma membrane Ca2+ pump. J Biol Chem

183 Freed, E., Symons, M., Macdonald, S. G., McCormick, F. and Ruggieri, R. (1994) Binding of 14-3-3 proteins to the protein kinase Raf and effects on its activation. Science 265, 1713-1716

184 Fantl, W. J., Muslin, A. J., Kikuchi, A., Martin, J. A., MacNicol, A. M., Gross, R. W. and Williams, L. T. (1994) Activation of Raf-1 by 14-3-3 proteins. Nature 371, 612-614

185 Papin, C., Denouel, A., Calothy, G. and Eychene, A. (1996) Identification of signalling proteins interacting with B-Raf in the yeast two-hybrid system. Oncogene 12, 2213-2221
186 Chaudhri, M., Scarabel, M. and Aitken, A. (2003) Mammalian and yeast 14-3-3 isoforms form distinct patterns of dimers in vivo. Biochem Biophys Res Commun 300, 679-685
187 Braselmann, S. and McCormick, F. (1995) Bcr and Raf form a complex in vivo via 14-3-3 proteins. Embo J 14, 4839-4848
188 Paul, A. L., Sehnke, P. C. and Ferl, R. J. (2005) Isoform-specific subcellular localization among 14-3-3 proteins in Arabidopsis seems to be driven by client interactions. Mol Biol Cell 16, 1735-1743
189 Leffers, H., Madsen, P., Rasmussen, H. H., Honore, B., Andersen, A. H., Walbum, E., Vandekerckhove, J. and Celis, J. E. (1993) Molecular cloning and expression of the transformation sensitive epithelial marker stratifin. A member of a protein family that has been involved in the protein kinase C signalling pathway. J Mol Biol 231, 982-998
190 Rena, G., Woods, Y. L., Prescott, A. R., Peggie, M., Unterman, T. G., Williams, M. R. and Cohen, P. (2002) Two novel phosphorylation sites on FKHR that are critical for its nuclear exclusion. Embo J 21, 2263-2271
191 Piwnica-Worms, H. (1999) Cell cycle. Fools rush in. Nature 401, 535, 537
192 Seimiya, H., Sawada, H., Muramatsu, Y., Shimizu, M., Ohko, K., Yamane, K. and Tsuruo, T. (2000) Involvement of 14-3-3 proteins in nuclear localization of telomerase. Embo J 19, 2652-2661
193 Preisinger, C., Short, B., De Corte, V., Bruyneel, E., Haas, A., Kopajtich, R., Gettemans, J. and Barr, F. A. (2004) YSK1 is activated by the Golgi matrix protein GM130 and plays a role in cell migration through its substrate 14-3-3zeta. J Cell Biol 164, 1009-1020
194 Middleton, F. A., Peng, L., Lewis, D. A., Levitt, P. and Mirnics, K. (2005) Altered expression of 14-3-3 genes in the prefrontal cortex of subjects with schizophrenia. Neuropsychopharmacology 30, 974-983
195 Green, A. J. (2002) Cerebrospinal fluid brain-derived proteins in the diagnosis of Alzheimer's disease and Creutzfeldt-Jakob disease. Neuropathol Appl Neurobiol 28, 427-440
196 Baxter, H. C., Liu, W. G., Forster, J. L., Aitken, A. and Fraser, J. R. (2002) Immunolocalisation of 14-3-3 isoforms in normal and scrapie-infected murine brain. Neuroscience 109, 5-14
197 Baxter, H. C., Fraser, J. R., Liu, W. G., Forster, J. L., Clokie, S., Steinacker, P., Otto, M., Bahn, E., Wiltfang, J. and Aitken, A. (2002) Specific 14-3-3 isoform detection and immunolocalization in prion diseases. Biochem Soc Trans 30, 387-391
198 Steinacker, P., Schwarz, P., Reim, K., Brechlin, P., Jahn, O., Kratzin, H., Aitken, A., Wiltfang, J., Aguzzi, A., Bahn, E., Baxter, H. C., Brose, N. and Otto, M. (2005) Unchanged survival rates of 14-3-3gamma knockout mice after inoculation with pathological prion protein. Mol Cell Biol 25, 1339-1346
199 Suzuki, H., Itoh, F., Toyota, M., Kikuchi, T., Kakiuchi, H. and Imai, K. (2000) Inactivation of the 14-3-3 sigma gene is associated with 5' CpG island hypermethylation in human cancers. Cancer Res 60, 4353-4357

200 Vercoutter-Edouart, A. S., Lemoine, J., Le Bourhis, X., Louis, H., Boilly, B., Nurcombe, V., Revillion, F., Peyrat, J. P. and Hondermarck, H. (2001) Proteomic analysis reveals that 14-3-3sigma is down-regulated in human breast cancer cells. Cancer Res 61, 76-80

201 Moreira, J. M., Ohlsson, G., Rank, F. E. and Celis, J. E. (2005) Down-regulation of the tumor suppressor protein 14-3-3sigma is a sporadic event in cancer of the breast. Mol Cell Proteomics 4, 555-569

202 Nowell, P. C. and Hungerford, D. A. (1960) Chromosome studies on normal and leukemic human leukocytes. J Natl Cancer Inst 25, 85-109

203 Sawyers, C. L. (1999) Chronic myeloid leukemia. N Engl J Med 340, 1330-1340

204 Li, W. J., Dreazen, O., Kloetzer, W., Gale, R. P. and Arlinghaus, R. B. (1989) Characterization of bcr gene products in hematopoietic cells. Oncogene 4, 127-138

205 McLaughlin, J., Chianese, E. and Witte, O. N. (1989) Alternative forms of the BCR-ABL oncogene have quantitatively different potencies for stimulation of immature lymphoid cells. Mol Cell Biol 9, 1866-1874

206 Kelliher, M., Knott, A., McLaughlin, J., Witte, O. N. and Rosenberg, N. (1991) Differences in oncogenic potency but not target cell specificity distinguish the two forms of the BCR/ABL oncogene. Mol Cell Biol 11, 4710-4716

207 Laurent, E., Talpaz, M., Kantarjian, H. and Kurzrock, R. (2001) The BCR gene and philadelphia chromosome-positive leukemogenesis. Cancer Res 61, 2343-2355

208 Levav-Cohen, Y., Goldberg, Z., Zuckerman, V., Grossman, T., Haupt, S. and Haupt, Y. (2005) C-Abl as a modulator of p53. Biochem Biophys Res Commun 331, 737-749

209 Wetzler, M., Talpaz, M., Van Etten, R. A., Hirsh-Ginsberg, C., Beran, M. and Kurzrock, R. (1993) Subcellular localization of Bcr, Abl, and Bcr-Abl proteins in normal and leukemic cells and correlation of expression with myeloid differentiation. J Clin Invest 92, 1925-1939

210 Pendergast, A. M., Gishizky, M. L., Havlik, M. H. and Witte, O. N. (1993) SH1 domain autophosphorylation of P210 BCR/ABL is required for transformation but not growth factor independence. Mol Cell Biol 13, 1728-1736

211 Sawyers, C. L., Callahan, W. and Witte, O. N. (1992) Dominant negative MYC blocks transformation by ABL oncogenes. Cell 70, 901-910

212 Stewart, M. J., Litz-Jackson, S., Burgess, G. S., Williamson, E. A., Leibowitz, D. S. and Boswell, H. S. (1995) Role for E2F1 in p210 BCR-ABL downstream regulation of c-myc transcription initiation. Studies in murine myeloid cells. Leukemia 9, 1499-1507

213 Cortez, D., Reuther, G. and Pendergast, A. M. (1997) The Bcr-Abl tyrosine kinase activates mitogenic signaling pathways and stimulates G1-to-S phase transition in hematopoietic cells. Oncogene 15, 2333-2342

214 Pendergast, A. M., Quilliam, L. A., Cripe, L. D., Bassing, C. H., Dai, Z., Li, N., Batzer, A., Rabun, K. M., Der, C. J., Schlessinger, J. and et al. (1993) BCR-ABL-induced oncogenesis is mediated by direct interaction with the SH2 domain of the GRB-2 adaptor protein. Cell 75, 175-185

215 Cortez, D., Kadlec, L. and Pendergast, A. M. (1995) Structural and signaling requirements for BCR-ABL-mediated transformation and inhibition of apoptosis. Mol Cell Biol 15, 5531-5541

216 Salomoni, P., Wasik, M. A., Riedel, R. F., Reiss, K., Choi, J. K., Skorski, T. and Calabretta, B. (1998) Expression of constitutively active Raf-1 in the mitochondria restores antiapoptotic and leukemogenic potential of a transformation-deficient BCR/ABL mutant. J Exp Med 187, 1995-2007

217 Okuda, K., Matulonis, U., Salgia, R., Kanakura, Y., Druker, B. and Griffin, J. D. (1994) Factor independence of human myeloid leukemia cell lines is associated with increased phosphorylation of the proto-oncogene Raf-1. Exp Hematol 22, 1111-1117

218 Burgess, G. S., Williamson, E. A., Cripe, L. D., Litz-Jackson, S., Bhatt, J. A., Stanley, K., Stewart, M. J., Kraft, A. S., Nakshatri, H. and Boswell, H. S. (1998) Regulation of the c-jun gene in p210 BCR-ABL transformed cells corresponds with activity of JNK, the c-jun N-terminal kinase. Blood 92, 2450-2460

219 Shuai, K., Halpern, J., ten Hoeve, J., Rao, X. and Sawyers, C. L. (1996) Constitutive activation of STAT5 by the BCR-ABL oncogene in chronic myelogenous leukemia. Oncogene 13, 247-254

220 Ilaria, R. L., Jr. and Van Etten, R. A. (1996) P210 and P190(BCR/ABL) induce the tyrosine phosphorylation and DNA binding activity of multiple specific STAT family members. J Biol Chem 271, 31704-31710

221 Reuther, J. Y., Reuther, G. W., Cortez, D., Pendergast, A. M. and Baldwin, A. S., Jr. (1998) A requirement for NF-kappaB activation in Bcr-Abl-mediated transformation. Genes Dev 12, 968-981

222 Skorski, T., Bellacosa, A., Nieborowska-Skorska, M., Majewski, M., Martinez, R., Choi, J. K., Trotta, R., Wlodarski, P., Perrotti, D., Chan, T. O., Wasik, M. A., Tsichlis, P. N. and Calabretta, B. (1997) Transformation of hematopoietic cells by BCR/ABL requires activation of a PI-3k/Akt-dependent pathway. Embo J 16, 6151-6161

223 Skorski, T., Kanakaraj, P., Nieborowska-Skorska, M., Ratajczak, M. Z., Wen, S. C., Zon, G., Gewirtz, A. M., Perussia, B. and Calabretta, B. (1995) Phosphatidylinositol-3 kinase activity is regulated by BCR/ABL and is required for the growth of Philadelphia chromosome-positive cells. Blood 86, 726-736

224 Gesbert, F., Sellers, W. R., Signoretti, S., Loda, M. and Griffin, J. D. (2000) BCR/ABL regulates expression of the cyclin-dependent kinase inhibitor p27Kip1 through the phosphatidylinositol 3-Kinase/AKT pathway. J Biol Chem 275, 39223-39230

225 Pierce, A., Spooncer, E., Wooley, S., Dive, C., Francis, J. M., Miyan, J., Owen-Lynch, P. J., Dexter, T. M. and Whetton, A. D. (2000) Bcr-Abl protein tyrosine kinase activity induces a loss of p53 protein that mediates a delay in myeloid differentiation. Oncogene 19, 5487-5497

226 Anastasi, J., Moinuddin, R. and Daugherty, C. (1999) The juxtaposition of ABL with BCR and risk for fusion may come at the time of BCR replication in late S-phase. Blood 94, 1137-1138

227 Neves, H., Ramos, C., da Silva, M. G., Parreira, A. and Parreira, L. (1999) The nuclear topography of ABL, BCR, PML, and RARalpha

genes: evidence for gene proximity in specific phases of the cell cycle and stages of hematopoietic differentiation. Blood 93, 1197-1207
228 Lugo, T. G., Pendergast, A. M., Muller, A. J. and Witte, O. N. (1990) Tyrosine kinase activity and transformation potency of bcr-abl oncogene products. Science 247, 1079-1082
229 Salesse, S. and Verfaillie, C. M. (2002) BCR/ABL: from molecular mechanisms of leukemia induction to treatment of chronic myelogenous leukemia. Oncogene 21, 8547-8559
230 Nagar, B., Bornmann, W. G., Pellicena, P., Schindler, T., Veach, D. R., Miller, W. T., Clarkson, B. and Kuriyan, J. (2002) Crystal structures of the kinase domain of c-Abl in complex with the small molecule inhibitors PD173955 and imatinib (STI-571). Cancer Res 62, 4236-4243
231 Schindler, T., Bornmann, W., Pellicena, P., Miller, W. T., Clarkson, B. and Kuriyan, J. (2000) Structural mechanism for STI-571 inhibition of abelson tyrosine kinase. Science 289, 1938-1942
232 Gorre, M. E., Mohammed, M., Ellwood, K., Hsu, N., Paquette, R., Rao, P. N. and Sawyers, C. L. (2001) Clinical resistance to STI-571 cancer therapy caused by BCR-ABL gene mutation or amplification. Science 293, 876-880
233 Goldman, J. M. and Melo, J. V. (2003) Chronic myeloid leukemia--advances in biology and new approaches to treatment. N Engl J Med 349, 1451-1464
234 Scherr, M., Battmer, K., Winkler, T., Heidenreich, O., Ganser, A. and Eder, M. (2003) Specific inhibition of bcr-abl gene expression by small interfering RNA. Blood 101, 1566-1569
235 Kurreck, J. (2003) Antisense technologies. Improvement through novel chemical modifications. Eur J Biochem 270, 1628-1644
236 Biernaux, C., Loos, M., Sels, A., Huez, G. and Stryckmans, P. (1995) Detection of major bcr-abl gene expression at a very low level in blood cells of some healthy individuals. Blood 86, 3118-3122
237 Bose, S., Deininger, M., Gora-Tybor, J., Goldman, J. M. and Melo, J. V. (1998) The presence of typical and atypical BCR-ABL fusion genes in leukocytes of normal individuals: biologic significance and implications for the assessment of minimal residual disease. Blood 92, 3362-3367
238 Wu, Y., Ma, G., Lu, D., Lin, F., Xu, H. J., Liu, J. and Arlinghaus, R. B. (1999) Bcr: a negative regulator of the Bcr-Abl oncoprotein. Oncogene 18, 4416-4424
239 Dhut, S., Dorey, E. L., Horton, M. A., Ganesan, T. S. and Young, B. D. (1988) Identification of two normal bcr gene products in the cytoplasm. Oncogene 3, 561-566
240 Stam, K., Heisterkamp, N., Reynolds, F. H., Jr. and Groffen, J. (1987) Evidence that the phl gene encodes a 160,000-dalton phosphoprotein with associated kinase activity. Mol Cell Biol 7, 1955-1960
241 Amson, R. B., Marcelle, C. and Telerman, A. (1989) Identification of a 130 Kda bcr related gene product. Oncogene 4, 243-247
242 McWhirter, J. R., Galasso, D. L. and Wang, J. Y. (1993) A coiled-coil oligomerization domain of Bcr is essential for the transforming function of Bcr-Abl oncoproteins. Mol Cell Biol 13, 7587-7595

243 Maru, Y. and Witte, O. N. (1991) The BCR gene encodes a novel serine/threonine kinase activity within a single exon. Cell 67, 459-468
244 Adams, J. M., Houston, H., Allen, J., Lints, T. and Harvey, R. (1992) The hematopoietically expressed vav proto-oncogene shares homology with the dbl GDP-GTP exchange factor, the bcr gene and a yeast gene (CDC24) involved in cytoskeletal organization. Oncogene 7, 611-618
245 Ron, D., Zannini, M., Lewis, M., Wickner, R. B., Hunt, L. T., Graziani, G., Tronick, S. R., Aaronson, S. A. and Eva, A. (1991) A region of proto-dbl essential for its transforming activity shows sequence similarity to a yeast cell cycle gene, CDC24, and the human breakpoint cluster gene, bcr. New Biol 3, 372-379
246 Diekmann, D., Brill, S., Garrett, M. D., Totty, N., Hsuan, J., Monfries, C., Hall, C., Lim, L. and Hall, A. (1991) Bcr encodes a GTPase-activating protein for p21rac. Nature 351, 400-402
247 Ma, G., Lu, D., Wu, Y., Liu, J. and Arlinghaus, R. B. (1997) Bcr phosphorylated on tyrosine 177 binds Grb2. Oncogene 14, 2367-2372
248 Zhao, X., Ghaffari, S., Lodish, H., Malashkevich, V. N. and Kim, P. S. (2002) Structure of the Bcr-Abl oncoprotein oligomerization domain. Nat Struct Biol 9, 117-120
249 Aitken, A. (1996) 14-3-3 and its possible role in coordinating multiple signalling pathways. Trends Cell Biol 6, 341-347
250 Takeda, N., Shibuya, M. and Maru, Y. (1999) The BCR-ABL oncoprotein potentially interacts with the xeroderma pigmentosum group B protein. Proc Natl Acad Sci U S A 96, 203-207
251 Maru, Y., Kobayashi, T., Tanaka, K. and Shibuya, M. (1999) BCR binds to the xeroderma pigmentosum group B protein. Biochem Biophys Res Commun 260, 309-312
252 Radziwill, G., Erdmann, R. A., Margelisch, U. and Moelling, K. (2003) The Bcr kinase downregulates Ras signaling by phosphorylating AF-6 and binding to its PDZ domain. Mol Cell Biol 23, 4663-4672
253 Malmberg, E. K., Andersson, C. X., Gentzsch, M., Chen, J. H., Mengos, A., Cui, L., Hansson, G. C. and Riordan, J. R. (2004) Bcr (breakpoint cluster region) protein binds to PDZ-domains of scaffold protein PDZK1 and vesicle coat protein Mint3. J Cell Sci 117, 5535-5541
254 Campbell, M. L., Li, W. and Arlinghaus, R. B. (1990) P210 BCR-ABL is complexed to P160 BCR and ph-P53 proteins in K562 cells. Oncogene 5, 773-776
255 Bennett, M. J., Schlunegger, M. P. and Eisenberg, D. (1995) 3D domain swapping: a mechanism for oligomer assembly. Protein Sci 4, 2455-2468
256 Smith, K. M., Yacobi, R. and Van Etten, R. A. (2003) Autoinhibition of Bcr-Abl through its SH3 domain. Mol Cell 12, 27-37
257 Beissert, T., Puccetti, E., Bianchini, A., Guller, S., Boehrer, S., Hoelzer, D., Ottmann, O. G., Nervi, C. and Ruthardt, M. (2003) Targeting of the N-terminal coiled coil oligomerization interface of BCR interferes with the transformation potential of BCR-ABL and increases sensitivity to STI571. Blood 102, 2985-2993

258 Hanks, S. K., Quinn, A. M. and Hunter, T. (1988) The protein kinase family: conserved features and deduced phylogeny of the catalytic domains. Science 241, 42-52

259 Cen, H., Papageorge, A. G., Zippel, R., Lowy, D. R. and Zhang, K. (1992) Isolation of multiple mouse cDNAs with coding homology to Saccharomyces cerevisiae CDC25: identification of a region related to Bcr, Vav, Dbl and CDC24. Embo J 11, 4007-4015

260 Hart, M. J., Eva, A., Evans, T., Aaronson, S. A. and Cerione, R. A. (1991) Catalysis of guanine nucleotide exchange on the CDC42Hs protein by the dbl oncogene product. Nature 354, 311-314

261 Hart, M. J., Eva, A., Zangrilli, D., Aaronson, S. A., Evans, T., Cerione, R. A. and Zheng, Y. (1994) Cellular transformation and guanine nucleotide exchange activity are catalyzed by a common domain on the dbl oncogene product. J Biol Chem 269, 62-65

262 Chuang, T. H., Xu, X., Kaartinen, V., Heisterkamp, N., Groffen, J. and Bokoch, G. M. (1995) Abr and Bcr are multifunctional regulators of the Rho GTP-binding protein family. Proc Natl Acad Sci U S A 92, 10282-10286

263 Korus, M., Mahon, G. M., Cheng, L. and Whitehead, I. P. (2002) p38 MAPK-mediated activation of NF-kappaB by the RhoGEF domain of Bcr. Oncogene 21, 4601-4612

264 Mahon, G. M., Wang, Y., Korus, M., Kostenko, E., Cheng, L., Sun, T., Arlinghaus, R. B. and Whitehead, I. P. (2003) The c-Myc Oncoprotein Interacts with Bcr. Curr Biol 13, 437-441

265 Rizo, J. and Sudhof, T. C. (1998) C2-domains, structure and function of a universal Ca2+-binding domain. J Biol Chem 273, 15879-15882

266 Maru, Y., Peters, K. L., Afar, D. E., Shibuya, M., Witte, O. N. and Smithgall, T. E. (1995) Tyrosine phosphorylation of BCR by FPS/FES protein-tyrosine kinases induces association of BCR with GRB-2/SOS. Mol Cell Biol 15, 835-842

267 Li, J. and Smithgall, T. E. (1996) Co-expression with BCR induces activation of the FES tyrosine kinase and phosphorylation of specific N-terminal BCR tyrosine residues. J Biol Chem 271, 32930-32936

268 Lowenstein, E. J., Daly, R. J., Batzer, A. G., Li, W., Margolis, B., Lammers, R., Ullrich, A., Skolnik, E. Y., Bar-Sagi, D. and Schlessinger, J. (1992) The SH2 and SH3 domain-containing protein GRB2 links receptor tyrosine kinases to ras signaling. Cell 70, 431-442

269 Liu, J., Wu, Y., Ma, G. Z., Lu, D., Haataja, L., Heisterkamp, N., Groffen, J. and Arlinghaus, R. B. (1996) Inhibition of Bcr serine kinase by tyrosine phosphorylation. Mol Cell Biol 16, 998-1005

270 Peters, K. L. and Smithgall, T. E. (1999) Tyrosine phosphorylation enhances the SH2 domain-binding activity of Bcr and inhibits Bcr interaction with 14-3-3 proteins. Cell Signal 11, 507-514

271 Salomon, A. R., Ficarro, S. B., Brill, L. M., Brinker, A., Phung, Q. T., Ericson, C., Sauer, K., Brock, A., Horn, D. M., Schultz, P. G. and Peters, E. C. (2003) Profiling of tyrosine phosphorylation pathways in human cells using mass spectrometry. Proc Natl Acad Sci U S A 100, 443-448

272 Obenauer, J. C., Cantley, L. C. and Yaffe, M. B. (2003) Scansite 2.0: Proteome-wide prediction of cell signaling interactions using short sequence motifs. Nucleic Acids Res 31, 3635-3641
273 Wu, Y., Liu, J. and Arlinghaus, R. B. (1998) Requirement of two specific tyrosine residues for the catalytic activity of Bcr serine/threonine kinase. Oncogene 16, 141-146
274 Brill, L. M., Salomon, A. R., Ficarro, S. B., Mukherji, M., Stettler-Gill, M. and Peters, E. C. (2004) Robust phosphoproteomic profiling of tyrosine phosphorylation sites from human T cells using immobilized metal affinity chromatography and tandem mass spectrometry. Anal Chem 76, 2763-2772
275 Symons, M. and Rusk, N. (2003) Control of vesicular trafficking by Rho GTPases. Curr Biol 13, R409-418
276 Boisguerin, P., Leben, R., Ay, B., Radziwill, G., Moelling, K., Dong, L. and Volkmer-Engert, R. (2004) An improved method for the synthesis of cellulose membrane-bound peptides with free C termini is useful for PDZ domain binding studies. Chem Biol 11, 449-459
277 Laura, R. P., Witt, A. S., Held, H. A., Gerstner, R., Deshayes, K., Koehler, M. F., Kosik, K. S., Sidhu, S. S. and Lasky, L. A. (2002) The Erbin PDZ domain binds with high affinity and specificity to the carboxyl termini of delta-catenin and ARVCF. J Biol Chem 277, 12906-12914
278 Mackie, S. and AItken, A. (2005) Neuronal Proteins that associate with 14-3-3. FEBS
279 Kolch, W. (2000) Meaningful relationships: the regulation of the Ras/Raf/MEK/ERK pathway by protein interactions. Biochem J 351 Pt 2, 289-305
280 Wellbrock, C., Karasarides, M. and Marais, R. (2004) The RAF proteins take centre stage. Nat Rev Mol Cell Biol 5, 875-885
281 Hekman, M., Wiese, S., Metz, R., Albert, S., Troppmair, J., Nickel, J., Sendtner, M. and Rapp, U. R. (2004) Dynamic changes in C-Raf phosphorylation and 14-3-3 protein binding in response to growth factor stimulation: differential roles of 14-3-3 protein binding sites. J Biol Chem 279, 14074-14086
282 Wetzler, M., Talpaz, M., Yee, G., Stass, S. A., Van Etten, R. A., Andreeff, M., Goodacre, A. M., Kleine, H. D., Mahadevia, R. K. and Kurzrock, R. (1995) Cell cycle-related shifts in subcellular localization of BCR: association with mitotic chromosomes and with heterochromatin. Proc Natl Acad Sci U S A 92, 3488-3492
283 Dahmus, M. E. (1981) Purification and properties of calf thymus casein kinases I and II. J Biol Chem 256, 3319-3325
284 Tuazon, P. T. and Traugh, J. A. (1991) Casein kinase I and II--multipotential serine protein kinases: structure, function, and regulation. Adv Second Messenger Phosphoprotein Res 23, 123-164
285 Braun, S., Raymond, W. E. and Racker, E. (1984) Synthetic tyrosine polymers as substrates and inhibitors of tyrosine-specific protein kinases. J Biol Chem 259, 2051-2054
286 Hoekstra, M. F., Dhillon, N., Carmel, G., DeMaggio, A. J., Lindberg, R. A., Hunter, T. and Kuret, J. (1994) Budding and fission yeast casein

kinase I isoforms have dual-specificity protein kinase activity. Mol Biol Cell 5, 877-886

287 Pulgar, V., Tapia, C., Vignolo, P., Santos, J., Sunkel, C. E., Allende, C. C. and Allende, J. E. (1996) The recombinant alpha isoform of protein kinase CK1 from Xenopus laevis can phosphorylate tyrosine in synthetic substrates. Eur J Biochem 242, 519-528

288 Gross, S. D. and Anderson, R. A. (1998) Casein kinase I: spatial organization and positioning of a multifunctional protein kinase family. Cell Signal 10, 699-711

289 Fish, K. J., Cegielska, A., Getman, M. E., Landes, G. M. and Virshup, D. M. (1995) Isolation and characterization of human casein kinase I epsilon (CKI), a novel member of the CKI gene family. J Biol Chem 270, 14875-14883

290 Rowles, J., Slaughter, C., Moomaw, C., Hsu, J. and Cobb, M. H. (1991) Purification of casein kinase I and isolation of cDNAs encoding multiple casein kinase I-like enzymes. Proc Natl Acad Sci U S A 88, 9548-9552

291 Zhang, J., Gross, S. D., Schroeder, M. D. and Anderson, R. A. (1996) Casein kinase I alpha and alpha L: alternative splicing-generated kinases exhibit different catalytic properties. Biochemistry 35, 16319-16327

292 Horiguchi, R., Tokumoto, M., Nagahama, Y. and Tokumoto, T. (2005) Molecular cloning and expression of cDNA coding for four spliced isoforms of casein kinase Ialpha in goldfish oocytes. Biochim Biophys Acta 1727, 75-80

293 Poulter, L., Ang, S. G., Gibson, B. W., Williams, D. H., Holmes, C. F., Caudwell, F. B., Pitcher, J. and Cohen, P. (1988) Analysis of the in vivo phosphorylation state of rabbit skeletal muscle glycogen synthase by fast-atom-bombardment mass spectrometry. Eur J Biochem 175, 497-510

294 Grasser, F. A., Scheidtmann, K. H., Tuazon, P. T., Traugh, J. A. and Walter, G. (1988) In vitro phosphorylation of SV40 large T antigen. Virology 165, 13-22

295 Kuret, J., Woodgett, J. R. and Cohen, P. (1985) Multisite phosphorylation of glycogen synthase from rabbit skeletal muscle. Identification of the sites phosphorylated by casein kinase-I. Eur J Biochem 151, 39-48

296 Flotow, H. and Roach, P. J. (1989) Synergistic phosphorylation of rabbit muscle glycogen synthase by cyclic AMP-dependent protein kinase and casein kinase I. Implications for hormonal regulation of glycogen synthase. J Biol Chem 264, 9126-9128

297 Flotow, H., Graves, P. R., Wang, A. Q., Fiol, C. J., Roeske, R. W. and Roach, P. J. (1990) Phosphate groups as substrate determinants for casein kinase I action. J Biol Chem 265, 14264-14269

298 Flotow, H. and Roach, P. J. (1991) Role of acidic residues as substrate determinants for casein kinase I. J Biol Chem 266, 3724-3727

299 Pulgar, V., Marin, O., Meggio, F., Allende, C. C., Allende, J. E. and Pinna, L. A. (1999) Optimal sequences for non-phosphate-directed phosphorylation by protein kinase CK1 (casein kinase-1)--a re-evaluation. Eur J Biochem 260, 520-526

300 Marin, O., Bustos, V. H., Cesaro, L., Meggio, F., Pagano, M. A., Antonelli, M., Allende, C. C., Pinna, L. A. and Allende, J. E. (2003) A

noncanonical sequence phosphorylated by casein kinase 1 in beta-catenin may play a role in casein kinase 1 targeting of important signaling proteins. Proc Natl Acad Sci U S A 100, 10193-10200
301 Gao, Z. H., Seeling, J. M., Hill, V., Yochum, A. and Virshup, D. M. (2002) Casein kinase I phosphorylates and destabilizes the beta-catenin degradation complex. Proc Natl Acad Sci U S A 99, 1182-1187
302 Rubinfeld, B., Tice, D. A. and Polakis, P. (2001) Axin-dependent phosphorylation of the adenomatous polyposis coli protein mediated by casein kinase 1epsilon. J Biol Chem 276, 39037-39045
303 Pendergast, A. M. and Traugh, J. A. (1985) Alteration of aminoacyl-tRNA synthetase activities by phosphorylation with casein kinase I. J Biol Chem 260, 11769-11774
304 Tipper, J. P., Bacon, G. W. and Witters, L. A. (1983) Phosphorylation of acetyl-coenzyme A carboxylase by casein kinase I and casein kinase II. Arch Biochem Biophys 227, 386-396
305 Liu, F., Virshup, D. M., Nairn, A. C. and Greengard, P. (2002) Mechanism of regulation of casein kinase I activity by group I metabotropic glutamate receptors. J Biol Chem 277, 45393-45399
306 Peters, J. M., McKay, R. M., McKay, J. P. and Graff, J. M. (1999) Casein kinase I transduces Wnt signals. Nature 401, 345-350
307 Haas, D. W. and Hagedorn, C. H. (1991) Casein kinase I phosphorylates the 25-kDa mRNA cap-binding protein. Arch Biochem Biophys 284, 84-89
308 Liu, Y., Loros, J. and Dunlap, J. C. (2000) Phosphorylation of the Neurospora clock protein FREQUENCY determines its degradation rate and strongly influences the period length of the circadian clock. Proc Natl Acad Sci U S A 97, 234-239
309 Gorl, M., Merrow, M., Huttner, B., Johnson, J., Roenneberg, T. and Brunner, M. (2001) A PEST-like element in FREQUENCY determines the length of the circadian period in Neurospora crassa. Embo J 20, 7074-7084
310 Desdouits, F., Cohen, D., Nairn, A. C., Greengard, P. and Girault, J. A. (1995) Phosphorylation of DARPP-32, a dopamine- and cAMP-regulated phosphoprotein, by casein kinase I in vitro and in vivo. J Biol Chem 270, 8772-8778
311 Huflejt, M. E., Turck, C. W., Lindstedt, R., Barondes, S. H. and Leffler, H. (1993) L-29, a soluble lactose-binding lectin, is phosphorylated on serine 6 and serine 12 in vivo and by casein kinase I. J Biol Chem 268, 26712-26718
312 Imazu, M., Strickland, W. G., Chrisman, T. D. and Exton, J. H. (1984) Phosphorylation and inactivation of liver glycogen synthase by liver protein kinases. J Biol Chem 259, 1813-1821
313 Oldfield, S. and Proud, C. G. (1992) Purification, phosphorylation and control of the guanine-nucleotide-exchange factor from rabbit reticulocyte lysates. Eur J Biochem 208, 73-81
314 Agostinis, P., Vandenheede, J. R., Goris, J., Meggio, F., Pinna, L. A. and Merlevede, W. (1987) The ATP,Mg-dependent protein phosphatase: regulation by casein kinase-1. FEBS Lett 224, 385-390

315 Agostinis, P., Marin, O., James, P., Hendrix, P., Merlevede, W., Vandenheede, J. R. and Pinna, L. A. (1992) Phosphorylation of the phosphatase modulator subunit (inhibitor-2) by casein kinase-1. Identification of the phosphorylation sites. FEBS Lett 305, 121-124
316 Wang, X., Paulin, F. E., Campbell, L. E., Gomez, E., O'Brien, K., Morrice, N. and Proud, C. G. (2001) Eukaryotic initiation factor 2B: identification of multiple phosphorylation sites in the epsilon-subunit and their functions in vivo. Embo J 20, 4349-4359
317 Hathaway, G. M., Lundak, T. S., Tahara, S. M. and Traugh, J. A. (1979) Isolation of protein kinases from reticulocytes and phosphorylation of initiation factors. Methods Enzymol 60, 495-511
318 Tuazon, P. T., Pang, D. T., Shafer, J. A. and Traugh, J. A. (1985) Phosphorylation of the insulin receptor by casein kinase I. J Cell Biochem 28, 159-170
319 Rapuano, M. and Rosen, O. M. (1991) Phosphorylation of the insulin receptor by a casein kinase I-like enzyme. J Biol Chem 266, 12902-12907
320 Beyaert, R., Vanhaesebroeck, B., Declercq, W., Van Lint, J., Vandenabele, P., Agostinis, P., Vandenheede, J. R. and Fiers, W. (1995) Casein kinase-1 phosphorylates the p75 tumor necrosis factor receptor and negatively regulates tumor necrosis factor signaling for apoptosis. J Biol Chem 270, 23293-23299
321 Rittschof, D. and Traugh, J. A. (1982) Identification of casein kinase II and phosphorylated proteins associated with messenger ribonucleoproteins particles from reticulocytes. Eur J Biochem 123, 333-336
322 Eichwald, C., Jacob, G., Muszynski, B., Allende, J. E. and Burrone, O. R. (2004) Uncoupling substrate and activation functions of rotavirus NSP5: phosphorylation of Ser-67 by casein kinase 1 is essential for hyperphosphorylation. Proc Natl Acad Sci U S A 101, 16304-16309
323 Vila, J., Payne, D. M., Zioncheck, T. F., Harrison, M. L., Itarte, E. and Weber, M. J. (1990) Phosphorylation and activation of p40 tyrosine kinase by casein kinase-1. FEBS Lett 264, 21-24
324 Yamamoto, A., Friedlein, A., Imai, Y., Takahashi, R., Kahle, P. J. and Haass, C. (2004) Parkin phosphorylation and modulation of its E3 ubiquitin ligase activity. J Biol Chem
325 Takano, A., Shimizu, K., Kani, S., Buijs, R. M., Okada, M. and Nagai, K. (2000) Cloning and characterization of rat casein kinase 1epsilon. FEBS Lett 477, 106-112
326 Takano, A., Isojima, Y. and Nagai, K. (2004) Identification of mPer1 phosphorylation sites responsible for the nuclear entry. J Biol Chem 279, 32578-32585
327 Vila, J., Walker, J. M., Itarte, E., Weber, M. J. and Sando, J. J. (1989) Phosphorylation of protein kinase C by casein kinase-1. FEBS Lett 255, 205-208
328 Vancurova, I., Choi, J. H., Lin, H., Kuret, J. and Vancura, A. (1999) Regulation of phosphatidylinositol 4-phosphate 5-kinase from Schizosaccharomyces pombe by casein kinase I. J Biol Chem 274, 1147-1155

329 Oetting, W. S., Tuazon, P. T., Traugh, J. A. and Walker, A. M. (1986) Phosphorylation of prolactin. J Biol Chem 261, 1649-1652
330 Waddell, D. S., Liberati, N. T., Guo, X., Frederick, J. P. and Wang, X. F. (2004) Casein kinase Iepsilon plays a functional role in the transforming growth factor-beta signaling pathway. J Biol Chem 279, 29236-29246
331 Bordin, L., Vargiu, C., Clari, G., Brunati, A. M., Colombatto, S., Salvi, M., Grillo, M. A. and Toninello, A. (2002) Phosphorylation of recombinant human spermidine/spermine N(1)-acetyltransferase by CK1 and modulation of its binding to mitochondria: a comparison with CK2. Biochem Biophys Res Commun 290, 463-468
332 Gross, S. D., Hoffman, D. P., Fisette, P. L., Baas, P. and Anderson, R. A. (1995) A phosphatidylinositol 4,5-bisphosphate-sensitive casein kinase I alpha associates with synaptic vesicles and phosphorylates a subset of vesicle proteins. J Cell Biol 130, 711-724
333 Marchal, C., Haguenauer-Tsapis, R. and Urban-Grimal, D. (1998) A PEST-like sequence mediates phosphorylation and efficient ubiquitination of yeast uracil permease. Mol Cell Biol 18, 314-321
334 Marchal, C., Haguenauer-Tsapis, R. and Urban-Grimal, D. (2000) Casein kinase I-dependent phosphorylation within a PEST sequence and ubiquitination at nearby lysines signal endocytosis of yeast uracil permease. J Biol Chem 275, 23608-23614
335 Shibayama, T., Shinkawa, K., Nakajo, S., Nakaya, K. and Nakamura, Y. (1986) Phosphorylation of muscle and non-muscle actins by casein kinase 1 in vitro. Biochem Int 13, 367-373
336 Karino, A., Okano, M., Hatomi, M., Nakamura, T. and Ohtsuki, K. (1999) Biochemical characterization of a casein kinase I-like actin kinase responsible for the actin-induced suppression of casein kinase II activity in vitro. Biochim Biophys Acta 1472, 603-616
337 Lu, P. W., Soong, C. J. and Tao, M. (1985) Phosphorylation of ankyrin decreases its affinity for spectrin tetramer. J Biol Chem 260, 14958-14964
338 Okochi, M., Walter, J., Koyama, A., Nakajo, S., Baba, M., Iwatsubo, T., Meijer, L., Kahle, P. J. and Haass, C. (2000) Constitutive phosphorylation of the Parkinson's disease associated alpha-synuclein. J Biol Chem 275, 390-397
339 Behrend, L., Stoter, M., Kurth, M., Rutter, G., Heukeshoven, J., Deppert, W. and Knippschild, U. (2000) Interaction of casein kinase 1 delta (CK1delta) with post-Golgi structures, microtubules and the spindle apparatus. Eur J Cell Biol 79, 240-251
340 Walter, J., Fluhrer, R., Hartung, B., Willem, M., Kaether, C., Capell, A., Lammich, S., Multhaup, G. and Haass, C. (2001) Phosphorylation regulates intracellular trafficking of beta-secretase. J Biol Chem 276, 14634-14641
341 Pastorino, L., Ikin, A. F., Nairn, A. C., Pursnani, A. and Buxbaum, J. D. (2002) The carboxyl-terminus of BACE contains a sorting signal that regulates BACE trafficking but not the formation of total A(beta). Mol Cell Neurosci 19, 175-185

342 Salvatori, S., Furlan, S. and Meggio, F. (1994) Dual role of calsequestrin as substrate and inhibitor of casein kinase-1 and casein kinase-2. Biochem Biophys Res Commun 198, 144-149
343 Cooper, C. D. and Lampe, P. D. (2002) Casein kinase 1 regulates connexin-43 gap junction assembly. J Biol Chem 277, 44962-44968
344 Cheng, H. L. and Louis, C. F. (1999) Endogenous casein kinase I catalyzes the phosphorylation of the lens fiber cell connexin49. Eur J Biochem 263, 276-286
345 Wang, C. C., Tao, M., Wei, T. and Low, P. S. (1997) Identification of the major casein kinase I phosphorylation sites on erythrocyte band 3. Blood 89, 3019-3024
346 Nakajo, S., Nakaya, K. and Nakamura, Y. (1987) Phosphorylation of actin-binding proteins by casein kinases 1 and 2. Biochem Int 15, 321-327
347 Harris, H. W., Jr., Levin, N. and Lux, S. E. (1980) Comparison of the phosphorylation of human erythrocyte spectrin in the intact red cell and in various cell-free systems. J Biol Chem 255, 11521-11525
348 Simkowski, K. W. and Tao, M. (1980) Studies on a soluble human erythrocyte protein kinase. J Biol Chem 255, 6456-6461
349 Manno, S., Takakuwa, Y., Nagao, K. and Mohandas, N. (1995) Modulation of erythrocyte membrane mechanical function by beta-spectrin phosphorylation and dephosphorylation. J Biol Chem 270, 5659-5665
350 Harris, H. W., Jr. and Lux, S. E. (1980) Structural characterization of the phosphorylation sites of human erythrocyte spectrin. J Biol Chem 255, 11512-11520
351 Waugh, M. G., Challiss, R. A., Berstein, G., Nahorski, S. R. and Tobin, A. B. (1999) Agonist-induced desensitization and phosphorylation of m1-muscarinic receptors. Biochem J 338 (Pt 1), 175-183
352 Tobin, A. B. (2002) Are we beta-ARKing up the wrong tree? Casein kinase 1 alpha provides an additional pathway for GPCR phosphorylation. Trends Pharmacol Sci 23, 337-343
353 Budd, D. C., McDonald, J. E. and Tobin, A. B. (2000) Phosphorylation and regulation of a Gq/11-coupled receptor by casein kinase 1alpha. J Biol Chem 275, 19667-19675
354 Tobin, A. B., Keys, B. and Nahorski, S. R. (1996) Identification of a novel receptor kinase that phosphorylates a phospholipase C-linked muscarinic receptor. J Biol Chem 271, 3907-3916
355 Tobin, A. B., Totty, N. F., Sterlin, A. E. and Nahorski, S. R. (1997) Stimulus-dependent phosphorylation of G-protein-coupled receptors by casein kinase 1alpha. J Biol Chem 272, 20844-20849
356 Singh, T. J., Akatsuka, A. and Huang, K. P. (1983) Phosphorylation of smooth muscle myosin light chain by five different kinases. FEBS Lett 159, 217-220
357 Singh, T. J., Akatsuka, A., Blake, K. R. and Huang, K. P. (1983) Phosphorylation of troponin and myosin light chain by cAMP-independent casein kinase-2 from rabbit skeletal muscle. Arch Biochem Biophys 220, 615-622

358 Floyd, C. C., Grant, P., Gallant, P. E. and Pant, H. C. (1991) Principal neurofilament-associated protein kinase in squid axoplasm is related to casein kinase I. J Biol Chem 266, 4987-4994
359 Link, W. T., Dosemeci, A., Floyd, C. C. and Pant, H. C. (1993) Bovine neurofilament-enriched preparations contain kinase activity similar to casein kinase I--neurofilament phosphorylation by casein kinase I (CKI). Neurosci Lett 151, 89-93
360 Mackie, K., Sorkin, B. C., Nairn, A. C., Greengard, P., Edelman, G. M. and Cunningham, B. A. (1989) Identification of two protein kinases that phosphorylate the neural cell-adhesion molecule, N-CAM. J Neurosci 9, 1883-1896
361 Elizarov, S. M. and Preobrazhensky, A. A. (1993) Phosphorylation of two human neurochordins by mammalian casein kinase 1. Brain Res Mol Brain Res 19, 310-312
362 Uemura, T., Tachihara, K., Tomitori, H., Kashiwagi, K. and Igarashi, K. (2005) Characteristics of the polyamine transporter TPO1 and regulation of its activity and cellular localization by phosphorylation. J Biol Chem
363 Walter, J., Grunberg, J., Schindzielorz, A. and Haass, C. (1998) Proteolytic fragments of the Alzheimer's disease associated presenilins-1 and -2 are phosphorylated in vivo by distinct cellular mechanisms. Biochemistry 37, 5961-5967
364 Walter, J., Schindzielorz, A., Grunberg, J. and Haass, C. (1999) Phosphorylation of presenilin-2 regulates its cleavage by caspases and retards progression of apoptosis. Proc Natl Acad Sci U S A 96, 1391-1396
365 Ohguro, H., Rudnicka-Nawrot, M., Buczylko, J., Zhao, X., Taylor, J. A., Walsh, K. A. and Palczewski, K. (1996) Structural and enzymatic aspects of rhodopsin phosphorylation. J Biol Chem 271, 5215-5224
366 Kani, S., Oishi, I., Yamamoto, H., Yoda, A., Suzuki, H., Nomachi, A., Iozumi, K., Nishita, M., Kikuchi, A., Takumi, T. and Minami, Y. (2004) The receptor tyrosine kinase Ror2 associates with and is activated by casein kinase Iepsilon. J Biol Chem 279, 50102-50109
367 Zhang, C., Williams, E. H., Guo, Y., Lum, L. and Beachy, P. A. (2004) Inaugural Article: Extensive phosphorylation of Smoothened in Hedgehog pathway activation. Proc Natl Acad Sci U S A 101, 17900-17907
368 Apionishev, S., Katanayeva, N. M., Marks, S. A., Kalderon, D. and Tomlinson, A. (2005) Drosophila Smoothened phosphorylation sites essential for Hedgehog signal transduction. Nat Cell Biol 7, 86-92
369 Hanger, D. P., Betts, J. C., Loviny, T. L., Blackstock, W. P. and Anderton, B. H. (1998) New phosphorylation sites identified in hyperphosphorylated tau (paired helical filament-tau) from Alzheimer's disease brain using nanoelectrospray mass spectrometry. J Neurochem 71, 2465-2476
370 Singh, T. J., Grundke-Iqbal, I. and Iqbal, K. (1995) Phosphorylation of tau protein by casein kinase-1 converts it to an abnormal Alzheimer-like state. J Neurochem 64, 1420-1423

371 Li, G., Yin, H. and Kuret, J. (2004) Casein kinase 1 delta phosphorylates tau and disrupts its binding to microtubules. J Biol Chem 279, 15938-15945
372 Singh, T. J., Zaidi, T., Grundke-Iqbal, I. and Iqbal, K. (1996) Non-proline-dependent protein kinases phosphorylate several sites found in tau from Alzheimer disease brain. Mol Cell Biochem 154, 143-151
373 Darnay, B. G., Singh, S. and Aggarwal, B. B. (1997) The p80 TNF receptor-associated kinase (p80TRAK) associates with residues 354-397 of the p80 cytoplasmic domain: similarity to casein kinase. FEBS Lett 406, 101-105
374 Krantz, D. E., Peter, D., Liu, Y. and Edwards, R. H. (1997) Phosphorylation of a vesicular monoamine transporter by casein kinase II. J Biol Chem 272, 6752-6759
375 Price, M. A. and Kalderon, D. (2002) Proteolysis of the Hedgehog signaling effector Cubitus interruptus requires phosphorylation by Glycogen Synthase Kinase 3 and Casein Kinase 1. Cell 108, 823-835
376 de Groot, R. P., den Hertog, J., Vandenheede, J. R., Goris, J. and Sassone-Corsi, P. (1993) Multiple and cooperative phosphorylation events regulate the CREM activator function. Embo J 12, 3903-3911
377 Cegielska, A., Gietzen, K. F., Rivers, A. and Virshup, D. M. (1998) Autoinhibition of casein kinase I epsilon (CKI epsilon) is relieved by protein phosphatases and limited proteolysis. J Biol Chem 273, 1357-1364
378 Kattapuram, T., Yang, S., Maki, J. L. and Stone, J. R. (2005) Protein kinase CK1alpha regulates mRNA binding by hnRNP-C in response to physiologic levels of hydrogen peroxide. J Biol Chem
379 Okamura, H., Garcia-Rodriguez, C., Martinson, H., Qin, J., Virshup, D. M. and Rao, A. (2004) A conserved docking motif for CK1 binding controls the nuclear localization of NFAT1. Mol Cell Biol 24, 4184-4195
380 Zhu, J., Shibasaki, F., Price, R., Guillemot, J. C., Yano, T., Dotsch, V., Wagner, G., Ferrara, P. and McKeon, F. (1998) Intramolecular masking of nuclear import signal on NF-AT4 by casein kinase I and MEKK1. Cell 93, 851-861
381 Christmann, J. L. and Dahmus, M. E. (1981) Phosphorylation of rat ascites tumor non-histone chromatin proteins. Differential phosphorylation by two cyclic nucleotide-independent protein kinases and comparison to in vivo phosphorylation. J Biol Chem 256, 3326-3331
382 Scheidtmann, K. H., Buck, M., Schneider, J., Kalderon, D., Fanning, E. and Smith, A. E. (1991) Biochemical characterization of phosphorylation site mutants of simian virus 40 large T antigen: evidence for interaction between amino- and carboxy-terminal domains. J Virol 65, 1479-1490
383 Cegielska, A. and Virshup, D. M. (1993) Control of simian virus 40 DNA replication by the HeLa cell nuclear kinase casein kinase I. Mol Cell Biol 13, 1202-1211
384 Cegielska, A., Moarefi, I., Fanning, E. and Virshup, D. M. (1994) T-antigen kinase inhibits simian virus 40 DNA replication by phosphorylation of intact T antigen on serines 120 and 123. J Virol 68, 269-275

385 Dumaz, N., Milne, D. M. and Meek, D. W. (1999) Protein kinase CK1 is a p53-threonine 18 kinase which requires prior phosphorylation of serine 15. FEBS Lett 463, 312-316

386 Milne, D. M., Palmer, R. H., Campbell, D. G. and Meek, D. W. (1992) Phosphorylation of the p53 tumour-suppressor protein at three N-terminal sites by a novel casein kinase I-like enzyme. Oncogene 7, 1361-1369

387 Knippschild, U., Milne, D. M., Campbell, L. E., DeMaggio, A. J., Christenson, E., Hoekstra, M. F. and Meek, D. W. (1997) p53 is phosphorylated in vitro and in vivo by the delta and epsilon isoforms of casein kinase 1 and enhances the level of casein kinase 1 delta in response to topoisomerase-directed drugs. Oncogene 15, 1727-1736

388 Winter, M., Milne, D., Dias, S., Kulikov, R., Knippschild, U., Blattner, C. and Meek, D. (2004) Protein kinase CK1delta phosphorylates key sites in the acidic domain of murine double-minute clone 2 protein (MDM2) that regulate p53 turnover. Biochemistry 43, 16356-16364

389 Dahmus, M. E. (1981) Phosphorylation of eukaryotic DNA-dependent RNA polymerase. Identification of calf thymus RNA polymerase subunits phosphorylated by two purified protein kinases, correlation with in vivo sites of phosphorylation in HeLa cell RNA polymerase II. J Biol Chem 256, 3332-3339

390 Itarte, E., Plana, M., Guasch, M. D. and Martos, C. (1983) Phosphorylation of fibrinogen by casein kinase 1. Biochem Biophys Res Commun 117, 631-636

391 Humble, E., Heldin, P., Forsberg, P. O. and Engstrom, L. (1985) Phosphorylation in vitro of fibrinogen from three mammalian species with four different protein kinases. Arch Biochem Biophys 241, 225-231

392 Dupuy, L. C., Dobson, S., Bitko, V. and Barik, S. (1999) Casein kinase 2-mediated phosphorylation of respiratory syncytial virus phosphoprotein P is essential for the transcription elongation activity of the viral polymerase; phosphorylation by casein kinase 1 occurs mainly at Ser(215) and is without effect. J Virol 73, 8384-8392

393 Xu, R. M., Carmel, G., Sweet, R. M., Kuret, J. and Cheng, X. (1995) Crystal structure of casein kinase-1, a phosphate-directed protein kinase. Embo J 14, 1015-1023

394 Longenecker, K. L., Roach, P. J. and Hurley, T. D. (1996) Three-dimensional structure of mammalian casein kinase I: molecular basis for phosphate recognition. J Mol Biol 257, 618-631

395 Graves, P. R. and Roach, P. J. (1995) Role of COOH-terminal phosphorylation in the regulation of casein kinase I delta. J Biol Chem 270, 21689-21694

396 Gietzen, K. F. and Virshup, D. M. (1999) Identification of inhibitory autophosphorylation sites in casein kinase I epsilon. J Biol Chem 274, 32063-32070

397 Takano, A., Uchiyama, M., Kajimura, N., Mishima, K., Inoue, Y., Kamei, Y., Kitajima, T., Shibui, K., Katoh, M., Watanabe, T., Hashimotodani, Y., Nakajima, T., Ozeki, Y., Hori, T., Yamada, N., Toyoshima, R., Ozaki, N., Okawa, M., Nagai, K., Takahashi, K., Isojima, Y., Yamauchi, T. and

Ebisawa, T. (2004) A missense variation in human casein kinase I epsilon gene that induces functional alteration and shows an inverse association with circadian rhythm sleep disorders. Neuropsychopharmacology 29, 1901-1909

398 Longenecker, K. L., Roach, P. J. and Hurley, T. D. (1998) Crystallographic studies of casein kinase I delta toward a structural understanding of auto-inhibition. Acta Crystallogr D Biol Crystallogr 54 (Pt 3), 473-475

399 Brockman, J. L. and Anderson, R. A. (1991) Casein kinase I is regulated by phosphatidylinositol 4,5-bisphosphate in native membranes. J Biol Chem 266, 2508-2512

400 Santos, J. A., Logarinho, E., Tapia, C., Allende, C. C., Allende, J. E. and Sunkel, C. E. (1996) The casein kinase 1 alpha gene of Drosophila melanogaster is developmentally regulated and the kinase activity of the protein induced by DNA damage. J Cell Sci 109 (Pt 7), 1847-1856

401 Cobb, M. H. and Rosen, O. M. (1983) Description of a protein kinase derived from insulin-treated 3T3-L1 cells that catalyzes the phosphorylation of ribosomal protein S6 and casein. J Biol Chem 258, 12472-12481

402 Elias, L., Li, A. P. and Longmire, J. (1981) Cyclic adenosine 3':5'-monophosphate-dependent and -independent protein kinase in acute myeloblastic leukemia. Cancer Res 41, 2182-2188

403 Rena, G., Bain, J., Elliott, M. and Cohen, P. (2004) D4476, a cell-permeant inhibitor of CK1, suppresses the site-specific phosphorylation and nuclear exclusion of FOXO1a. EMBO Rep 5, 60-65

404 Meek, D. W. (1999) Mechanisms of switching on p53: a role for covalent modification? Oncogene 18, 7666-7675

405 Meek, D. W. (2004) The p53 response to DNA damage. DNA Repair (Amst) 3, 1049-1056

406 Bode, A. M. and Dong, Z. (2004) Post-translational modification of p53 in tumorigenesis. Nat Rev Cancer 4, 793-805

407 Appella, E. and Anderson, C. W. (2001) Post-translational modifications and activation of p53 by genotoxic stresses. Eur J Biochem 268, 2764-2772

408 Knippschild, U., Gocht, A., Wolff, S., Huber, N., Lohler, J. and Stoter, M. (2005) The casein kinase 1 family: participation in multiple cellular processes in eukaryotes. Cell Signal 17, 675-689

409 Banin, S., Moyal, L., Shieh, S., Taya, Y., Anderson, C. W., Chessa, L., Smorodinsky, N. I., Prives, C., Reiss, Y., Shiloh, Y. and Ziv, Y. (1998) Enhanced phosphorylation of p53 by ATM in response to DNA damage. Science 281, 1674-1677

410 Canman, C. E., Lim, D. S., Cimprich, K. A., Taya, Y., Tamai, K., Sakaguchi, K., Appella, E., Kastan, M. B. and Siliciano, J. D. (1998) Activation of the ATM kinase by ionizing radiation and phosphorylation of p53. Science 281, 1677-1679

411 Desdouits, F., Siciliano, J. C., Greengard, P. and Girault, J. A. (1995) Dopamine- and cAMP-regulated phosphoprotein DARPP-32:

phosphorylation of Ser-137 by casein kinase I inhibits dephosphorylation of Thr-34 by calcineurin. Proc Natl Acad Sci U S A 92, 2682-2685

412 Desdouits, F., Siciliano, J. C., Nairn, A. C., Greengard, P. and Girault, J. A. (1998) Dephosphorylation of Ser-137 in DARPP-32 by protein phosphatases 2A and 2C: different roles in vitro and in striatonigral neurons. Biochem J 330 (Pt 1), 211-216

413 Brockman, J. L., Gross, S. D., Sussman, M. R. and Anderson, R. A. (1992) Cell cycle-dependent localization of casein kinase I to mitotic spindles. Proc Natl Acad Sci U S A 89, 9454-9458

414 Gross, S. D., Simerly, C., Schatten, G. and Anderson, R. A. (1997) A casein kinase I isoform is required for proper cell cycle progression in the fertilized mouse oocyte. J Cell Sci 110 (Pt 24), 3083-3090

415 Sillibourne, J. E., Milne, D. M., Takahashi, M., Ono, Y. and Meek, D. W. (2002) Centrosomal anchoring of the protein kinase CK1delta mediated by attachment to the large, coiled-coil scaffolding protein CG-NAP/AKAP450. J Mol Biol 322, 785-797

416 Wong, W. and Scott, J. D. (2004) AKAP signalling complexes: focal points in space and time. Nat Rev Mol Cell Biol 5, 959-970

417 Witczak, O., Skalhegg, B. S., Keryer, G., Bornens, M., Tasken, K., Jahnsen, T. and Orstavik, S. (1999) Cloning and characterization of a cDNA encoding an A-kinase anchoring protein located in the centrosome, AKAP450. Embo J 18, 1858-1868

418 Takahashi, M., Shibata, H., Shimakawa, M., Miyamoto, M., Mukai, H. and Ono, Y. (1999) Characterization of a novel giant scaffolding protein, CG-NAP, that anchors multiple signaling enzymes to centrosome and the golgi apparatus. J Biol Chem 274, 17267-17274

419 Dubois, T., Kerai, P., Zemlickova, E., Howell, S., Jackson, T. R., Venkateswarlu, K., Cullen, P. J., Theibert, A. B., Larose, L., Roach, P. J. and Aitken, A. (2001) Casein kinase I associates with members of the centaurin-alpha family of phosphatidylinositol 3,4,5-trisphosphate-binding proteins. J Biol Chem 276, 18757-18764

420 Sobrado, P., Jedlicki, A., Bustos, V. H., Allende, C. C. and Allende, J. E. (2004) Basic region of residues 228-231 of protein kinase CK1alpha is involved in its interaction with axin: Binding to axin does not affect the kinase activity. J Cell Biochem

421 Dubois, T., Howell, S., Zemlickova, E. and Aitken, A. (2002) Identification of casein kinase Ialpha interacting protein partners. FEBS Lett 517, 167-171

422 Zemlickova, E., Johannes, F. J., Aitken, A. and Dubois, T. (2004) Association of CPI-17 with protein kinase C and casein kinase I. Biochem Biophys Res Commun 316, 39-47

423 Hammonds-Odie, L. P., Jackson, T. R., Profit, A. A., Blader, I. J., Turck, C. W., Prestwich, G. D. and Theibert, A. B. (1996) Identification and cloning of centaurin-alpha. A novel phosphatidylinositol 3,4,5-trisphosphate-binding protein from rat brain. J Biol Chem 271, 18859-18868

424 Tanaka, K., Horiguchi, K., Yoshida, T., Takeda, M., Fujisawa, H., Takeuchi, K., Umeda, M., Kato, S., Ihara, S., Nagata, S. and Fukui, Y.

(1999) Evidence that a phosphatidylinositol 3,4,5-trisphosphate-binding protein can function in nucleus. J Biol Chem 274, 3919-3922
425 Venkateswarlu, K., Oatey, P. B., Tavare, J. M., Jackson, T. R. and Cullen, P. J. (1999) Identification of centaurin-alpha1 as a potential in vivo phosphatidylinositol 3,4,5-trisphosphate-binding protein that is functionally homologous to the yeast ADP-ribosylation factor (ARF) GTPase-activating protein, Gcs1. Biochem J 340 (Pt 2), 359-363
426 Kreutz, M. R., Bockers, T. M., Sabel, B. A., Hulser, E., Stricker, R. and Reiser, G. (1997) Expression and subcellular localization of p42IP4/centaurin-alpha, a brain-specific, high-affinity receptor for inositol 1,3,4,5-tetrakisphosphate and phosphatidylinositol 3,4,5-trisphosphate in rat brain. Eur J Neurosci 9, 2110-2124
427 Hanahan, D. (1983) Studies on transformation of Escherichia coli with plasmids. J Mol Biol 166, 557-580
428 Inoue, H., Nojima, H. and Okayama, H. (1990) High efficiency transformation of Escherichia coli with plasmids. Gene 96, 23-28
429 Jones, D. H., Ley, S. and Aitken, A. (1995) Isoforms of 14-3-3 protein can form homo- and heterodimers in vivo and in vitro: implications for function as adapter proteins. FEBS Lett 368, 55-58
430 Dubois, T., Zemlickova, E., Howell, S. and Aitken, A. (2003) Centaurin-alpha 1 associates in vitro and in vivo with nucleolin. Biochem Biophys Res Commun 301, 502-508
431 Nelson, M. and McClelland, M. (1992) Use of DNA methyltransferase/endonuclease enzyme combinations for megabase mapping of chromosomes. Methods Enzymol 216, 279-303
432 Bradford, M. M. (1976) A rapid and sensitive method for the quantitation of microgram quantities of protein utilizing the principle of protein-dye binding. Anal Biochem 72, 248-254
433 King, J. and Laemmli, U. K. (1971) Polypeptides of the tail fibres of bacteriophage T4. J Mol Biol 62, 465-477
434 Sambrook, J., Fritsch, E. F. and Maniatis, T. (1989) Molecular Cloning - A laboratory manual. Cold Spring Harbour Laboratory Press
435 Aitken, A. and Learmonth, M. (2002) Protein identification by in-gel digestion and mass spectrometric analysis. Mol Biotechnol 20, 95-97
436 Li, W. J., Kloetzer, W. S. and Arlinghaus, R. B. (1988) A novel 53 kDa protein complexed with P210bcr-abl in human chronic myelogenous leukemia cells. Oncogene 2, 559-566
437 Chijiwa, T., Hagiwara, M. and Hidaka, H. (1989) A newly synthesized selective casein kinase I inhibitor, N-(2-aminoethyl)-5-chloroisoquinoline-8-sulfonamide, and affinity purification of casein kinase I from bovine testis. J Biol Chem 264, 4924-4927
438 Faundez, V. V. and Kelly, R. B. (2000) The AP-3 complex required for endosomal synaptic vesicle biogenesis is associated with a casein kinase Ialpha-like isoform. Mol Biol Cell 11, 2591-2604
439 Nathalie Bouchard, R. B., Ming Li, Chris Bunker, Mike Melnik and Daniel Chelsky Ultra-Sensitive Detection of Akt Kinase Activity Using AlphaScreen™.

440 Xu, R. M., Carmel, G., Kuret, J. and Cheng, X. (1996) Structural basis for selectivity of the isoquinoline sulfonamide family of protein kinase inhibitors. Proc Natl Acad Sci U S A 93, 6308-6313
441 Michaud, G. A., Salcius, M., Zhou, F., Bangham, R., Bonin, J., Guo, H., Snyder, M., Predki, P. F. and Schweitzer, B. I. (2003) Analyzing antibody specificity with whole proteome microarrays. Nat Biotechnol 21, 1509-1512
442 Hopp, T. P. (1988) A Short Polypeptide Marker Sequence Useful for Recombinant Protein Identification and Purification. Biotechnology 6, 1204-1210
443 Kristensen, C., Wiberg, F. C. and Andersen, A. S. (1999) Specificity of insulin and insulin-like growth factor I receptors investigated using chimeric mini-receptors. Role of C-terminal of receptor alpha subunit. J Biol Chem 274, 37351-37356
444 Schafer, K. and Braun, T. (1995) Monoclonal anti-FLAG antibodies react with a new isoform of rat Mg2+ dependent protein phosphatase beta. Biochem Biophys Res Commun 207, 708-714
445 Mackie, S., Aitken, A Novel brain 14-3-3 interacting proteins involved in neurodegenerative disease. FEBS
446 Toker, A., Sellers, L. A., Amess, B., Patel, Y., Harris, A. and Aitken, A. (1992) Multiple isoforms of a protein kinase C inhibitor (KCIP-1/14-3-3) from sheep brain. Amino acid sequence of phosphorylated forms. Eur J Biochem 206, 453-461
447 Comeau, S. R., Gatchell, D. W., Vajda, S. and Camacho, C. J. (2004) ClusPro: a fully automated algorithm for protein-protein docking. Nucleic Acids Res 32, W96-99
448 Martin, H., Patel, Y., Jones, D., Howell, S., Robinson, K. and Aitken, A. (1993) Antibodies against the major brain isoforms of 14-3-3 protein. An antibody specific for the N-acetylated amino-terminus of a protein. FEBS Lett 331, 296-303
449 Zhang, J., Ma, Y., Taylor, S. S. and Tsien, R. Y. (2001) Genetically encoded reporters of protein kinase A activity reveal impact of substrate tethering. Proc Natl Acad Sci U S A 98, 14997-15002
450 Mackie, S. and Aitken, A. (2005) Novel brain 14-3-3 interacting proteins involved in neurodegenerative disease. Febs J 272, 4202-4210
451 Petosa, C., Masters, S. C., Bankston, L. A., Pohl, J., Wang, B., Fu, H. and Liddington, R. C. (1998) 14-3-3zeta binds a phosphorylated Raf peptide and an unphosphorylated peptide via its conserved amphipathic groove. J Biol Chem 273, 16305-16310
452 Agostinis, P., Pinna, L. A., Meggio, F., Marin, O., Goris, J., Vandenheede, J. R. and Merlevede, W. (1989) A synthetic peptide substrate specific for casein kinase I. FEBS Lett 259, 75-78
453 Zemlickova, E., Dubois, T., Kerai, P., Clokie, S., Cronshaw, A. D., Wakefield, R. I., Johannes, F. J. and Aitken, A. (2003) Centaurin-alpha(1) associates with and is phosphorylated by isoforms of protein kinase C. Biochem Biophys Res Commun 307, 459-465
454 Venkateswarlu, K., Brandom, K. G. and Lawrence, J. L. (2004) Centaurin-alpha1 is an in vivo phosphatidylinositol 3,4,5-trisphosphate-

dependent GTPase-activating protein for ARF6 that is involved in actin cytoskeleton organization. J Biol Chem 279, 6205-6208

455 Bustos, V. H., Marin, O., Meggio, F., Cesaro, L., Allende, C. C., Allende, J. E. and Pinna, L. A. (2005) Generation of protein kinase CK1alpha mutants which discriminate between canonical and non canonical substrates. Biochem J

456 Wolff, S., Xiao, Z., Wittau, M., Sussner, N., Stoter, M. and Knippschild, U. (2005) Interaction of casein kinase 1 delta (CK1delta) with the light chain LC2 of microtubule associated protein 1A (MAP1A). Biochim Biophys Acta

457 Tam, J. P. and Zavala, F. (1989) Multiple antigen peptide. A novel approach to increase detection sensitivity of synthetic peptides in solid-phase immunoassays. J Immunol Methods 124, 53-61

458 Biomol SA-315 pSer antibody kit. http://www.biomol.com/SiteData/docs/productdata/sa315.pdf

459 Yuan, H., Michelsen, K. and Schwappach, B. (2003) 14-3-3 dimers probe the assembly status of multimeric membrane proteins. Curr Biol 13, 638-646

460 Clokie, S. J., Cheung, K. Y., Mackie, S., Marquez, R., Peden, A. H. and Aitken, A. (2005) BCR kinase phosphorylates 14-3-3 Tau on residue 233. Febs J 272, 3767-3776

461 Vancura, A., Sessler, A., Leichus, B. and Kuret, J. (1994) A prenylation motif is required for plasma membrane localization and biochemical function of casein kinase I in budding yeast. J Biol Chem 269, 19271-19278

462 Toker, A., Ellis, C. A., Sellers, L. A. and Aitken, A. (1990) Protein kinase C inhibitor proteins. Purification from sheep brain and sequence similarity to lipocortins and 14-3-3 protein. Eur J Biochem 191, 421-429

463 Sato, S., Fujita, N. and Tsuruo, T. (2002) Regulation of kinase activity of 3-phosphoinositide-dependent protein kinase-1 by binding to 14-3-3. J Biol Chem 277, 39360-39367

464 Cheng, X., Ma, Y., Moore, M., Hemmings, B. A. and Taylor, S. S. (1998) Phosphorylation and activation of cAMP-dependent protein kinase by phosphoinositide-dependent protein kinase. Proc Natl Acad Sci U S A 95, 9849-9854

465 Xu, Y., Padiath, Q. S., Shapiro, R. E., Jones, C. R., Wu, S. C., Saigoh, N., Saigoh, K., Ptacek, L. J. and Fu, Y. H. (2005) Functional consequences of a CKIdelta mutation causing familial advanced sleep phase syndrome. Nature 434, 640-644

10. Publications

Aitken A, Baxter H, Dubois T, Clokie S, Mackie S, Mitchell K, Peden A, Zemlickova E. Specificity of 14-3-3 isoform dimer interactions and phosphorylation. Biochem Soc Trans. 2002 Aug;30(4):351-60.

Baxter HC, Fraser JR, Liu WG, Forster JL, Clokie S, Steinacker P, Otto M, Bahn E, Wiltfang J, Aitken A. Specific 14-3-3 isoform detection and immunolocalization in prion diseases. Biochem Soc Trans. 2002 Aug;30(4):387-91.

Zemlickova E, Dubois T, Kerai P, Clokie S, Cronshaw AD, Wakefield RI, Johannes FJ, Aitken A. Centaurin-alpha(1) associates with and is phosphorylated by isoforms of protein kinase C. Biochem Biophys Res Commun. 2003 Aug 1;307(3):459-65

Clokie SJ, Cheung KY, Mackie S, Marquez R, Peden AH, Aitken A. BCR kinase phosphorylates 14-3-3 Tau on residue 233. FEBS J. 2005 Aug; 272(15):3767-76.

14-3-3 Proteins in Cell Regulation

Molecular Enzymology Group Colloquium Organized and Edited by A. Aitken (Division of Biomedical and Clinical Laboratory Sciences, University of Edinburgh). 676th Meeting held at Heriot-Watt University, Edinburgh, 8–10 April 2002.

Specificity of 14-3-3 isoform dimer interactions and phosphorylation

A. Aitken[1], H. Baxter, T. Dubois, S. Clokie, S. Mackie, K. Mitchell, A. Peden and E. Zemlickova
University of Edinburgh, Division of Biomedical and Clinical Laboratory Sciences, Hugh Robson Building, George Square, Edinburgh EH8 9XD, Scotland, U.K.

Abstract

Proteins that interact with 14-3-3 isoforms are involved in regulation of the cell cycle, intracellular trafficking/targeting, signal transduction, cytoskeletal structure and transcription. Recent novel roles for 14-3-3 isoforms include nuclear trafficking the direct interaction with cruciform DNA and with a number of receptors, small G-proteins and their regulators. Recent findings also show that the mechanism of interaction is also more complex than the initial finding of the novel phosphoserine/threonine motif. Non-phosphorylated binding motifs that can also be of high affinity may show a more isoform-dependent interaction and binding of a protein through two distinct binding motifs to a dimeric 14-3-3 may also be essential for full interaction. Phosphorylation of specific 14-3-3 isoforms can also regulate interactions. In many cases, they show a distinct preference for a particular isoform(s) of 14-3-3. A specific repertoire of dimer formation may influence which of the 14-3-3-interacting proteins could be brought together. Mammalian and yeast 14-3-3 isoforms show a preference for dimerization with specific partners *in vivo*.

Introduction

The name 14-3-3 was given to an abundant mammalian brain protein family due to its particular migration pattern on two-dimensional DEAE-cellulose chromatography and starch gel electrophoresis [1]. The first function ascribed to this family of proteins was activation of tyrosine and tryptophan hydroxylases, the rate-limiting enzymes involved in catecholamine and serotonin biosynthesis, essential for the synthesis of dopamine and other neurotransmitters [2]. Subsequently we showed that 14-3-3 could regulate (inhibit) activity of protein kinase C (PKC) [3,4]. 14-3-3 was then implicated as a novel type of chaperone protein that modulates interactions between components of signal-transduction pathways [5]. A large number of publications began to appear in the mid-1990s showing that 14-3-3 proteins could interact with a range of protein kinases, phosphatases and other signalling proteins. This implied a role for the 14-3-3 family of proteins to mediate the formation of protein complexes involved in signal transduction, trafficking and secretion, perhaps to bind to different signalling proteins on each subunit of the dimer, as a novel type of 'adapter protein'. It is now clear that 14-3-3 isoforms are involved in many other cell functions and this is only one of their many roles. A number of intrinsic enzymic activities have been ascribed to 14-3-3, but none have been substantiated in the literature.

The five major mammalian brain 14-3-3 isoforms are named α–η in order of their respective elution positions on HPLC [2,6] and we showed that α and δ are the phosphoforms of β and ζ respectively [7]. Two other isoforms, τ and σ, are expressed in T-cells and epithelial cells respectively, although the former is also widely expressed in other tissues, including brain.

Muslin and co-workers [8] showed that target-protein phosphorylation is important for

Key words: phosphorylation, protein-interaction motif, signalling.
Abbreviations used: PKC, protein kinase C; AANAT, arylalkylamine N-acetyltransferase.
[1]To whom correspondence should be addressed (e-mail Alastair.Aitken@ed.ac.uk).

Table 1

14-3-3-interacting sequences in mammalian systems

pS, phosphoserine; pT, phosphothreonine; GM-CSF, granulocyte/macrophage colony-stimulating factor; TNF, tumour necrosis factor.

Target protein and motifs	Sequence	Reference
(a) Protein kinases		
Breakpoint cluster region protein (Bcr)	RSQSTPS^{303}EQ	[33]
Ca^{2+}/calmodulin-dep myosin light-chain kinase, skeletal	HSPpS^{161}CP	[35]
PCTAIRE-1, protein kinase	KRLpS^{119}LP	[38]
PKCμ (PKD)	RLpS^{205}NVS^{208}, RTSpS^{219}AELpS^{223}	[39]
PKCζ	RHDMpS^{186}YMP	[30]
c-Raf-1 kinase	RSTpS^{259}TP, RSApS^{621}EP	[40]
B-Raf	RSApS^{728}EP	[41]
Testicular protein kinase (TESK1)	RCRpS^{439}LP	[42]
Wee1 cell-cycle Y kinase	RSVpS^{642}LT	[43]
(b) Phosphatases		
PTPH1, tyrosine phosphatase	RSLpS^{359}VE, RVDpS^{853}EP	[44]
Cdc25A, cell-cycle dual-specificity phosphatase	RSPpS^{290}MP	[45]
Cdc25C, cell-cycle phosphatase	RSPpS^{216}MP	[46,47]
(c) Receptors, G-proteins and related proteins		
α-Chain of interleukin 9 receptor (IL-9R)	RpS^{519}WpT^{521}F	[48]
β-Chain of GM-CSF, interleukin-3 and -5 receptors	HSRS^{585}LP	[49]
CLIC4 (p64H1), chloride channel	R^{219}YLpTNAYpS	[50]
Exoenzyme-S, ADP-ribosylation	DALDL^{428}	[51]
GPIbα subunit of platelet membrane glycoprotein Ib-IX-V	RLpS^{166}LTDP, RYSGHSL^{610}$_{-COOH}$	[52]
Insulin growth factor I receptor	S VPLDPSASSSpS^{1283}LP	[53]
Iip35, major histocompatibility complex-associated	RSRpS^{8}CR	[54]
Insulin receptor substrate 1 (IRS-1)	RSKpS^{270}QS, HSRpS^{374}IP, KSVpS^{641}AP	[53]
Na^+/H^+ exchanger isoform-1 (NEH1)	RIGpS^{703}DP	[55]
Nicotinic acetylcholine receptor α 4 subunit	RSLS^{441}VQ	[56]
Nuclear receptor (Nur77)	RLPpS^{350}KP	[57]
Phosducin (photoreceptor G$\beta\gamma$-binding protein)	RQMpS^{54}SP, RKpS^{73}IQ	[58]
RAS effector protein RIN1	RSMpS^{351}AA	[59]

Regulators of G-protein signalling, RGS3, RGS7 (and others)	EKDpS^{496}YP, KSDpS^{434}YP	[60]
p190RhoGEF, guanine nucleotide exchange factor	I^{1370}QAIQNL	[61]
(d) Apoptosis-regulating proteins		
A20, zinc finger protein, inhibitor of TNF-induced apoptosis	RSKpS DP	[62]
Apoptosis signal-regulating kinase 1 (ASK1)	RSIpS^{967}LP	[63]
BAD, apoptosis-regulating	RHSpS^{112}YP, RSRpS^{136}AP, RRMpS^{155}DFE	[64,65]
(e) Adaptor proteins		
KSR (kinase suppressor of Ras)	RSKpS^{297}HE, RTEpS^{392}VP	[65a]
Cbl	RHpS^{619}LPFpS^{623}, RLGpS^{639}TFpS^{642}	[66]
(f) Transcription factors and nuclear proteins		
Forkhead transcription factor (FKHRL1)	RPRSCpT^{32}WP, RRRAVpS^{253}MD	[67,68]
Histone deacetylase, HDAC4	RKTApS^{246}EP, RTQpS^{467}AP, RAQpS^{632}SP	[69]
Histone deacetylase, HDAC5	RKTApS^{259}EP, RTQpS^{498}SP	[70]
Histone deacetylase, HDAC7	RKTVpS^{178}EP, RTRpS^{344}EP, RAQpS^{479}SP	[71]
Transcriptional co-activator with PDZ-binding domain (TAZ)	RSHpS^{89}SP	[72]
Nuclear factor of activated T-cells (NFAT3)	RRYpS^{272}pSpS, RRGpS^{289}	[73]
p53 tumour-suppressor/transcription factor	KGQSTpS^{378}RH/G	[10]
(g) Enzymes and others		
43 kDa inositol polyphosphate 5-phosphatase	ELVLRSESEEKVV^{371}	[74]
KIF1C, kinesin-like protein	RRQRpS^{1092}AP	[75]
Keratin 18 cytoskeletal component	RPVpSSAApS^{33}	[76]
Middle T antigen, polyoma virus	RSHpS^{257}YP	[77]
Serotonin N-acetyltransferase	RRHpT^{31}LP	[20]
Tyrosine hydroxylase	RRAVpS^{19}ELD	[78]

14-3-3 binding via a novel phosphoserine sequence motif. It has subsequently been shown that while many 14-3-3-interacting proteins contain this motif, many others do not, indicating that additional sequences and modes of interaction/contacts also allow 14-3-3 binding. Co-crystal structures with non-phosphorylated motifs suggest that the same binding pocket or 'groove' is involved [9]. Not only can phosphorylation of the motif be an important regulatory component of the interaction but dephosphorylation can also lead to creation of an interaction motif. Waterman et al. [10] showed that ionizing radiation led to dephosphorylation of Ser-376 in the sequence $KGQS^{376}TS^{378}RH/G$ in the p53 tumour-suppressor protein (see Table 1), creating a consensus binding site for 14-3-3 proteins which led to association of p53 with 14-3-3. This in turn increased the affinity of p53 for sequence-specific DNA.

14-3-3 isoforms and sequence conservation

The 14-3-3 family is highly conserved over a wide range of mammalian species, where the individual isoforms β, ε, η, γ, τ (also called θ), ζ and σ are either identical or contain a few conservative substitutions. Homologues of 14-3-3 proteins have also been found in a broad range of eukaryotic organisms and are probably ubiquitous (reviewed in [11,12]). In every organism studied, at least two isoforms of 14-3-3 have been observed.

The chromosomal location of 14-3-3 isoforms has been deduced from the human genome database. The haemopoietic ε sequence variant, ... VEL<u>D</u>VE ..., where the underlined D replaces T in this most highly conserved 14-3-3, is on chromosome 2 in the current draft genome sequence. No variants in the amino acid sequence of ε are otherwise known in any mammalian species. We have identified this haemopoietic tissue ε variant in human, ovine, bovine and rodent ε 14-3-3, in the same individual animal ([13] and A. Aitken, A. Toker and Y. Soneji, unpublished results). This form may also be present at low levels in keratinocytes. Structure analysis of the variation on the outer surface of ε 14-3-3 suggests this may have an important effect on interaction with other proteins. The most striking finding in the genome analysis is a large number of sequences matching the ζ isoform; at least nine protein translations in a number of chromosomes, most of which are presumably pseudogenes.

14-3-3 proteins are quite distinct in sequence and structural topology from other protein families in the database. Exceptions may be tertiary structure similarity with tetratricopeptide repeat ('TPR') helices [14] and primary structure similarity with α-synuclein in particular regions [15].

14-3-3 dimers, binding motifs and their interactions

Crystal structures of both the τ and ζ isoforms of 14-3-3 [16,17] show that they are highly helical, dimeric proteins. Each monomer is composed of nine anti-parallel α-helices, organized into an N-terminal and a C-terminal domain. The dimer creates a large negatively charged channel. Those regions of the 14-3-3 protein which are invariant throughout all the isoforms are mainly found lining the interior of this channel, while the variable residues are located on the surface of the protein.

This channel would recognize common features of target proteins, so the specificity of interaction of 14-3-3 isoforms with diverse target proteins may involve the outer surface of the protein. The N-terminal residues of all 14-3-3 homologues are variable, and as these residues are important for dimer formation there may be a limit to the number of possible homo- or hetero-dimer combinations. Residues involved in dimerization are 5–21 in the A-helix of one subunit and residues 58–89 of the C and D helices of the other (see Figure 1).

After the demonstration by Muslin and co-workers [8] that a novel phosphoserine-containing motif initially identified in Raf kinase was important for interaction, the motif was further refined into two subtypes and the structural details of the interaction with 14-3-3 were elucidated [18,19]. The binding site for the phosphoserine consists of a basic pocket composed of Lys-49, Arg-56 and Arg-127, as well as Tyr-128, within the C and E helices (see the underlined residues in Figure 1).

The proline residues are in different conformations in the two classes of phosphopeptide consensus motif. In the mode 1 phosphopeptide [18] the proline is in a *cis*-conformation while in the mode 2 phosphopeptide [19] the proline has a *trans*-conformation. Nevertheless, both proline conformations result in a sharp alteration in chain direction, allowing the peptide to exit the binding groove. This is also clear in the recent deter-

mination of the arylalkylamine N-acetyltransferase (AANAT)/14-3-3 co-crystal structure [20].

The ligand-binding groove runs in opposite directions in the two subunits of the dimer and a highly stable and isoform-specific interaction may result, distinct from the involvement of 14-3-3 dimer in binding two distinct target proteins together in a chaperone-like role.

Many of the 14-3-3-interacting proteins contain either one or both of two consensus motifs, R(S/Ar)(+)pSXP and RX(Ar)(+)pSXP [18] where pS is phosphoserine, Ar is an aromatic residue (particularly Tyr or Phe in mode 2) and + is a basic amino acid. Residue X following the phosphoserine is commonly Leu, Glu, Ala or Met. The phosphorylated residue may also be a threonine. Although most motifs contain Ser some well-characterized ones, e.g. AANAT, have Thr and there seem to be no structural reasons why this residue could not fit equally well into the cleft. Other motifs that are listed in Table 1 may be categorized as RSXpS motifs, $RX_{1-2}SX_{2-3}S$ motifs and non-phosphorylated motifs.

When phosphopeptide libraries were tested on six of the 14-3-3 isoforms and the yeast BMH1 and BMH2, all the isoforms were found to have very similar preferences for the individual residues within each consensus motif. There are seven mammalian isoforms of 14-3-3 that are all highly conserved and one supposes that each isoform would have a distinct function or subset of functions. For example, several isoforms of 14-3-3 are involved in the G_2/M cell-cycle checkpoint: 14-3-3 σ is responsible for sequestering the Cdc2–cyclin B1 complex in the cytoplasm, while the β and ε isoforms bind Cdc25C [21].

The complete sequence conservation in the observed ligand-binding regions of 14-3-3 would support the hypothesis that there may be little isoform specificity in the interaction between 14-3-3 and protein ligands; therefore many isoform-specific functions of 14-3-3 observed *in vivo* may result either from subcellular localization or transcriptional regulation of particular isotypes rather than from inherent differences in their ability to bind to particular ligands. However, the finding that phosphorylated 14-3-3 negatively regulates the interaction with the Raf N-terminal domain [22] suggests that additional interactions may occur on the outer surface of 14-3-3 or its dimer. A number of publications in the literature confirm recently that for full functionality in at least some cases the dimer of 14-3-3 is essential [23].

Figure 1

Human ζ 14-3-3 phosphorylation sites and motifs

The positions of the known phosphorylation sites on various isoforms are shown in large type and the phosphopeptide-binding residues are underlined. Ac denotes the N-terminus of the monomer (this is *N*-acetylmethionine, residue 1 in most isoforms). The numbering is that of the alignment of the correctly processed longer members of the family (i.e. ε and longer form of β that commence at residue 1) and the introduction of gaps of two residues maximize the alignment.

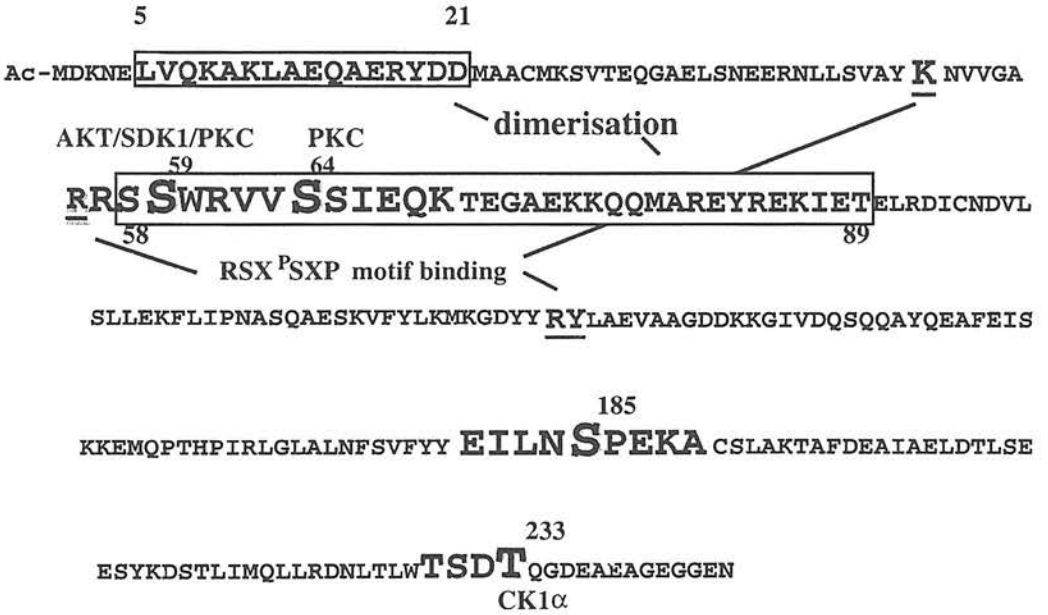

Recent findings relating to the structures and mechanism of interaction of 14-3-3 with its partners strengthen the evidence that interaction is not simply mediated by the canonical phosphoserine-containing motif. Some well-characterized interacting proteins such as Raf kinase have been shown to have additional binding site(s) for 14-3-3 on their cysteine-rich regions. Bcr and Ksr also bind via serine-rich regions. The interaction between 14-3-3 and Raf is complex and the exact role of 14-3-3 remains controversial. The fact that Raf contains a third interaction domain in the cysteine-rich region would add further complexity. This could also confer isoform specificity. It has also been suggested that due to the very common occurrence of two binding sites or motifs on one polypeptide chain of an interacting protein, the synergy between the two may also lead to isoform preference of interaction. Interaction motifs that are near the optimum, as determined by surface plasmon resonance spectroscopy [18], show no specificity but less optimal ones do. The binding of a protein in both (lower) affinity sites may greatly increase target-protein specificity of recognition and affinity. This suggests a dual site-recognition mechanism in which, for example, a 14-3-3 ζ dimer interacts with both glycoprotein I (GPI)bα (unphosphorylated motif) and GPIbβ (with a phosphorylation-dependent binding site), resulting in high-affinity binding (see Table 1).

The 14-3-3 phosphoserine-binding motif is also a common feature in plant and other eukaryotic species [24]. The plant plasma membrane H^+-ATPase motif, $QQYpT^{947}V\text{-}_{COOH}$, is noteworthy in that it has so far been found only in plant proteins [25].

Around 100 proteins have been shown to interact with 14-3-3. The well-characterized 14-3-3-interacting proteins and the motif(s) that have been identified are listed in Table 1. Some target proteins contain more than one motif that has been shown to be involved in 14-3-3 binding and they are listed only once. In many cases the actual residue numbers will be different in mammalian species other than the one(s) that were studied, although the site will be equivalent; for example, Ser-178 is the most important in mouse HDAC7. The equivalent residues in the human sequence are Ser-156, Ser-318 and Ser-446 in the motif $RAQS^{446}SP$.

In addition to those listed in Table 1, mammalian proteins that have been shown to interact include the following. (a) Protein kinases; CK1α, Chk1 kinase, MEKK1, -2 and -3, type I PKC (α,β,γ), PKCε, PKCθ and PKUα. (b) Phosphatase Cdc25B; see also (g). (c) Receptors; α2-adrenergic, γ-aminobutyric acid (GABA) (B), glucocorticoid, adrenergic, α and β oestrogen, nuclear receptor co-repressor RIP140 and small G-proteins and their regulators, Rad and Rem. (d) Proteins involved in apoptosis including α-synuclein and the neurotrophin receptor (p75NTR)-associated cell death executor NADE. (e) Adaptor/scaffolding molecules p130Cas, Grb2 and Shc (p66). (f) Transcription factors and other proteins involved in transcriptional control, TATA box-binding proteins TBP and TFIIB, histone acetyltransferase 1, Msn2p and 4p, other forkhead family members, the co-activator YAP (Yes-associated protein), myocyte enhancer binding factor 2 (MEF2D) proteins in the MADS [MCM1, AGAMOUS, DEFICIENS and SRF (where SRF is serum response factor)] box family of transcription factors, FKBP12-rapamycin-associated protein (FRAP), primary response gene BRF1, PHDfinger-HD, topoisomerase IIα, initiation factor EIF2α, integrin CD18 chain, TLX-2 homeodomain transcription factor and histones. (g) Enzymes and others including tryptophan hydroxylase, catalytic subunit (p110) of phosphoinositide 3-kinase, calmodulin, mitochondrial uncoupling protein (UCP) and CMP-NeuAc:GM1 α-2,3-sialyltransferase; structural and cytoskeletal proteins including keratin K8, Kif1C, Tau and vimentin; proteins involved in cell-cycle control including cell-cycle phosphatase Cdc25B and telomerase catalytic subunit (TERT).

14-3-3-binding motif kinases

Kinases that have been shown to phosphorylate the phosphoserine or threonine in the phosphorylated binding motifs include protein kinase B (also called Akt), cAMP-dependent protein kinase, p21-activated protein kinase 1 (PAK), Ras-mitogen-activated protein kinase (RSK1, also known as MAPKAP-K1), MAP kinase-activated protein kinase-2 (MAPKAP-K2) and PKC, as would be expected from their substrate specificity. In most cases the physiological kinases(s) have not been demonstrated but those that co-localize in the cell would be prime candidates; e.g. Cdc25C has been reported to be phosphorylated by a number of kinases such as Cds-1/Chk2, Chk1 and Cdc25C-associated kinase 1 (C-TAK1). The first two are nuclear-located. In addition, Ca^{2+}-calmodulin-dependent kinase II (CAM kinase II), p90 ribosomal S6K, protein kinase D (also known

as PKCμ) and casein kinase II (CKII) have also been implicated in phosphorylation of the motifs.

14-3-3 isoform phosphorylation

Our sequence analysis of brain 14-3-3 separated by reversed-phase HPLC failed to show any differences between α and β on the one hand and δ and ζ on the other [26]. We subsequently showed by mass spectrometric analysis that α and δ were the phosphorylated forms of β and ζ respectively and we identified the site as Ser-185 [7] using the numbering of the generic mammalian 14-3-3. The acetylation at the N-terminus of 14-3-3 isoforms, with or without removal of the initiator methionine, has been verified by mass spectrometry for all isoforms except σ [26].

β 14-3-3 is expressed at alternate start sites, 40% of which is co-translationally processed, resulting in an additional threonine residue at the N-terminus. There is no evidence that this would affect dimer formation.

This phosphorylation of Ser-185 may not 'turnover', as high levels of the phospho-forms are recovered without precautions taken to inhibit phosphatases. Although the ε and σ isoforms contain a serine residue in equivalent positions (SPDR and SPEE respectively), they are not known to be phosphorylated at this site. The ε isoform is particularly abundant in brain; therefore it would have been identified by mass spectrometric analysis when we characterized the α and δ isoforms. We have found no evidence for α and δ phospho-forms in a wide range of tissue types and cell lines other than brain. Inspection of the many two-dimensional gel electrophoretograms that are in the literature lend support to the idea that this phosphorylation may be specific to brain 14-3-3.

We identified casein kinase 1α (CKIα) as the brain kinase that phosphorylated 14-3-3 ζ and τ isoforms on Thr- and Ser-233 respectively. 14-3-3 ζ is phosphorylated on Thr-233 in HEK-293 cells [22]. Residue 233 is located within a region involved in the association of 14-3-3 with target proteins. *In vivo* phosphorylation of 14-3-3 ζ at this site negatively regulates its binding to c-Raf, and may be important in Raf-mediated signal transduction. We have also shown (S. Mackie, T. Dubois and A. Aitken, unpublished work) that CK1α binds to 14-3-3 isoforms *in vitro*.

Some isoforms of 14-3-3 have been shown to be phosphorylated by a sphingosine-dependent kinase [27] and PKB/Akt [27a]. The site these authors determined, Ser-59, is masked in the dimer interface [16]. If phosphorylation occurs, it could be a mechanism for regulation of dimer formation. However, it might be difficult under physiological conditions for a kinase to gain access, since the 14-3-3 dimer is very stable under normal conditions (see Figure 2). Our results have shown that while brain PKC did phosphorylate some 14-3-3 isoforms on an adjacent residue, Ser-64, the phosphorylation did not appear to occur to any physiologically significant extent [6], although there is an excellent motif in this region. In contrast, in our deletion mutants that exposed

Figure 2

Structure of the τ 14-3-3 dimer interface

The interface between the monomers is mainly hydrophobic, comprising 70% of the total 2150 Å^2 of inaccessible surface [16].

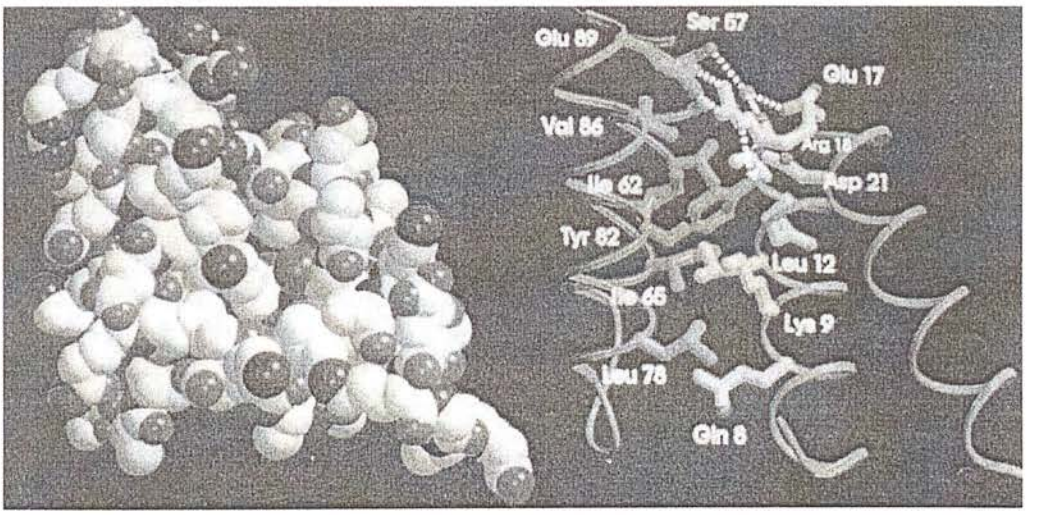

this site [28] there are very high levels of phosphorylation. We also showed that large synthetic peptides are also stoichiometrically phosphorylated at Ser-59 and there were low levels of phosphorylation at Ser-64 [29].

Van Der Hoeven et al. [30] showed that 14-3-3 β and τ were substrates for PKC-ζ (sites not determined) and Autieri and Carbone [31] showed phosphorylation of human 14-3-3 γ by PKC isoforms on undetermined site(s). However, their cDNA sequence was quite different from previous γ sequences (including that in the human genome) and included changes in residues known to be invariant.

Reuther and co-workers [32] showed that 14-3-3 τ interacted with c-Bcr and with Bcr/Abl. Their results indicated that 14-3-3 τ was a substrate for the Bcr serine/threonine kinase and was also phosphorylated on tyrosine by Brc/Abl but not by c-Abl. On attempting to identify this site(s) of phosphorylation on these and other 14-3-3 isoforms we have evidence (S. Clokie, S. Mackie and A. Aitken, unpublished work) that the phosphorylation is due to a co-immunoprecipitating kinase at a known site of phosphorylation.

Dimerization of mammalian and yeast 14-3-3 isoforms *in vivo*

In many cases, interaction between 14-3-3 and other signalling proteins shows a distinct preference for particular isoform(s) of 14-3-3. The existence of particular combinations of heterodimeric 14-3-3 isoforms *in vivo* has important implications for function as an adaptor protein in signalling. This may allow the interaction between signalling proteins that do not directly associate with each other. Bcr and Raf, for example, do not associate directly but form a complex mediated through 14-3-3 [33]. β and τ 14-3-3 associate with Bcr while the ζ and β 14-3-3 isoforms interact with Raf. We have shown that isoforms of 14-3-3 can form homo- and hetero-dimers *in vivo* and *in vitro* and a specific repertoire of dimer formation may influence which of the 14-3-3-interacting proteins could in turn be brought together [34]. Since the residues involved in dimerization exhibit some isoform variation, this may limit the possible homo- or hetero-dimer combinations and may confer specificity on 14-3-3 function.

The dimers of 14-3-3 are stable and do not readily exchange unless they are denatured and renatured [34]. It should be noted that a single recombinant 14-3-3 isoform will form homodimers regardless of the actual preference *in vivo* since a monomeric form would be thermodynamically unstable. 14-3-3 proteins also have a slow rate of turnover.

We analysed the pattern of dimer formation for two of the most abundant isoforms of 14-3-3 ε and γ, following their stable expression in the neuronal pheochromocytoma PC12 cell line (M. Chaudhri and A. Aitken, unpublished work). This revealed a distinct preference for particular dimer combinations that is largely independent of cellular conditions. γ 14-3-3 formed homo- and hetero-dimers, mainly with ε. In turn, the ε isoform formed heterodimers with all the 14-3-3 isoforms tested (β, η, γ and ζ), but no homodimers were detected. This suggests that the observed dimer combinations may be due to structural properties of the dimer interface of the individual isoforms. This pattern may be generally applicable since the dimerization patterns of γ and ε isoforms in transiently transfected COS cells were also similar overall. The pattern of dimer formation was not simply a reflection of the amounts of available 14-3-3 isoform present in the cell or in a particular subcellular location. Analysis of the two 14-3-3 homologues, BMH1 and BMH2, from the budding yeast *Saccharomyces cerevisiae* also revealed that between 65 and 80 % are heterodimers (M. Chaudhri and A. Aitken, unpublished work).

Homo- and hetero-dimers of 14-3-3 proteins may play different roles. It is possible that homodimers of a particular isoform will function to sequester or chaperone a protein, while heterodimers are more likely to act as adaptor proteins, modulating the interaction of two distinct proteins, each of which specifically associates with one of the isoforms of the heterodimer. The γ isoform may be more involved in sequestration functions, while the ε isoform is more likely to function as an adaptor protein in signal-transduction events. Indeed, γ 14-3-3 has been found to be the major isoform in Golgi and is implicated in secretion and protein trafficking while the ε isoform is more generally found in association with proteins involved in signal transduction.

In conclusion, association with 14-3-3 isoforms has led to the activation or stabilization of some proteins, and the inactivation of others, while for many proteins 14-3-3 isoforms have played an organizational role as a 'scaffold'. In the complex multistep process of Raf activation, 14-3-3 appears to play several of these roles. It is likely that its ability to form homo- and various heterodimeric combinations is crucial and the analysis of the exact combinations of homo- and hetero-dimers of

14-3-3 isoforms that are present within cell compartment(s) and that are involved in interactions with particular proteins will be important.

The work in the authors' laboratory was supported by the Medical Research Council.

References

1 Moore, B. E. and Perez, V. J. (1967) in Physiological and Biochemical Aspects of Nervous Integration (Carlson, F. D., ed.), pp. 343–359, Prentice-Hall Englewood Cliffs, NJ
2 Ichimura, T., Isobe, T., Okuyama, T., Takahashi, N., Araki, K., Kuwano, R. and Takahashi, Y. (1988) Proc. Natl. Acad. Sci. U.S.A. **85**, 7084–7088
3 Aitken, A., Ellis, C. A., Harris, A., Sellers, L. A. and Toker, A. (1990) Nature (London) **344**, 594
4 Toker, A., Ellis, C. A., Sellers, L. A. and Aitken, A. (1990) Eur. J. Biochem. **191**, 421–429
5 Aitken, A. (1996) Trends Cell Biol. **6**, 341–347
6 Toker, A., Sellers, L. A., Amess, B., Patel, Y., Harris, A. and Aitken, A. (1992) Eur. J. Biochem. **206**, 453–461
7 Aitken, A., Howell, S., Jones, D., Madrazo, J. and Patel, Y. (1995) J. Biol. Chem. **270**, 5706–5709
8 Muslin, A. J., Tanner, J. W., Allen, P. M. and Shaw, A. S. (1996) Cell **84**, 889–898
9 Fu, H., Subramanian, R. R. and Masters, S. C. (2000) Annu. Rev. Pharmacol. Toxicol. **40**, 617–647
10 Waterman, M. J., Stavridi, E. S., Waterman, J. L. and Halazonetis, T. D. (1998) Nat. Genet. **19**, 175–178
11 Wang, W. and Shakes, D. C. (1996) J. Mol. Evol. **43**, 384–398
12 Rosenquist, M., Sehnke, P., Ferl, R. J., Sommarin, M. and Larsson, C. (2000) J. Mol. Evol. **51**, 446–458
13 Pietromonaco, S. F., Seluja, G. A., Aitken, A. and Elias, L. (1996) Blood Cells Molecules Dis. **22**, 225–237
14 Das, A. K., Cohen, P. W. and Barford, D. (1998) EMBO J. **17**, 1192–1199
15 Ostrerova, N., Petrucelli, L., Farrer, M., Mehta, N., Choi, P., Hardy, J. and Wolozin, B. (1999) J. Neurosci. **19**, 5782–5791
16 Xiao, B., Smerdon, S. J., Jones, D. H., Dodson, G. G., Soneji, Y., Aitken, A. and Gamblin, S. J. (1995) Nature (London) **376**, 188–191
17 Liu, D., Bienkowska, J., Petosa, C., Collier, R. J., Fu, H. and Liddington, R. (1995) Nature (London) **376**, 191–194
18 Yaffe, M. B., Rittinger, K., Volinia, S., Caron, P. R., Aitken, A., Leffers, H., Gamblin, S. J., Smerdon, S. J. and Cantley, L. C. (1997) Cell **91**, 961–971
19 Rittinger, K., Budman, J., Xu, J., Volinia, S., Cantley, L. C., Smerdon, S. J., Gamblin, S. J. and Yaffe, M. B. (1999) Mol. Cell **4**, 153–166
20 Ganguly, S., Gastel, J. A., Weller, J. L., Schwartz, C., Jaffe, H., Namboodiri, M. A., Coon, S. L., Hickman, A. B., Rollag, M., Obsil, T. et al. (2001) Proc. Natl. Acad. Sci. U.S.A. **98**, 8083–8088
21 Zeng, Y., Forbes, K. C., Wu, Z., Moreno, S., Piwnica-Worms, H. and Enoch, T. (1998) Nature (London) **395**, 507–510
22 Dubois, T., Rommel, C., Howell, S., Steinhusen, U., Soneji, Y., Moelling, K. and Aitken, A. (1997) J. Biol. Chem. **272**, 28882–28888
23 Tzivion, G. and Avruch, J. (2002) J. Biol. Chem. **277**, 3061–3064
24 Moorhead, G., Douglas, P., Cotelle, V., Harthill, J., Morrice, N., Meek, S., Deiting, U., Stitt, M., Scarabel, M., Aitken, A. and MacKintosh, C. (1999) Plant J. **18**, 1–12
25 Svennelid, F., Olsson, A., Piotrowski, M., Rosenquist, M., Ottman, C., Larsson, C., Oecking, C. and Sommarin, M. (1999) Plant Cell. **11**, 2379–2391
26 Martin, H., Patel, Y., Jones, D., Howell, S., Robinson, K. and Aitken, A. (1993) FEBS Lett. **331**, 296–303
27 Megidish, T., Cooper, J., Zhang, L., Fu, H. and Hakomori, S. (1998) J. Biol. Chem **273**, 21834–21845
27a Powell, D. W., Rane, M. J., Chen, Q., Singh, S. and McLeish, K. R. (2002) J. Biol. Chem **277**, 21639–21642
28 Jones, D., Martin, H., Madrazo, J., Robinson, K., Nielsen, P., Roseboom, P., Patel, Y., Howell, S. and Aitken, A. (1995) J. Mol. Biol. **245**, 375–384
29 Dubois, T., Howell, S., Amess, R., Kerai, P., Learmonth, M. P., Madrazo, J., Chaudhri, M., Rittinger, K., Scarabel, M., Soneji, Y. and Aitken, A. (1997) J. Prot. Chem. **16**, 513–522
30 Van Der Hoeven, P. C., Van Der Wal, J. C., Ruurs, P. and VanBlitterswijk, J. (2000) Biochem. J. **347**, 781–785
31 Autieri, M. V. and Carbone, C. J. (1999) DNA Cell Biol. **18**, 555–564
32 Reuther, G. W., Fu, H., Cripe, L. D., Collier, R. J. and Pendergast, A. M. (1994) Science **266**, 129–133
33 Braselmann, S. and McCormick, F. (1995) EMBO J. **14**, 4839–4848
34 Jones, D., Ley, S. and Aitken, A. (1995) FEBS Lett. **368**, 55–58
35 Haydon, C. E., Watt, P. W., Morrice, N., Knebel, A., Gaestel, M. and Cohen, P. (2002) Arch. Biochem. Biophys. **397**, 224–231
36 Reference deleted
37 Reference deleted
38 Graeser, R., Gannon, J., Poon, R., Dubois, T., Aitken, A. and Hunt, T. J. (2002) J. Cell Sci., in the press
39 Hausser, A., Storz, P., Link, G., Stoll, H., Liu, Y. C., Altman, A., Pfizenmaier, K. and Johannes, F. J. (1999) J. Biol. Chem. **274**, 9258–9264
40 Michaud, N. R., Fabian, J. R., Mathes, K. D. and Morrison, D. K. (1995) Mol. Cell. Biol. **15**, 3390–3397
41 MacNicol, M. C., Muslin, A. J. and MacNicol, A. M. (2000) J. Biol. Chem. **275**, 3803–3809
42 Toshima, J. Y., Toshima, J., Watanabe, T. and Mizuno, K. (2001) J. Biol. Chem. **276**, 43471–43481
43 Honda, R., Ohba, Y. and Yasuda, H. (1997) Biochem. Biophys. Res. Commun. **230**, 262–265
44 Zhang, S. H., Kobayashi, R., Graves, P. R., Piwnica-Worms, H. and Tonks, N. K. (1997) J. Biol. Chem. **272**, 27281–27287
45 Conklin, D. S., Galaktionov, K. and Beach, D. (1995) Proc. Natl. Acad. Sci. U.S.A. **92**, 7892–7896
46 Dalal, S. N., Schweitzer, C. M., Gan, J. and DeCaprio, J. A. (1999) Mol. Cell. Biol. **19**, 4465–4479
47 Peng, C. Y., Graves, P. R., Ogg, S., Thoma, R. S., Byrnes, 3rd, M. J., Wu, Z., Stephenson, M. T. and Piwnica-Worms, H. (1998) Cell Death Differ. **19**, 197–208
48 Sliva, D., Gu, M., Zhu, Y. X., Chen, J., Tsai, S., Du, X. and Yang, Y. C. (2000) Biochem. J. **345**, 741–747
49 Stomski, F. C., Dottore, M., Winnall, W., Guthridge, M. A., Woodcock, J., Bagley, C. J., Thomas, D. T., Andrews, R. K., Berndt, M. C. and Lopez, A. F. (1999) Blood **94**, 1933–1942

50 Suginta, W., Karoulias, N., Aitken, A. and Ashley, R. H. (2001) Biochem. J. **359**, 55–64
51 Henriksson, M. L., Troller, U. and Hallberg, B. (2000) Biochem. J. **349**, 697–701
52 Andrews, R. K., Harris, S. J., McNally, T. and Berndt, M. C. (1998) Biochemistry **37**, 638–647
53 Craparo, A., Freund, R. and Gustafson, T. A. (1997) J. Biol. Chem. **272**, 11663–11669
54 Kuwana, T., Peterson, P. A. and Karlsson, L. (1998) Proc. Natl. Acad. Sci. U.S.A **95**, 1056–1061
55 Lehoux, S., Ji, A., Florian, J. A. and Berk, B. C. (2001) J. Biol. Chem. **276**, 15794–15800
56 Jeanclos, E. M., Lin, L., Treuil, M. W., Rao, J., DeCoster, M. A. and Anand, R. (2001) J. Biol. Chem. **276**, 28281–28290
57 Masuyama, N., Oishi, K., Mori, Y., Ueno, T., Takahama, Y. and Gotoh, Y. (2001) J. Biol. Chem. **276**, 32799–32805
58 Thulin, C. D., Savage, J. R., McLaughlin, J. N., Truscott, S. M., Old, W. M., Ahn, N. G., Resing, K. A., Hamm, H. E., Bitensky, M. W. and Willardson, B. M. (2001) J. Biol. Chem. **276**, 23805–23815
59 Wang, Y., Waldron, R. T., Dhaka, A., Patel, A., Riley, M. M., Rozengurt, E. and Colicelli, J. (2002) Mol. Cell. Biol. **22**, 916–926
60 Benzing, T., Yaffe, M. B., Arnould, T., Sellin, L., Schermer, B., Schilling, B., Schreiber, R., Kunzelmann, K., Leparc, G. G., Kim, E. and Walz, G. (2000) J. Biol. Chem. **275**, 28167–28172
61 Zhai, J., Lin, H., Shamim, M., Schlaepfer, W. W. and Canete-Soler, R. (2001) J. Biol. Chem. **276**, 41318–41324
62 Vincenz, C. and Dixit, V. M. (1996) J. Biol. Chem. **271**, 20029–20034
63 Zhang, L., Chen, J. and Fu, H. (1999) Proc. Natl. Acad. Sci. U.S.A. **96**, 8511–8515
64 Fang, X., Yu, S., Eder, A., Mao, M., Bast, Jr, R. C., Boyd, D. and Mills, G. B. (1999) Oncogene **18**, 6635–6640
65 Lizcano, J. M., Morrice, N. and Cohen, P. (2000) Biochem. J. **349**, 547–557
65a Cacace, A. M., Michaud, N. R., Therrien, M., Mathes, K., Copeland, T., Rubin, G. M. and Morrison, D. K. (1999) Mol. Cell. Biol. **19**, 229–240
66 Liu, Y. C., Liu, Y., Elly, C., Yoshida, H., Lipkowitz, S. and Altman, A. (1997) J. Biol. Chem. **272**, 9979–9985
67 Brunet, A., Bonni, A., Zigmond, M. J., Lin, M. Z., Juo, P., Hu, L. S., Anderson, M. J., Arden, K. C., Blenis, J. and Greenberg, M. E. (1999) Cell **96**, 857–868
68 Rena, G., Prescott, A. R., Guo, S., Cohen, P. and Unterman, T. G. (2001) Biochem. J. **354**, 605–612
69 Wang, A. H., Kruhlak, M. J., Wu, J., Bertos, N. R., Vezmar, M., Posner, B. I., Bazett-Jones, D. P. and Yang, X. J. (2000) Mol. Cell. Biol. **20**, 6904–6912
70 McKinsey, T. A., Zhang, C. L. and Olson, E. N. (2000) Proc. Natl. Acad. Sci. U.S.A. **97**, 14400–14405
71 Kanai, F., Marignani, P. A., Sarbassova, D., Yagi, R., Hall, R. A., Donowitz, M., Hisaminato, A., Fujiwara, T., Ito, Y., Cantley, L. C. and Yaffe, M. B. (2000) EMBO J. **19**, 6778–6791
72 Kao, H. Y., Verdel, A., Tsai, C. C., Simon, C., Juguilon, H. and Khochbin, S. (2001) J. Biol. Chem. **276**, 47496–47507
73 Chow, C. W. and Davis, R. J. (2000) Mol. Cell. Biol. **20** 702–712
74 Campbell, J. K., Gurung, R., Romero, S., Speed, C. J., Andrews, R. K., Berndt, M. C. and Mitchell, C. A. (1997) Biochemistry **36**, 15363–15370
75 Dorner, C., Ullrich, A., Haring, H. U. and Lammers, R. (1999) J. Biol. Chem. **274**, 33654–33660
76 Ku, N. O., Liao, J. and Omary, M. B. (1998) EMBO J. **17**, 1892–1906
77 Cullere, X., Rose, P., Thathamangalam, U., Chatterjee, A., Mullane, K. P., Pallas, D. C., Benjamin, T. L., Roberts, T. M. and Schaffhausen, B. S. (1998) J. Virol. **72**, 558–563
78 Itagaki, C., Isobe, T., Taoka, M., Natsume, T., Nomura, N., Horigome, T., Omata, S., Ichinose, H., Nagatsu, T., Greene, L. A. and Ichimura, T. (1999) Biochemistry **38**, 15673–15680

Received 10 April 2002

Survival-promoting functions of 14-3-3 proteins

S. C. Masters, R. R. Subramanian, A. Truong, H. Yang, K. Fujii, H. Zhang and H. Fu[1]
Department of Pharmacology, Emory University School of Medicine, 1510 Clifton Road, Atlanta, GA 30322, U.S.A.

Abstract

The 14-3-3 proteins are a family of phosphoserine/phosphothreonine-binding molecules that control the function of a wide array of cellular proteins. We suggest that one function of 14-3-3 is to support cell survival. 14-3-3 proteins promote survival in part by antagonizing the activity of associated proapoptotic proteins, including Bad and apoptosis signal-regulating kinase 1 (ASK1). Indeed, expression of 14-3-3 inhibitor peptides in cells is sufficient to induce apoptosis. Interestingly, these 14-3-3 antagonist peptides can sensitize cells for effective killing by anticancer agents such as cisplatin. Thus, 14-3-3 may be part of the cellular machinery that maintains cell survival, and targeting 14-3-3–ligand interactions may be a useful strategy to enhance the efficacy of conventional anticancer agents.

Key words: apoptosis, ASK1, Bad, difopein.
Abbreviations used: PKB, protein kinase B; ASK1, apoptosis signal-regulating kinase 1; EYFP, enhanced yellow fluorescent protein.
[1]To whom correspondence should be addressed (e-mail hfu@emory.edu).

Introduction

14-3-3 proteins can bind a variety of proteins that are critical mediators of intracellular signalling

Specific 14-3-3 isoform detection and immunolocalization in prion diseases

H. C. Baxter*[1], J. R. Fraser†, W.-G. Liu†, J. L. Forster*, S. Clokie*, P. Steinacker‡, M. Otto‡, E. Bahn‡, J. Wiltfang‡ and A. Aitken*

*Department of Biomedical Sciences, University of Edinburgh, George Square, Edinburgh EH8 9XD, U.K., †Institute for Animal Health, Neuropathogenesis Unit, Edinburgh EH9 3JF, U.K., and ‡Departments of Neurology, Neuropathology and Psychiatry, University of Gottingen, D-37075, Gottingen, Germany

Abstract

14-3-3 proteins are involved in signalling processes in neuronal cells. Using isoform-specific antibodies we have examined the variation in 14-3-3 isoform neurolocation in normal and scrapie-infected murine brain and show that in defined areas of the brain there are significant changes associated with the pathology of the disease process. The appearance of 14-3-3 proteins in the cerebrospinal fluid (CSF) is a consequence of neuronal disease and the detection of specific isoforms of the 14-3-3 proteins in the CSF is characteristic of some neurodegenerative diseases. In this study, monitoring specifically for the γ 14-3-3 isoform in the CSF by both Western-blot analysis and ELISA we can show a level of correlation between the assays.

Introduction

Transmissible spongiform encephalopathies are a group of diseases which affect both humans and animals. These are commonly called prion diseases [1] and include the human diseases sporadic Creutzfeldt–Jakob disease (CJD), variant CJD and iatrogenic CJD and the animal diseases bovine spongiform encephalopathy (BSE) and natural scrapie in sheep [2]. All of these involve rapid neurodegeneration and are invariably fatal. Definitive diagnosis of prion diseases is currently only carried out post-mortem by neurohistopathological examination for the detection of abnormal form of the prion protein.

Concern over the link between BSE and variant CJD and the requirement for early or pre-mortem diagnosis of CJD has resulted in the evaluation of a number of proteins identified in the cerebrospinal fluid (CSF) of patients with neurodegenerative diseases for uses as surrogate markers. These include 14-3-3 proteins [3,4], neuron-specific enolase [5], S100β [6] and Tau protein [7], and of these proteins 14-3-3 has the highest specificity. At present only Western-blot analysis of 14-3-3 has been advanced by the World Health Organization as a pre-mortem biochemical indicator to aid early diagnosis of clinically characterized sporadic CJD.

The 14-3-3 proteins are a highly conserved family of multifunctional proteins that are primarily found in high levels in neurons but which are expressed in a wide range of other cells and tissues. 14-3-3 proteins have a typical monomeric molecular mass of approx. 30 kDa and have been shown to form homo- and hetero-dimeric structures which complex with other proteins. There are seven distinct isoforms (β, γ, ε, ζ, τ, η and σ), named from their reversed-phase HPLC elution profile [8]. The β and ζ forms have also been isolated as phosphorylated forms, which are named α and δ respectively [9]. Multiple isoforms of 14-3-3 have been shown to interact with distinct regulatory proteins of the signalling, regulatory and apoptotic pathways [10]. Many of these protein–protein interactions have been shown to be modulated by phosphorylation of the interacting 14-3-3 partner [11,12]. This is exemplified in the regulation of the Bcl-2 apoptotic pathway; here sequestration of phosphorylated BAD (Bcl-2-associated death promoter) in the cytosol by 14-3-3 proteins results in inhibition of the pro-apoptotic action of BAD [13].

Early immunohistochemical studies of the human brain showed that the 14-3-3 proteins are predominantly localized in neuronal cells [14]. Gene expression studies have shown that the ε, γ, η, β and ζ isoforms are expressed in neuronal cells in the grey matter area of the brain, including the hippocampus, thalamus and the cerebellar cortex [15,16], but that the τ isoform (also known as θ) is also expressed in white matter areas of the brain [17]. Characterization of the subcellular location of 14-3-3 [18] had shown the ε, γ, η, β and ζ isoforms to be present in synaptic vesicle mem-

Key words: CSF, ELISA, immunocytochemistry, neurodegeneration.

Abbreviations used: BAD, Bcl-2-associated death promoter; BSE, bovine spongiform encephalopathy; CSF, cerebrospinal fluid; CJD, sporadic Creutzfeldt–Jakob disease; LGN, lateral geniculate nucleus.

[1]To whom correspondence should be addressed (e-mail hbaxter@ed.ac.uk).

branes whereas η, ε and γ isoforms are located at the synaptic junction and that the ε isoform binds to the synaptic plasma membrane through its N-terminal domain [19].

Using two-dimensional analysis an increase of the levels of the ε and η isoforms has been shown in the cortical region of the brain in both Alzheimer's disease and Down's syndrome [20].

Studies on the immunolocalization of 14-3-3 isoforms in neurodegenerative brain disease has shown 14-3-3 to co-localize with neurofibrillary tangles in the brain of patients with Alzheimer's disease [21] and in the Lewy bodies in Parkinson's disease and in Diffuse Lewy Body disease [22].

Immunocytochemistry

In a comparative analysis of the neurolocation of the individual 14-3-3 isoforms in normal and scrapie-infected murine brain we have shown that in areas where severe pathological changes occur there are distinct changes in the isoform labelling [23]. This is clearly shown in the hippocampus and in the thalmus. In the hippocampus there is a loss of labelling of the τ isoform and the number of pyrimidal cell bodies in the CA1 decreases with a corresponding loss of labelling of the β, η, γ and ζ isoforms (Figure 1), yet in the molecular layer of the dentate gyrus there is a significant increase in the intensity of labelling. In the lateral geniculate nucleus (LGN) of the thalmus we observe a marked decrease in the isoform labelling in the dorsal LGN but this is not observed in the ventral LGN. As the 14-3-3 isoform labelling in the central nervous system in terminal scrapie is lost in some areas, but increases in others, this would suggest that the processing of these proteins during neurodegeneration may be much more complex than previously recognized.

Although the pathogenic role of the 14-3-3 isoforms in the prion diseases is unknown these proteins do modulate the apoptotic pathway by interaction with the Bcl-2 complex and by inhibiting the pro-apoptotic action of BAD.

Since changes in distribution pattern of various 14-3-3 isoforms is provoked by transmissible spongiform encephalopathy infection it is of intrinsic importance to determine the fate of these proteins in the disease process.

CSF

As 14-3-3 proteins are not normally detected in the CSF the appearance of small quantities of specific 14-3-3 isoforms in the CSF during the disease processes tends to suggest that the pathway from neuron to CSF may be isoform-specific. Here it is of importance to note that of the six isoforms, β, γ, ε, ζ, τ and η, that are normally found in the brain, only four of these, the β, γ, ε and η isoforms, are present in the CSF of patients with sporadic CJD [24,25]. It is also noteworthy that the only isoform consistently observed in the CSF of patients with Alzheimer's disease is the η isoform [24] and that the ζ 14-3-3 isoform is not typically found in the CSF in either of these diseases. Currently the World Health Organization protocol for the use of 14-3-3 proteins as surrogate markers in CSF of sporadic CJD patients uses Western-blot analysis, which is not isoform-specific.

Figure 1

Immunolabelling of β14-3-3 isoform

β-Labelling of the cell bodies of pyramidal cells in CA1 hippocampus (**a**) in normal brain and (**b**) in ME7 scrapie-infected murine brain. Scale bar, 100 μm.

Western analysis

Of the β, ε, γ and η 14-3-3 isoforms typically identified in the CSF of patients with sporadic CJD the γ isoform appears to be the most abundant. Figure 2(A) shows specific detection of the γ 14-3-3 isoform in the CSF of sporadic CJD patients after treatment by SDS/PAGE followed by Western-blot analysis. The SDS gels were blotted and probed for the presence of the γ isoform using a polyclonal antibody raised to a 14-3-3 γ N-terminal peptide and the bands were semi-quantitatively classified into five groups according to the strength of the signal. Clearly there is a distinct difference in the levels of the individual isoforms found in the CSF after the onset of sporadic CJD (see Figure 2B).

Figure 2

Western-blot analysis of CSF from CJD patients using 14-3-3 isoform-specific antisera

(A) A standard mixture of 14-3-3 isoforms isolated from sheep brain and CSF samples from patients 2 and 4 were analysed using γ, ε, η and β 14-3-3 isoform-specific antisera. (B) CSF samples from CJD patients 1–4 were analysed using γ 14-3-3 isoform-specific antisera with the following scoring regime: −, no detectable signal; +, very faint signal; ++, faint signal; +++, moderate signal; ++++, strong signal.

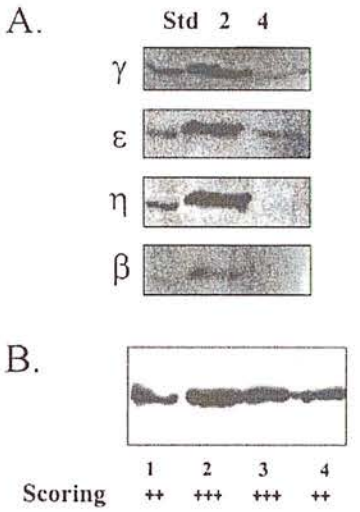

ELISA

In developing our present ELISA procedures the capture antibody used was a monoclonal antibody raised against a heterogeneous 14-3-3 peptide. The detecting antibody used is a biotinylated form of the polyclonal anti-γ 14-3-3 antibody used in the Western analysis, followed by streptavidin–horseradish peroxidase-conjugated secondary antibody and tetramethybenzidine peroxide substrate. The absorbance was measured at 450 nm. The standard mixture of 14-3-3 isoforms used in the study was isolated from sheep brain and the isoform ratio in this mixture was quantified by calibration of the isoform HPLC profile using purified γ 14-3-3 protein as a standard. The

Figure 3

(**A**) Two-site ELISA for γ 14-3-3 and (**B**) correlation between Western-blotting and ELISA γ14-3-3 isoform-specific analysis of CSF from CJD patients and patients with multiple sclerosis

A

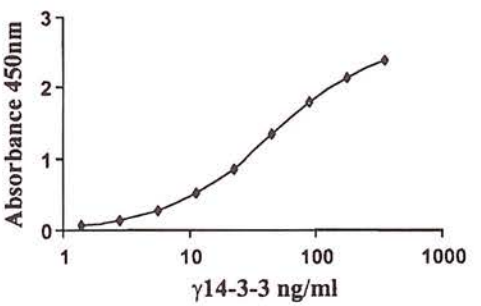

B

CSF Samples	Western scoring analysis from figure 2	Elisa for γ 14-3-3
CJD 1	++ (lane 1)	30 ng/ml
CJD 2	+++ (lane 2)	122 ng/ml
CJD 3	+++ (lane 3)	144 ng/ml
CJD 4	++ (lane 4)	20 ng/ml
CJD 5	+ (data not shown)	7 ng/ml
MS 1-5	not tested	below the detectable level.

coefficients of variation for the within-batch and between-batch precision of the assay were 25% and 13% respectively. Our current ELISA protocol has a working range of 10–100 ng/ml. A typical standard curve is shown in Figure 3(A).

Testing of CSF samples from patients with neurodegenerative diseases

The CSF samples contain dimeric 14-3-3 proteins complexed with other interacting proteins. In this heterogeneous mixture the 14-3-3 proteins are not as readily detectable by ELISA as by Western-blot analysis and for this reason all of the protein samples were concentrated (× 5) and heat-treated before being assayed.

In our preliminary studies the ELISA protocol was used to determine the levels of γ 14-3-3 in the CSF of patients with two neurological disorders: (a) from patients with sporadic CJD and (b) from patients with multiple sclerosis. Elevated levels of 14-3-3 in the CSF of multiple sclerosis patients has previously been reported by Sathoh et al. [26].

As shown in Figure 2(B), each of the CJD patients tested by ELISA recorded positive for γ 14-3-3 with good correlation between the scoring analysis from Western blotting and the differential levels of 14-3-3 recorded by the ELISA. In contrast, the multiple sclerosis samples tested were all below the detectable limit for the γ 14-3-3 protein. However, it may be that the CSF of multiple sclerosis patients contains other isoforms of 14-3-3 protein.

Conclusion

Kenney et al. [27] have shown the total 14-3-3 protein content present in the CSF of sporadic CJD patients during neurodegeneration to be in the ng/ml range. If the appearance of small quantities of specific 14-3-3 isoforms in the CSF is consistent with the loss of neurons in neurodegenerative conditions, then the variation in the pattern of isoforms suggests that control of the pathway from neuron to CSF may be isoform-specific.

While our analysis indicates that at present the Western-blot analysis of 14-3-3 in CSF is more sensitive than the current ELISA, the positive correlation between the assays indicates that development of an isoform-specific ELISA using adaptations of the method is valid. The optimization of selectivity and sensitivity of our ELISA protocol is in progress.

References

1 Prusiner, S. B. (1982) Science **216**, 136–144
2 Wells, G. A., Scott, A. C., Johnson, C. T., Gunning, R. F., Hancock, R. D., Jeffrey, M., Dawson, M. and Bradley, R. (1987) Vet. Rec. **121**, 419–420
3 Hsich, G., Kenney, K., Gibbs, C. J., Lee, K. H. and Harrington, M. G. (1996) N. Engl. J. Med. **335**, 924–930
4 Lee, K. H. and Harrington, M. G. (1997) Electrophoresis **18**, 502–506
5 Zerr, I., Bodemer, M., Racker, S., Grossche, S., Poser, S., Kretzschmar, H. A. and Weber, T. (1995) Lancet **345**, 1609–1610
6 Otto, M., Stein, H., Szudra, A., Zerr, I., Bodemer, M., Gefeller, O., Poser, S., Kretzschmar, H. A., Mader, M. and Weber, T. (1997) J. Neurol. **244**, 566–570
7 Otto, M., Wiltfang, J., Tumani, H., Zerr, I., Lantsch, M., Kornhuber, J., Weber, T., Kretzschmar, H. A. and Poser, S. (1997) Neurosci. Lett. **225**, 210–212
8 Ichimura, T., Isobe, T., Okuyama, T., Takahashi, N., Araki, K., Kuwano, R. and Takahashi, Y. (1989) Proc. Natl. Acad. Sci. U.S.A. **85**, 7084–7088
9 Aitken, A., Howell, S., Jones, D., Madrazo, J. and Patel, Y. (1995) J. Biol. Chem. **270**, 5706–5709
10 Aitken, A. (1996). Trends Cell Biol. **6**, 341–347
11 Muslin, A. J., Tanner, J. W., Allen, P. M. and Shaw, A. S. (1996) Cell **84**, 889–897
12 Yaffe, M. B., Rittinger, K., Volinia, S., Caron, P. R., Aitken, A., Leffers, H., Gambin, S. J., Smerdon, S. J. and Cantley, L. C. (1997) Cell **91**, 961–971
13 Zha, J., Harada, H., Yang, E., Jockel, J. and Korsmeyer, S. J. (1996) Cell **87**, 619–628
14 Isobe, T., Ichimura, T. and Okuyama, T. (1989) Arch. Histol. Cytol. **52** (Suppl.), 25–32
15 Watanabe, M., Isobe, T., Ichimura, T., Kuwano, R., Takahashi, Y. and Kondo, H. (1993) Brain Res. Dev. Brain Res. **73**, 225–235
16 Watanabe, M., Isobe, T., Ichimura, T., Kuwano, R., Takahashi, Y., Kondo, H. and Inoue, Y. (1994) Brain Res. Mol. Brain Res. **25**, 113–121
17 Watanabe, M., Isobe, T., Okuyama, T., Ichimura, T., Kuwano, R., Takahashi, Y. and Kondo, H. (1991) Brain Res. Mol. Brain Res. **10**, 151–158
18 Martin, H., Rostas, J., Patel, Y. and Aitken, A. (1994) J. Neurochem. **63**, 2259–2265
19 Jones, D. H., Martin, H., Madrazo, J., Robinson, K. A., Nielsen, P., Roseboom, P. H., Patel, Y., Howell, S. A. and Aitken, A. (1995) J. Mol. Biol. **245**, 375–384
20 Fountoulakis, M., Cairns, N. and Lubec, G. (1999) J. Neural. Transm. Suppl. **57**, 323–335
21 Layfield, R., Fergusson, J., Aitken, A., Lowe, J., Landon, M. and Mayer, R. J. (1996) Neurosci. Lett. **209**, 57–60
22 Kawamoto, Y., Akiguchi, I., Nakamura, S., Honjyo, Y., Shibasaki, H. and Budka, H. (2002) J. Neuropathol. Exp. Neurol. **61**, 245–253
23 Baxter, H. C., Liu, W. G., Forster, J. L., Aitken, A. and Fraser, J. R. (2002) Neuroscience **109**, 5–14

24 Wiltfang, J., Otto, M., Baxter, H. C., Bodemer, M., Steinacker, P., Bahn, E., Zerr, I., Kornhuber, J., Kretzschmar, H. A., Poser, S. et al. (1999) J. Neurochem. **73**, 2485–2490
25 Takahashi, H., Iwata, T., Kitagawa, Y., Takahashi, R. H., Sato, Y., Wakabayashi, H., Takashima, M., Kido, H., Nagashima, K., Kenney, K. et al. (1999). Clin. Diagn. Lab. Immunol. **6**, 983–985
26 Sathoh, J., Kurohara, K., Yukitake, M. and Kuroda, Y. (1999) Eur. Neurol. **41**, 216–225
27 Kenney, K., Brichetel, C., Takchashi, H., Kurohara, K., Anderson, P. and Gibbs, C. J. (2000) Ann. Neurol. **48**, 395–398

Received 10 April 2002

Effect of multiple phosphorylation events on the transcription factors FKHR, FKHRL1 and AFX

Y. L. Woods[1] and G. Rena[2]
MRC Protein Phosphorylation Unit, School of Life Sciences, MSI/WTB Complex, University of Dundee, Dow Street, Dundee DD1 5EH, Scotland, U.K.

Abstract

The insulin-stimulated phosphoinositide 3-kinase (PI 3-kinase)/3-phosphoinositide-dependent kinase-1 (PDK1)/protein kinase B (PKB) kinase cascade is believed to play a critical role in metabolic control and cell survival, largely mediated through PKB phosphorylation of many proteins. Recent findings demonstrate that the transcription factors FKHR (forkhead in rhabdomyosarcoma), AFX (ALL1 fused gene from chromosome X) and FKHRL1 (FKHR-like 1; termed FKHR isoforms) are phosphorylated by PKB in cells, leading to their exit from the nucleus. These exciting results suggest that FKHR isoforms may be critical effectors of PI 3-kinase/PDK1/PKB signalling *in vivo*.

Introduction

Many of insulin's intracellular actions are transmitted through a conserved kinase cascade. In brief, insulin-stimulated autophosphorylation of the insulin receptor brings about the activation of phosphoinositide 3-kinase (PI 3-kinase), leading to the recruitment of protein kinase B (PKB) to the plasma membrane and its activation by 3-phosphoinositide-dependent kinase-1 (PDK1). The PI 3-kinase/PKB signalling pathway has a critical role in metabolic control and cell survival [1]. These effects are largely mediated through PKB phosphorylation of many proteins, of which the first to be identified was glycogen synthase kinase-3 (GSK3) [2].

Given that insulin alters the transcription of at least 100 genes [3] it is likely that many of the effects of PI 3-kinase/PKB signalling are due to altered gene expression. Until recently, however, no PKB-regulated transcription factor had been identified. This situation changed in 1999, when we and others reported that the transcription factors FKHR (forkhead in rhabdomyosarcoma), AFX (ALL1 fused gene from chromosome X) and FKHRL1 (FKHR-like 1) are phosphorylated directly by PKB in cells, preventing them from stimulating gene transcription and leading to their exit from the nucleus [4–10]. These findings have stimulated much more detailed analysis of the effect of phosphorylation on the regulation of FKHR isoforms, the results of which are the major focus of this review.

DAF16 regulation by an insulin-like signalling pathway

Mechanistic evidence suggesting that FKHR isoforms are regulated by PKB was initially obtained from genetic studies in *Caenorhabditis elegans* [11,12]. An insulin-receptor-like signalling pathway regulates dauer formation, a developmental stage of the nematode that causes animals to shift metabolism towards fat storage and to live longer [13,14]. Inactivating mutations in the insulin/insulin-like growth factor 1 (IGF-1) receptor homologue DAF-2 (where DAF stands for dauer arrest phenotype) [15], in the PI 3-kinase hom-

Key words: AKT, CK1, dual-specificity tyrosine-phosphorylated and -regulated kinase (DYRK), forkhead, nuclear exclusion.
Abbreviations used: PI 3-kinase, phosphoinositide 3-kinase; PKB, protein kinase B; PDK1, 3-phosphoinositide-dependent kinase-1; GSK3, glycogen synthase kinase-3; FKHR, forkhead in rhabdomyosarcoma; FKHRL1, FKHR-like 1; AFX, ALL1 fused gene from chromosome X; daf, dauer arrest phenotype; MAPKAP-K1, mitogen-activated protein kinase-activated protein kinase-1; SGK, serum- and glucocorticoid-induced kinase; IGF-1, insulin-like growth factor 1; NES, nuclear export signal; NLS, nuclear localization signal; DYRK, dual-specificity tyrosine-phosphorylated and -regulated kinase.
[1]Present address: Department of Surgery and Oncology, University of Dundee Medical School, Ninewells Hospital, Dundee, Scotland, U.K.
[2]To whom correspondence should be addressed (e-mail grena1@biochem.dundee.ac.uk).

ACADEMIC PRESS

Available online at www.sciencedirect.com

SCIENCE DIRECT®

Biochemical and Biophysical Research Communications 307 (2003) 459–465

BBRC

www.elsevier.com/locate/ybbrc

Centaurin-α_1 associates with and is phosphorylated by isoforms of protein kinase C☆

Eva Zemlickova,[a,b] Thierry Dubois,[a,c] Preeti Kerai,[d] Sam Clokie,[a] Andy D. Cronshaw,[e] Robert I.D. Wakefield,[a] Franz-Josef Johannes,[f,1] and Alastair Aitken[a,*]

[a] *University of Edinburgh, School of Biomedical and Clinical Laboratory Sciences, Hugh Robson Building, George Square, Edinburgh EH8 9XD, UK*
[b] *Unidad de Investigacion, Hospital Universitario de Canarias, Ofra s/n, La Cuesta, Tenerife 38320, Spain*
[c] *Institut Curie-Section Recherche, CNRS UMR 144, 26 rue d'Ulm, Paris, Cédex 05 75248, France*
[d] *Wolfson Institute for Biomedical Research, University College London, WC1E 6BT, UK*
[e] *University of Edinburgh, ICMB, Kings Buildings, Edinburgh, UK*
[f] *Fraunhofer Institute for interfacial Engineering and Biotechnology, Nobelstrasse 12, Stuttgart 70569, Germany*

Received 10 June 2003

This article is dedicated to the memory of our colleague Franz-Josef Johannes, whose contributions to protein kinase C research will be greatly missed.

Abstract

Centaurin-α_1 is a member of the family of ADP-ribosylation factors (ARF) GTPase activating proteins (GAPs), although ARF GAP activity has not yet been demonstrated. The human homologue, centaurin-α_1 functionally complements the ARF GAP activity of Gcs1 in yeast. Although Gcs1 is involved in the formation of actin filaments in vivo, the function of centaurin remains elusive. We have identified a number of novel centaurin-α_1 binding partners; including CKIα and nucleolin. In this report, we have focused on the interaction of centaurin-α_1 with PKC. All groups of PKC associate directly through their cysteine rich domains. Centaurin-α_1 is also a substrate for all PKC classes and we have identified the two sites of phosphorylation. This is the first report of a kinase that phosphorylates centaurin-α_1.

Keywords: Centaurin; PtdIns-(3,4,5)-P_3-binding protein; PKC; Protein kinase C; Isoforms; PKD; Phosphorylation site; Mass spectrometry; Affinity chromatography

Centaurin-α_1 was purified from rat brain as a PtdIns-(3,4,5)-P_3-binding protein [1]. The human homologue, centaurin-α_1, functionally complements the ARF GAP activity of Gcs1, a yeast centaurin homologue [2], although it is not yet known whether centaurin-α has this activity. The latter has a common domain of 70 amino acids that includes a zinc finger motif that has been shown to be essential for GAP activity [3]. In addition, centaurins contain two pleckstrin homology (PH) domains [1]. Centaurin-α_1 is found in the cytoplasm as well as in the nucleus [2,4] and in support of a possible involvement of centaurin-α_1 in nuclear processes, we have shown the association of centaurin-α_1 with the nucleolar protein nucleolin [4]. Centaurin-α_1 is ubiquitously expressed, with particularly high levels in brain [5]. The main location is the neurons of hippocampus, cortex, cerebellum, and in the hypothalamus [6].

Centaurin-α has recently been shown to be upregulated in neurons in patients with Alzheimer's disease [7]. Apart from their potential GAP activity, the in vivo function of centaurins remains elusive. However, it has been shown that Gcs1 is involved in the formation of actin filaments in vivo [8]. Involvement in actin reorganisation has also been shown for other members of the

☆ *Abbreviations:* ARF, ADP-ribosylation factors; CKI, casein kinase I; GAP, GTPase activating proteins; GFP, green fluorescent protein; GST, glutathione *S*-transferase; PAGE, polyacrylamide gel electrophoresis; PCR, polymerase chain reaction; PKC, protein kinase C; C1, cysteine rich domain; MS–MS, tandem mass spectrometry.

* Corresponding author. Fax: +44-131-650-3711.
E-mail address: Alastair.Aitken@ed.ac.uk (A. Aitken).

[1] Deceased.

0006-291X/03/$ - see front matter © 2003 Elsevier Inc. All rights reserved.
doi:10.1016/S0006-291X(03)01187-2

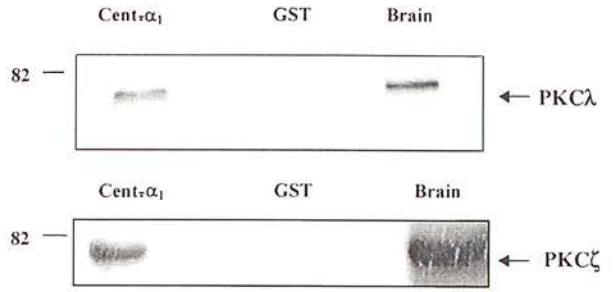

Fig. 1. PKCλ and ζ associate with the centaurin-α_1 column. Protein (5 μg) eluted from the GST–centaurin-α_1 (Cent.-α_1) and GST column was separated on 10% SDS–PAGE, transferred onto nitrocellulose, and Western blotted with PKCλ and ζ antibodies. A brain extract (Brain) was used as a positive control for the antibodies. The position of one of the molecular weight markers (kDa) is indicated.

ARF GAP family; such as ASAP1 [9] which supports the idea that ARF GAP proteins are involved in cytoskeletal reorganisation, possibly in PtdIns-(3,4,5)-P_3 signalling. We showed the association of centaurin-α_1 with casein kinase Iα (CKIα) [10], a kinase that has been shown to be involved in membrane trafficking and/or actin cytoskeleton rearrangement [11,12].

PKCs comprise a family of serine/threonine kinases classified into different groups according to activation parameters: conventional PKCs (PKC α, βI, βII, and γ), novel PKCs (PKCδ, ε, η, and θ), atypical PKCs (PKCζ and ι/λ), and PKD/PKCμ, which can be considered as a separate class [13]. Among many other functions, PKC isoforms are involved in the regulation of cytoskeletal organisation and in mediating muscle contraction. PKC isoforms are also involved in nuclear functions such as cell proliferation, differentiation, and apoptosis. Members of the PKC family are regulated by several lipid second messengers, such as PtdIns-(3,4,5)-P_3 [13]. In this report, we show that centaurin-α_1 binds to all members of the PKC family and is phosphorylated by isoforms from all PKC classes. We also identified the two PKC phosphorylation sites.

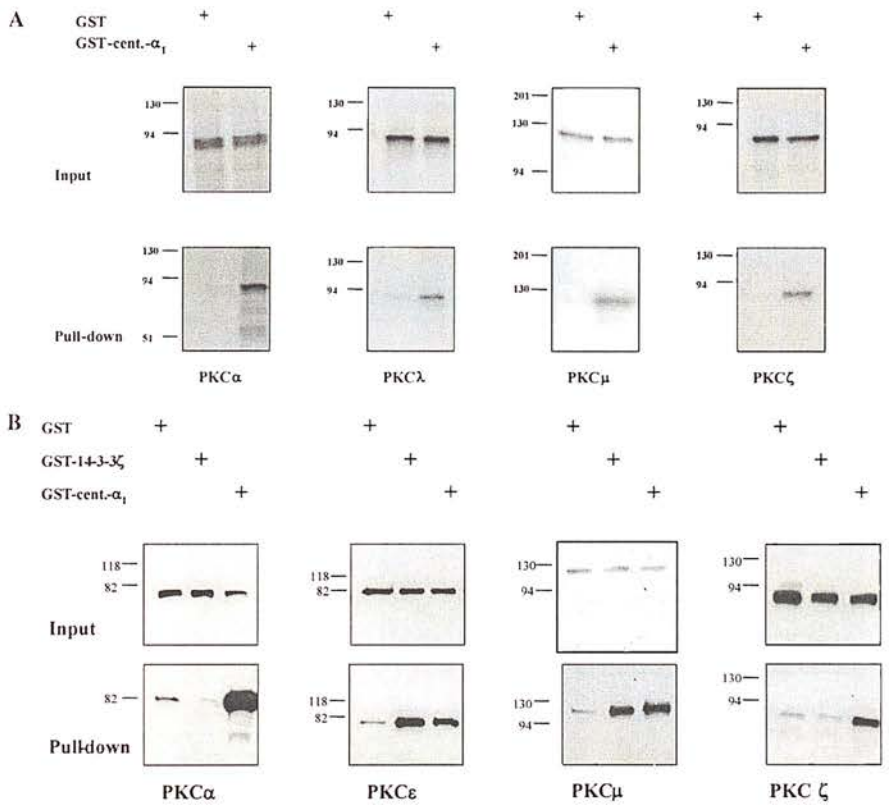

Fig. 2. Centaurin-α_1 associates with all PKC isoforms tested. (A) Centaurin-α_1 associates with all PKC isoforms. PKCα, λ, μ, and ζ were expressed and labelled with [^{35}S]methionine in a reticulocyte lysate and incubated for 15 min at 30 °C with 5 μg GST and GST–centaurin-α_1 in the presence of 1% Nonidet P-40. Glutathione–Sepharose beads were added and incubated at room temperature for 1 h. Beads were washed and samples analysed by 10% SDS–PAGE followed by autoradiography (panel "Pull-down"). An aliquot of the lysate was loaded on the gel to visualise expressed PKCs (panel "Input"). The positions of the molecular weight markers (kDa) are indicated. (B) Centaurin-α_1 directly associates with PKC isoforms from all sub-families. Five micrograms each of GST, GST-14-3-3ζ, and GST–centaurin-α_1 was incubated with 0.1 μg of human recombinant PKCα, PKCε, PKCμ, and PKCζ. The samples were analysed on 10% SDS–PAGE, transferred onto nitrocellulose, and Western blotted with PKCα, ε, μ, and ζ antibodies as indicated. Top panels represent an aliquot of the assays to visualise the PKCs (panels "Input"). Bottom panels represent the GST pull-down assays (panel "Pull-down"). The positions of molecular weight markers (kDa) are indicated.

Materials and methods

Plasmids and recombinant proteins. Centaurin-α_1 cloned within *Eco*RI/*Sal*I sites into pGEX-4T3 was from Venkateswarlu and Cullen [1]. PKCα (pCO2) was from Peter Parker and PKCλ (pcDNA3) from Terje Johansen. The construction of PKCμ mutants (WT, 1–340, ΔAC, and ΔPH) in pcDNA3 has been described [14] and PKCζ/pcDNA3.1 was obtained from Feng Liu. GST–centaurin-α_1 was constructed and purified as previously described [10].

Affinity chromatography on a centaurin-α_1 column. The affinity chromatography was performed as described previously [4]. Eluted proteins from the GST and GST–centaurin-α_1 columns were analysed by 10% SDS–PAGE, transferred onto nitrocellulose, and Western blotted using PKCλ (Transduction Laboratories, all 1:1000) and PKCζ antibodies (W.J. van Blitterswijk, 1:1000).

In vitro binding between purified PKC isoforms and centaurin-α_1. GST, GST-14-3-3ζ, and GST–centaurin-α_1 (5 μg) were incubated with human recombinant PKCα, ε, μ, and ζ (1 U) (Calbiochem) in binding buffer (20 mM Tris, pH 7.4, 100 mM NaCl, 10% glycerol, 1 mM DTT, 1% Nonidet-P40 [NP40], and 0.1% BSA) for 2 h at 4 °C. GSH beads were then added and incubated for a further 1 h. Bead precipitates were then washed 4 times with binding buffer and bound proteins were eluted using SDS sample buffer. The samples were analysed by 10% SDS–PAGE, transferred onto nitrocellulose, and Western blotted using PKC antibodies.

In vitro transcription and translation and GST pull-down assays. PKCα, λ, μ, and ζ were expressed in vitro using a T7 TNT coupled transcription/translation reticulocyte lysate (Promega, Madison, WI). The reactions (50 μl) were performed following the manufacturer's instructions using [^{35}S]methionine (Amersham) for 90 min at 30 °C. Samples were then diluted 3-fold with binding buffer (20 mM Tris, pH 7.4, 100 mM NaCl, 10% glycerol, 1 mM DTT, and 1% Nonidet-P40 [NP40]) and incubated for 15 min at 30 °C with 5 μg of GST, GST-14-3-3ζ, and GST–centaurin-α_1. GSH beads and binding buffer (300 μl) were added to the reactions and incubated at room temperature for a further 1 h. The beads were washed 5 times with 1 ml of binding buffer and electrophoresed on 12.5% SDS–PAGE. After staining/destaining, the gels were incubated for 30 min with Amplify (Amersham Pharmacia), dried, and exposed to film.

Phosphorylation of centaurin-α_1 by PKC. Centaurin-α_1 (5 μg) was incubated with 1 U of PKCα, PKCε, PKCμ, and PKCζ in a buffer containing 40 mM Hepes, pH 7.4, 20 mM $MgCl_2$, 2 mM EGTA (for PKCα 3 mM $CaCl_2$ was included), 30 μg/ml phosphatidylserine, 8 μg/ml diacylglycerol, and 50 μM ATP including [γ-^{32}P]ATP). The reaction was performed at 30 °C for 15 min in a final volume of 40 μl. The reactions were stopped by the addition of SDS sample buffer and analysed on 12.5% SDS–PAGE. Gels were stained with Coomassie blue and autoradiographed.

Identification of the PKC in vitro phosphorylation sites. Recombinant human centaurin-α_1 phosphorylated by PKCα was loaded on 12.5% SDS–PAGE to separate phosphorylated substrate from the autophosphorylated PKC. Centaurin was visualised on the gel by GelCODE (Pierce) staining. The band containing centaurin-α_1 was digested with trypsin and peptides extracted as described [15]. The peptides were purified by reverse phase HPLC on a Surveyor AS (ThermoFinnigan) with a PepMap C_{18} 150 mm, 1.0 mm diameter,

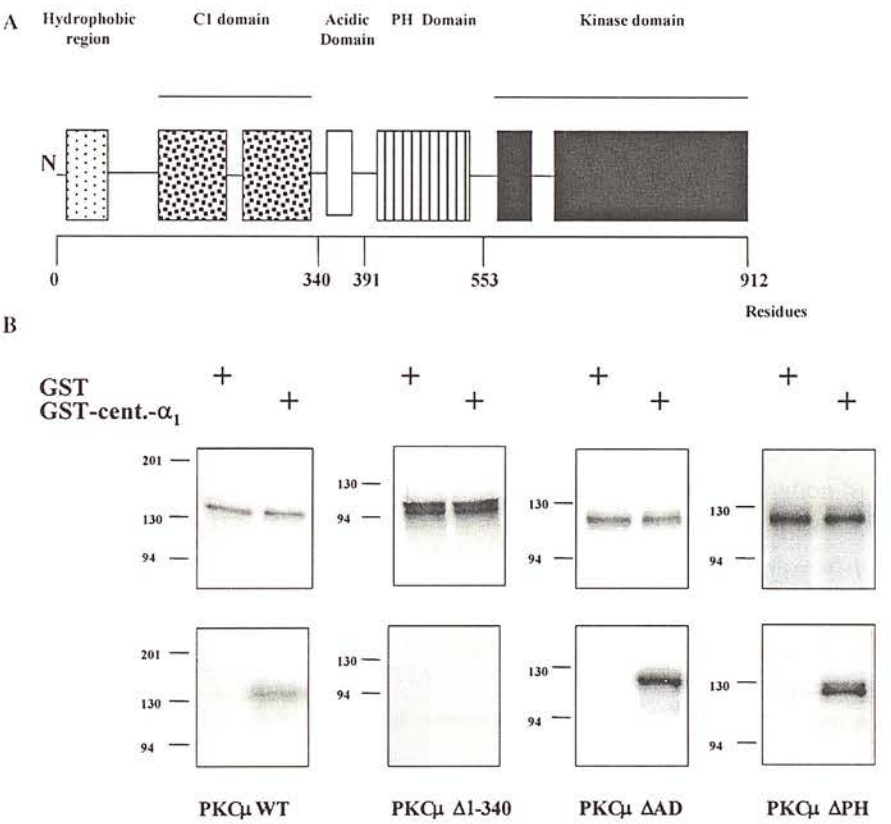

Fig. 3. Centaurin-α_1 binds to the C1 domain of PKCμ. (A) Schematic representation of the known functional domains of PKCμ. (B) Centaurin-α_1 binds to the C1 domain of PKCμ. PKCμ wt and PKCμ deletion mutants Δ1–340 (ΔC); Δ336–391 (ΔAD); and Δ417–553 (ΔPH) were expressed in a reticulocyte lysate, and incubated with 5 μg each of GST and GST–centaurin-α_1 as described in Fig. 2A. GST pull-down assays were analysed by SDS–PAGE and autoradiographed (panel "Pull-down"). An aliquot of the lysate was loaded on the gel (panel "Input"). The positions of molecular weight markers (kDa) are indicated.

0.5 μm 100 Å column (LC Packings), using a flow rate of 50 μl/min with a gradient 0–1% B over 0–4 min, 1–3% B over 4–20 min, 3–23% B over 20–25 min, 23–40.5% B over 25–95 min, 40.5–48% B over 95–110 min, 48–68% B over 110–150 min, and 68–85% B over 150–155 min. Solvent A was aqueous 0.1% formic acid, and solvent B was 100% acetonitrile with 0.1% formic acid. Fifty microliter fractions were collected. The elution positions of the ^{32}P-labeled peptides were determined by Cerenkov counting and the phosphopeptide fractions were analysed by ion-trap mass spectrometry as described [15]. LC–ESI-MS/MS was carried out on a LCQ Deca ion trap (ThermoFinnigan, Hemel Hempstead). The instrument settings for an on-line LC flow rate of 50 μl/min were as follows: Sheath Gas Flow Rate 100, Tube Lens offset −30 V, ESI Spray Voltage 4.50 kV, capillary voltage 3.0 V, and capillary temperature 325.0 °C. The MS data were acquired in the 'Triple-Play' data-dependent mode that included three scan events: a full-range (50–2000 m/z) MS scan; a narrow-range, high resolution zoom scan on a selected ion from the MS scan; and an MS–MS scan of the selected ion.

Solid phase sequencing. After phosphorylation of the protein and separation of the centaurin-α_1 from ATP and autophosphorylated PKC by SDS-PAGE, followed by trypsin digestion, release of ^{32}P from the phosphopeptides was measured at each cycle of automatic Edman degradation. Peptides were covalently coupled to arylamine membrane and sequenced in an ABI Procise sequencer as in [16].

Results and discussion

Centaurin-α_1 binds to c, n, and aPKCs and PKD/PKCμ

We identified novel centaurin-α_1 interacting proteins by affinity chromatography of sheep brain lysate, pre-incubated with GST to remove non-specific binding. Western blotting revealed that PKCλ and ζ associated with the GST–centaurin-α_1 (Fig. 1).

To investigate whether all PKC isoforms associated with centaurin-α_1, PKCα, λ, μ, and ζ were expressed in an in vitro transcription/translation (IVTT) assay and incubated with GST, GST-14-3-3ζ, and GST–centaurin-α_1. All four PKC isoforms associated with GST–centaurin-α_1 but not with GST (Fig. 2A).

In order to analyse whether the association between centaurin-α_1 and PKC isoforms was direct, binding assays were performed using purified recombinant proteins. The results in Fig. 2B show that GST–centaurin-α_1 directly bound to all PKC isoforms tested in an in vitro GST pull-down assay. In addition, as a control for specificity of interaction, 14-3-3ζ directly associated with PKCε and PKCμ, but not with PKCα or PKCζ. Our results in Fig. 2B are in agreement with a reported interaction between 14-3-3ζ and the C1 domain of PKCμ [17]. We have shown that centaurin-α_1 specifically and directly associated with PKC. The fact that centaurin-α_1 interacted with all PKC isotypes suggested that it associated with a domain common to all PKC isoforms, i.e., the cysteine rich domain (C1) or the kinase domain.

Centaurin-α_1 binds to the C1 domain of PKCμ

PKCμ isoform was used to map the centaurin-α_1 binding site. PKCμ wt and PKCμ deletion mutants, Δ1–340 (ΔC); Δ336–391 (ΔAD); and Δ417–553 (ΔPH) (Fig. 3A) were expressed with [^{35}S]methionine and incubated with GST and GST–centaurin-α_1. PKCμ wt bound to GST–centaurin-α_1 (Fig. 3B). Deletion of the acidic domain or the PH domain of PKCμ did not affect the binding to centaurin-α_1. No binding was observed between centaurin-α_1 and PKCμ Δ1–340 (Fig. 3B), therefore residues 1–340 of PKCμ were necessary for the association, indicating that the C1 domain of PKCμ could represent the target region for binding. This is not unexpected as several proteins have been identified in association with the C1 region of PKCμ [14,17]. Since all PKC isoforms have at least one C1 domain [13] these results complement those from Figs. 2A and B showing that all PKC isoforms associated in vitro with centaurin-α_1.

Phosphorylation of centaurin-α_1 by distinct PKC isoforms

Using recombinant purified PKC isoforms, we showed that centaurin-α_1 (5 μg) was phosphorylated in vitro with PKCα, ε, μ, and ζ (1 U each, Fig. 4).

Identification of the PKC phosphorylation sites

The sites of phosphorylation by PKCα on centaurin-α_1 were identified as S87 (peptide ARFESK) and T276

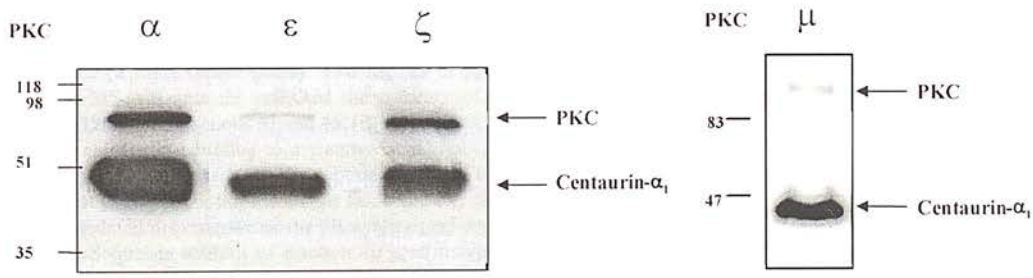

Fig. 4. Centaurin-α_1 is phosphorylated by all classes of PKC. One unit each of PKCα, ε, μ, and ζ was incubated with 5 μg centaurin-α_1 in the presence of 50 μM [γ-^{32}P]ATP and kinase buffer at 30 °C for 15 min and for 30 min (by which time phosphorylation was near maximal). The samples were analysed on 10% SDS–PAGE followed by autoradiography.

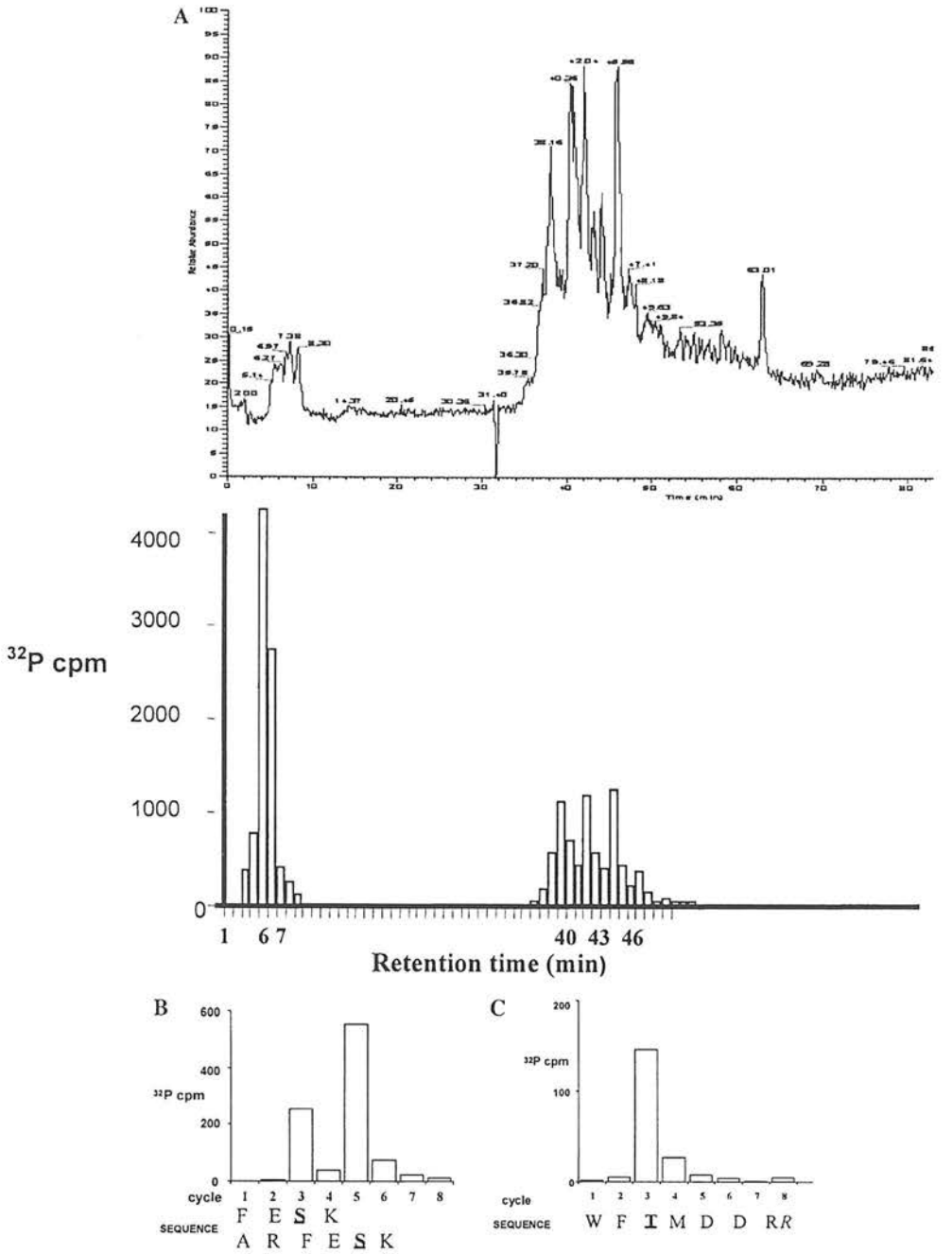

Fig. 5. Sites of phosphorylation by PKC. (A) Recombinant human centaurin was phosphorylated by PKCα and separated on SDS–PAGE. The radioactive band was located by autoradiography, then subjected to trypsin digestion and extraction [15]. Upper panel shows the separation of the peptides by reverse phase HPLC as described in Materials and methods. The eluted fractions were analysed by Cerenkov counting to determine the presence of ^{32}P-labelled peptides (lower panel). Two regions of phosphopeptide were identified (fractions 6 and 7, and multiple peaks from fractions 40–46). On-line MS–MS analysis indicated the presence of two peptides in fractions 6 and 7 (FESK and ARFESK) and peptides WFTMDDR and WFTMDDRR in fractions 43 and 46. (B) Represents the release of ^{32}P at each cycle of Edman degradation of the phosphorylated peptide (fraction 6) after covalently coupling to arylamine membrane [16]. Sequence data from fraction 7 were similar (not shown). The results indicate that the radioactivity incorporated into the peptide is released in cycle 3 and cycle 5 corresponding to Ser87 within the peptides FESK and ARFESK. The presence of multiple peptides from the same site has resulted from partial cleavage as expected from the known endoproteolytic behaviour of trypsin. (C) Edman degradation of the phosphorylated peptide from fraction 43 indicated that the radioactivity is released in cycle 3, corresponding to Thr276. Sequence analysis of fraction 46 gave similar results. Fraction 40 gave a poor recovery of ^{32}P (only around 150 cpm Cerenkov were loaded) but this could represent the peptide(s) RWFTDDR(R). The additional arginine residue(s), which is/are hydrophilic, results in the peptide eluting earlier. In contrast, for the peptide ARFESK there is an additional (slightly hydrophobic) alanine as well as arginine. These would compensate for each other resulting in no significant difference in hydrophobicity from the peptide FESK. We observed no separation of these two peptides on reverse phase HPLC (both eluted in fractions 6 and 7).

(peptide WFTMDDR*R*) (Fig. 5). We noted that in the PepMap column the phosphoform of the peptide eluted 2 min later than the dephospho-form using this particular gradient and 0.1% formic acid. This is a similar situation to that in a Vydac "low TFA" column which also uses a much lower level of ion-suppression agent (less than 0.01% TFA). This is in contrast to the general situation in reverse phase HPLC where phosphopeptides elute with a typical gradient around 1 min earlier when 0.1% TFA is used.

The identification of the peptides was confirmed by tandem MS–MS (data not shown). Fig. 5A indicates that around 60% of the radioactivity is incorporated into Ser87 and 40% into peptides originating from Thr276. Since the latter site is more hydrophobic, it is possible that these peptides were extracted less efficiently and the true ratio might be more equal. The phosphorylation site analysis was carried out twice after phosphorylation of centaurin-α_1 with PKCα and once with PKCε. A similar pattern of phosphopeptides was obtained each time. Under the phosphorylation conditions used the stoichiometry was around 0.3 mol/mol.

Centaurin-α_1 is expressed at particularly high levels in brain [5] and PKC isoforms are also widely distributed in different tissues including brain [18]. Centaurin-α_1 is mainly found in the nucleus of different cell lines, but also associates with the plasma membrane and is present in the cytosol [2,4,19,20].

Most PKC isoforms have also been identified in the nucleus and increasing evidence has implicated a role for PKC in nuclear functions, such as cell proliferation, cell differentiation, and apoptosis, reviewed in [21]. The presence of a PtdIns-(3,4,5)-P_3-binding site in centaurin-α_1 suggests possible roles for centaurin-α_1 and PKC in signalling downstream of PI 3-K. Since novel and atypical PKC isoforms are activated by lipid second messengers including the PI 3-K products PtdIns-(3,4)-P_2 and PtdIns-(3,4,5)-P_3 [13] this could link PKC isoforms and centaurin-α_1 to the phosphoinositide signalling pathway. The interaction between PKC and centaurin-α_1 also further strengthens the possibility of involvement of centaurin-α_1 in cytoskeletal processes. Our identification of a major PKC site on centaurin-α_1 at Thr276 in the C-terminal PH domain suggests that phosphorylation at this site may affect phosphoinositide binding to centaurin-α_1. The other phosphorylation site that we identified, Ser 87, is in the putative ARF-GAP domain.

In this study, PKC was identified as a novel centaurin-α_1 interacting protein by affinity chromatography and GST pull-down assay. Centaurin-α_1 associated directly with all PKC isoforms possibly via their C1 domain. Centaurin-α_1 was also phosphorylated by all PKCs tested probably on the same two sites that we identified in this study, using PKCα. This is the first report of a kinase that phosphorylates centaurin-α_1.

Acknowledgments

This work was supported by the Medical Research Council Programme Grant and a Faculty of Medicine Scholarship, University of Edinburgh (to E.Z.). The phosphopeptide analysis was a contribution from the Edinburgh Protein Interaction Centre funded by the Wellcome Trust.

References

[1] K. Venkateswarlu, P.J. Cullen, Molecular cloning and functional characterization of a human homologue of centaurin-alpha, Biochem. Biophys. Res. Commun. 262 (1999) 237–244.
[2] K. Venkateswarlu, P.B. Oatey, J.M. Tavare, T.R. Jackson, P.J. Cullen, Identification of centaurin-alpha1 as a potential in vivo phosphatidylinositol 3,4,5-trisphosphate-binding protein that is functionally homologous to the yeast ADP-ribosylation factor (ARF) GTPase-activating protein, Gcs1, Biochem. J. 340 (1999) 359–363.
[3] J.G. Donaldson, Filling in the GAPs in the ADP-ribosylation factor story, Proc. Natl. Acad. Sci. USA 97 (2000) 3792–3794.
[4] T. Dubois, E. Zemlickova, S. Howell, A. Aitken, Centaurin-α_1 associates in vivo with nucleolin in a RNA dependent manner, Biochem. Biophys. Res. Commun. 301 (2003) 502–508.
[5] L.P. Hammonds-Odie, T.R. Jackson, A.A. Profit, I.J. Blader, C.W. Turck, G.D. Restwich, A.B. Theibert, Identification and cloning of centaurin-alpha. A novel phosphatidylinositol 3,4,5-trisphosphate-binding protein from rat brain, J. Biol. Chem. 271 (1996) 18859–18868.
[6] M.R. Kreutz, T.M. Bockers, B.A. Sabel, E. Hulser, R. Stricker, G. Reiser, Expression and subcellular localization of p42IP4/centaurin-alpha, a brain-specific, high-affinity receptor for inositol 1,3,4,5-tetrakisphosphate and phosphatidylinositol 3,4,5-trisphosphate in rat brain, Eur. J. Neurosci. 9 (1997) 680–685.
[7] G. Reiser, H.G. Bernstein, Neurons and plaques of Alzheimer's disease patients highly express the neuronal membrane docking protein p42IP4/centaurin alpha, Neuroreport 13 (2002) 2417–2419.
[8] I.J. Blader, M.J.T.V. Xopw, T.R. Jackson, A.A. Profit, A.F. Greenwood, D.G. Drubin, G.D. Prestwich, A.B. Theibert, GCS1, an Arf guanosine triphosphatase-activating protein in *Saccharomyces cerevisiae*, is required for normal actin cytoskeletal organization in vivo and stimulates actin polymerization in vitro, Mol. Biol. Cell 10 (1999) 581–596.
[9] P.A. Randazzo, J. Andrade, K. Miura, M.T. Brown, Y.Q. Long, S. Stauffer, P. Roller, J.A. Cooper, The Arf GTPase-activating protein ASAP1 regulates the actin cytoskeleton, Proc. Natl. Acad. Sci. USA 97 (2000) 4011–4016.
[10] T. Dubois, P. Kerai, E. Zemlickova, S. Howell, T.R. Jackson, K. Venkateswarlu, P.J. Cullen, A.B. Theibert, L. Larose, P.J. Roach, A. Aitken, Casein kinase I associates with members of the centaurin-alpha family of phosphatidylinositol 3,4,5-trisphosphate-binding proteins, J. Biol. Chem. 276 (2001) 18757–18764.
[11] S.D. Gross, D.P. Hoffman, P.L. Fisette, P. Baas, R.A. Anderson, A phosphatidylinositol 4,5-bisphosphate-sensitive casein kinase I alpha associates with synaptic vesicles and phosphorylates a subset of vesicle proteins, J. Cell Biol. 130 (1995) 711–724.
[12] V.V. Faundez, R.B. Kelly, The AP-3 complex required for endosomal synaptic vesicle biogenesis is associated with a casein kinase I alpha-like isoform, Mol. Biol. Cell 11 (2000) 2591–2604.
[13] A. Toker, Signaling through protein kinase C, Front. Biosci. 3 (1998) D1134–D1147.
[14] F.J. Johannes, A. Hausser, P. Storz, L. Truckenmuller, G. Link, T. Kawakami, K. Pfizenmaier, Bruton's tyrosine kinase (Btk) associates with protein kinase C mu, FEBS Lett. 461 (1999) 68–72.

[15] A. Aitken, M.P. Learmonth, Protein identification by in-gel digestion and mass spectrometric analysis, Mol. Biotechnol. 20 (2002) 95–97.
[16] T. Dubois, P. Kerai, M. Learmonth, A. Cronshaw, A. Aitken, Identification of syntaxin-1A sites of phosphorylation by casein kinase I and casein kinase II, Eur. J. Biochem. 269 (2002) 909–914.
[17] A. Hausser, P. Storz, G. Link, H. Stoll, Y.C. Liu, A. Altman, K. Pfizenmaier, F.J. Johannes, Protein kinase C mu is negatively regulated by 14-3-3 signal transduction proteins, J. Biol. Chem. 274 (1999) 9258–9264.
[18] J.P. Liu, Protein kinase C and its substrates, Mol. Cell. Endocrinol. 116 (1996) 1–29.
[19] K. Tanaka, K. Horiguchi, T. Yoshida, M. Takeda, H. Fujisawa, K. Takeuchi, M. Umeda, S. Kato, S. Ihara, S. Nagata, Y. Fukui, Evidence that a phosphatidylinositol 3,4,5-trisphosphate-binding protein can function in nucleus, J. Biol. Chem. 274 (1999) 3919–3922.
[20] F. Sedehizade, T. Hanchk, R. Stricker, A. Horstmayer, H.G. Bernstain, G. Reiser, Cellular expression and subcellular localization of the human Ins(1,3,4,5)P(4)-binding protein, p42(IP4), in human brain and in neuronal cells, Brain Res. Mol. Brain Res. 99 (2002) 1–11.
[21] A.M. Martelli, N. Sang, P. Borgatti, S. Capitani, L.M. Neri, Multiple biological responses activated by nuclear protein kinase C, J. Cell. Biochem. 74 (1999) 499–521.

the FEBS Journal

BCR kinase phosphorylates 14-3-3 Tau on residue 233

Samuel J. Clokie[1], Kin Y. Cheung[1], Shaun Mackie[1,*], Rodolfo Marquez[2], Alex H. Peden[1,†] and Alastair Aitken[1]

1 School of Biomedical and Clinical Laboratory Sciences, University of Edinburgh, UK
2 School of Life Sciences, University of Dundee, UK

Keywords
14-3-3 isoforms; phosphorylation; BCR kinase; protein interactions

Correspondence
A. Aitken, School of Biomedical and Clinical Laboratory Sciences, Darwin Building, University of Edinburgh, King's Buildings, Mayfield Road, Edinburgh EH8 9XD, UK
Fax/Tel: +44 131 650 5357
E-mail: alastair.aitken@ed.ac.uk

Present addresses
*Psychiatric Genetics Section, Molecular Medicine Centre, University of Edinburgh, UK
†The National Creutzfeldt–Jakob Disease Surveillance Unit, Western General Hospital, Edinburgh, UK

(Received 21 February 2005, revised 4 May 2005, accepted 13 May 2005)

doi:10.1111/j.1742-4658.2005.04765.x

The breakpoint cluster region protein, BCR, has protein kinase activity that can auto- and *trans*-phosphorylate serine, threonine and tyrosine residues. BCR has been implicated in chronic myelogenous leukaemia as well as important signalling pathways, and as such its interaction with 14-3-3 is of major interest. 14-3-3τ and ζ isoforms have been shown previously to be phosphorylated *in vitro* and *in vivo* by BCR kinase on serine and threonine residue(s) but site(s) were not determined. Phosphorylation of 14-3-3 isoforms at distinct sites is an important mode of regulation that negatively affects interaction with Raf kinase and Bax, and potentially influences the dimerization of 14-3-3. In this study we have further characterized the BCR–14-3-3 interaction and have identified the site phosphorylated by BCR. We show here that BCR interacts with at least five isoforms of 14-3-3 *in vivo* and phosphorylates 14-3-3τ on Ser233 and to a lesser extent 14-3-3ζ on Thr233. We have previously shown that these two isoforms are also phosphorylated at this site by casein kinase 1, which, in contrast to BCR, preferentially phosphorylates 14-3-3ζ.

The term breakpoint cluster region (BCR) refers to an area of 5.8 kb on chromosome 22 that by a reciprocal translocation event with the oncogene Abl, from chromosome 9, produces the chimera BCR–Abl [1]. It is this reciprocal translocation event that creates an aberrant chromosome called the Philadelphia chromosome (ph^1) that is the hallmark of chronic myeloid leukaemia (CML) and which is found in over 90% of patients with CML [2]. BCR–Abl proteins can vary in size, depending on the breakpoint within the BCR. The resultant fusion protein, containing different amounts of the BCR gene fused to ABL, gives rise to different clinical outcomes with ranging clinical severity [3,4]. The constitutively active tyrosine kinase activity of Abl, essential for the progression of CML [5], has been the focus of many studies to find an effective inhibitor [6], of which the compound Gleevec or Imatinib has proved to be highly successful. However, the many varied domains of BCR are also essential for the transforming potential of BCR–Abl [1].

The normal BCR product is 160 kDa and contains a number of domains (Fig. 1) (reviewed in [1]). These include an oligomerization domain [7], an atypical S/T kinase domain [8–10], a Src homology 2 (SH2)-binding domain [11], guanine nucleotide exchange factor (GEF) domain [12,13] and a GTPase activity (GAP)

Abbreviations
BCR, breakpoint cluster region; CK1, casein kinase 1; CML, chronic myeloid leukaemia; D4476, 4-[4-[2,3-dihydro-benzo (1,4)dioxin-6-yl]-5-pyridin-2-yl-1H-imidazol-2-yl]benzamide; ERBIN, ERB2 interacting protein; GAP, GTPase activity; GEF, guanine nucleotide exchange factor; JNK, c-Jun N-terminal kinase; ph^1, Philadelphia chromosome; PI3K, phosphatidylinositol 3-kinase; PKC, protein kinase C; SH2, Src homology 2; XPB, xeroderma pigmentosum group B protein.

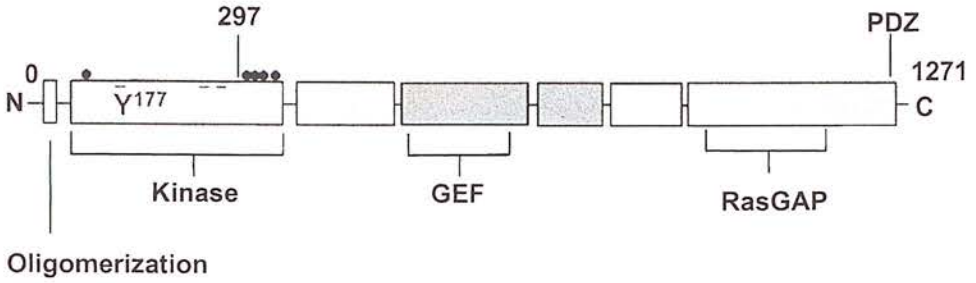

Fig. 1. Domains of BCR. Possible 14-3-3 binding sites are indicated as filled circles on top. These and the kinase domain are located within exon 1. The positions of the RacGAP, GEF, oligomerization and SH_2 binding domains are indicated; the tyrosine residues in SH_2 domains by short lines.

domain [14]. BCR binds 14-3-3 [9], Xeroderma pigmentosum group B protein (XPB) [15] and chromatin [16]. BCR binds to Grb2 when phosphorylated on Tyr177 in the SH2 binding domain, thus linking it to a role in the Ras pathway [11]. Recently a functional PDZ binding domain was identified in BCR, associating through a motif consisting of S-T-E-V, with the ERB2 interacting protein (ERBIN) [17].

The 14-3-3 family forms protein complexes involved in neurodegeneration, apoptosis, signal transduction, trafficking and secretion [18–20]. In many cases, these complexes show a distinct preference for a particular isoform(s) of 14-3-3. 14-3-3 proteins are established adaptors of signalling proteins that bind primarily, but not solely, to proteins containing phosphorylated serine/threonine residues. Using a phosphopeptide library, an optimal motif for 14-3-3 binding was identified as R(S)XpS/TXP [21] which was later refined to RXXXpS/TXP where pS is phosphoserine and X is any amino acid [22]. The crystal structures of 14-3-3 dimers [23,24] led to identification of the binding site of the novel phosphopeptide motif $RSX_{1,2}SpXP$ and unphosphorylated motifs [22,25].

Recent findings also show that the mechanism of interaction is more complex than simply acting through the phosphoserine/threonine motif. Nonphosphorylated binding motifs can also be of high affinity and may show more isoform-dependence in their interaction [25]. Some well-characterized interacting proteins such as Raf kinase have been shown to have additional binding site(s) for 14-3-3 on their cysteine-rich regions. BCR also binds via a serine-rich region. Binding of a protein through two distinct binding motifs to a dimeric 14-3-3 may also be essential for full interaction [26]. Dimerization with specific isoforms *in vivo* has important implications for the role of 14-3-3 in the formation of signalling complexes [19], and phosphorylation of specific 14-3-3 isoforms can also regulate interactions [18,20].

The BCR protein has four potential R(S)XXpSXP motifs [27] and the association with 14-3-3 is of major biological significance due to their respective involvement in signalling pathways including the association with Raf kinase [28]. 14-3-3 has been shown to bind the p110 subunit of phosphatidylinositol 3-kinase (PI3K) [29] and the authors suggested that 14-3-3 negatively regulates the activity of PI3K in activated T cells by ≥50%. Interestingly the authors noted enhanced binding of 14-3-3τ to PI3K with inclusion of the tyrosine phosphatase inhibitor pervanadate to the lysis buffer, suggesting that 14-3-3 may bind through phosphotyrosine residues as well as phosphoserine/threonine residues.

We showed that α and δ were phosphorylated forms of β and ζ, respectively, and are more than 50% phosphorylated on Ser185 in brain 14-3-3 [30], but we find no evidence for phospho-forms in a wide range of other tissue types and cell lines. Casein kinase 1 (CK1, reviewed in [31,32]) colocalizes in neurons with synaptic vesicle markers and can phosphorylate some synaptic vesicle associated proteins. We identified CK1α as the brain kinase that phosphorylated 14-3-3ζ on Thr233 [33]. 14-3-3τ and yeast 14-3-3s (BMH1 and 2) were also phosphorylated on the equivalent sites. *In vivo* phosphorylation of 14-3-3ζ at this site negatively regulates its binding to c-Raf and may be important in Raf mediated signal transduction [28,33].

The β, η and ζ isoforms of 14-3-3 (but not ε and γ although they also contain serine at the equivalent site) are phosphorylated by a sphingosine-dependant kinase, SDK1, now identified as the kinase domain of protein kinase C (PKC) δ produced after caspase-3 cleavage [34].

Phosphorylation of 14-3-3 by BCR could affect the ability of 14-3-3 to bind other signalling proteins; for example we have shown that phosphorylation of 14-3-3 by CK1 negatively regulates binding to Raf *in vivo* [33].

Ser185 is located in the tertiary structure adjacent to residue 233 [19], and Gotoh's group [35] have recently shown that activated c-Jun N-terminal kinase (JNK) promotes Bax translocation to the mitochondria through phosphorylation of 14-3-3σ and ζ at sites equivalent to Ser185, which led to the dissociation of Bax. Expression of phosphorylation defective mutants of 14-3-3 blocked JNK-induced Bax translocation to mitochondria, cytochrome *c* release and apoptosis.

14-3-3τ isoform has been shown to interact with full length BCR and with BCR-Abl [9]. The authors indicated that 14-3-3τ was a substrate for the BCR serine-threonine kinase activity and in this study we have determined the site to be residue 233. This is of major potential physiological relevance since this C-terminal region has recently been proposed as a general inhibitor of 14-3-3–ligand interactions [36]. The observation here that BCR phosphorylates 14-3-3 on the same residue, 233, as CK1 indicates a conserved mode of regulation, whereby phosphorylation could affect the ability of 14-3-3 to bind target proteins.

Results

BCR associates with 14-3-3 isoforms *in vitro* and *in vivo*

14-3-3 isoforms τ and ζ and β have previously been shown to interact with BCR [9,10]. To investigate the possibility that additional isoforms may also interact with BCR, two approaches were taken. Firstly BCR–FLAG was overexpressed in 293 cells, GST–14-3-3 fusion proteins were incubated with the lysate, glutathione beads added and the 'pull downs' were subjected to SDS/PAGE and western blotted using anti-FLAG (Fig. 2A). Recombinant GST fusion constructs of all 14-3-3 isoforms pulled down BCR–FLAG from transfected cells which verified that all 14-3-3 isoforms have the ability to interact with BCR. However, relatively more BCR associated with the 14-3-3η and γ isoform constructs (Fig. 2A). Pull down experiments were repeated, with consistent results. The example shown was carried out at a time when the phosphorylation site had been identified, which is the reason for the inclusion of the T233Dζ–14-3-3 construct. Secondly, BCR–FLAG was overexpressed in cells, immunoprecipitated, and western blotting used to detect interaction with endogenous 14-3-3 isoforms. The results show that

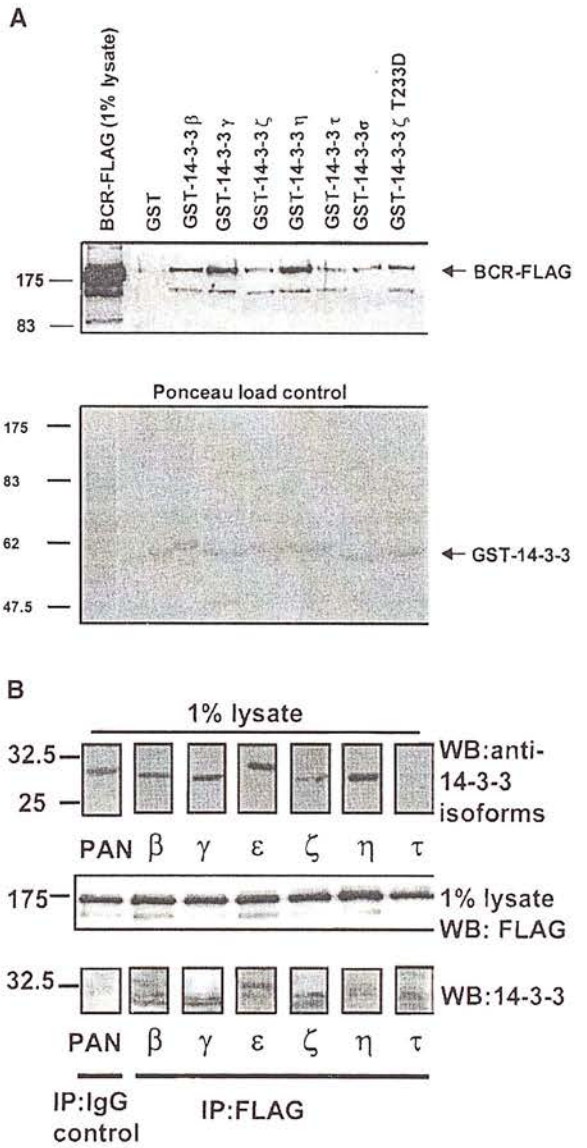

Fig. 2. (A) BCR interacts with all 14-3-3 isoforms in 293 cells. HEK293 -cells were transfected with BCR–FLAG, lysed and incubated with the indicated GST–14-3-3 isoform. A loading control for 14-3-3 stained with Ponceau S is shown in the lower panel. GST–14-3-3ζ T233D construct was also assayed, right-hand lane. An equivalent amount of 1% of the lysate used for each incubation is shown in lane 1, and a GST-only incubation is shown in lane 2. (B) 293 cells were transfected with BCR–FLAG, the lysates pooled and divided into seven aliquots for immunoprecipitation with anti-FLAG Ig. An aliquot containing 1% of the input of each lysate was western blotted with anti-14-3-3 Igs to verify endogenous levels (top panel). The input lysate (1%) was western blotted with anti-FLAG Igs (middle panel) to check expression levels of the BCR construct. The 14-3-3 isoforms were coimmunoprecipitated with anti-Flag Ig and each anti-FLAG immunoprecipitation was western blotted with antibodies specific for a 14-3-3 isoform [54] as indicated (bottom panel). To demonstrate that 14-3-3 isoforms do not bind nonspecifically to the resin beads, the left lane is an immunoprecipitation with control IgG followed by a western blot with antibodies that recognize all 14-3-3 isoforms (PAN).

14-3-3β, γ, ε, ζ, τ and η isoforms associate with BCR–FLAG (Fig. 2B). Tau14-3-3 is expressed at low levels in 293 cells; nevertheless interaction with this isoform can be seen. 14-3-3σ is expressed at high levels only in epithelial cells and is present at such low levels in the 293 cell line that the interaction could not be detected. Negative controls using nonimmune sera were added to BCR–FLAG transfections. These showed that none of the isoforms tested associate with the agarose bead/antibody matrix.

As well as verifying the binding of 14-3-3 isoforms β, ζ and τ shown previously [9,10] we have thus shown in this study that γ, η and ε14-3-3 can also associate with BCR *in vivo* and *in vitro*.

BCR phosphorylates 14-3-3τ and 14-3-3ζ *in vitro*

BCR kinase has previously been shown to phosphorylate 14-3-3 on serine/threonine residues [9]. It has also been shown that BCR when treated with alkaline phosphatase reduced ability to associate with 14-3-3 [37]. However it is not known if association of BCR with 14-3-3 facilitates phosphorylation. Two vectors suitable for mammalian expression containing full length BCR were produced; an N-terminal GST fusion construct and a C-terminal FLAG construct. The purpose of creating a GST N-terminal fusion was to determine whether the dimerization ability of GST could increase the kinase activity of BCR, because Maru *et al.* [38] showed that GST could replace the oligomerization domain of BCR. It has also been shown that BCR purifies as an oligomer [8]. A C-terminal FLAG tag construct was created in case the GST itself would create steric hindrance between BCR and 14-3-3 as substrate. In addition, production in mammalian cells would allow any necessary post-translational modifications such as phosphorylation and correct processing and folding of BCR. The tagged BCR transcripts were overexpressed in COS-1 and human embryonic kidney (HEK) 293 cells, and lysed in NP-40 buffer designed to maintain the phosphorylated state of BCR. GST–BCR was affinity purified using glutathione–Sepharose beads, extensively washed and incubated with exogenous 14-3-3 under appropriate assay conditions. In agreement with previous studies, the 14-3-3τ and ζ isoforms were phosphorylated (Fig. 3), the latter to a much lower level than τ. None of the other mammalian isoforms β, γ, ε, η and σ were phosphorylated. BCR–FLAG constructs immunoprecipitated with M2 α-FLAG antibody gave a slightly higher level of phosphorylation and so were used for further studies. There was no difference in substrate specificity between GST–BCR and BCR–FLAG (data not shown). Alignment of the mammalian 14-3-3 isoform

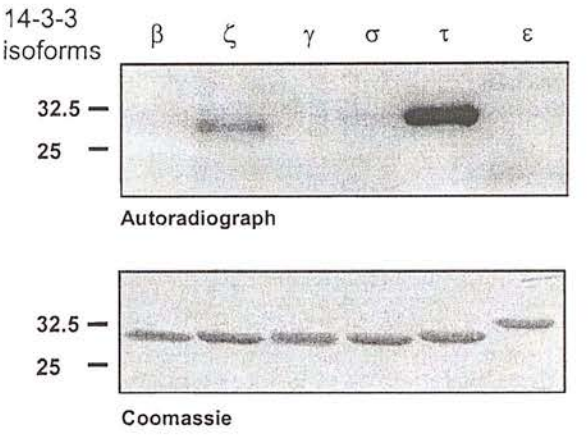

Fig. 3. BCR kinase phosphorylation of isoforms of 14-3-3. GST–BCR was 'pulled down' and a protein kinase assay with each mammalian 14-3-3 isoform was carried out, followed by autoradiography of the SDS/PAGE. The lower panel shows the loading control of each 14-3-3 isoform (stained with Coomassie blue).

sequences indicate that the only Ser/Thr residues common to τ and ζ, but not present in the other isoforms, are S233 in 14-3-3τ and T233 in 14-3-3ζ. Using Ala mutants of these phosphorylation sites, kinase assays were carried out as previously. The Ser→Ala mutant (S233A) of 14-3-3τ (Fig. 4A) and the Thr→Ala mutant (T233A) of 14-3-3ζ were not phosphorylated by BCR (Fig. 4B). There was no change in phosphorylation by BCR of the Ser→Ala mutant (S185A) of 14-3-3ζ (Fig. 4B). The phosphorylation of the 14-3-3ζ constructs at residue T233 was very poor in comparison to phosphorylation of wild type 14-3-3τ and mutation of this residue to Ala completely abolished phosphorylation. The lack of phosphorylation of the T233A construct of 14-3-3ζ indicates that BCR does not phosphorylate residue 185 in 14-3-3ζ, which was shown by Gotoh's group to be a substrate for JNK [35].

Ser58, common to all 14-3-3 isoforms except σ, is phosphorylated by a variety of protein kinases (SDK1 [39], PKB [40] and by PKC in a synthetic peptide corresponding to residues 49–68 of the other isoforms [41]). We show that there is complete lack of phosphorylation of 14-3-3σ (Fig. 3), which acts as a natural negative control. The S185A mutant of 14-3-3ζ as well as the S233A and T233A variants still include Ser58, which rules out the possibility of Ser58 being a site of phosphorylation by BCR.

Phosphorylation of 14-3-3 isoforms is not due to coimmunoprecipitation of CK1

Casein kinase 1 has been shown to phosphorylate 14-3-3τ and ζ specifically on residue 233 both *in vitro*

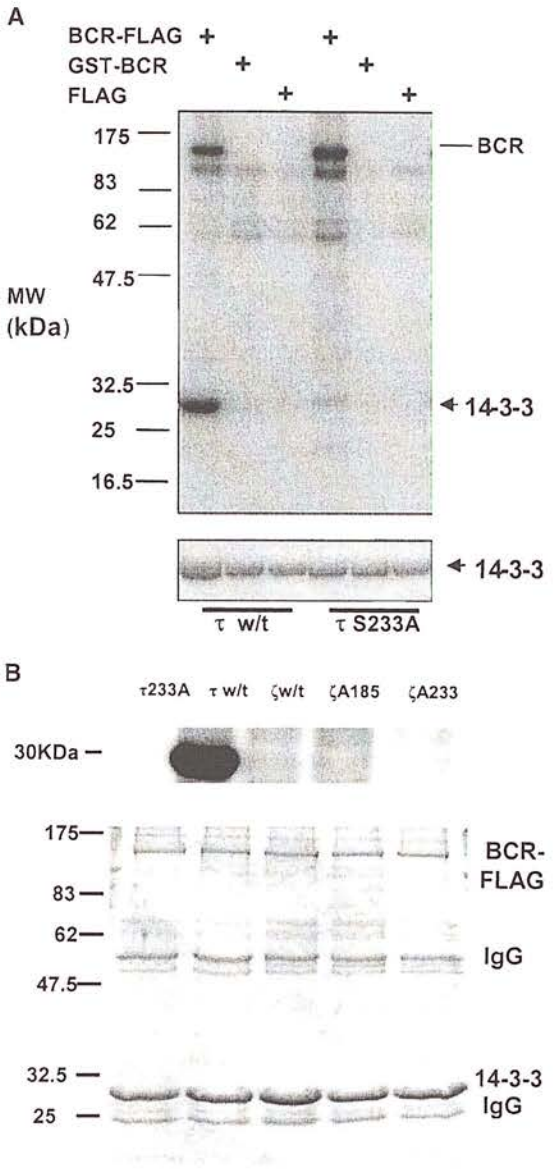

Fig. 4. Ala mutation at residue 233 abolishes phosphorylation by BCR *in vitro*. (A) BCR–FLAG and the empty flag vector were transfected into 293 cells and immunoprecipitated with anti-FLAG Igs as described in the Experimental procedures. Kinase assays of 14-3-3τ were performed and SDS/PAGE of the radiolabelled protein was carried out. The top panel shows an autoradiograph of tau 14-3-3 wild type (left 3 lanes) and tau 14-3-3 S233A (right 3 lanes). The control (middle lanes) is a transfection with the GST–BCR construct, which we then attempted to pull down with the anti-FLAG Ig to verify the specificity of the immunoprecipitation. The bottom panel shows the 14-3-3 protein levels (Coomassie blue stained) in the corresponding lanes of the autoradiograph. (B) A similar experiment was carried out with the zeta 14-3-3 T233A and zeta S185A constructs. Wild type tau and zeta 14-3-3 were phosphorylated in parallel. The bottom panel shows the 14-3-3 protein levels (Coomassie blue stained) in the corresponding lanes of the autoradiograph.

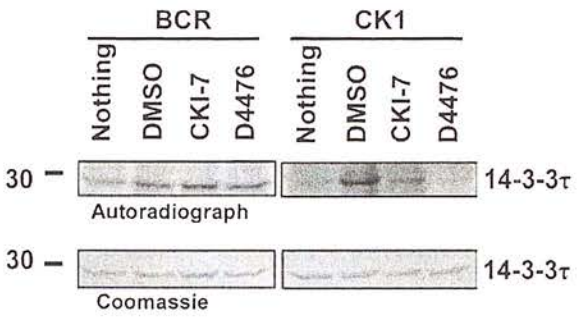

Fig. 5. CK1 specific inhibitors do not affect BCR kinase activity. The figure shows an autoradiograph of 14-3-3 τ wt protein phosphorylated by BCR (left 4 lanes) and by CKIα (right 4 lanes) in the presence and absence of the inhibitors as indicated. The bottom panels show the 14-3-3 protein levels (Coomassie blue stained) in the corresponding lanes of the autoradiograph. Dimethylsulfoxide was included as a vehicle control. CKI-7 and D4476 were both used at 20 μM.

and *in vivo* [33]. We have also shown that CK1 associates with 14-3-3 (S. Clokie and A. Aitken, unpublished results; [42]). The possibility existed that endogenous 14-3-3 could be acting as a 'molecular bridge' between BCR and endogenous CK1 and that the latter activity was phosphorylating 14-3-3τ. To exclude this possibility, the CK1 inhibitor CKI-7 was added to kinase assays at concentrations up to 100 μM. Little effect was seen, even at the highest concentration, and only slight inhibition was seen when BCR was preincubated with CKI-7 for 1 h. However the IC_{50} of this compound is rather high and it is possible that it is causing a general inhibition of kinase activity when used at such high concentrations. We then used the newly developed inhibitor of CK1 4-{4-[2,3-dihydro-benzo (1,4)dioxin-6-yl]-5-pyridin-2-yl-1H-imidazol-2-yl}benzamide (D4476) [43]. This has an IC_{50} of approximately 1 μM, and is therefore 10-fold more inhibitory than CKI-7 towards CK1 and has been shown to be highly specific [43]. This had no effect on the phosphorylation of 14-3-3τ or ζ by BCR kinase, but completely inhibited CK1 assayed in parallel with BCR (Fig. 5).

Discussion

Reuther *et al.* [9] showed that 14-3-3 binds to BCR downstream of residue 297 (Fig. 1), and these authors alluded to the possibility of 14-3-3 binding elsewhere on the protein, but to a lesser extent. Indeed BCR has many potential 14-3-3 binding sites – RASA-S95-RP, RSG-S301-TS, RL-T310-WPR, RSY-S317-P and RSP-S371-QN [28,45] – four of them C-terminal to residue 297. Recently the sequence RL-T310-WPR has been shown to be phosphorylated *in vivo* [44].

We have now shown that the 14-3-3 isoforms (β, γ, ε, ζ and η) that are expressed at a detectable level in 293 cells bind BCR *in vivo*. The fact that 14-3-3τ was detected in the BCR–FLAG immunoprecipitation, even though not detectable in the 293 lysate shows the interaction may be of higher affinity than the other isoforms. We also showed that 14-3-3 isoforms incubated with a cell lysate containing BCR–FLAG were able to associate. Therefore, in addition to the τ, ζ and β isoforms previously shown, 14-3-3 ε, η and γ can also interact with BCR. Our results suggest that while there is the capacity of all 14-3-3 isoforms to bind BCR, there is a preference for binding certain 14-3-3 isoforms. It may be difficult to ascertain true binding specificities, *in vivo*, due to the ability of 14-3-3 to form a limited repertoire of heterodimers [45]. A T233D mutant of 14-3-3ζ was incubated with the BCR lysate (Fig. 2A) to determine whether mimicking a phosphorylated T233 could negatively affect binding, as reported previously [28,33]. However, the mutant had no significant effect, possibly due to the fact that sometimes an Asp mutation that introduces a carboxyl group does not have the same effect as a phosphate group.

The increased number of 14-3-3 isoforms that are shown here to bind BCR opens up further potential roles for BCR in cellular signalling. Even though these extra 14-3-3 isoforms are not substrates for BCR, they may well affect BCR activity and/or subcellular location.

Using specific mutants of 14-3-3 we have shown that BCR phosphorylates the tau isoform on serine 233 only. There is a rational explanation why phosphorylation at Ser233 in this isoform led to the observation by Reuther *et al.* [9] of four phosphopeptide spots on thin layer electrophoresis. From our own extensive protein sequence analysis ([46] and A. Aitken, unpublished results) we have shown that tryptic cleavage of 14-3-3 isoforms produces the following two C-terminal peptides: (R)DNLTLWTSDSAGEECDAAEGAEN(223–245) and (K)DSTLIMQLLRDNLTLWTSDSAGEE CDAAEGAEN(213–245). This is due to partial cleavage at Arg223 (underlined). The unique cysteine residue (also underlined) in the tau isoform may undergo modification, such as partial oxidation to cysteic acid during thin layer electrophoresis when exposed to air, which changes its electrophoretic mobility. Phosphorylation at residue 233 would yield two radiolabelled phosphopeptides due to partial cleavage by trypsin, multiplied by two due to the partially modified cysteine residues (which have a more acidic mobility), and producing a total of four spots on thin layer electrophoresis.

BCR has a clear preference for phosphorylation of 14-3-3τ rather than 14-3-3ζ (in agreement with previous studies [9]), possibly due to increased binding affinity. In three separate experiments we observed an approximately 10-fold higher phosphorylation of τ than ζ 14-3-3 (Fig. 3 and data not shown). This is in contrast to the preference of CK1α for 14-3-3ζ over 14-3-3τ [34]. It may be worth noting that 14-3-3τ, the major isoform substrate for BCR is expressed in T-cells to a greater extent than in other tissues [47,48].

Western blots of immunoprecipitated BCR using phospho-Tyr antibodies showed the presence of phosphorylated tyrosine residues (data not shown). One study has shown that tyrosine phosphorylation on residue 177 (by Fes kinase) actually reduced the association with 14-3-3, while at the same time increasing the SH2 binding to GRB2 [49]. The kinase that phosphorylates BCR on Tyr177 in HEK293 cells is currently not known. A study of the Philadelphia positive cell line K562 showed that Tyr177 is phosphorylated *in vivo* [44], but this residue is a known substrate for BCR–Abl, also expressed in this cell line [50,51]. The possibility remains that 14-3-3 association with BCR may perturb Tyr177 phosphorylation and/or affect SH2 binding at this site.

Experimental procedures

Materials

All chemicals and reagents were from Sigma (St Louis, MO, USA), apart from Redivue [^{32}P]ATP[γP] (triethylammonium salt) from Amersham (Buckinghamshire, UK) and prestained protein markers from New England Biolabs (Beverly, MA, USA). Protease inhibitor tablets were from Roche (Indianapolis, IN, USA); recombinant CK1 was from Upstate Biotechnology (Lake Placid, NY, USA) and CKI-7 was from Seikagaku (Tokyo, Japan).

A vector containing the *bcr* sequence was a kind gift from O. Witte (Department of Cell Biology, Harvard Medical School, Boston, MA, USA). The coding sequence for bcr was amplified by PCR using two oligonucleotides 5′-GATCGCGGCCGCGCGCCATGGTGGACCCGGTG GGCTT-3′ and 3′-GATCGAATTCGACTTCGGTGGAG AACAGGATGCTCTGTCT-5′ creating the restriction sites *Not*1 and *Eco*R1, respectively (underlined), and ligated into the pEBG-2T GST vector for mammalian expression (kind gift from D. Alessi, University of Dundee, UK) creating an N-terminally fused bcr construct. Two oligonucleotides (5′-GATCGAATTCATGGTGGACCCGGTGGGCTTCG-3′ and 3′-GATCGCGGCCGCTTAGACTTCGGTGGAGAA CAGGATGCTCTGTCT-5′) were used to produce bcr cDNA, containing the restriction sites *Eco*R1 and *Not*1 for ligation

into the pCMV-4A vector (Stratagene, La Jolla, CA, USA), producing a C-terminal fusion with the FLAG tag.

The cDNAs for 14-3-3 isoforms were from various sources. 14-3-3β is an IMAGE clone (4843961/gi14060448), and was subcloned from the supplied vector (pOTB7) PCR with two oligonucleotides: 5′-GATCGAATTCATGACAA TGGATAAAAGTGAGCTGGTA-3′ and 3′-GATCGTC GACTTAGTTCTCTCCCTCCCCAG-5′, creating an *Eco*R1 and a *Sal*1 restriction site, respectively (underlined). The PCR product was inserted into pGEX-4T1 (Amersham), creating an N-terminal GST fusion. 14-3-3η, 14-3-3γ and 14-3-3σ were a gift from H. Leffers (University of Copenhagen, Denmark), the η and γ clones were present as an N-terminal GST fusion in the vector pGEX-2TK (Amersham). The 14-3-3σ was subcloned from the vector pGPT-delta 6 using the oligonucleotides 5′-GATCGAATTCATGGAGA GAGCCAGTCTGATC-3′ and 3′-GATCGTCGACTCAG CTCTGGGGCTCCT-5′ creating an *Eco*R1 site and *Sal*1 site, respectively (underlined). The PCR product was inserted into pGEX-4T1. 14-3-3ζ was from a human T-cell cDNA library and has been produced as an N-terminal GST fusion in the pGEX-2T vector [33,47,52]. 14-3-3ε was produced as an N-terminal maltose binding protein (MBP) fusion, from a rat cDNA (accession no. m84416) [53]. 14-3-3τ was from a human source [48,49]. All cDNAs were checked by sequencing both strands (in house sequencing core and Cytomyx, Cambridge, UK).

Tissue culture and immunoprecipitation

SV40 transformed African green monkey kidney cells (COS-1) and adenovirus 5E1A/B transformed human embryonic kidney (HEK) 293 cells were transiently transfected with 8 μg DNA with 24 μL Lipofectamine 2000 (Invitrogen, Carlsbad, CA, USA). Cells were routinely cultured in Dulbecco's modified Eagle's medium (DMEM, Invitrogen) supplemented with 10% (w/v) fetal bovine serum (Invitrogen), penicillin, streptomycin and L-glutamine at 1 $U \cdot mL^{-1}$, 1 $\mu g \cdot mL^{-1}$ and 0.292 $mg \cdot mL^{-1}$, respectively, at 5% (v/v) CO_2 and 37 °C until lysis. For transient transfections, 2–4 × 10^6 cells were added to 100 mm plates, using antibiotic-free media, left until 80–90% confluent, then incubated for 24 h after addition of the DNA–Lipofectamine complex at 5% (v/v) CO_2, 37 °C. The plates were washed twice with ice cold $NaCl/P_i$ and lysed on ice with ice-cold NP-40 buffer using a cell scraper. The lysate was clarified by centrifugation at 16 000 *g* for 30 min at 4 °C, the addition of 50 μL washed Pansorbin A cells (Calbiochem) for 60 min to remove endogenous IgG, then a further 30 min at 16 000 *g*, 4 °C.

Glutathione 'pull-down' immunoprecipitation kinase assay

Glutathione–Sepharose 4B (Amersham Pharmacia) beads or a 1 : 1 mix of protein A and G beads (Amersham) were used to pull down the GST fusion and immunoprecipitate the FLAG-tagged BCR, respectively. To the clarified cell lysates, GSH beads were added for 2 h before washing. For immunoprecipitation with FLAG antibody (M2) the antibody was incubated in the lysate overnight, then incubated with protein AG beads for 2 h. The beads were then centrifuged at 8000 *g* in a benchtop centrifuge for 20 s and washed three times in lysis buffer [50 mM Tris, pH 7.5, 10% (v/v) glycerol, 137 mM NaCl, 2 mM β-glycerol phosphate, 1 mM NaF, 1 mM $NaVO_4$, 1 mM EDTA, 1 mM dithiothreitol and protease inhibitor cocktail tablet, EDTA-free (Roche)]. The beads were then washed twice in kinase assay buffer (see below, without ATP and dithiothreitol). After the last wash, the beads were resuspended in a final volume of 25 μL kinase assay buffer, with a final concentration of 50 mM Hepes, pH 7.05, 10 mM MgCl, 20 μM ATP (containing 10 μCi [^{32}P]ATP) and 20 μM dithiothreitol, and 2 μg of 14-3-3 isoform was used for each assay. The reaction was carried out for 30 min at 30 °C and stopped in Laemmli buffer prior to SDS/PAGE, followed by autoradiography.

Casein kinase 1 inhibitors

CKI-7 was dissolved in dimethylsulfoxide as a 10 mM stock. For preincubation experiments with CKI-7, during the last wash of the IP, BCR–FLAG immunoprecipitates were turned end over end while suspended in kinase assay buffer including 100 μM CKI-7 (minus ATP). Where stated, CKI-7 was added just prior to addition of the substrate (20 μM). D4476 inhibitor was dissolved in dimethylsulfoxide to a stock of 1 mM and was used at 20 μM in the final assay. This was added immediately prior to addition of the substrate. No preincubation with D4476 was required to observe an inhibitory effect. Dimethylsulfoxide (2 μL) was used as a vehicle control.

Recombinant protein purification

All GST–14-3-3 fusion cDNAs were transformed into *E. coli* BL21(DE3)pLysS competent cells (Novagen, Madison, WI, USA), using the appropriate antibiotic. The cells were grown at 37 °C until an attenuation of 0.9, then induced using isopropyl thio-β-D-galactoside (ICN, Costa Mesa, CA, USA) for 3.5 h at 30 °C, in a shaking incubator. The same procedure was used for the MBP–14-3-3ε, but with the addition of glucose at 2 $g \cdot L^{-1}$ at all stages. Cell pellets, resuspended in lysis buffer [$NaCl/P_i$, 1 mM phenylmethanesulfonyl fluoride, 1 mM EDTA, 1 mM dithiothreitol, protease inhibitor tablet and 0.1% (v/v) Triton], were sonicated six times for 30 s with amplitude of 5 microns. The Triton X-100 concentration was increased to 1%; the cell suspensions were rotated for 30 min at 4 °C and clarified by centrifugation at 16 000 *g* for 30 min. The supernatant was then passed through a 0.22 μm filter and

the GST fusion protein was recovered from the lysate using glutathione–Sepharose 4B beads (Amersham). The beads were washed extensively and the 14-3-3 cleaved from the GST tag using 50 U thrombin (Sigma) or 50 U Factor Xa (New England Biolabs) for MBP–14-3-3ε, for each litre of original culture. The 14-3-3 was then concentrated and buffer-exchanged into NaCl/P_i containing protease inhibitors (Roche) using a Vivaspin 10K MWCO concentrator and stored in small aliquots at −70 °C until required.

Acknowledgements

A vector containing the *bcr* sequence was a kind gift from Owen Witte (Department of Cell Biology, Harvard Medical School, Boston, MA, USA). We thank Sir Philip Cohen and Carol MacKintosh (MRC protein phosphorylation unit, University of Dundee) for the suggestion to use D4476 and for the use of lab facilities. The pEBG-2T GST vector for mammalian expression was a kind gift from Dario Alessi.

References

1 Laurent E, Talpaz M, Kantarjian H & Kurzrock R (2001) The BCR gene and philadelphia chromosome-positive leukemogenesis. *Cancer Res* **61**, 2343–2355.
2 Nowell PC & Hungerford DA (1960) Chromosome studies on normal and leukemic human leukocytes. *J Natl Cancer Inst* **25**, 85–109.
3 Li WJ, Dreazen O, Kloetzer W, Gale RP & Arlinghaus RB (1989) Characterization of bcr gene products in hematopoietic cells. *Oncogene* **4**, 127–138.
4 McLaughlin J, Chianese E & Witte ON (1989) Alternative forms of the BCR-ABL oncogene have quantitatively different potencies for stimulation of immature lymphoid cells. *Mol Cell Biol* **9**, 1866–1874.
5 Lugo TG, Pendergast AM, Muller AJ & Witte ON (1990) Tyrosine kinase activity and transformation potency of bcr-abl oncogene products. *Science* **247**, 1079–1082.
6 Salesse S & Verfaillie CM (2002) BCR/ABL: from molecular mechanisms of leukemia induction to treatment of chronic myelogenous leukemia. *Oncogene* **21**, 8547–8559.
7 McWhirter JR, Galasso DL & Wang JY (1993) A coiled-coil oligomerization domain of BCR is essential for the transforming function of BCR-Abl oncoproteins. *Mol Cell Biol* **13**, 7587–7595.
8 Maru Y & Witte ON (1991) The BCR gene encodes a novel serine/threonine kinase activity within a single exon. *Cell* **67**, 459–468.
9 Reuther GW, Fu H, Cripe LD, Collier RJ & Pendergast AM (1994) Association of the protein kinases c-BCR and BCR-Abl with proteins of the 14-3-3 family. *Science* **266**, 129–133.
10 Braselmann S & McCormick F (1995) BCR and Raf form a complex in vivo via 14-3-3 proteins. *EMBO J* **14**, 4839–4848.
11 Pendergast AM, Quilliam LA, Cripe LD, Bassing CH, Dai Z, Li N, Batzer A, Der Rabun KMCJ, Schlessinger J *et al.* (1993) BCR-ABL-induced oncogenesis is mediated by direct interaction with the SH2 domain of the GRB-2 adaptor protein. *Cell* **75**, 175–185.
12 Adams JM, Houston H, Allen J, Lints T & Harvey R (1992) The hematopoietically expressed vav proto-oncogene shares homology with the dbl GDP-GTP exchange factor, the bcr gene and a yeast gene (CDC24) involved in cytoskeletal organization. *Oncogene* **7**, 611–618.
13 Ron D, Zannini M, Lewis M, Wickner RB, Hunt LT, Graziani G, Tronick SR, Aaronson SA & Eva A (1991) A region of proto-dbl essential for its transforming activity shows sequence similarity to a yeast cell cycle gene, CDC24, and the human breakpoint cluster gene, bcr. *New Biol* **3**, 372–379.
14 Diekmann D, Brill S, Garrett MD, Totty N, Hsuan J, Monfries C, Hall C, Lim L & Hall A (1991) BCR encodes a GTPase-activating protein for p21rac. *Nature* **351**, 400–402.
15 Takeda N, Shibuya M & Maru Y (1999) The BCR-ABL oncoprotein potentially interacts with the xeroderma pigmentosum group B protein. *Proc Natl Acad Sci USA* **96**, 203–207.
16 Wetzler M, Talpaz M, Yee G, Stass SA, Van Etten RA, Andreeff M, Goodacre AM, Kleine HD, Mahadevia RK & Kurzrock R (1995) Cell cycle-related shifts in subcellular localization of BCR: association with mitotic chromosomes and with heterochromatin. *Proc Natl Acad Sci USA* **92**, 3488–3492.
17 Boisguerin P, Leben R, Ay B, Radziwill G, Moelling K, Dong L & Volkmer-Engert R (2004) An improved method for the synthesis of cellulose membrane-bound peptides with free C termini is useful for PDZ domain binding studies. *Chem Biol* **11**, 449–459.
18 Fu H, Subramanian RR & Masters SC (2000) 14-3-3 proteins: structure, function, and regulation. *Annu Rev Pharmacol Toxicol* **40**, 617–647.
19 Aitken A (2002) Functional specificity in 14-3-3 isoform interactions through dimer formation and phosphorylation. Chromosome location of mammalian isoforms and variants. *Plant Mol Biol* **50**, 993–1010.
20 MacKintosh C (2004) Dynamic interactions between 14 and 3–3s and phosphoproteins regulate diverse cellular processes. *Biochem J* **381**, 329–342.
21 Muslin AJ, Tanner JW, Allen PM & Shaw AS (1996) Interaction of 14-3-3 with signaling proteins is mediated by the recognition of phosphoserine. *Cell* **84**, 889–897.
22 Yaffe MB, Rittinger K, Volinia S, Caron PR, Aitken A, Leffers H, Gamblin SJ, Smerdon SJ & Cantley LC

(1997) The structural basis for 14-3-3: phosphopeptide binding specificity. *Cell* **91**, 961–971.
23 Xiao B, Smerdon SJ, Jones DH, Dodson GG, Soneji Y, Aitken A & Gamblin SJ (1995) Structure of a 14-3-3 protein and implications for coordination of multiple signalling pathways. *Nature* **376**, 188–191.
24 Liu D, Bienkowska J, Petosa C, Collier RJ, Fu H & Liddington R (1995) Crystal structure of the zeta isoform of the 14-3-3 protein. *Nature* **376**, 191–194.
25 Henriksson ML, Francis MS, Peden A, Aili M, Stefansson K, Palmer R, Aitken A & Hallberg B (2002) A nonphosphorylated 14-3-3 binding motif on exoenzyme S that is functional *in vivo*. *Eur J Biochem* **269**, 4921–4929.
26 Tzivion G & Avruch J (2002) 14-3-3 proteins: active cofactors in cellular regulation by serine/threonine phosphorylation. *J Biol Chem* **277**, 3061–3064.
27 Aitken A (1996) 14-3-3 and its possible role in coordinating multiple signalling pathways. *Trends Cell Biol* **6**, 341–347.
28 Rommel C, Radziwill G, Lovric J, Noeldeke J, Heinicke T, Jones D, Aitken A & Moelling K (1996) Activated Ras displaces 14-3-3 protein from the amino terminus of c-Raf-1. *Oncogene* **12**, 609–619.
29 Bonnefoy-Berard N, Liu YC, von Willebrand M, Sung A, Elly C, Mustelin T, Yoshida H, Ishizaka K & Altman A (1995) Inhibition of phosphatidylinositol 3–kinase activity by association with 14-3-3 proteins in T cells. *Proc Natl Acad Sci USA* **92**, 10142–10146.
30 Aitken A, Howell S, Jones D, Madrazo J & Patel Y (1995) 14-3-3 alpha and delta are the phosphorylated forms of raf-activating 14-3-3 beta and zeta. In vivo stoichiometric phosphorylation in brain at a Ser-Pro-Glu-Lys MOTIF. *J Biol Chem* **270**, 5706–5709.
31 Gross SD & Anderson RA (1998) Casein kinase I: spatial organization and positioning of a multifunctional protein kinase family. *Cell Signal* **10**, 699–711.
32 Vielhaber E & Virshup DM (2001) Casein kinase I: from obscurity to center stage. *IUBMB Life* **51**, 73–78.
33 Dubois T, Rommel C, Howell S, Steinhussen U, Soneji Y, Morrice N, Moelling K & Aitken A (1997) 14-3-3 is phosphorylated by casein kinase I on residue 233. Phosphorylation at this site in vivo regulates Raf/14-3-3 interaction. *J Biol Chem* **272**, 28882–28888.
34 Hamaguchi A, Suzuki E, Murayama K, Fujimura T, Hikita T, Iwabuchi K, Handa K, Withers DA, Masters SC, Fu H & Hakomori S (2003) Sphingosine-dependent protein kinase-1, directed to 14-3-3, is identified as the kinase domain of protein kinase C delta. *J Biol Chem* **278**, 41557–41565.
35 Tsuruta F, Sunayama J, Mori Y, Hattori S, Shimizu S, Tsujimoto Y, Yoshioka K, Masuyama N & Gotoh Y (2004) JNK promotes Bax translocation to mitochondria through phosphorylation of 14-3-3 proteins. *EMBO J* **23**, 1889–1899.
36 Truong AB, Masters SC, Yang H & Fu H (2002) Role of the 14-3-3 C-terminal loop in ligand interaction. *Proteins* **49**, 321–325.
37 Michaud NR, Fabian JR, Mathes KD & Morrison DK (1995) 14-3-3 is not essential for Raf-1 function: identification of Raf-1 proteins that are biologically activated in a 14-3-3- and Ras-independent manner. *Mol Cell Biol* **15**, 3390–3397.
38 Maru Y, Afar DE, Witte ON & Shibuya M (1996) The dimerization property of glutathione S-transferase partially reactivates BCR-Abl lacking the oligomerization domain. *J Biol Chem* **271**, 15353–15357.
39 Megidish T, Cooper J, Zhang L, Fu H & Hakomori S (1998) A novel sphingosine-dependent protein kinase (SDK1) specifically phosphorylates certain isoforms of 14-3-3 protein. *J Biol Chem* **273**, 21834–21845.
40 Powell DW, Rane MJ, Chen Q, Singh S & McLeish KR (2002) Identification of 14-3-3zeta as a protein kinase B/Akt substrate. *J Biol Chem* **277**, 21639–21642.
41 Dubois T, Howell S, Amess B, Kerai P, Learmonth M, Madrazo J, Chaudhri M, Rittinger K, Scarabel M, Soneji Y & Aitken A (1997) Structure and sites of phosphorylation of 14-3-3 protein: role in coordinating signal transduction pathways. *J Protein Chem* **16**, 513–522.
42 Pozuelo Rubio M, Geraghty KM, Wong BH, Wood NT, Campbell DG, Morrice N & MacKintosh C (2004) 14-3-3-affinity purification of over 200 human phosphoproteins reveals new links to regulation of cellular metabolism, proliferation, and trafficking. *Biochem J*
43 Rena G, Bain J, Elliott M & Cohen P (2004) D4476, a cell-permeant inhibitor of CK1, suppresses the site-specific phosphorylation and nuclear exclusion of FOXO1a. *EMBO Report* **5**, 60–65.
44 Salomon AR, Ficarro SB, Brill LM, Brinker A, Phung QT, Ericson C, Sauer K, Brock A, Horn DM, Schultz PG & Peters EC (2003) Profiling of tyrosine phosphorylation pathways in human cells using mass spectrometry. *Proc Natl Acad Sci USA* **100**, 443–448.
45 Chaudhri M, Scarabel M & Aitken A (2003) Mammalian and yeast 14-3-3 isoforms form distinct patterns of dimers *in vivo*. *Biochem Biophys Res Commun* **300**, 679–685.
46 Toker A, Sellers LA, Amess B, Patel Y, Harris A & Aitken A (1992) Multiple isoforms of a protein kinase C inhibitor (KCIP-1/14-3-3) from sheep brain. Amino acid sequence of phosphorylated forms. *Eur J Biochem* **206**, 453–461.
47 Nielsen PJ (1991) Primary structure of a human protein kinase regulator protein. *Biochim Biophys Acta* **1088**, 425–428.
48 Jones DH, Martin H, Madrazo J, Robinson KA, Nielsen P, Roseboom PH, Patel Y, Howell SA & Aitken A (1995) Expression and structural analysis of 14-3-3 proteins. *J Mol Biol* **245**, 375–384.
49 Peters KL & Smithgall TE (1999) Tyrosine phosphorylation enhances the SH2 domain-binding activity of

BCR and inhibits BCR interaction with 14-3-3 proteins. *Cell Signal* **11**, 507–514.

50 Puil L, Liu J, Gish G, Mbamalu G, Bowtell D, Pelicci PG, Arlinghaus R & Pawson T (1994) BCR-Abl oncoproteins bind directly to activators of the Ras signalling pathway. *EMBO J* **13**, 764–773.

51 Lozzio CB & Lozzio BB (1975) Human chronic myelogenous leukemia cell-line with positive Philadelphia chromosome. *Blood* **45**, 321–334.

52 Jones DH, Ley S & Aitken A (1995) Isoforms of 14-3-3 protein can form homo- and heterodimers *in vivo* and *in vitro*: implications for function as adapter proteins. *FEBS Lett* **368**, 55–58.

53 Roseboom PH, Weller JL, Babila T, Aitken A, Sellers LA, Moffett JR, Namboodiri MA & Klein DC (1994) Cloning and characterization of the epsilon and zeta isoforms of the 14-3-3 proteins. *DNA Cell Biol* **13**, 629–640.

54 Martin H, Rostas J, Patel Y & Aitken A (1994) Subcellular localisation of 14-3-3 isoforms in rat brain using specific antibodies. *J Neurochem* **63**, 2259–2265.